NUREG/CR-5855
EGG-2671

Thermal-Hydraulic Processes During Reduced Inventory Operation with Loss of Residual Heat Removal

Prepared by
S. A. Naff, G. W. Johnsen, D. E. Palmrose,
E. D. Hughes, C. M. Kullberg, W. C. Arcieri

Idaho National Engineering Laboratory
EG&G Idaho, Inc.

Prepared for
U.S. Nuclear Regulatory Commission

NUREG/CR-5855
EGG-2671
R2, R4

Thermal-Hydraulic Processes During Reduced Inventory Operation with Loss of Residual Heat Removal

Manuscript Completed: February 1992
Date Published: April 1992

Prepared by
S. A. Naff, G. W. Johnsen, D. E. Palmrose,
E. D. Hughes, C. M. Kullberg, W. C. Arcieri

Idaho National Engineering Laboratory
Managed by the U.S. Department of Energy

EG&G Idaho, Inc.
Idaho Falls, ID 83415

Prepared for
Division of Systems Research
Office of Nuclear Regulatory Research
U.S. Nuclear Regulatory Commission
Washington, DC 20555
NRC FIN L1893
Under DOE Contract No. DE-AC07-76ID01570

ABSTRACT

Nuclear power plant conditions during outages differ markedly from those prevailing at normal full-power operation on which most past research has concentrated. This report identifies the topics needed to understand pressurized water reactor response to an extended loss-of-residual heat removal event during refueling and maintenance outages. By identifying the possible plant conditions and cooling methods that might be used, the controlling thermal-hydraulic processes and phenomena were identified. Gravity drain into the reactor coolant system, core water boil-off, and reflux condensation cooling were investigated in detail for example plants from each of the three U.S. pressurized water reactor vendors. The reactor coolant system pressure that would result from reflux cooling was calculated under various assumed conditions and compared to threshold pressures for various temporary closures that might be in use. The viability of various potential gravity feed-and-bleed approaches also was studied.

CONTENTS

LIST OF FIGURES

LIST OF TABLES

EXECUTIVE SUMMARY

Recent plant experience has included many events occurring during outages at pressurized water reactors. A recent example is the loss of residual heat removal system event that occurred March 20, 1990 at the Vogtle-1 plant following refueling. Plant conditions during outages differ markedly from those prevailing at normal full-power operation on which most past research has concentrated. During outages, the core power is low, the coolant system may be in a drained state with air or nitrogen present, and various primary system closures may be unsecured. With the residual heat removal system operating, the core decay heat is readily removed. However, if the residual heat removal system capability is lost and alternate heat removal means cannot be established, heatup of the coolant could lead to core coolant boil-off, fuel rod heatup, and core damage.

By identifying the possible plant conditions and cooling methods that might be used, the controlling thermal-hydraulic processes and phenomena were identified. Controlling processes and phenomena include gravity drain into the reactor coolant system, core water boil-off, and the reflux condensation cooling process. Important subcategories of the reflux cooling processes include the initiation of reflux cooling from various plant conditions, the effects of noncondensable gas on reflux cooling, core level depression effects, issues regarding the steam generator secondaries, and the special case of boiler-condenser cooling with once-through steam generators.

Recommendations for assisting staff in evaluating utility capability so they can effectively respond to a loss of the residual heat removal system include evaluating the capability for using gravity-drain processes and other means of feeding the reactor coolant system without ac power, determining the best options for using secondary system vents and backup sources of feedwater, and determining the capabilities of high point vents for removing air from the reactor coolant system. The primary area needing research regarded initiating and continuing reflux cooling in a reactor coolant system containing air. Specific issues were the primary pressure increase needed to start and maintain the reflux process, and the effects of steam and air migration.

This report gives plant-specific analyses of alternate cooling modes in the absence of residual heat removal system capability. Two basic types of analyses were performed: feed-and-bleed cooling of an open reactor coolant system through the refueling water storage tank or accumulators, and reflux condensation cooling of a closed system using the steam generators as heat sinks (boiler-condenser mode in once-through steam generators). A total of five different reactor plants were evaluated, three for feed-and-bleed and two for condensation cooling. Major conclusions reached in the study are summarized below.

- For the three plants examined (one for each PWR vendor), all are theoretically capable of establishing a drain path between the refueling water storage tank (RWST) and the reactor coolant system (RCS). However, the relative elevation difference between the RWST and the RCS that determines how much water is available can vary significantly from plant to plant.

- Under ideal conditions for the three plants studied, RWST feed-and-bleed of the RCS could maintain core cooling for as little as 0.4 hours (Waterford) to as much as 18 hours (Davis-Besse), assuming the loss of RHR occurred two days after shutdown.

- Feeding from the RWST and venting steam through a manway extends the time RWST water could be used to keep the core cool. However, the capability to control flow to achieve sufficient inventory needs to be established.

- The accumulators are not a practical source of makeup water as currently configured.

- Environmental heat loss from the RCS will only be a small fraction of even the lowest levels of decay heat.

- Closed RCS condensation cooling through one or more steam generators is a viable strategy to maintain core cooling after a loss-of-RHR event. However, there is a possibility that the "steady-state" pressure level in the RCS will threaten the integrity of temporary RCS closures.

- Analysis indicates that the RCS pressure level reached under quasi-stable conditions is dependent on a number of situational and phenomenological conditions. The model developed in this study predicted pressures ranging from 38 to 90 psia for H. B. Robinson and 49 to 71 psia for Oconee.

These results provide a better understanding of plant response to events occurring during outages. This understanding will be useful in achieving plant safety improvements in operating procedures, training, instrumentation, equipment availability, and risk quantification.

This study has concentrated on loss-of-residual heat removal events during reduced inventory operation in pressurized water reactors. Studies may also be needed regarding analogous operations in boiling water reactors.

Thermal-Hydraulic Processes During Reduced Inventory Operation with Loss of Residual Heat Removal

1. INTRODUCTION

This report identifies and analyzes the important thermal-hydraulic phenomena in pressurized water reactors following loss of vital ac power and consequent loss of the residual heat removal (RHR) system during reduced inventory operation. The following steps were undertaken:

- Plant configurations and alternative cooling modes were identified for the variety of potential plant conditions during such events
- Controlling phenomena were identified for each potential cooling mode
- The phenomena that are sufficiently well understood, such that they present no new issues requiring further study, were identified
- Plant-specific analyses were carried out to evaluate alternative reactor cooling schemes.

The research results will provide a better understanding of plant response to events occurring during refueling and maintenance outages and will be useful in achieving plant safety improvements in the following areas: operating procedures, training, instrumentation, equipment availability, and risk quantification.

Events involving loss of RHR during planned outages for maintenance or refueling with different initiators and plant conditions were reviewed, catalogued, and documented in References 1, 2, and 3. The primary emphasis was placed on the March 20, 1990 Vogtle event (LER42490006) and special attention also was given to the April 10, 1987 Diablo Canyon 2 event (LER32387005) and the Waterford 3 event that occurred on July 14, 1986 (LER38286015). Review of these events, each of which lead to reactor coolant system (RCS) heat up, was instrumental in understanding the various potential plant conditions and cooling modes. For brevity, only the Vogtle event is summarized here.

During a refueling outage, the Vogtle-1 plant (Westinghouse 4-loop design) experienced a loss of the RHR system on March 20, 1990. The incident occurred with Unit 1 shut down during a refueling outage. The water level had been lowered to the mid-loop level and as a result, air occupied the upper volume of the RCS. The event was initiated by an accident in the switchyard that interrupted the ac power supply to the RHR system. Diesel generator power was not immediately available; it required 36 minutes to get one of the generators operating and thus restore power to the RHR system. During this period, the reactor coolant temperature increased from 90°F to 136°F and the coolant level remained at mid-loop. The restoration of RHR cooling reversed the coolant heatup and the plant was recovered. A schematic of the Vogtle 1 plant, highlighting component elevations, is shown in Figure 1.

The NRC Incident Investigation Team's report on the Vogtle event is documented in Reference 1. Of particular interest is Section 8 of that document, entitled "Coping with the Loss of the Residual Heat Removal System," which studies the feasibility of alternate core cooling methods. The effect and response of nonboiling and boiling methods were discussed under various scenarios including: (a) whether the RCS is open or closed, (b) various operator actions, and (c) different initial primary coolant levels. Alternate cooling

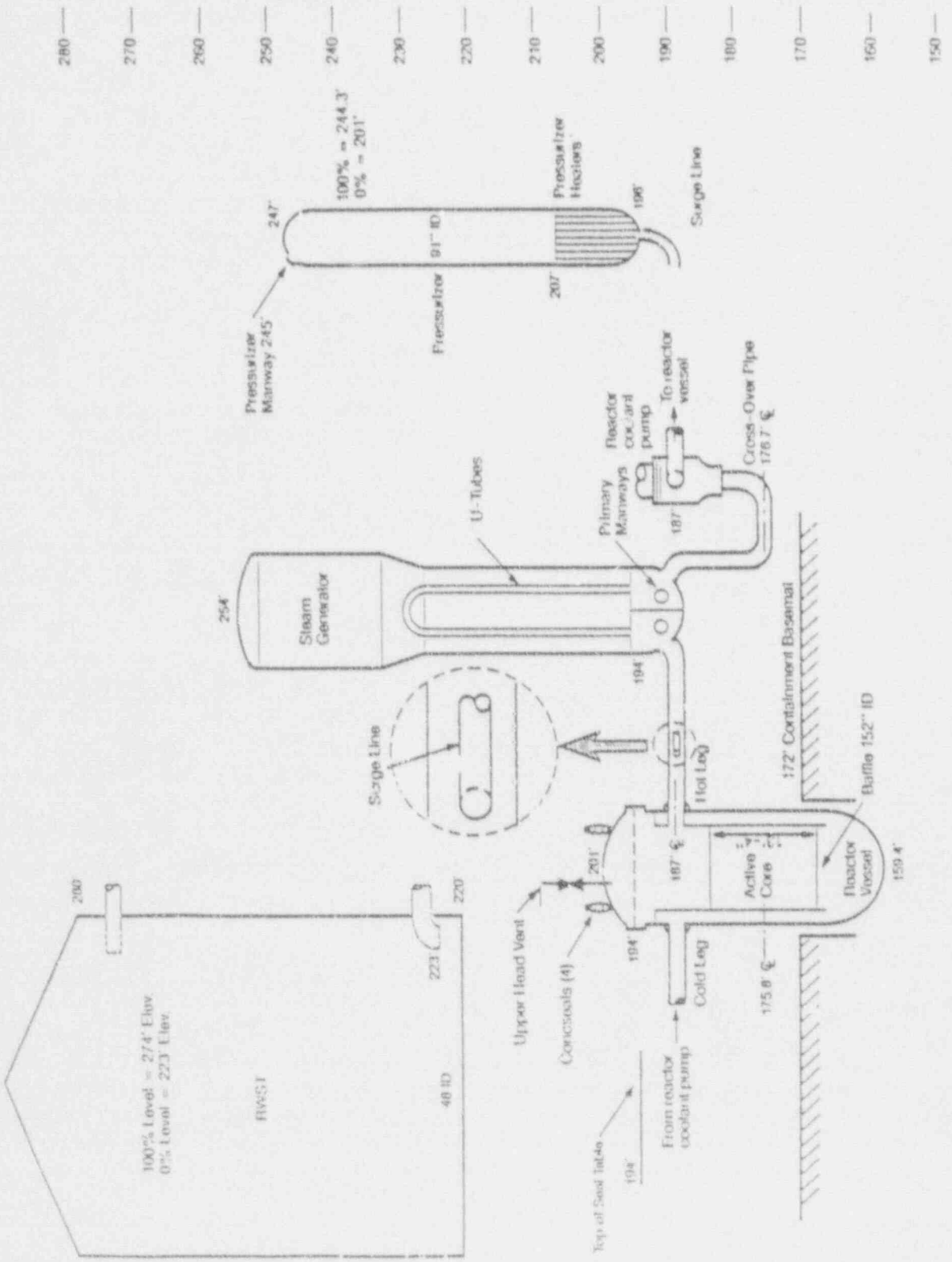

Figure 1. Schematic of Vogtle plant.

mechanisms include reflux condensation cooling and/or gravity feed of water from the refueling water storage tank (RWST). In most cases, the reflux cooling option is available when core boiling cannot be prevented by gravity-feed cooling and when the RCS is closed (i.e., manways and reactor vessel upper head are secured).

This report builds on the analysis provided in Reference 1 by exploring in greater detail the thermal-hydraulic processes and phenomena expected to occur during the cooling modes potentially available following a loss of ac power and RHR. The research support areas were defined in Section III D of the appendix to the NRC's staff plan for evaluating safety risks during shutdown and low power operation.[a] These are

- Systematically examine event sequences that might lead to a loss of RHR cooling. These are addressed in Section 2 of this report.

- Identify and assess sequences that can lead to recovery from loss of RHR events, including natural circulation cooling in pressurized water reactors (PWRs). Controlling processes involved in these sequences and our ability to model them are discussed in Section 3.

- Evaluate the effectiveness of alternate cooling methods including

  - Initiation and promotion of convective core cooling using the refueling water storage tank and accumulators as coolant sources. Example analyses for each vendor plant type is addressed in Section 4.

  - Maintenance of the inventory during core boiling using the refueling water storage tank and accumulators as cooling sources. The analysis of this issue is also presented in Section 4.

  - Initiation and promotion of reflux cooling. This is the subject of Section 5.

a. Private communication from T. E. Murley to J. M. Taylor, October 10, 1990.

2. POTENTIAL PLANT CONDITIONS AND COOLING METHODS

In the event of loss of RHR during plant maintenance or refueling, the reactor has been shut down for many hours or days, the decay heat level is low (relative to power operation), and the plant is either in Mode 5 (cold shutdown) or Mode 6 (refueling) operation. A cold shutdown condition consists of an effective reactivity less than 0.99, no thermal power except decay heat, and an average coolant temperature of 200°F or less. A refueling condition consists of fuel in the reactor vessel, vessel head closure bolts less than fully tensioned or with the upper head removed, an effective reactivity of 0.95 or less, no thermal power except decay heat, and an average coolant temperature of 140°F or less. Core decay heat generally is less than 15 MW, corresponding to approximately 2 days after reactor shutdown. These and, in general, other example data presented are for Vogtle-1, a four-loop, 3411 MW_t, pressurized water reactor of Westinghouse[b] design. Notes are included indicating any classes of plants for which the presented data are not representative regarding response following a loss-of-RHR event.

2.1 Plant Configuration

In the refueling mode, the RCS can be partially drained, and the high point (pressurizer, hot leg, reactor vessel head) vents, which are opened to promote draining, can have nitrogen or air drawn into the upper RCS. If the RCS water level is lower than three feet below the reactor vessel flange, the condition is termed "reduced inventory" operation. Core decay heat is removed by the RHR system that takes suction flow from one or two hot legs, cools the water with a heat exchanger, and returns it through the four cold legs to the core. The status of the containment may be open or closed; openings are possible at many locations.

During maintenance and refueling, the steam generator secondary systems are often in "wet layup" status and are essentially filled with cold water and pressurized to about 5 psig with a nitrogen blanket. For steam generators undergoing maintenance operations, the secondaries may instead be drained.

In addition to vents opened for draining the RCS, other RCS openings often are present during maintenance and refueling outages. These additional openings may include one or more of the following: pressurizer relief valves or manways, steam generator manways, main coolant pump shaft seals, cold leg valves, or the reactor vessel upper head. Reduced inventory operations normally are performed with one or more openings in the RCS; however, a closed system is possible under certain circumstances (for example, in the Vogtle event).[1] A refueling and maintenance outage generally requires about 40 to 80 days, depending on the maintenance required; the reactor vessel upper head is off for about half that time.

The actual RCS water level at reduced inventory operation may vary considerably. For steam generator maintenance operations, nozzle dams may be installed in the hot and cold legs near the steam generator plena. These dams, which can support a differential pressure of 50 psig,[1] may be in one or more coolant loops. There is no restriction on the number of loops with nozzle dams; however, operations at Vogtle are generally performed with nozzle dams in no more than two of its four loops. The presence of nozzle dams reduces the volume of the RCS. This isolated volume typically will contain air and interacts with the containment through open steam generator manways. Nozzle dam failure results in an effective increase in system volume and the potential opening of a flow path to the containment.

b. Mention of specific products and/or manufacturers in this document implies neither endorsement or preference, nor disapproval by the U.S. Government, any of its agencies, or EG&G Idaho Inc. of the use of a specific product for any purpose.

2.2 Possible Scenarios Following Loss of Alternating Current Power and Residual Heat Removal

The process flow chart in Figure 2 shows plant behavior following a loss-of-RHR event. The following discussion pertains to pressurized water reactors employing U-tube type steam generators (i.e., plants of Westinghouse and Combustion Engineering, Inc. design). The expected response of reactors employing once-through steam generators (i.e., plants of Babcock and Wilcox design) is also noted. The initiating event is assumed to be a station blackout (loss of all station ac power, offsite and onsite) that stops operation of the RHR pumps.

Plant behavior is divided into the two main paths shown in Figure 2, one with an open RCS and the other with a closed RCS. If the system is open, early action may allow its closure (as depicted by the dashed line in the figure). This action would consist of securing any open manways or valves. If the reactor vessel head is off, it could potentially be secured, although eight hours or more may be required for this operation. Closure of openings during an event appears unlikely because of increasing coolant temperatures and steam flow through the openings. A closed RCS provides the operators flexibility to maintain core cooling and to maintain it longer if an extended station blackout occurs. Furthermore, if core cooling is lost, a closed RCS provides an additional fission product barrier, increased time before core melt occurs if means for removing heat are not found, potential for heat removal methods exist that may not exist with an open system, and there is an ability to work in the containment building for a longer time following loss of RHR systems.

2.2.1 Open Reactor Coolant System. Consider the upper main path in Figure 2, where the RCS is open. The RCS is open to the containment (through the upper head, manways, etc.) during about half of an average refueling and maintenance outage period. With no ac power available, two sources of borated water for the RCS may be available without offsite assistance: the accumulators and the gravity drain of the RWST. In addition, the makeup water storage tank is a potential source of nonborated water. Offsite assistance in the form of a pumper truck provides a possible additional source of coolant for the RCS. Water may be added to the RWST and, with some reconfiguring of piping, it may be feasible to add water directly to the RCS in a timely manner. Generic plant capabilities in these regards have not been established, but example studies were performed and are detailed in Appendix A.

The status of the accumulators can vary at reduced inventory operation. In general, the accumulators are expected to be depressurized with their isolation valves closed; however, accumulators could also be in a pressurized state. In a four loop plant, accumulator liquid volume is about 3000 ft^3 (22,000 gal). Depressurized accumulators are potential gravity-drain water sources to the RCS in those plants where they are sufficiently elevated (accumulator elevations are plant specific). If fully-pressurized, discharging the accumulators by opening the isolation valves presents a potential control problem. Another possibility for advantageously using accumulators involves a gradual pressurization of the accumulator (using its nitrogen pressurization system) that would result in a controlled transfer of the accumulator water to the RCS.

The second potential source of water for the RCS is gravity-draining from the RWST, which typically contains about 53,300 ft^3 (400,000 gal) of borated water. The elevation of the RWST with respect to the RCS varies, so in some plants gravity feed may not be possible. For the Vogtle plant, only a portion of the RWST is above the top of the pressurizer; therefore, the quantity of water available for gravity feed without an RCS heatup depends on the elevation of the lowest opening in the RCS. For example, if the only opening is the manway on the top of the pressurizer, then the RWST would drain to that elevation and flow would stop. After that time, the remaining RWST fluid could flow into the RCS (a) as a result of an

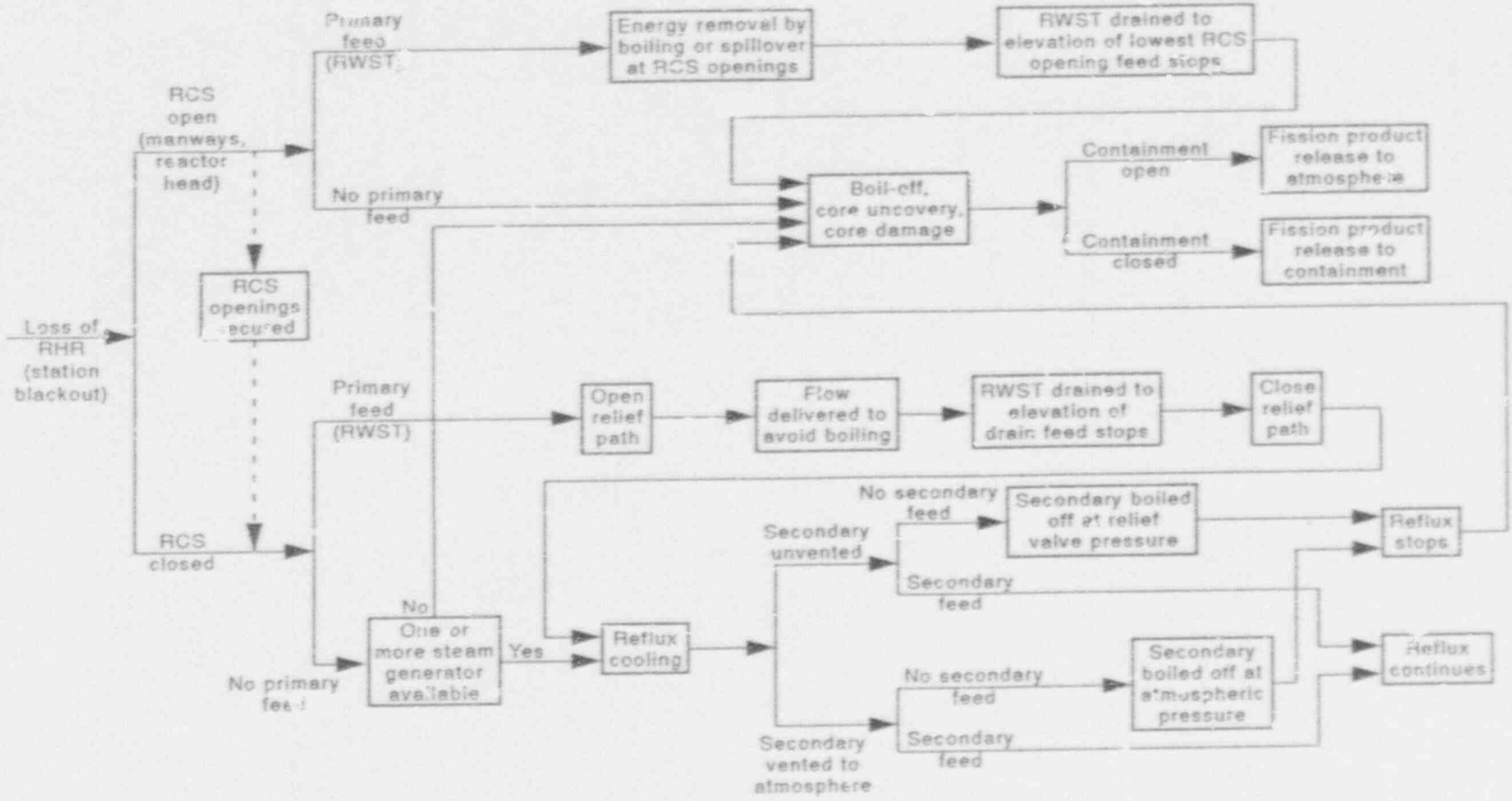

Figure 2. Potential plant conditions and cooling methods during loss of RHR and station blackout.

altered hydrostatic balance as the reactor system fluid is heated, or (b) to replace any core steam expelled through the pressurizer manway. Depending on the situation and plant, it may be possible to open alternate drain paths. This would increase the RWST liquid available for delivery without primary system heatup or control the drain rate, and thus delay RWST depletion. The desirability of employing drain paths in this manner has not been established. It may be possible to control the RWST drain rate to the minimum flow needed to prevent core boiling (thus conserving RWST inventory while eliminating concerns regarding boron precipitation from solution). Example calculations for this potential cooling method were performed for a sample plant from all three U.S. PWR vectors. The results are reported in Appendix A.

As an alternate source of coolant, a pumper truck could inject fluid into the cold legs. The time required to align the necessary plant systems for such operation is not known. The water injected would not be borated. If, during pumper truck injection, core coolant boiling was the only sink for removing water, then the average core boron concentration would remain constant. If a sufficiently large water drain was opened, however, the core boron concentration would decrease because of flushing with the nonborated water. This concern is greatest when new fuel is present because the initial boron concentration is the highest then. For new fuel, it is likely the control rod worth is insufficient to maintain a subcritical core in this situation.

If no water is available to replenish inventory (or if an established source is lost or depleted), then boiling of the core coolant will ensue. With the reactor system open, the size and location of the opening determines whether steam condenses and remains in the system, escapes through the openings, or partially condenses and partially escapes. The boil-off of the core coolant could lead to core uncovering and damage. If the core is damaged and the containment is open, fission products will be released to the environment; with it closed, the release to the environment will not be as likely.

2.2.2 Closed Reactor Coolant System. The closed RCS condition is represented by the lower main logic paths in Figure 2. With the manways and reactor vessel head closed, core cooling may still be accomplished by gravity-draining the RWST into the cold legs. Eventually, when core boiling occurs or when RCS pressure increases sufficiently to stop RWST draining, a drain path must be opened to continue feeding from the RWST. This cooling mode is comparable to that described in Section 2.2.1. If the RCS drain paths are small, the onset of core boiling could rapidly increase system pressure and stop the injection flow. As with the open system, RWST draining will continue until its level reaches the drain path vent elevation where the gravity-driven flow will stop. The necessary operator response will then be to close the hot leg drain paths to completely close the RCS in anticipation of a transition to reflux condensation cooling decay heat removal.

In the reflux condensation cooling mode, core decay heat is removed by boiling; the steam flows to the steam generators where it is condensed on the [illegible] surfaces of the steam generator tubes. The condensate from the upflow side of the [illegible] flows downward, against the upward flowing steam, into the steam generator inlet plenum, hot leg, reactor vessel upper plenum, and back to the core. The condensate from the downflow side of the U-tubes is returned to the cold leg. To be viable, the reflux cooling mode requires that one or more steam generators be operational. In other words, at least one steam generator secondary must contain cold water and nozzle dams must not be present in the hot and cold leg piping of the loop with that steam generator. If one or more steam generators are not operational, then boil-off and core damage might occur.

In Babcock and Wilcox plants (with once-through steam generators), the cooling mode analogous to reflux cooling is the "boiler-condenser" mode, in which condensate is returned to the cold leg and need not flow against the steam flow. The boiler-condenser mode requires that the primary and secondary side coolant levels be situated such that an adequate condensing surface is available on the inside of the tubes. The secondary side level must be sufficiently elevated,

and the primary side level sufficiently depressed, so that both a cooling sink and a steam path to the tubes at its elevation are available. At reduced inventory operation, air will reside in the upper regions of the tubes. Boiler-condenser cooling thus requires this air to be compressed, allowing steam to find a condensing surface inside the upper tube region. The reactor vessel vent valves present in Babcock and Wilcox plants preclude core coolant level depression, relative to coolant levels in the rest of the system, because of system pressurization and static head effects.

Reflux cooling results in the transfer of the decay heat to the steam generator secondary sides. Since the secondary systems are generally isolated and nitrogen-pressurized, continual reflux cooling will result in a heating and pressurizing of the secondary liquid. Although intervention normally would be expected, if valves could not be opened, a closed secondary system would be expected to continue heating (in the extreme, its temperature would reach saturation at the secondary relief valve opening setpoint pressure). To continue condensation, the primary system temperature must exceed the secondary system temperature, and thus the primary system pressure will rise along with the secondary. The primary system pressure increase has the potential to jeopardize the integrity of the RCS (i.e., temporary thimble seals, nozzle dams, and the Tygon tubing used for level instrumentation during outages). With an elevated secondary pressure, operation of the turbine-driven auxiliary feedwater pump is possible. If this pump is started, it can provide feedwater from the condensate storage tank to the steam generators, allowing the reflux process to continue indefinitely. If some feedwater supply cannot be established, the secondary inventory would be boiled off at the steam generator relief valve setpoint pressure. When the secondary inventory was depleted, the reflux process would cease and core boil-off and damage would occur.

Another procedure is to vent the steam generator secondary systems to the atmosphere by manually opening the atmospheric dump valves. This action would limit the heating and pressurizing of the primary and secondary systems. More importantly, however, depressurized secondary systems could allow offsite assistance (for example, a pumper truck) to be used to indefinitely replenish the secondary inventory and continue the reflux process.

To establish reflux cooling, the core boiling must sufficiently pressurize the RCS to compress the nitrogen or air in the upper regions of the RCS to expose a tube condensing surface to the steam flow. Furthermore, the required pressure increase will be a function of various plant conditions such as the decay heat and initial reactor vessel water level. The magnitude of the required pressure rise is significant because the integrity of any nozzle dams, temporary instrument tube thimble seals, and temporary level instrumentation may be challenged. If these plant features fail, then the event sequence is made more complex by the resulting loss of coolant.

The thermal hydraulics of reflux cooling was studied in detail and sample calculations were performed for both U-tube and once-through steam generator plants. Two calculation techniques were used. The first used a calculational tool developed for this purpose at the INEL, and results are reported in Appendix B. The second used the RELAP5/MOD3 code.[c] These results are reported in Appendix C.

---

c. RELAP5/MOD3, Version 5m5.

3. CONTROLLING PROCESSES AND THERMAL-HYDRAULIC PHENOMENA

This section discusses the processes and thermal-hydraulic phenomena that control the cooling methods presented in Section 2, with the intent of indicating the current understanding regarding them. The discussion is separated into three subjects: (a) gravity-drain processes, (b) core boil-off processes, and (c) reflux cooling processes. The specific areas evaluated for each of these processes are shown in Table 1.

3.1 Gravity-Drain Processes

As described in Section 2, for a station blackout loss-of-RHR event, gravity-drain of the RWST is a process with potential to delay core boil-off and damage. RWST gravity draining may deliver core coolant either when the RCS is open [pressurizer power-operated (PORV), manways, pump shaft seals, or reactor vessel upper head] or when it is closed (in which case an RCS drain path eventually needs to be opened). To be effective, all or part of the RWST must be at an elevation above the lowest opening in the RCS. The hydrostatic head of the RWST water forces borated coolant into the cold legs and reactor vessel downcomer, making it available for core cooling. Water heated by the core flows out RCS openings (pressurizer or steam generator manways, reactor coolant pump seals, or reactor vessel upper head) or drain valves and falls to the containment sump. In the Vogtle event, the RWST water level was 76 ft above the hot leg centerline and 16 ft above the pressurizer manway elevation, which is within the normal operating range. Reference 1 indicates that the Vogtle RWST water available above the pressurizer manway is 216,600 gal. Therefore, the RWST is available for gravity-feed in the Vogtle-1 plant. However, RWST elevations relative to the RCS vary from plant to plant. A generic plant survey regarding the capability for RWST draining does not exist, but sample calculations were performed for one plant from each U.S. PWR vendor. Drain rates and durations are reported in Appendix A.

The drain rate required to prevent net core boiling may be readily calculated, given the core decay heat. For the Vogtle event, that rate was 130 gpm. A plant-specific analysis for Vogtle indicates the RWST is capable of providing this drain rate with a small driving head of only 0.8 ft. The drain rate is determined by the driving head and the resistance of the flow path through the injection lines and fittings, reactor core, and leakage paths to the containment. The drain rate therefore will be totally dependent on the elevations of the particular plant and on the losses and flow areas of openings in the RCS. Generic information regarding the period of time that RWST gravity-draining might delay core boil-off similarly is not known. For Vogtle, analysis indicates this period will be 25 hours with the pressurizer manway open. The capabilities, control, and observation of the drain rates were referenced in the Vogtle report.[1] These quantitative results were not incorporated in the Vogtle procedures, although when questioned, the operators were aware of multiple modes of RWST draining (through the chemical volume and control, safety injection, and residual heat removal systems). If the RCS is closed, any one of several suitable drain paths could potentially be opened under blackout conditions. However, a hot leg drain path is preferred since the RWST injection would flow through the core to the RCS opening. Ability to open hot leg drains appears to be limited to the RHR suction piping. If only cold leg drains are available, the RWST fluid will maintain core coverage but will not flow through the core. Instead, the RWST fluid will be bypassed out the drain. Therefore, water boiling is more likely with a cold leg drain than with a hot leg drain.

When the drain rate is sufficient to avoid boiling, the core boron concentration approaches that in the RWST. However, if the water boils, the steam produced does not carry off boron and the core boron concentration increases, providing the potential for boron precipitation. This precipitation could, in the extreme, partially block the core

Table 1. Factors evaluated for controlling processes.

Process	Factors
Gravity drain	Availability in all plants
	Rate needed to avoid boiling
	Actual rates attainable
	If boiling occurs, boron overconcentration
	Control of drain rate
	Instrumentation available
	Drains available
Core boil-off	Time to uncovery and damage
	Heat losses
Reflux cooling	Initiation process
	Horizontal stratification in hot leg
	Two-phase natural circulation
	Steam/air mixing
	Buoyancy, turbulent mixing, diffusion
	Conservatism of "no-mixing"
	Air absorption in condensate
	Humidity within the air
	Core level depression
	Tube flooding
	Hot leg flooding
	Applicable countercurrent flow limiting models
	Loop seal depression
	Primary pressure required
	Nozzle dams
	Temporary thimble tube seals
	Temporary level instrumentation
	Primary coolant pump seals
	Steam generator secondary effects
	Vent availability and effect
	Viability of feedwater processes
	Heatup and boil-off times
	Babcock and Wilcox plants
	No core level depression
	Vent availability and effectiveness
	Adequate condensing surface
	Heating at top of tubes

flow or cover fuel and result in core damage. The Vogtle report[1] estimates that precipitation would not occur until after 10 days of core boiling, based on an initial core decay heat of 2.5 MW. This was only an approximation and more detailed calculations should be performed for this and other scenarios. Also, this concern would arise sooner if the loss-of-RHR event occurred sooner after

reactor shutdown. Conversely, if the RWST is refilled with nonborated water, or some other source of nonborated water is used, the reactivity effect of diluting the core boron concentration must be considered.

If the RCS is closed and the core coolant boils, the rise in system pressure will reduce the flow from the RWST. Some or all of the core steam may be condensed in the steam generators in the presence of air (see discussion of reflux cooling in Section 3.3). However, the interaction between a gravity-driven injection system and a reflux cooling process is not well understood.

In summary, gravity-drain injection involves relatively simple thermal-hydraulic phenomena. However, the significant process variables (for example, elevations and piping lengths) vary considerably from plant to plant, or are dependent on specific event assumptions (system configuration, status of openings, etc.). The interaction of a gravity-drain RWST system with steam generator reflux boiling involves more complex phenomena (unique plant features, coupled manometer considerations, and low system pressures).

3.2 Core Boil-Off Processes

As indicated in Section 2, core water boil-off is a controlling process in situations where (a) feed to the RCS is not available or has been lost, (b) steam generators are unavailable for reflux cooling, and (c) reflux cooling is established but later lost. The boil-off may occur near atmospheric pressure when the RCS is open, or at elevated pressures when it is closed.

The starting point for a loss-of-RHR event is subcooled water in the RCS. Before boiling occurs, the water must be heated to saturation. Reference 1 estimates this would have required 109 minutes for the Vogtle event; however, this time could be much shorter for some events.

During boiling, steam pressurizes the RCS and escapes through any openings. In equilibrium, the pressure rise is that required to force the steam out the vent; the smaller the vent, the higher the resulting pressure. If the system is unvented, the pressure will continue to rise. The limit of the pressurization is the opening setpoint pressure of the pressurizer code safety valves, typically about 2500 psia.

As the core water boil-off progresses, the mixture level will drop into the core. For the Vogtle event, boil-off of the mixture level to the top of the core is estimated to require about 11 hours,[2] but could occur much sooner under some other conditions. Steam cooling of the upper core region will prove effective in limiting the fuel temperature rise for some time thereafter. Eventually, however, the core uncovering becomes deeper, the steam production rate declines, and the steam cooling is ineffective in preventing fuel heatup and damage.

Phenomena involved in the core water boil-off appear to be relatively well understood. Timing will be determined by the initial water inventory, system pressure, core power (the time after shutdown), the core axial power shape, and the openings in the RCS. One uncertainty regards the "best" correlation to use to determine the two-phase mixture level, however this affects only the sequence timing.

Because the decay heats are low, there is a potential for ambient heat loss to be a significant effect during the late stages of a boil-off. During normal operation (with an average coolant temperature of 570°F), typical reactor coolant heat loss is about 2–4 MW. The thermal driving potentials and heat transfer mechanisms for heat loss in a boil-off situation are different than for normal operation. Estimates of the magnitude of such heat losses are reported in Appendix A.

3.3 Reflux Cooling Processes

As described in Section 2, reflux cooling processes are important for delaying core boil-off after a loss-of-RHR system event. The following sections describe various aspects of the reflux cooling process in a closed RCS as it pertains to this event. Section 3.3.1 describes initiation of reflux cooling, and Section 3.3.2 describes possible effects of noncondensable gas (air) in the

upper portion of the RCS. Section 3.3.3 describes the possibility for core level depression effects. Section 3.3.4 discusses steam generator secondary issues affecting reflux cooling, and Section 3.3.5 discusses boiler-condenser considerations unique to the once-through steam generators of Babcock and Wilcox plants.

Reflux cooling calculations under various conditions were performed for both U-Tube and once-through steam generator plants. The results are reported in detail in Appendices B and C.

3.2.1 Initiation of Reflux Cooling. Initiation of reflux condensation cooling depends on the ability of steam, produced by core boiling, to reach condensing surfaces in the steam generator U-tubes. During a plant shutdown condition, the reactor coolant level may be at reduced inventory, with air or nitrogen occupying the upper volumes of the primary system. This air inhibits steam flow from the reactor vessel to the steam generator U-tubes. Important aspects of reflux initiation are (a) the initial reactor coolant water level, (b) the need to establish and preserve horizontal stratification of the liquid in the hot legs, (c) the primary system pressure requirements and limitations, and (d) the possible need to drain or vent the primary system to obtain a stable reflux cooling mode at an acceptable pressure.

Until very recently, initiating reflux from a shutdown reduced inventory operating condition had not been thoroughly examined in reflux experiments with noncondensable gases present. Most existing experiments investigating reflux with noncondensables[4,5,6,7] were initiated from a stable reflux condition by injecting noncondensable gas into the reactor system. A recent experiment in the PKL-III facility,[8] investigating reflux starting from mid-loop operation with noncondensables, showed that refluxing is readily initiated from such conditions with only one steam generator available, a decay heat of 0.7, and 1.0% of full power. Thermal hydraulic systems codes have been used to calculate some reflux phenomena in steam-water systems, but they have simplistic models for the phenomena associated with mixing or stratifying two gas phases (air and steam) that are relevant to this situation. In spite of this, RELAP5/MOD3 was used to calculate such conditions, and global results appear reasonable. These results are reported in Appendix C.

The Vogtle report[1] evaluated the effect of four different primary water levels on the initiation of reflux: top of core, mid-pipe with an uncovered pressurizer surge line, hot and cold legs filled with liquid and air in the upper reactor vessel, and a filled reactor vessel. The first two cases are expected to result in stable reflux cooling modes at relatively low system pressures. It was noted that these cases would be similar to the reflux conditions experienced at Diablo Canyon in April 1987.[3] Hand calculations for the last two cases determined that an intermittent or cyclic refluxing mode was possible as water was forced into and out of the pressurizer, the U-tubes were drained, and condensation occurred in the steam generator U-tubes. Draining or venting may be necessary to control reactor system pressure and/or to obtain a stable refluxing mode similar to the first two cases.

The Vogtle report (Reference 1) noted that none of these initial water levels leads to a core heatup as long as the RCS remains intact (i.e., pressurization or dynamic effects do not affect the integrity of temporary thimble tube seals). Not identified in the Vogtle report is the potential for establishing two-phase net loop natural circulation flow. The initiation of boiling in the core when the vessel is filled with water results in a liquid swell and pressurization that forces two-phase mixture into the pressurizer and steam generator U-tubes. If the liquid in the steam generator tubes reaches the elevation of the steam generator tube U-bends, a buoyancy driven two-phase natural circulation flow over the U-bends will result. Uncertainties or variables associated with the initiation of two-phase net loop natural circulation include the decay heat level, the pressure, the behavior of the flow into and out of the pressurizer, and the flow of noncondensable gas both before and after the initiation of two-phase natural circulation.

Reflux includes horizontal stratification of the liquid in the hot legs. If the steam flow is too high,

horizontal stratification cannot be sustained, and steam may still be able to reach the steam generators through slug or bubbly flow regimes. Scoping calculations were performed using the Taitel-Dukler criteria[9] to determine the threshold for horizontal stratification. Figure 3 presents the results of the calcula[illegible]s at atmospheric pressure for a hot leg water level at mid-pipe and for differing numbers of active steam generators. In practice, a higher hot leg water level usually will be present. Calculations for lower water levels indicate that horizontal stratification exists for all decay heats of interest even if only one steam generator is active. For higher water levels and fewer active steam generators, the likelihood for loss of horizontal stratification increases. Results for these other cases appear in Appendix D.

The presence of noncondensable gases in the steam generator U-tubes impedes the condensation of steam. Primary system pressure increases as necessary to (a) compress the noncondensable gas so that a condensing surface is exposed in the steam generator U-tubes, and (b) provide the primary-to-secondary temperature difference. Reference 3 indicated that if all the noncondensable gas in the primary system during the Diablo Canyon event was isothermally compressed into the steam generator U-tubes, the resulting pressure would be 20 psig. A more reasonable estimate was obtained by considering only those noncondensable gas volumes that must be compressed into the steam generator U-tubes to initiate reflux cooling. One calculation assumed that most of the gas in the pressurizer and pressurizer surge line remained there, while another calculation assumed that these gases also had to be compressed into the steam generator U-tubes. The pressure estimates assumed a two-foot condensation region. The pressure rise needed to initiate reflux was 10 psig. This was obtained by averaging the results of the above two calculations. This value agrees well with the rise in pressure experienced in the Diablo Canyon incident, which was roughly estimated to have been 7 to 10 psi.[3]

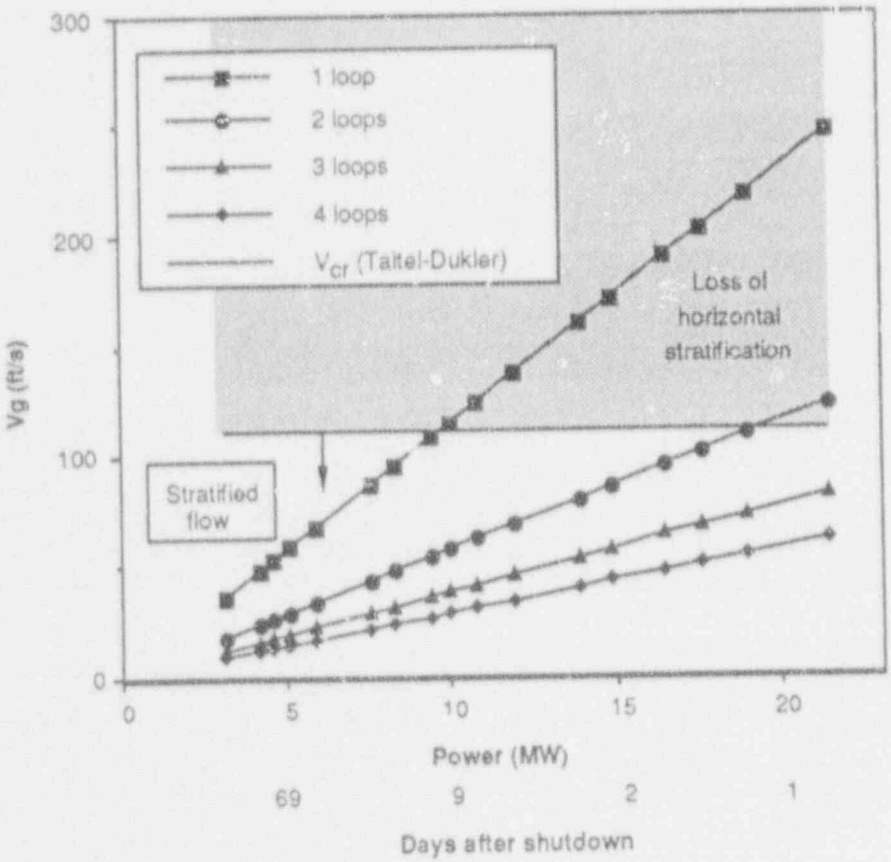

Figure 3. Horizontal stratification behavior in the hot leg.

However, the presence of nozzle dams in one or more primary loops significantly increases the pressure required to initiate reflux (assuming there are no openings in the pressurizer). The nozzle dams effectively reduce the volume into which noncondensable gases from locations outside the steam generator U-tubes must be compressed. Based on an isothermal compression of Diablo Canyon volumes, 18 psig is a rough estimate for the pressure rise necessary to initiate reflux when nozzle dams isolate two primary loops. This value is much closer to the design pressure (25 psig) of the temporary thimble tube seals[1]; therefore, their integrity may be challenged.

Investigation of the different primary water levels[1] indicated the potential need for sufficient vent paths from the primary system that may be used to control primary system pressure or to remove noncondensable gas from the system. Draining might be beneficial if steam flow to the steam generator U-tubes is impeded by a reactor liquid level above the top of the hot leg piping. In this situation, an accurate vessel level indication is needed to interpret plant response. References 1 and 3 discuss problems associated with the reactor vessel level instrumentation system.

In summary, initiation of reflux from mid-loop operation with significant amounts of noncondensable gas in the upper elevations of the primary system required further investigation. The effects of different primary water levels on the initiation of reflux are discussed in Reference 1. Verification of these postulated initiation phenomena was necessary, as well as the consideration of other phenomena such as the initiation of two-phase loop natural circulation under certain conditions. Additional study was needed to determine the pressure rise necessary to start reflux as a function of initial water level and noncondensable gas concentration.

3.3.2 Noncondensable Effects. The primary concern regarding noncondensable gases in plants with U-tube steam generators is gas accumulation in the steam generator tubes that could prevent steam from reaching a condensing surface. The effects of noncondensables on reflux cooling have been investigated in the high pressure (≈1000 psia) Semiscale facility[10,11] and the reduced pressure (≈100 psia) PKL,[5,12,13] FLECHT-SEASET,[6] and EPRI/SRI[7] facilities. Integral test facility data at atmospheric pressure have not been found in the literature. Local or separate effects experiments at atmospheric pressure have been performed.[14,15,16] The noncondensable and reflux experiments in the integral facilities mentioned above were initiated by discrete injections of noncondensable gases after a steady refluxing mode had been established. The problems associated with initiating reflux from a mid-loop operating condition with significant amounts of noncondensables in the upper elevations of the primary loop have not yet been investigated, except for the recent PKL-III experiment.[8]

Experiments indicate that noncondensable gases in the steam generator U-tubes tend to shift the steam condensation region to the lower portions of the upflow sides of the U-tubes. Consequently, the steam generator is divided into "active" and "passive" zones, active meaning steam condensation occurs in that zone. This effectively reduces the primary-to-secondary heat transfer area; therefore, a larger primary-to-secondary temperature difference is needed to remove the core decay heat. For a given steam generator secondary temperature, the primary temperature and pressure must rise to provide this temperature difference.

Reflux cooling is not possible if noncondensables occupy all of the steam generator U-tubes and prevent steam from reaching a condensing surface. For a situation like the Vogtle event, the pressure increase initially required to start reflux may not be sufficient to maintain the condensing surface. Additional noncondensable gas from the reactor vessel may be swept along with the steam to the steam generator U-tubes. Steam is condensed and drained from the tubes, leaving the noncondensable gas behind to further impede the condensation process. This accumulation of additional noncondensable gas in the steam generator U-tubes requires an added pressurization to compress the additional gas volume and maintain an

adequate condensing surface. Reduced-pressure experiments (less than 75 psia) by EPRI/SRI demonstrated that significant amounts of noncondensables may be accommodated by the reactor system in this manner without jeopardizing adequate core cooling.[7] Because of buoyancy, thermal mixing, and diffusion effects, some mixing of steam and air might be expected in this situation.

Challenges to the integrity of the RCS (for example, the temporary thimble tube seals and nozzle dams) could alter the reflux cooling mechanism and limit its effectiveness if openings are sufficiently large.

The noncondensable gas migration and mixing tendencies within the primary loop are important issues. Basic phenomena include the tendency for air to accumulate at the condensation site and for air to be returned to the reactor vessel via absorption into the condensate. Additional phenomena regard the split of the steam-gas mixture flow among the three paths from the core.[3] The first path is into the reactor vessel upper head where venting may be possible through the reactor vessel upper head vent valve and the core bypass flow paths. The second flow path is into the hot leg piping and pressurizer via the surge line. Venting from the pressurizer may be accomplished with the PORVs (some plants do not have these valves, and in others opening them may not be possible at low pressures). The third path is into the hot leg piping and to the steam generator U-tubes. During reflux condensation in a closed RCS, a vent path does not exist in the U-tube steam generators (i.e., the steam generator manways are closed).

The steam-gas mixture flow split among these paths is an important variable for determining the thermal hydraulic response of the system and the potential for vents to remove gas from the system. Note that the first two paths allow venting, while the third path does not. The third steam-gas path provides cooling through reflux condensation, but it may also transport additional noncondensable gas to the steam generator U-tubes and therefore may be self-limiting if tube condensation is impeded.

Buoyancy effects may also play a role in determining the effectiveness of reflux cooling. Air is heavier than steam so the buoyancy effect would tend to promote mixing of steam upward into the air-filled steam generator tubes.

The establishment of reflux cooling during a loss-of-RHR event with the RCS in a mid-loop operating condition was demonstrated at Diablo Canyon on April 10, 1987. It is believed that the steam generators provided cooling in the reflux mode for approximately three quarters of an hour. The primary system pressure increase was estimated at 7 to 10 psi. Most of the steam produced in the core is believed to have been condensed and returned to the reactor vessel. Initially, condensation occurred on the cool walls of the upper reactor vessel. Eventually, the steam reached a condensing surface in the steam generator U-tubes and reflux condensation removed the core decay heat.[3]

The use of thermal-hydraulic system codes to simulate the complex phenomena associated with condensation in the presence of significant amounts of noncondensable gases is not presently defensible because the area of application is well beyond its assessment base. The problem is that there are no models capable of simulating the mixing and/or stratifying of two gas phases that may occur. The mass transfer model in the presence of noncondensable gases also needs to be improved. However the RELAP5/MOD3 code was used to calculated reflux conditions in the H. B. Robinson plant and the global results appear reasonable. The results of this study are reported in Appendix C.

The reflux condensation process is described in detail in Section D-2.1 of Appendix D. The effects of noncondensable gases on the reflux cooling mode are discussed in greater detail in Section D-2.4 of Appendix D.

3.3.3 Core Level Depression Effects.

Three effects that could potentially lead to core level depression are discussed below: steam generator tube flooding, hot leg flooding, and pressurizer surge line flooding.

3.3.3.1 Steam Generator Tube Flooding. The countercurrent flow of steam into the U-tubes and condensate return during reflux cooling has the potential to cause a depression of the core level. On the upflow side of the U-tubes, the upward flowing steam opposes the return of condensate, thus "holding up" liquid within the tubes. On the downflow side of the U-tubes, the steam flow assists the draining of condensate. Any resulting differential liquid inventory between the U-tube upflow and downflow sides provides a hydrostatic head that depresses the core level. This issue is of concern because if the core level depression is sufficient, the upper regions of the core may be uncovered. Flooding has been observed in a number of reflux condensation experiments.[14,15,17,18,19,20,21] Section D-2.2 of Appendix D summarizes the various modes of tube flooding and applicable experiments. Large thermal-hydraulic systems codes generally have the capability of simulating tube flooding phenomena during reflux condensation in steam and water systems. However, current code capability for simulating flooding in reflux processes with air present is questionable.[14]

Previous evaluations of steam generator tube flooding phenomena have regarded system performance following a small break loss-of-coolant accident (LOCA). Plant conditions following a loss-of-RHR event during reduced inventory operation differ in two significant respects. First, for reduced inventory operation, the primary system pressure is much lower than is the case for the LOCA (near atmospheric vs. about 1000 psia). The steam density at atmospheric pressure is much smaller than at the elevated pressure; therefore, for a given steam mass flow its velocity is much higher at atmospheric pressure. This steam density effect tends to promote tube flooding. Second, the core decay heats of interest for reduced inventory operation are much lower than for post-LOCA operation. This decay heat effect tends to reduce the likelihood of tube flooding.

To evaluate the net result of the effects of low steam density and low core decay heat at mid-loop operation on steam generator tube flooding, a calculation was performed. Assuming atmospheric pressure, the Wallis non-dimensional vapor velocity in the steam generator U-tubes was calculated as a function of the core decay heat. A parametric study was added to evaluate the effect of one or more steam generators being unusable for reflux cooling. Details of this calculation are found in Appendix E. The results of the calculation (shown in Figure 4) are significant because they show the nondimensional tube steam velocities to be much lower than the threshold value of 0.5 needed for tube flooding (based on a Wallis-type flooding correlation) for most decay heats of interest. The figure shows that core level depression caused by steam generator tube flooding is only of concern when one steam generator is refluxing, and then only for decay heats greater than about 15 MW (approximately 2 days after shutdown).

3.3.3.2 Hot Leg Flooding. There is a potential for flooding in the vertically-inclined portion of the hot leg. Typically, the hot leg rises about 3 ft from its horizontal elevation to the steam generator. If flooding occurs at this location, then there is a potential to accumulate water in the steam generator inlet plenum or tubes as well. The diameter of the hot leg is large and a Kutateladze-type correlation is more applicable than a Wallis-type flooding correlation for hot leg applications. Because the diameter of the hot legs is much larger than that of the steam generator tubes, hot leg flooding would at first appear to be less likely than tube flooding. However, because the steam generator tube flow area is about three times that in the hot leg, the hot leg velocity is higher than the tube velocity, increasing the relative likelihood of hot leg flooding.

To evaluate the net result of the effects of low steam density and low core decay heat at mid-loop operation (as compared with a post-LOCA situation) on hot leg flooding, a calculation was performed. Assuming atmospheric pressure, the Kutateladze non-dimensional vapor velocity in the hot legs was calculated as a function of the core decay heat. A parametric study was added to evaluate the effect of one or more steam generators being unusable for reflux cooling. Details of this calculation are found in Appendix E. The

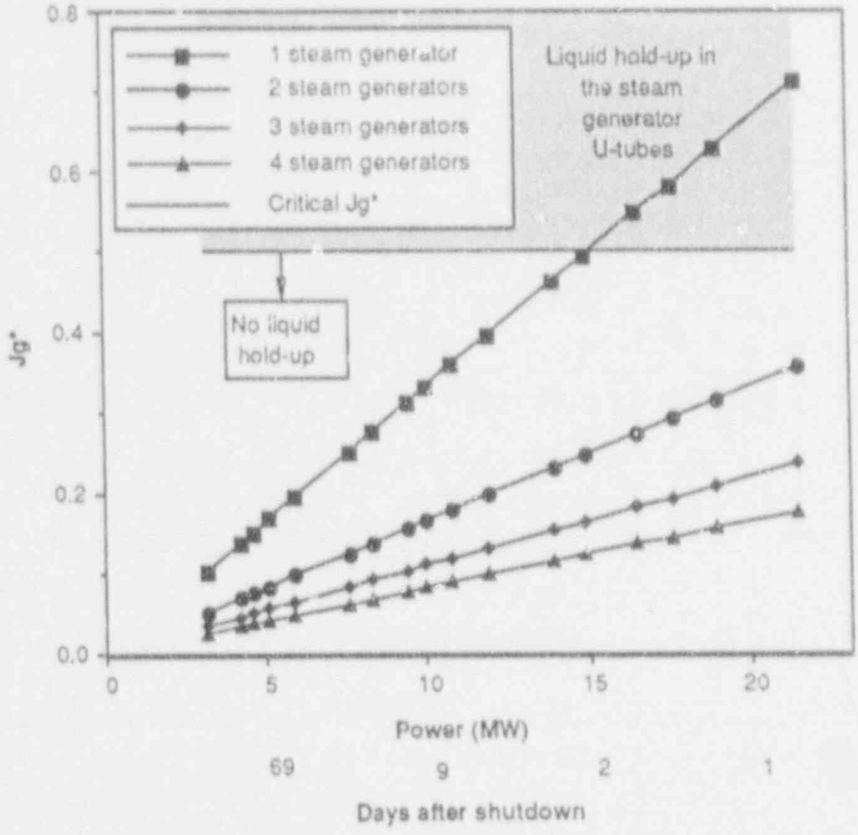

Figure 4. Steam generator tube flooding behavior.

results of the calculation (shown in Figure 5) are significant because they show the nondimensional hot leg velocities to be much lower than the threshold value of 3.2 needed for liquid holdup (based on a Kutateladze-type flooding correlation) for virtually all decay heats of interest. The figure shows that hot leg flooding is only of concern when one steam generator is refluxing, and then only for decay heats greater than about 10 MW (approximately seven days after shutdown). The potential for hot leg liquid holdup from flooding therefore appears to be only slightly greater than for steam generator tube flooding discussed in the previous section. Because this potential is even less at higher primary system pressures, core level depression effects from liquid holdup caused by flooding in the hot legs are not a concern for a loss-of-RHR event as long as two or more steam generators are active.

3.3.3.3 Pressurizer Surge Line Flooding. Flooding in the vertical section of the pressurizer surge line could allow retention of liquid within the line itself and within the pressurizer, an effect that has the potential to depress the core level. Since the pressurizer is air-filled during mid-loop operation, this issue appears limited to situations when there is an opening on the top of the pressurizer, allowing convection of liquid into the pressurizer through the surge line.

To evaluate the possibilities for pressurizer surge line flooding, a calculation was performed. Assuming atmospheric pressure, the Kutateladze nondimensional velocity in the 14-in. diameter surge line was calculated as a function of the core decay heat. A parametric study was added to evaluate the effect of only a portion of the steam production passing to the pressurizer, as might occur in the presence of reflux cooling. Details of the

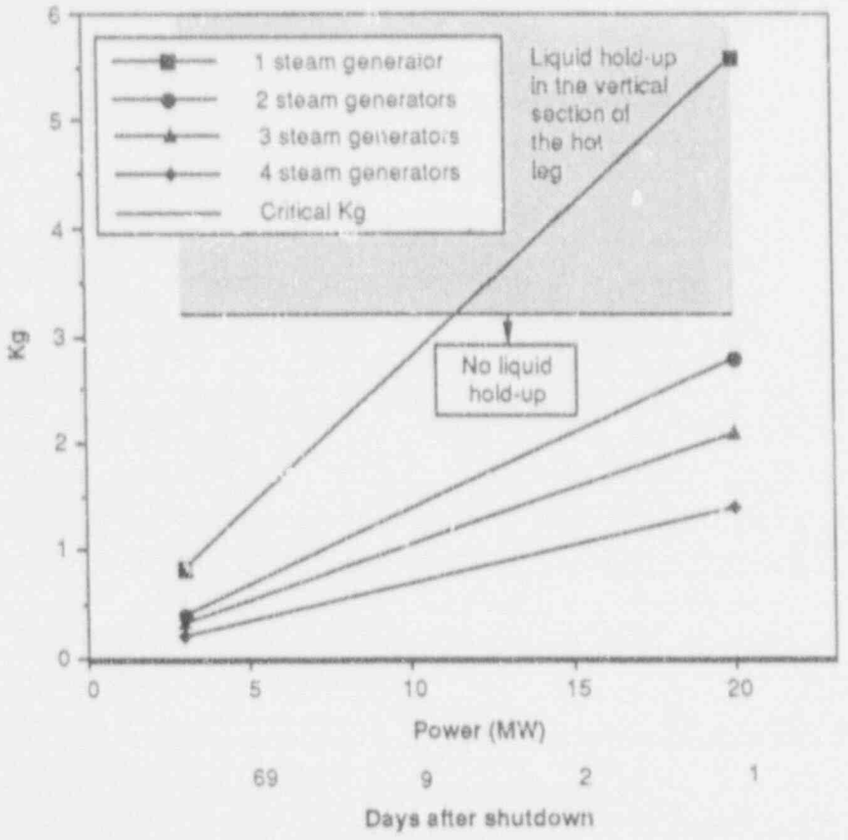

Figure 5. Hot leg vertical section flooding behavior.

calculation appear in Appendix E. Figure 6 shows the results of these calculations, indicating pressurizer surge line flooding is generally to be expected over the decay heat range of interest if the PORV is open. Pressurizer surge line flooding is indicated at decay heats above about 3 MW (corresponding to 100 days after shutdown) if all steam passes to the pressurizer and at decay heats above about 10 MW (corresponding to about 9 days after shutdown) if only 25% of the steam passes to the pressurizer.

Initially, when the RCS temperature reaches the saturation temperature steam flow to the pressurizer should be large, because of condensation on the walls, even with the PORV's closed, and surge line flooding should be expected. Later in time, after the pressurizer walls are heated through condensation of in-flowing steam, surge line flows should be minimal and flooding is not expected. This behavior can potentially cause displacement of liquid into the pressurizer and accompanying RCS inventory reduction. Also the interchange of steam and noncondensables into and out of the pressurizer remains an area of uncertainty and is probably a function of plant specific surge line routing and other conditions. This could affect the final, steady-state RCS pressure reached during refluxing. Further discussion of this is given in Section 5 and Appendix B.

3.3.4 Steam Generator Secondary Issues. Experiments performed during the late 1970's in the low-pressure PKL facility[13] investigated the effects of reduced steam generator secondary inventory on the effectiveness of reflux cooling. The results indicated that the primary-to-secondary differential temperature increased significantly when either (a) the secondary level was lowered, or (b) when noncondensable gases were present within the tubes.

For the loss-of-RHR/station blackout event, reflux condensation is expected to occur in the

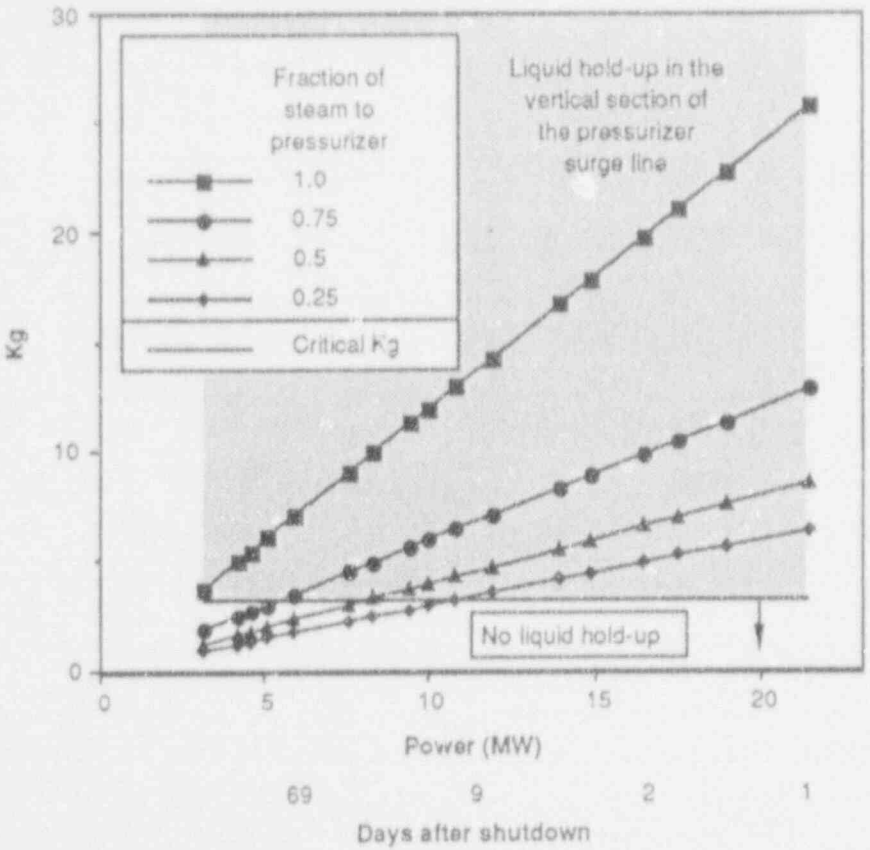

Figure 6. Pressurizer surge line flooding behavior.

lower portion of the steam generator tubes, near the tubesheet. This is the location where steam is most likely to be present, regardless of steam/air mixing concerns. On the secondary side, water will be warmed at the bottom and, because of buoyancy, the secondary side will be well-mixed. Therefore, for this event with U-tube steam generators in "wet layup" (a) the reflux process will be insensitive to the secondary level, and (b) virtually all the secondary-side liquid will be available as a reflux cooling heat sink.

Calculations indicate that for the Vogtle event (core decay heat of 2.5 MW), approximately 4 hours is required to heat up the steam generator secondaries from 90°F to 212°F. At a decay heat rate of 17.1 MW, this time is reduced to 34 minutes. The time required to boil-off all secondary water at atmospheric pressure is 120 hours at a decay heat of 2.5 MW and 18 hours at a decay heat of 17.1 MW. These calculations place into perspective the worth (with respect to delaying core boil-off) of the steam generators as a reflux cooling heat sink.

The venting of steam generators was discussed in Section 2.2.2. If no operator action is taken, reflux cooling heat transfer will heat the secondary fluid, increasing its pressure. The pressure increase raises the saturation temperature and therefore delays the onset of secondary-side boiling. If the secondary system remains sealed, then its pressure could increase to a limiting condition of the secondary safety valve opening setpoint pressure, about 1100 psia. If the secondary side is vented to the atmosphere by manually opening the atmospheric dump valves, then the secondary side pressure will be lower and secondary side boiling will occur sooner.

Based on a limited review, it appears that plant procedures currently do not address secondary-side venting for a Vogtle-like event. Discussions with operators indicate they likely would choose to vent the secondaries early in the event

sequence. Vented secondaries allow the use of low-pressure backup feedwater sources to replace any secondary fluid lost through boiling. Candidate sources for this feedwater include the plant fire protection system and pumper trucks. If such a backup feedwater source is available, the core reflux cooling process could be continued indefinitely. Unvented secondaries would likely preclude use of these low-pressure backup feedwater sources. The higher secondary pressures associated with unvented secondaries would, however, provide a possibility of starting the turbine-driven auxiliary feedwater pump. Secondary side pressures as low as 100 psia may be sufficient to drive the pump. However, control of this pump could be critical because of the low core decay heat. If the secondary side is fed too rapidly, its steaming rate and pressure would fall, perhaps leading to a loss of the pumping capability. Additionally, there are unknowns regarding venting of the secondaries: the ability to open and control valves, and appropriate timing for venting operations.

In summary, operators would likely vent the secondary system if possible. Options for providing feedwater to either vented or unvented secondaries have been examined for three example plants. The results are reported in Appendix A.

3.3.5 Boiler-Condenser Cooling In Babcock and Wilcox Plants. The discussion provided here addresses the differences between the reflux cooling processes described for plants with U-tube steam generators and the analogous boiler-condenser cooling processes present in Babcock and Wilcox designed plants with once-through steam generators. With once-through steam generators, condensate is returned to the cold leg and need not flow against the steam flow. Boiler-condenser cooling during a loss-of-RHR/station blackout event requires the primary and secondary side levels to be situated such that an adequate condensing surface is available on the inside of the tubes. The secondary side level must therefore be sufficiently elevated and the primary side level must be sufficiently depressed so that both a cooling sink and steam path to the tubes at the elevation of that sink are available. The effectiveness of pool boiler condensing heat removal (i.e., to a pool of secondary liquid) has been demonstrated experimentally.[22,23,24]

The secondary-side level requirement would generally be met for the loss-of-RHR event because the steam generators are in wet-layup and are filled with cold liquid virtually up to the upper tube sheet. The primary-side level requirement is also met because the upper regions of the RCS have been drained.

The primary question regarding the effectiveness of boiler-condenser cooling for the event studied here is the ability of core steam to reach the condensing surface in the steam generators. Experimental data for this issue are very limited. High-pressure tests were conducted in the Multiloop Integral System Test (MIST) facility to determine the effects of noncondensable gases, but these tests also included a cold leg break.[22] Low-pressure noncondensable gas experiments were conducted by EPRI/SRI[23] in a facility modeling a Babcock and Wilcox plant. These experiments indicated that noncondensable gas in the steam generator tubes dictated the elevation where the condensation process occurred. Because the steam had been condensed out of a steam/air mixture that flowed into the tubes, high concentrations of noncondensable gas accumulated within the tubes. Since the presence of noncondensables impedes the condensation process, the condensing region may be forced to a higher elevation in the steam generator. Note that this is opposite to the effect observed for the U-tube steam generators where the condensing process tends to occur in the lower regions of the tube bundle.

If the condensation process is unable to remove the core decay heat because of the accumulation of noncondensables, the RCS pressurizes and temperatures will increase and expose more condensing surface. These observations led to the conclusion that the pressure limits of the facility determine the amount of noncondensable gas that may be accommodated.[23] This pressure limit is important, especially because it might affect the

integrity of the reactor coolant pump seals or temporary liquid level instruments.

Because the active condensing region is at the top of the once-through steam generator secondary, warming of the secondary fluid occurs at the top of the boiler region as compared to the bottom of the secondary side in U-tube generators. This difference is significant because thermal stratification is likely in the once-through steam generator secondary side. This stratification effectively reduces the liquid available for use as a secondary heat sink, accelerates the onset of secondary-side boiling, and may aggravate pressurization of the primary system.

A feature of the Babcock and Wilcox plants not available in all plants of other design is the high point vents. These vents are located on the reactor vessel upper head and at the top of each hot leg U-bend (most Westinghouse and Combustion Engineering plants have reactor vessel head vents but none have vents comparable to those on the Babcock and Wilcox hot leg U-bends). These vent paths provide a potential for removing air from the upper regions of the RCS. Note, however, that the effectiveness of the high point vents for purging air from the upper regions of the RCS has not been demonstrated. The vents are opened by solenoid-activated valves that are powered through inverters by the station batteries. The valves therefore could be opened during the early stages of a station blackout event. It is envisioned that the vents would be opened, allowing core steam production to flush air out of the upper regions of the RCS. The vents would then be closed, allowing boiler-condenser heat removal using a pure steam flow to the steam generators. Appropriate timing for these valve operations has not yet been addressed. The vent configuration varies from plant to plant; in some plants, the vents lead to the containment and in others they lead to the pressurizer relief tank.

In summary, once-through steam generator boiler-condenser cooling will likely be established following a loss-of-RHR/station blackout event. The high secondary and low primary levels provide a large condensing surface. Continuation of the condensation process appears to be jeopardized, however, by accumulation of air within the tubes. This phenomenon forces the condensation process higher into the tubes. In the limit, the primary system pressure must rise to expose more condensing surface. This pressure rise may challenge the integrity of temporary closures such as level instruments. The localization of heat removal at the tops of the steam generators effectively limits the secondary heat sink and accelerates the onset of secondary boiling. Generally, the effects of air on the condensation process are not well understood. There appears to be a potential to use the high point vents to purge air from the RCS; however, these vents are quite small and their use in this application has not yet been demonstrated.

4. SUGGESTIONS FOR EVALUATING INDUSTRY CAPABILITIES

This section suggests areas where, based on the discussions in Section 3, additional plant-specific analyses should prove useful for determining industry capability to effectively respond to a loss of the RHR system. Appendix A gives example analyses for one plant from each U.S. PWR vendor.

4.1 Refueling Water Storage Tank Gravity-Drain Potential

The capability for establishing RWST gravity drain needs to be determined for each plant. The major process variables for RWST gravity drain include RWST elevations, geometries and normal water levels, and elevations and sizes of maintenance and refueling primary coolant system openings. These parameters differ significantly from plant to plant.

4.2 Refueling Water Storage Tank Gravity-Drain without Core Boiling

The capability of the flow from the RWST to prevent core boiling has been evaluated for three plants. Process variables evaluated include (a) the driving head between the lowest permitted level in the RWST and the highest reactor coolant vent location, (b) the minimum achievable coolant flow rate from the RWST considering flow resistances throughout the system, and (c) a realistic convective heat transfer rate that exceeds decay heat levels based on coolant temperatures and flow rates.

4.3 Secondary Venting and Options for Replenishing Inventory

The usefulness of venting the steam generator secondary system has been considered. Venting appears to be desirable; however, the capability to do so, proper timing, and appropriate cooldown rates should be ascertained for each plant. The capability to replenish secondary inventory through low pressure sources (if the secondary is vented) or through turbine-driven auxiliary feedwater (if the secondary is unvented) should be confirmed.

4.4 Use of High-Point Vents for Venting Air

Babcock and Wilcox plants include high-point vents on the hot legs and reactor vessel upper head. Most plants of other designs include reactor vessel upper head vents. Since the presence of air impedes the reflux process, the use of high-point vents to flush air from the primary coolant system could be considered, but all such vents are relatively small (approximately one inch).

4.5 Ambient Heat Loss Effects During Core Boil-Off

The ambient heat loss from the reactor system to containment at normal operation is about 2–4 MW and is within the decay heat range of interest. The limits of core cooling by ambient heat loss during a core boil-off was considered and found to be small relative to decay heat levels for reduced inventory conditions.

4.6 Summary of Results from Sample Plant Evaluations

Various drain and vent strategies were examined for the three plants described in Table 2, and a summary of RWST information for each plant is given in Table 3. Unthrottled flow rates from the RWST and the minimum flow required to prevent boiling for the three example plants chosen is given in Table 4, and length of time the RWST could supply cooling is given in Table 5.

Various RCS venting concepts were studied to use in minimizing system pressurization. These concepts prolong potential cooling through

RWST gravity draining. Table 6 summarizes the results for Catawba, Table 7 for Waterford, and Table 8 for Davis-Besse.

To minimize RCS pressure under refluxing conditions, steam generator secondary pressures also need to be minimized. Various secondary venting paths were considered and the resulting secondary side pressures are given in Table 9 for Catawba, Table 10 for Waterford, and Table 11 for Davis-Besse.

Table 2. Summary of plant examples.

Plant name	Vendor	Core power (MW)	Comments
Catawba Units 1 and 2	Westinghouse	3411	Four hot and cold legs with U-tube steam generators
Waterford	Combustion Engineering	3390	Two hot legs and four cold legs with U-tube steam generators
Davis–Besse	Babcock and Wilcox	2772	Raised loop plant with two candy-cane hot legs and four cold legs with once-through steam generators

Table 3. Summary of RWST data.

Plant	Nominal initial RWST–RCS differential elevation head (ft)	Tank cross-sectional area (ft^2)	Nominal capacity at power operations (gal)	Storage tank description
Catawba	66	1,259	363,000	Refueling water storage tank
Waterford	3	3,809	584,000	Refueling storage water pool
Davis–Besse	48	1,735	467,000	Borated water storage tank

Table 4. Summary of hydraulic line loss factors and RWST/RCS flow rates.

Plant	Drain path	R (ft^{-4})	Initial unthrottled flow (lbm/s)	Minimum flow to prevent boiling after 2 days (lbm/s)
Catawba	Single train RWST/RHR line and cold legs	327	230	97
Davis–Besse	Single train RWST/RHR line and vessel	158	276	79
Waterford	RWST/RHR to single hot leg	16	215	96

Table 5. Summary of times to lose RWST/RCS flow.

Plant	Drain path	Estimated time to lose gravity head for unthrottled flow (h)	Estimated time to lose gravity head for throttled flow (h)
Catawba	Single train RWST/RHR/RCS. Fill RCS to the top of the pressurizer manway and spill out. Core boiling is likely to develop before drain flow stops.	3.2	7.6
	Single train RWST/RHR/RCS SG manway is an RCS spillover path. Core boiling is not expected to develop before flow is lost.	4.4	10.4
Waterford	RWST/RHR/single hot leg. There is no RCS spill-out path. Significant core boiloff is not expected to develop until all flow is lost.	0.2	0.4
Davis–Besse	Single train RWST/RHR/RCS fill to center of pressurizer. There is no RCS spillover into containment. It is possible that core boiling will develop before flow is lost.	0.5	1.7
	Single train RWST/RHR/RCS. RCS spill out is through the hot leg to containment sump. Core boiling is not expected before flow is lost.	5.2	18.2

Table 6. Estimated RCS venting conditions after a loss of RHR for Catawba.[a]

Venting configuration	Hours after shutdown			Gravity drain time (h)[b]
	48	83	167	
	Corresponding RCS steady-state pressure[c] (psia)			
SG manway (1)	14.9	14.8	14.8	62.7
SG manway (4)	14.7	14.7	14.7	63.6
Three code safety lines open to containment	23.8	21.9	20.2	29.6
Pressurizer manway through surge line (1)	18.6	17.7	16.9	49.0
PORV (3)	753.1	623.0	507.6	None
PORV (3), upper head vent, and pressurizer vent (assume orifices are removed)	489.7	410.6	337.2	None

a. At 48 hours the saturated steaming rate is 13.2 lbm/s and the initial gravity drain RCS shut off head is 43.5 psia.

b. Drain times are calculated by conservatively assuming maximum steam flow at 48 hours with maximum back pressure at 48 hours.

c. All RCS steady-state pressures are based on the assumption that there is no primary/secondary side heat sink, and that containment pressure remains at atmospheric conditions.

Table 7. Estimated RCS venting conditions after a loss-of-RHR event for Watts Bar.[a]

Venting configuration	Hours after shutdown			Gravity drain time (h)[b]
	48	83	167	
	Corresponding RCS steady-state pressure[c] (psia)			
SG manway (1)	15.1	15.0	14.9	10.0
SG manway (4)	14.7	14.7	14.7	14.7
Pressurizer manway through surge line (1)	20.3	19.0	17.9	None
Pressurizer safety line (1) (assume open to containment)	79.3	68.4	57.9	None
Pressurizer safety line (3) (assume open to containment)	29.0	25.6	22.3	None

a. At 48 hours, the saturated steaming rate is 13.2 lbm/s and the initial gravity drain RCS shut off head is 16.0 psia.

b. Drain times are calculated by conservatively assuming maximum steam flow at 48 hours with maximum back pressure at 48 hours.

c. All RCS steady-state pressures are based on the assumption that there is no primary/secondary side heat sink, and that containment pressure remains at atmospheric conditions.

Table 8. Estimated RCS venting conditions after a loss-of-RHR event for Davis-Besse.[a]

Venting conditions	Hours after shutdown			Gravity drain time (h)[b]
	48	83	167	
	Corresponding RCS steady-state pressure[c] (psia)			
Upper SG manway (1)	16.7	16.2	15.8	87.7
Upper SG manway (2)	15.2	15.1	15.0	97.0
Pressurizer manway through surge line (1)	21.7	20.2	18.9	55.7
PORV (1)	416.4	350.1	288.2	None
PORV (1), high point vent valve (2) (assume orifices are removed)	303.8	256.4	212.0	None

a. At 48 hours, the saturated steaming rate is 10.8 lbm/s and the initial gravity drain RCS shut off head is 35.5 psia.

b. Drain times are calculated by conservatively assuming maximum steam flow at 48 hours with maximum back pressure at 48 hours.

c. All RCS steady-state pressures are based on the assumption that there is no primary/secondary side heat sink, and that containment pressure remains at atmospheric conditions.

Table 9. Estimated steady–state SG secondary pressures after a loss-of-RHR event for Catawba.

Venting configuration	Hours after shutdown		
	48	83	167
	Corresponding SG steady-state pressure (psia)		
One SG with one opened manway	15.1	15.0	14.9
Four SGs, each with one opened manway	14.7	14.7	14.7
One SG with one opened code safety	88.1	75.8	64.1
Four SGs, each with one opened code safety	18.5	17.6	16.9
One SG with one opened PORV	112.7	96.6	81.3
Four SGs, each with one opened PORV	20.4	19.1	18.0
One SG with one opened vent line	928.6	759.6	612.5
Four SGs, each with one opened vent line	184.2	156.6	130.6

Table 10. Estimated steady-state ... nting pressures after a loss-of-RHR event for Waterford.

Venting configuration	Hours after shutdown		
	48	83	167
	Corresponding SG steady-state pressure (psia)		
One SG with one opened manway	15.1	15.0	14.9
Two SGs, each with one opened manway	14.8	14.8	14.7
One SG with one opened code safety	48.9	42.6	36.5
Two SGs, each with one opened code safety	16.0	15.7	15.4
One SG with an opened atmospheric vent valve	164.9	140.4	117.4
Two SGs, each with an opened atmospheric vent valve	24.5	22.6	20.7
One SG with one opened vent line	920.9	753.6	607.9
Two SGs, each with one opened vent line	395.2	332.5	273.9

Table 11. Estimated steady-state SG venting pressures after a loss-of-RHR event for Davis-Besse.

Venting configuration	Hours after shutdown		
	48	83	167
	Corresponding SG steady-state pressure (psia)		
One SG with one opened manway	15.0	14.9	14.8
Two SGs, each with one opened manway	14.8	14.7	14.7
One SG with one opened code safety	58.4	50.6	43.2
Two SGs, each with one opened code safety	20.6	19.3	18.2
One SG with an opened atmospheric dump valve (ADV)	114.8	98.3	82.7
Two SGs, each with an opened ADV	30.7	27.7	24.8
One SG with one opened vent line	1040[a]	1040.0[a]	984.0
Two SGs, each with one opened vent line	612.0	511.3	418.2

a. Dump valve will open at a set point of 1040 psia.

5. REFLUX COOLING STUDY

The thermal-hydraulic response of a nuclear steam supply system (NSSS) with a closed RCS to loss-of-RHR cooling capability is investigated and reported in Appendix B. The specific processes investigated include boiling of the coolant in the core and reflux condensation in the steam generators, the corresponding pressure increase on the primary side, the heat transfer mechanisms on the primary and secondary sides of the steam generators, the effects of air or other noncondensable gas on the heat transfer processes, and void fraction distributions on the primary side of the system. Mathematical models of these physical processes have been developed. The models are validated against available experimental data and are applied to analyses of two typical NSSS plants to estimate the response of the plant to a loss-of-RHR incident.

Sensitivity studies show which thermal-hydraulic parameters are the most important relative to the critical aspects of the plant response. In the case of boiling in the core and reflux condensation in the steam generators, sensitivity studies show that the secondary side pressure/temperature, the heat transfer mode in the primary side, the number of nozzle dams installed, and the behavior of noncondensables in the pressurizer are the most important factors relative to RCS pressure increases. Conversely, the decay heat level and number of steam generators (as long as nozzle dams are not installed in others) has only a second-order effect.

Existing system code (RELAP5 and TRAC-PF1) capabilities in this area were thought to be limited because noncondensable gases are tracked with, and are in thermal equilibrium with, the steam phase. They are therefore not capable of simulating separate migration behavior for steam and noncondensable gas. The significance of this behavior to the overall simulation of refluxing under reduced inventory conditions might not be as important as originally thought since calculations were performed for the H. B. Robinson Plant using RELAP5/MOD3, and the global results (reported in Appendix C) appear reasonable. This is probably because the initial rapid rise in froth level when boiling first occurs in the core and the continued flow of steam from the core (source) to the steam generator tubes (sink) forces the noncondensables into noncondensing regions of the RCS and makes the migration of steam through the noncondensables a non-problem. However, some caution must be taken in that RCS pressures predicted by RELAP5/MOD3 are similar to the lower end of the pressure range predicted using the "Piston Model," and some details of the RELAP calculations do not look realistic (e.g., mass of noncondensables is not conserved). The RELAP5/MOD3 calculations are reported in detail in Appendix C, and will not be repeated here.

A number of calculations were performed for various plant conditions using the "Piston Model" described in Appendix B. Calculations were performed for one U-tube steam generator plant (H. B. Robinson) and one once-through steam generator plant (Oconee). Variables investigated included time after shutdown, RCS inventory, secondary pressure, number of active steam generators, and number of loops containing nozzle dams (H. B. Robinson only). Sensitivity studies investigated the effects of whether steam only or a steam-water mix enters the steam generator tubes, and the distribution of noncondensable gas into and out of the pressurizers. The conditions studied are shown in Table 12 for H. B. Robinson and Table 13 for Oconee. A brief summary of the results is given in Table 14. Detailed results are given in Appendix B.

To further refine the results and more accurately calculate RCS pressures would require currently unavailable experimental data, at least in the area of pressurizer and surge line noncondensable gas behavior. It is questionable whether further refinement is necessary because in a number of cases for U-tube plants, at least instrument thimble seals would be, or are near being, challenged. Since the once-through steam generator plants don't use nozzle dams or thimble seals, their only areas of concern appear to be

level measuring tygon tubing and, in some cases, primary coolant pump seals. However, since pressures calculated are not too different from the various failure thresholds, vendors could potentially propose improved (higher pressure threshold) temporary closures. If that were the case, improved calculational ability would be desirable.

Table 12. Analysis for H. B. Robinson.

Run number	Number of SGs used as a heat sink	Number of SGs with dams installed	Secondary side pressure (psia)	Flow regime on SG tube primary side	RCS water level	Comments
1	1	0	14.7[a]	Two-phase annular	Mid-loop operation	—
2	1	2	14.7	Two-phase annular	Mid-loop operation	—
3	3	0	14.7	Two-phase annular	Mid-loop operation	—
4	1	0	29.4[b]	Two-phase annular	Mid-loop operation	—
5	1	0	44.1[c]	Two-phase annular	Mid-loop operation	—
6	1	0	14.7	Two-phase annular	Core outlet	Shutdown for 48 h
7	1	0	14.7	Two-phase annular	25% of hot leg volume	Shutdown for 48 h
8	1	0	14.7	Two-phase annular	75% of hot leg volume	Shutdown for 48 h
9	1	0	14.7	Two-phase nonannular	Mid-loop operation	—
10	1	0	14.7	Single-phase liquid	Mid-loop operation	—
11	1	2	14.7	Two-phase annular	Mid-loop operation	Pressurizer gas "partitioning," shutdown for 48 h
12	3	0	14.7	Two-phase annular	Mid-loop operation	Pressurizer gas "purging," shutdown for 48 h

a. 1 atm = 14.7 psia.

b. 2 atm = 29.4 psia.

c. 3 atm = 44.1 psia.

Table 13. Analysis for Oconee.

Run number	Number of SGs used as a heat sink	Secondary side pressure (psia)	RCS water level	Secondary boiling time (h)	Comments
1	1	14.7[a]	Mid-loop operation	0	Make-up feedwater available
2	2	14.7	Mid-loop operation	0	Make-up feedwater available
3	1	29.4[b]	Mid-loop operation	0	Make-up feedwater available
4	1	44.1[c]	Mid-loop operation	0	Make-up feedwater available
5	1	14.7	Core outlet	0	Shutdown for 48 h
6	1	14.7	25% of hot leg volume	0	Shutdown for 48 h
7	1	14.7	75% of hot leg volume	0	Shutdown for 48 h
8–12	1	14.7	Mid-loop operation	1,2,2.5,3,3.25	Shutdown for 48 h, no make-up feedwater available
13	1	14.7	Mid-loop operation	0	Pressurizer gas "partitioning," shutdown for 48 h
14	2	14.7	Mid-loop operation	0	Pressurizer gas "purging," shutdown for 48 h

a. 1 atm = 14.7 psia.

b. 2 atm = 29.4 psia.

c. 3 atm = 44.1 psia

Table 14. Pressurizer and nozzle dam sensitivity data.

	RCS pressure (psia)			
	H. G. Kobinson		Oconee	
Condition of pressurizer	1 SG available with 2 dam pairs	3 SGs available	1 SG available	2 SGs available
Gas partition	[illegible]9	8.3	48.8	48.5
No gas exchange	[illegible]0.4	43.4	54.0	53.[illegible]
Gas purge	90.4	52.6	71.4	70.6

6. REFERENCES

1. NRC, *Loss of Vital AC Power and the Residual Heat Removal System During Mid-*Loop Operations at Vogtle Unit 1 on March 20, 1990*, NUREG-1410, June 1990.

2. T. L. Chu et al., *Improved Reliability of Residual Heat Removal Capability in PWRs as Related to Resolution of Generic Issue 99*, NUREG/CR-5015, Brookhaven National Laboratory, May 1988.

3. J. L. Crews et. al., *Loss of Residual Heat Removal System, Diablo Canyon, Unit 2, April 10, 1987 (Augmented Inspection Team Report April 15–21, 29 [illegible] 87)*, NUREG-1269, June 1987.

4. K. Soda and G. G. Loomis, "Effect of Noncondensable Gas on Natural Circulation in the Semiscale Mod-2A Facility," *Proceedings of the International Meeting Thermal Nuclear Reactor Safety, Chicago, Illinois, August 29–September 2, 1982*, NUREG/CP-0027, February 1983.

5. R. M. Mandl and P. A. Weiss, "PKL Tests on Energy Transfer Mechanisms During Small-Break LOCAs," *Nuclear Safety, 23*, March–April 1982, p. 148.

6. L. E. Hochreiter et al., *PWR FLECHT-SEASET Systems Effects Natural Circulation and Reflux Condensation.*, NUREG/CR-3654, EPRI NP-3497, WCAP-10415, August 1984.

7. R. L. Kiang et. al., *Decay Heat Removal Experiments in a UTSG Two-Loop Test Facility*, EPRI NO-2621, Electric Power Research Institute, September 1982.

8. D. E. Palmrose and R. Mandl, "A Model for Calculation of RCS Pressure During Reflux Boiling Under Reduced Inventory Conditions and Its Assessment Against PKL Data," *Nineteenth Water Reactor Safety Information Meeting, Bethesda, Maryland, October 1991*.

9. Y. Taitel and A. Dukler, "A Model of Predicting Flow Regime Transitions in Horizontal and Near Horizontal Gas-Liquid Flow," *AICHE Journal, 22*, 1976, pp. 47–55.

10. G. Loomis, *Summary of the Semiscale Program (1965–1986)*, NUREG/CR-4945, EGG-2509, July 1987.

11. D. J. Shinnock and G. W. Johnsen, "Natural Circulation Cooling in a PWR Geometry Under Accident-Induced Conditions," *Nuclear Science and Engineering, 88*, p. 311.

12. H. Weisshauph and B. Brand, "PKL Small Break Tests and Energy Transport Mechanisms," *Proceedings of the ANS Specialists' Meeting on Small Break Loss-of-Coolant Accidents Analyses in LWRs, Monterey, California, August 25–27, 1981*, EPRI-WS-81-201, 1981.

13. D. Hein and F. Winkler, "A Synopsis of PKL Small Break Tests," *Eighth Water Reactor Safety Research Information Meeting, Gaithersburg, Maryland, October 27-31, 1980*, NUREG/CP-0023, Vol. 2, 1980.

14. Q. T. Nguyen, *Condensation in Inverted U-Tube Heat Exchangers*, Ph.D. dissertation, University of California at Santa Barbara, August 1988.

15. C. Calia and P. Griffith, "Modes of Circulation in an Inverted U-Tube Array with Condensation," *Journal of Heat Transfer, 104*, pp. 769–773, November 1982.

16. D. Hein et al., "The Distribution of Gas in a U-Tube Heat Exchanger and Its Influence on the Condensation Process," *Proceedings of the Seventh International Heat Transfer Conference, Munich, Federal Rep. of Germany, 1982.*

17. M. T. Leonard, "Vessel Coolant Depletion During a Small Break LOCA," EGG-SEMI-6010, September 1982.

18. Y. Kukita et al., "Flooding at Steam Generator Inlet and Its Impacts on Simulated PWR Natural Circulation," *ASME Winter Meeting, December 13–18, 1987,* Fluids Engineering Division (FED)-Vol. 61, Heat Transfer Division (HTD)-Vol. 92.

19. Y. Kukita et al., "Nonuniform Steam Generator U-tube Flow Distribution During Natural Circulation Tests in ROSA-IV Large Scale Test Facility," *24th ASME/AIChE National Heat Transfer Conference, Pittsburgh, Pennsylvania, August 9–12, 198*

20. P. Bazin et al., "Natural Circulation Under Variable Primary Mass Inventories at BETHSY Facility," *Fourth International Meeting on Nuclear Reactor Thermal-Hydraulics, NURETH-4, Karlsruhe, Federal Republic of Germany, October 10-13, 1989,* p. 504.

21. S. D. Rupprecht et al., "Results of the FLECHT-SEASET Natural Circulation Experiments," *Transamerican Nuclear Society, 45,* 1983, p. 460.

22. J. R. Gloudemans, *Multiloop Integral System Test (MIST): Final Report,* NUREG/CR-5395, EPRI/NP-6480, BAW-2066, Vol. 7, July 1989.

23. R. L. Kiang, *Two-Phase Natural Circulation Experiments in a Test Facility Modeled After Three Mile Island Unit-2,* EPRI-NP-2069, October 1981.

24. J. R. Gloudemans et. al., *Once-Through Integral System (OTIS): Final Report,* NUREG/CR-4567, EPRI NP-4572, BAW-1905, September 1986.

Appendix A

Plant Recovery Schemes Including Gravity Drain, Accumulator Injection, and Environmental Heat Losses

CONTENTS

Appendix A

Plant Recovery Schemes Including Gravity Drain Accumulator Injection, and Environmental Heat Losses

A-1. GRAVITY DRAIN ANALYSIS

A-1.1 Introduction

This section presents an approach to evaluate gravity drain alignment schemes for plant recovery following the loss of RHR. Drain alignments using both the RWST and accumulators are considered. For the analysis, it is assumed that the loss-of-RHR event occurs during mid-loop operation.

The following two-step approach is presented to define recovery schemes:

- Conduct a survey to identify possible gravity drain paths that can be aligned in a timely manner
- Employ standard computational methods to quantify gravity drainage flow rates needed to maintain adequate core cooling.

Plant specific data were used to illustrate how the methodology is applied. Three plants were chosen as sample cases and are listed in Table A-1.

The remainder of Section 1 is outlined as follows: Section A-1.2 gives required flow to maintain core at liquid saturation conditions or to match core boiloff. Section A-1.3 surveys the three plants in terms of the potential for refueling water storage tank (RWST) gravity feed alignment. Section A-1.4 uses plant specific data to calculate gravity drain response under differing conditions. Section A-1.5 examines the use of accumulators or flood tanks for plant recovery. Section A-1.6 gives conclusions.

A-1.2 Mass Flow Envelopes to Maintain Core Cooling

This section presents calculations for two envelopes. The first is an estimate of the minimum mass flow rate needed to maintain the core bulk temperature at liquid saturation conditions. The second is an estimate of the flow needed to match the core saturation boiloff rate. Envelopes of the first kind are applicable in situations where liquid inflow is balanced with reactor coolant system (RCS) liquid outflow. These feed and bleed schemes are contingent on available drain paths out of the RCS. Envelopes of the second kind are applicable to feed and boil situations, which are contingent on available RCS steam venting paths.

Table A-1. Summary of plant examples.

Plant name	Vendor	Core power (MW)	Comments
Catawba Units I and II	Westinghouse	3,411	Four hot and cold legs with U-tube steam generators
Waterford	Combustion Engineering	3,390	Two hot legs and four cold legs with U-tube steam generators
Davis-Besse	Babcock and Wilcox	2,772	Raised loop plant with two candy-cane hot legs and four cold legs with once-through steam generators

In practice, such flow envelopes may not be directly usable by plant operators unless appropriate instrumentation is in place and a method of controlling flow is available. Calculating the envelopes was done in two steps:

- A normalized core decay power curve was generated using the 1979 American Nuclear Society (ANS) standard.[1,2]

- A steady-state energy balance was done to estimate mass flow envelopes required to just prevent boiling and those required to just replace water boiled away at a given decay heat.

For steady-state conditions with the core inlet at subcooled conditions, the energy balance can be expressed as

$$m_{drain} = Q(t)/\Delta h \qquad \text{(A-1)}$$

where

m_{drain} = mass flow rate from the drain (lbm/s)

$Q(t)$ = decay power (Btu/s)

Δh = coolant enthalpy change between the vessel inlet and outlet in Btu/lbm

Equation (A-1) was applied to no-boiling and boiling cases. In both cases, the vessel inlet enthalpy was based on an assumed RWST coolant temperature of 70°F. Figure A-1 shows the no-boiling flow envelope with an outlet liquid saturation temperature of 212°F for initial power levels of 3411 and 2772 MW, respectively. In the second case, steady-state boiling is assumed with makeup liquid being converted to saturated vapor. The corresponding flows (Figure A-2) are much lower for the boiling case because of the relatively large latent heat of vaporization. In practice, it would hardly be prudent to try to control the flow to match the boiloff rate.[3] The values shown are mainly useful in establishing a low flow limit to maintain core cooling.

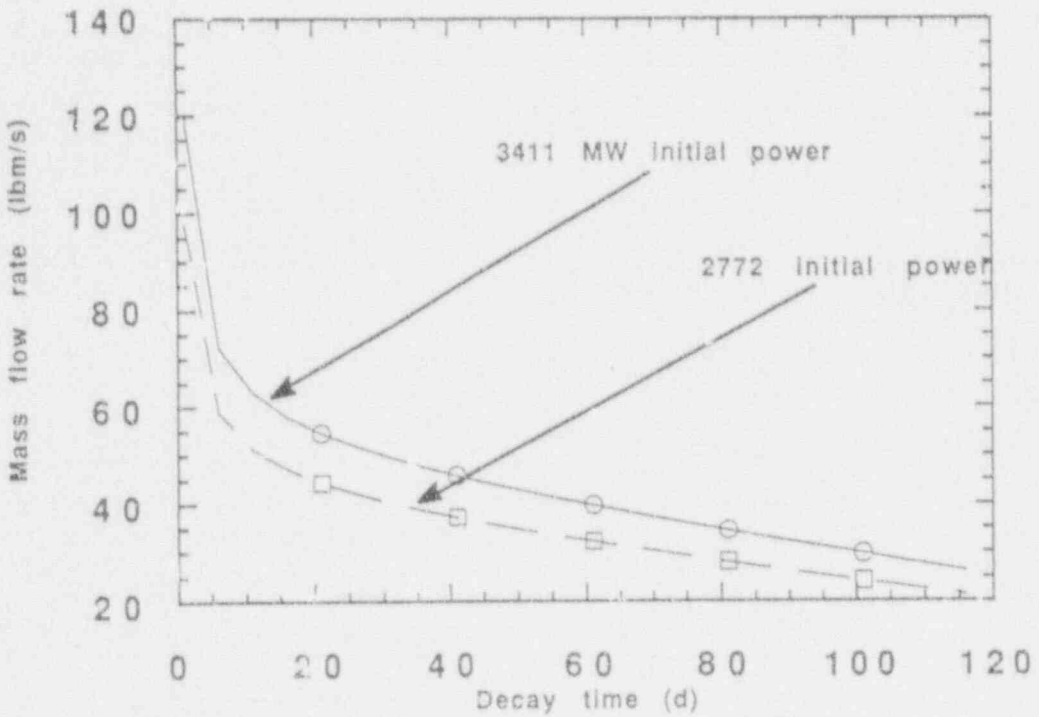

Figure A-1. No-boiling core flow envelope as a function of decay time.

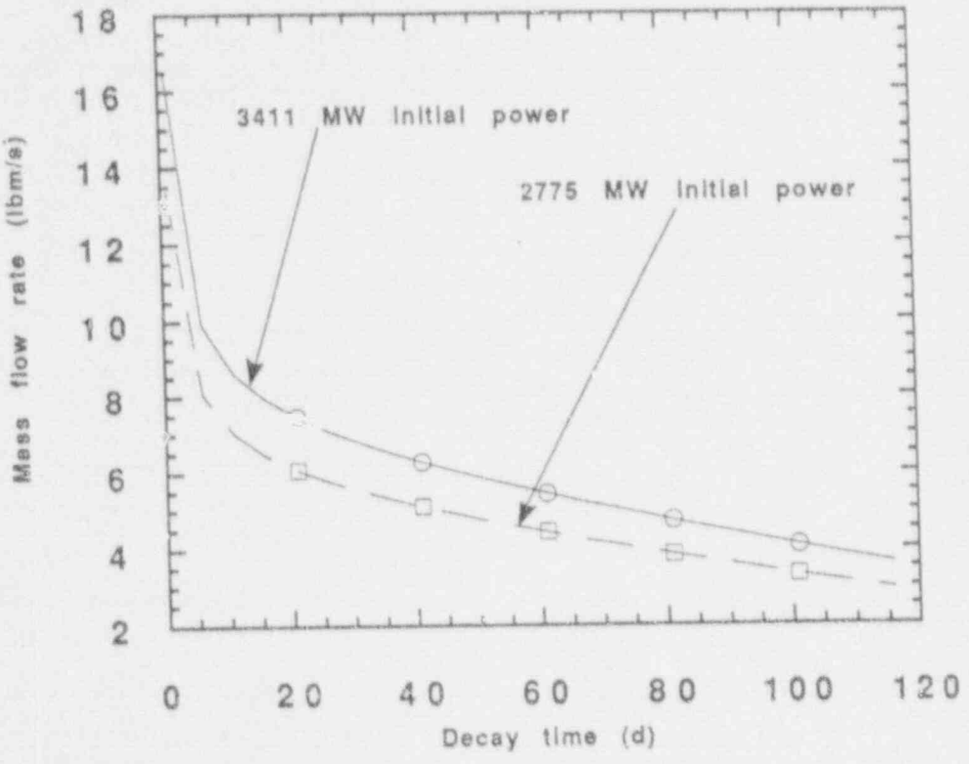

Figure A-2. Boiling core flow envelope as a function of decay time.

A-1.3 RWST/RCS Drain Path Survey

A partial survey was conducted to identify potential gravity drain paths for the three plants. Flow paths from the RWST through piping in the emergency core cooling (ECC) and residual heat removal (RHR) systems into the RCS are considered as plant specific examples. Charging and high-pressure injection (HPI) flow paths are also possible but are generally constrained by high hydraulic resistances. In particular, flow restriction orifices or control valves in these piping trains can significantly limit drainage mass flow rates. Criteria for plausible gravity drain pathways to the RCS system include

1. There must be a net positive differential pressure between the RWST and RCS injection point
2. It must be possible to align the system to allow gravity drain for a particular path from the RWST to the RCS
3. To maintain cooling, a drainage path out of the RCS into the containment building is required
4. The RCS must be adequately vented (such as an open pressurizer manway) to allow for inflowing liquid to displace air or steam out of the RCS (see Section A-2).

The first three criteria are discussed below.

Depending on the particular plant configuration and vendor design, there is a wide range of possible elevation heads to drive gravity drainage through various paths.[3,4,5,6] Differential elevation heads are dependent on the geometry of the RWST, plant operating conditions, and the RWST location relative to the RCS. Typically, the RWST is a large stainless steel tank located outside of the containment building. These tanks are the order of 40 ft in elevation and at full power conditions have nominal capacities that range from 300,000 to 580,000 gal. During refueling operations with the vessel head removed, the RWST system inventory is generally much lower. In this

maintenance mode, much of the RWST inventory has been transferred to the refueling pool.

Table A-2 shows a summary of the relative elevation heads between the liquid level in the RWST and the cold leg centerline for the three plants. These heads were estimated using nominal RWST levels for normal operation and therefore should be considered as "maximum" estimates. The name given to the RWST differs for each vendor, as indicated in Table A-2. In general, there will be some variation in the actual level based on plant technical specifications and other operating conditions. For low power subcritical conditions that occur during RHR cooling modes, the RWST levels can be significantly lower. This variability alone may prevent the possibility of gravity draining. In particular, the level in the RWST tank for the Waterford plant can be below the emergency core cooling system (ECCS) injection cold leg injection point by at least 1.5 ft.

The second criterion is that a viable drainage path exists between the RWST and RCS. Viable means that not only does the path exist, but that the proper alignments can be made to effectively use the path. The latter is much more complex and requires plant specific operational knowledge. The possibility of accomplishing the intended alignment is constrained by the operational characteristics of each drain path component. Such constraints may introduce unacceptable delay times in making an alignment. Some of the more significant constraints include the following:

- Gravity drain alignment could be difficult with a loss of vital ac power because key valves would require manual opening, if they can be opened at all.
- Alignment strategies may result in configurations that conflict with existing plant operational procedures.
- Valves that require manual opening or closing may be located in radiological areas that are not easily accessed by plant personnel.
- Depending on maintenance schedules, certain valves may be down for repairs.
- If an intended gravity drain alignment attempt is unsuccessful, core boiling and significant RCS pressurization may ensue. Under this circumstance, it would be important to isolate any low-pressure systems from the RCS.[a]

a. Failure to isolate low-pressure piping trains such as the RHR lines could lead to pipe ruptures and possible RCS coolant releases into the auxiliary building.[7]

Table A-2. Summary of RWST data.

Plant	Nominal initial RWST/RCS differential elevation head (ft)	Tank cross-sectional area (ft^2)	Nominal capacity at power operations (gal)	Storage tank description
Catawba	66	1,259	363,000	Refueling water storage tank
Waterford	3	3,809	584,000	Refueling storage water pool
Davis-Besse	48	1,735	467,000	Borated water storage tank

- Trip signals could be generated after a loss-of-RHR event that lock certain valves into a configuration that is incompatible with a potential gravity drain alignment.

In the following sample survey, it is shown that there are a number of possible pathways for gravity drainage from the RWST to the RCS. Table A-3 is a summary of the survey findings. With regard to Westinghouse plants, gravity drain alignment schemes with and without vital power have been documented.[3,8] The Table A-3 summary is not an exhaustive list of all possible gravity drain path routes. Generally, the piping pathways between the RWST and the RCS are long and complex. Many of these pathways have a relatively high hydraulic resistance, some in part because of flow restriction orifices or control valves that limit ECCS pump run out.

Figure A-3 shows a generic RWST/ECCS/RCS alignment scheme for a four-loop Westinghouse plant.[9] The Babcock & Wilcox (B&W) and Combustion Engineering (CE) plants have similar configurations between the RWST and RCS.[b] The HPI, RHR, and charging lines are viable drain paths for the Catawba and Davis-Besse plants because of the relatively high RWST/RCS gravity heads. For Waterford, these pathways were judged to be less usable because of the low RWST/RCS differential head. However, Waterford has a low resistance/high mass flow rate pathway from the RWST that connects directly to the RCS hot leg. Gravity drain capacities for some of the above listed pathways are quantified in Section A-4.

As a plant-specific example, consider the low resistance Waterford RWST/RHR/hot leg drain path. Table A-4 presents a component summary for this proposed pathway and Figure A-4 presents a simplified drawing of the pathway. This pathway also contains multiple check valves that are not shown but would allow flow in the desired direction.

One major constraint on this proposed alignment is that the hydraulic containment isolation valve number 3 remains open if there is a loss of vital ac power. Upon loss of vital power, the hydraulic gear drive loses power and the valve tends to drift shut. Once this valve has drifted shut, it becomes extremely difficult to reopen it unless ac power is restored. Thus, timely manual intervention by plant staff is required.

Blanket conclusions cannot be derived from the above example. In some cases, key valve components have backup power systems that allow for operation without vital power. In some cases, a pneumatic system connected to an accumulator tank serves as a backup power supply. Trigger energy to remotely operate these systems is generally supplied from backup dc battery power.

The third criterion mentioned earlier is that an adequate drain path out of the RCS must be established for successful feed-and-bleed decay heat removal. The approach for evaluating potential RCS outflow passageways is similar to that for inflow pathways. Table A-5 is a partial survey of potential RCS drainage path ways for the Catawba, Davis-Besse, and Waterford plants. There are also a host of potential drain paths through the ECCS system into the auxiliary building. Because of radiological concerns outside of containment, these paths were not considered. Depending on the RCS inventory and relative liquid level, many of the openings listed in Table A-5 could also be used for venting purposes in a core boiling mode. This is discussed in Section A-2. The relative effectiveness of an RCS drain path for plant recovery depends on its location relative to the RWST injection location and its size. Relatively large RCS system openings will provide minimal hydraulic resistance and maximum cooling flows when injection and drain locations cause flow through the core. Small drain paths may result in flows too small to meet core cooling needs (see Section A-1.2).

b. One major difference between B&W and Westinghouse or CE ECCS configurations is the accumulator/CFT connections. In Westinghouse and CE plants, the accumulators generally connect to the cold legs. In B&W plants, the CFT discharge lines are connected to the vessel.

Table A-3. Summary of potential gravity drain paths.

Plant	Gravity drain path	Number of trains available	Comments
Catawba	RWST/RHR/cold leg	2 trains with each train splitting to 4 cold leg injection points	Moderate resistance path with flow restriction orifices
	RWST/HPI/cold leg	2 trains with each train splitting to 4 cold leg injection points	High resistance path with flow restriction orifices
	RWST/chemical and volume control system (CVCS)/cold leg	2 trains into 2 cold legs	High resistance path with flow restriction orifices
	RWST/RHR suction/hot leg	1 path that splits to 2 hot legs	Direct low resistance path that bypasses pump and heat exchangers (is most direct pathway to the RCS)
Davis-Besse	RWST/RHR/vessel	2 trains to 2 vessel upper plenum injection points	Moderate resistance path with flow restriction orifices
	RWST/HPI/cold leg	2 trains with each train splitting to 4 cold leg injection points	High resistance path
	RWST/CVCS/cold leg	2 trains to 2 cold leg injection points	High resistance path
Waterford	RWST/hot leg	1 path to each hot leg	This is a direct low resistance path
	RWST/HPI/cold leg	2 trains with each train splitting to 4 cold leg injection points	High resistance path (system has 1 standby HPI pump)
	RWST/RHR/cold leg	2 trains connect with each splitting to 4 cold leg injection points	Moderate resistance path with flow control valves

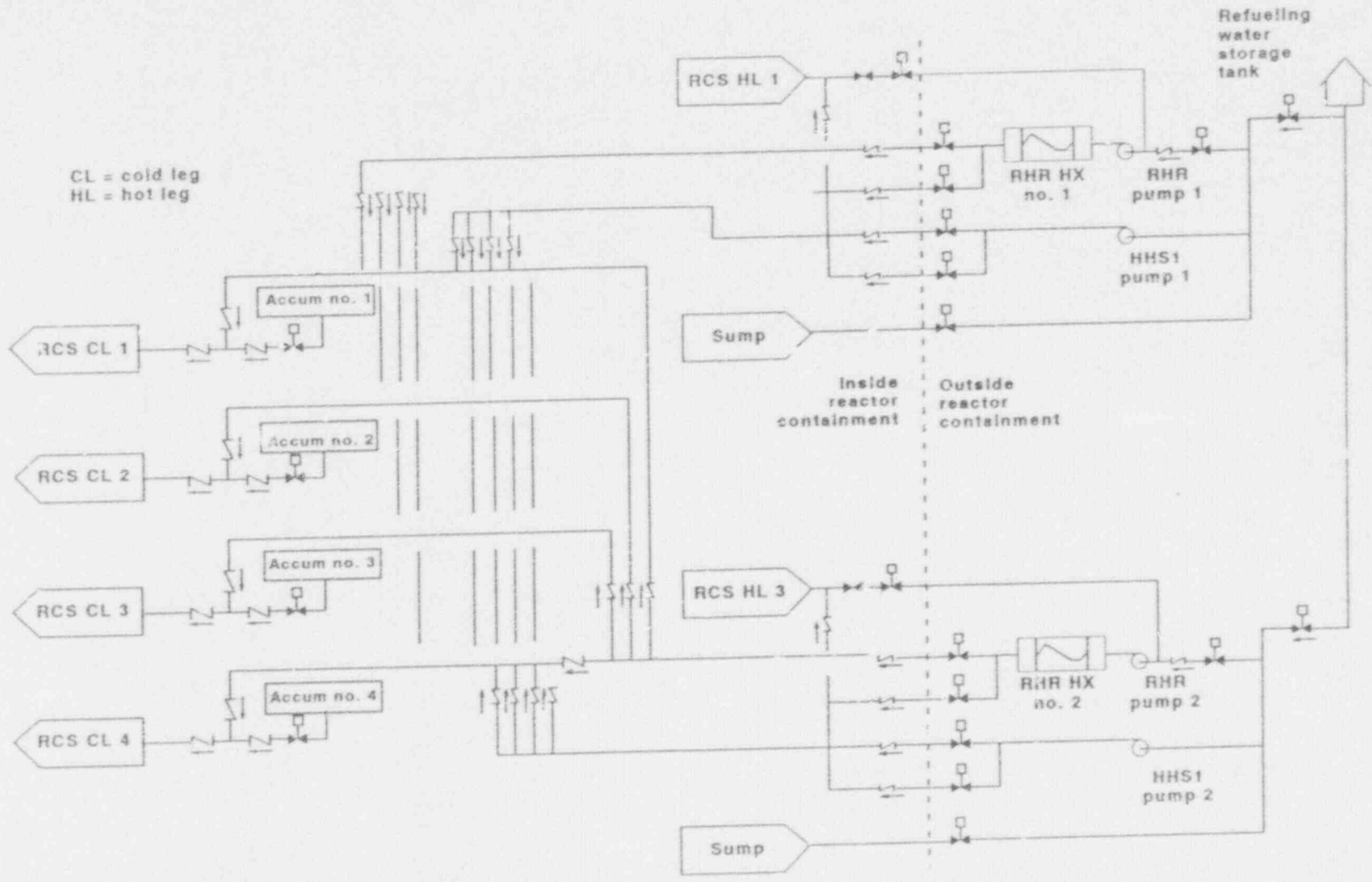

Figure A-3. Westinghouse ECCS/RWST flow path schematic.

Table A-4. RWST/RCS component summary for Waterford.

Valve number identifier (from Figure A-4)	Valve type	Failure mode upon loss of ac power	Comments
1	Manual globe valve	None	During mid-loop operation, this valve is closed to prevent inadvertent RWST drainage Personnel may be able to adjust the valve to throttle RWST flow
2,4	Motor-operated globe valves	Fail in existing position	During mid-loop operation, these valves are open
3	Hydraulic-operated globe valve	Fail in existing position	Loss of ac power will cause the valve drive mechanism to drift shut

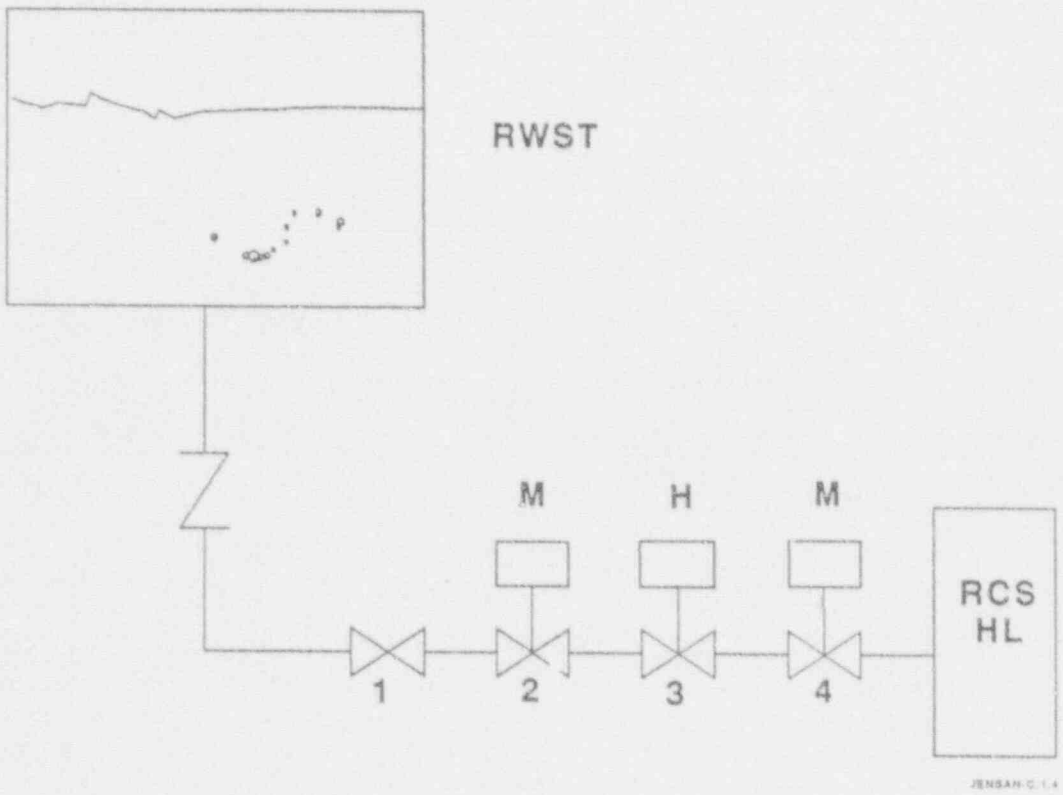

Figure A-4. Waterford RWST/HL gravity drain path.

Table A-5. Summary of RCS outflow paths.

Plant	Drain path	Number of paths available	Comments
Catawba	Primary steam generator manways (two per steam generator)	8	Steam generator nozzle dams may block this pathway.
	Pressurizer manway	1	Because of the small RWST/pressurizer manway differential head, this pathway will result in only partial drainage of the RWST.
	Pressurizer power-operated relief valve	3	Can be remotely opened with or without loss of vital power. May not drain to containment if quench tank is closed. Because of limited quench tank volume, this will inhibit long-term drainage. Its high elevation will also limit drainage.
	Pressurizer safety lines	3	The spring-loaded safety valves may be removed for maintenance. These lines may be temporarily opened to containment. High elevation will also limit drainage flow.
	Letdown line to hold up tanks	2	Some valves on letdown line may fail shut if vital power is lost. It is a time-consuming task to manually open valves on this line.
	Hot leg to sump intake line	2	If loss of vital power occurs, a motor-operated valve located in an encapsulation container must be accessed and opened, which is a time-consuming effort.
	Hot leg to sump bypass line	2	There are 1-inch bypass lines around the motor-operated valves in the encapsulation containers. These valves can be manually opened. Drainage flow is expected to be small.

Table A-5. (continued).

Plant	Drain path	Number of paths available	Comments
Catawba	Hot leg/RHR drain and vent lines to containment	2	These drain and vent lines are connected to the RHR lines coming off of the hot legs. The drain lines are 0.375 inch orificed 2-inch lines that drain directly into containment. The vent lines are 0.375 orificed 3/4-inch lines. These vents and drains can be manually opened on loss of vital ac power.
	Hot leg resistance temperature detectors bypass manifold vent and drain lines	20	The twelve 1-inch drain and eight 3/4-inch vent lines are 0.375 orificed and go directly into containment. These lines could be opened manually if vital ac power is lost. Drainage mass flow rates are expected to be small.
Davis-Besse	Primary steam generator manways (two per steam generator)	4	One at each inlet plenum and outlet plenum of each once-through steam generator. The inlet plenum is too high to be a practical drain opening. The outlet plenum can drain through the cold leg, which may cause core bypass problems.
	Pressurizer manway	1	Because of the low RWST/RCS differential head liquid drainage out, this entrance is not expected.
	Hot leg RHR to containment sump	2	if loss of vital power occurs, a motor-operated containment isolation valve located in an encapsulation container must be accessed and opened. This is a time-consuming effort.
	Letdown line to rad waste tank	4	This is a high resistance, low flow, 2-1/2 inch line connected to each cold leg. These may be difficult to manually align if vital power is lost.

Table A-5. (continued).

Plant	Drain path	Number of paths available	Comments
Waterford	Steam generator manways (two per steam generator)	4	Because of the low RWST/RCS differential head liquid drainage out, this opening is not expected.
	Pressurizer manway	1	Because of the low RWST/RCS differential head liquid drainage out, this opening is not possible.
	Hot leg to sump	2	Blocked by check valves.
	Hot leg to reactor drain tank	2	This 1-inch line connects to the RHR piping and flows into the reactor drain tank. Because of the small drain tank volume, this path way is not expected to be practical.
	Letdown line to hold-up tanks	1	This high resistance path is not available if vital ac power is lost.

A-1.4 RWST/RCS Drain Scoping Calculations

The principal parameters needed to estimate gravity drain flow rates are the hydraulic line losses, the geometric features of the RWST and RCS, and the initial differential pressure head. There is a wide plant-to-plant variation in these parameters and corresponding gravity drain rates.

An approximation technique for estimating RWST/RCS hydraulic line losses relies on direct methods that draw from a known data base of hydraulic information to calculate a total line loss resistance factor. This approach uses the following data:

- Pipe diameters, lengths, and friction factors
- Bends and elevation changes
- Valve and orifice form loss factors
- Pump rotor resistances, locked or freely spinning.

For a gravity feed train composed of piping of variable sizes and lengths and interconnected valves and bends, the total frictional pressure drop is given as

$$\Delta P_{floss} = \dot{m}^2 \sum_{i=1}^{n} (K_i + f_i l_i/d_i)/\left(288\varrho g_c A_i^2\right)$$

$$= \dot{m}^2 R/(288\varrho g_c) \qquad \text{(A-2)}$$

where

$\dot{m}$ = mass flow rate (lbm/s)

K_i = local form loss factor for a specific valve, orifice, pipe bend, etc.

f_i = friction factor for a particular pipe

l_i = corresponding component length (ft)

d_i = corresponding hydraulic diameter (ft)

ϱ = RWST liquid density (lbm/ft^3)

g_c = gravitational constant (32.2 lbm-ft/lbf-s^2)

A_i = flow area for a particular component or piping length (ft^2)

R = lumped piping train resistance, which equals

$$\sum_{i=1}^{n} (K_i + f_i l_i / d_i) / A_i^2 \qquad \text{(A-3)}$$

Once a line resistance factor has been calculated, an estimated mass flow drainage rate can be calculated by equating the total frictional pressure drop, ΔP_{floss}, with the total differential pressure, ΔP_{diff}, between the RWST and RCS. Using Equation (A-2) and solving for the initial drainage mass flow rate gives

$$\dot{m}_{drain} = (288 g_c \varrho \Delta P_{diff} / R)^{1/2} \qquad \text{(A-4)}$$

Equation (A-4) was used to estimate maximum initial gravity drain rates with the elevation data in Table A-2. The magnitudes of the initial drainage flows (each case assumes one pipe train) are summarized in Table A-6. In these calculations, it was assumed that the RCS was at mid-loop conditions, and that the RCS and RWST system pressures were at atmospheric conditions. Also shown for comparison are the flow rates required to prevent boiling if feed-and-bleed commences two days after shutdown. In all cases, the unthrottled flow rate exceeds the no-boiling minimum flow rate.

The initial mass flow rates into the RCS will decrease if the RCS pressure rises above atmospheric pressure. Figure A-5 shows unthrottled mass flow rates for a single train as a function of RCS back pressure for the Catawba, Davis-Besse, and Waterford plants, respectively. For a given decay power, the data in Figure A-5 can be used in tandem with the flow envelopes presented in Figures A-1 and A-2 to estimate maximum RCS back pressures and still avoid core boiling or uncovery. For instance, consider the Davis-Besse plant with 40 days of decay power. From Figure A-2 we need on the order of 40 lbm/s to maintain subcooling. From Figure A-5, the RCS back pressure can be as high as 20 psig and still accommodate core subcooling.

Although initial gravity drain mass flow rates can be more than adequate to cool the core, as time progresses these flow rates will decay as the liquid level in the RWST drops. Knowing these decay times is an important factor in predicting times to core damage if recovery procedures cannot be implemented. RWST/RCS flow can be lost because (a) the RWST level has dropped to reach hydrostatic balance with the RCS, (b) the RWST

Table A-6. Summary of hydraulic line loss factors and RWST/RCS flow rates.

Plant	Drain path	R (ft^{-4})	Initial unthrottled flow (lbm/s)	Minimum flow to prevent boiling after 2 days (lbm/s)
Catawba	Single train RWST/ RHR line/cold legs	327	230	97
Davis-Besse	Single train RWST/ RHR line/vessel	158	276	79
Waterford	RWST/RHR/to single hot leg	16	215	96

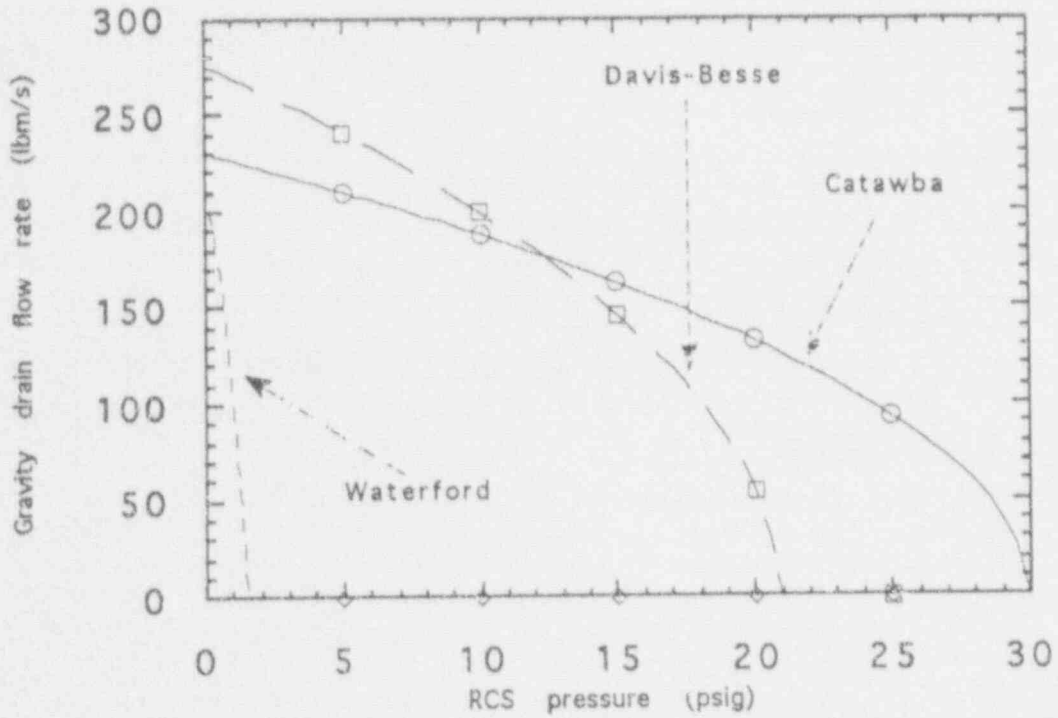

Figure A-5. Unthrottled RWST gravity drain flow rates as a function of RCS pressure.

has become empty, or (c) boiling begins coincident with a lack of RCS venting so that the RCS pressurizes above the RWST/RCS hydrostatic head shut off point. In the following examples, the RCS system pressure was assumed to be maintained at atmospheric conditions (if adequate RCS venting was available). Various differential heads and assumed RCS spill-out points were examined. In situations where RCS spill-out points were not available, the time to loss of RCS/RWST flow is relatively short. If spillover openings are available or if the flow can be throttled, the flow time becomes significantly longer.

Cross-sectional areas of the RWST are significantly larger than the average cross-sectional area of the RCS. As a consequence, several feet of liquid from the RWST can lead to significant refill of the RCS. Cross-sectional RWST data were summarized in Table A-2 for the Catawba, Davis-Besse, and Waterford plants. From the table, we note these areas are on the order of 2000–4000 ft^2. In contrast, the RCS cross-sectional areas are on the order of 100–120 ft^2. Thus, a small drop in the RWST has the potential of significantly raising the level in the RCS if the initial RWST/RCS differential head is large.

Estimating times for volumetric displacement changes in the RWST are calculated using the following approximation[10,11]:

$$t_{loss} \approx \Delta M / m_{avg} \qquad \text{(A-5)}$$

where

ΔM = mass displaced from the RWST into the RCS between the initial and final RWST/RCS differential head (lbm)[c]

c. Calculating the precise volumetric displacement from the RWST to the RCS is complicated by the fact that the RCS volume is not uniform with respect to RCS elevation changes.

m_{avg} = average mass flow rate between the corresponding initial and final differential RWST/RCS differential heads (lbm/s).[d]

The above approximation was applied to estimating RWST/RCS flow loss times with and without RCS spillover openings. The results are summarized in Table A-7. All throttled flows are based on the minimum cooling requirements for two days after shutdown to initially maintain the core just below boiling conditions (see Figure A-2). Whether it is practical to throttle the RWST/RCS flow is an operational matter that cannot be addressed here. Times to core damage may occur at significantly earlier times than the RWST/RCS flow loss times if the flow drops below the minimum core cooling flow rate for an extended time period.

As an example, consider the Waterford plant that is initially in a well vented mid-loop cooling configuration at atmospheric pressure, with a differential RWST/RCS head of 3 ft. Following a loss-of-RHR event coincident with a loss of vital power, how long will it take to reach a hydrostatic balance between the RCS and RWST and terminate gravity drain flow? Using the above formula, the time to lose complete gravity drain for unthrottled flow is about 12 minutes. In this circumstance, it was assumed that there was no RCS spill-out point available to help prolong RWST/RCS gravity drain. If the drain flow is assumed to be throttled to initially match minimum subcooling requirements (this may be impractical), the decay time is about 24 minutes.

If the initial RWST/RCS gravity head is large, the flow loss time for both throttled and unthrottled flow conditions becomes significantly longer. In the case of Catawba, using the steam generator manway spillover path, the loss time for unthrottled and throttled flow conditions are 4.4 and 10.4 hours respectively. In the case of Davis-Besse, using a postulated hot leg/RHR/containment spillover path, the loss times for unthrottled and throttled flow conditions are 5.2 and 18.2 hours, respectively. In the above two drain schemes, the final differential heads before the RWST has drained still yield flows large enough to sustain significant core cooling. This is because the bottom of the RWST is well above the corresponding RCS spillover locations.

A-1.5 The Potential Use of Accumulator Injection

There are possible scenarios where accumulators or core flood tanks (CFTs) may be used as an auxiliary source of short-term core cooling. During mid-loop operation the accumulators are generally isolated from the RCS by closing motor-operated valves on the discharge lines between the tanks and RCS. In general, it is possible to manually open these isolation valves if there is a loss of vital power. Depending on the plant, the isolated accumulator/flood tanks can remain pressurized or be depressurized. Maximum pressures, depending on the plant, range from 200–650 psig. If the accumulators or CFTs are pressurized, it is not likely that an attempt would be made to manually open the discharge line isolation valves. Therefore, this scenario will not be considered further.

Table A-8 shows a summary of the accumulator/flood tank characteristics for the Catawba, Waterford, and Davis-Besse plants. Table A-9 shows the estimated initial flows and times to loss of flow for each of the plants. The flow rates and times were calculated as previously described in A-1.4, in which the RCS remains at atmospheric pressure, an adequate spill path exists, and the flow is unthrottled.

Developing a strategy to throttle and monitor flow from the accumulator or CFT lines is complicated by several operational issues, including

- Controlled injection of accumulator or CFT liquid into the RCS is complicated by a lack of direct flow instrumentation.

d. If the RCS and RWST reach a hydrostatic balance, the final drain flow rate is zero. If the bottom of the RWST is well above the RCS drain-out point, the final flow rate at the instant the RWST empties can still be very large.

Table A-7. Summary of times to lose RWST/RCS flow.

Plant	Drain path	Estimated time to lose gravity head for unthrottled flow (h)	Estimated time to lose gravity head for throttled flow (h)
Catawba	Single train RWST/RHR/RCS. Fill RCS to top of pressurizer manway and spill out. Core boiling is likely to develop before drain flow stops.	3.2	7.6
	Single train RWST/RHR/RCS steam generator manway. This manway is an RCS spill over path. Core boiling is not expected to develop before flow is lost.	4.4	10.4
Waterford	RWST/RHR/single hot leg. There is no RCS spill out path. Significant core boiloff is not expected to develop until all flow is lost.	0.2	0.4
Davis-Besse	Single train RWST/RHR/RCS fill to center of pressurizer. There is no RCS spill over into containment. It is possible that core boiling will develop before flow is lost.	0.5	1.7
	Single train RWST/RHR/RCS. RCS spill out is through the hot leg to containment sump. Core boiling is not expected before flow is lost.	5.2	18.2

Table A-8. Summary of plant accumulator or CFT operational characteristics.

Plant	Can accumulator or CFT system be pressurized during mid-loop operation with loss of vital power?	How accumulator or CFT is isolated during mid-loop operation	Nominal set point pressure at full power operation (psig)	Can isolation MOV be opened if there is loss of vital power?
Catawba	Yes	With MOV	400	Yes
Waterford	No	With MOV	600	Yes
Davis-Besse	Yes	With MOV	600	Yes

Table A-9. Summary of plant accumulator/flood tank characteristics.

Plant	Number of tanks	Nominal liquid inventory per tank (gal)	Maximum initial flow rate for unpressurized accumulator or CFT (gpm)	Time to loss of unthrottled flow (min)
Catawba	4	7,480	2,273	6.6
Waterford	4	13,000	5,874	4.4
Davis-Besse	2	7,780	6,065	2.6

- If vital power is not available, discharge line isolation valves must be operated manually. This entails entry into a potentially high radiation zone in containment.

- In a manual operational mode, the motor-operated valve (MOV) stem positions may not easily translate into meaningful flow rates unless some calibrations were made beforehand.

The use of the accumulator or CFT level instrumentation is one potential measurement. However, the sensitivity for transient flow conditions may not give accurate readings.

A-1.6 Conclusions

It has been shown that gravity drain of coolant from the RWST to the RCS is one potential option to temporarily maintain core cooling after a loss-of-RHR event. A limited analysis of three different plants and gravity drain configurations were presented. Beginning two days after shutdown under ideal conditions, core cooling could be maintained for up to 0.4, 10.4, and 18.2 hours for the Waterford, Catawba, and Davis-Besse plants, respectively. The relatively short period for Waterford is due to the initially low RWST/RCS differential head. It was assumed that the RWST/RCS flows could be throttled and that spill-out paths were available for Davis-Besse and Catawba. In practice, these assumptions may not be realistic and core cooling times may be significantly shorter.

An additional survey was made to see if accumulator/flood tank systems could be used as an alternate way of passively injecting liquid into the RCS during a loss-of-RHR scenario. The use of this system is problematic for long term cooling because of the limited water volume and difficulties in properly throttling the injection flow rate.

A-2. VENTING ANALYSIS

A-2.1 Introduction

This section presents a simplified approach to evaluating RCS venting capabilities following a loss of RHR event. Venting capabilities play a key role in any analysis to quantify RWST gravity drain potential (see Section A-1) as well as limiting potentially damaging RCS pressure excursions. In the event that no RCS drain path is available to maintain core subcooling, vented boiloff may be the only way of removing core decay heat from the RCS. Plant specific examples from Table A-1 are used to demonstrate how this analysis was applied.[4,5,6] Survey methods used to identify possible vent paths are similar to those used to identify gravity drain paths in Section A-1. In some situations, depending on the variability of the RCS inventory, a vent path has the dual potential of functioning as a RCS liquid drain path. This section addresses the following issues:

- For a given system pressure and decay power what venting configurations are adequate to relieve boiloff?

- Conversely, for a given venting configuration what envelope of steady-state pressures and decay powers can the configuration operate in?

- For scenarios where boiling has not been initiated what RCS vent sizes are needed to sustain gravity drain without RCS pressurization?

The motivation for performing such vent analysis includes

- Developing a methodology to evaluate whether large vent paths open to containment during a loss-of-RHR cooling accident are adequate to minimize RCS pressurization and allow for RWST gravity drain.

- Developing a similar methodology to evaluate what small vent paths are appropriate to relieve core boiloff at pressures above the RWST gravity head.

- Obtaining estimates of RCS steady-state pressure levels while venting through various RCS openings, using data from three representative plants.

- Obtaining rough estimates of steam generator steady-state pressure levels while venting through various openings, again for three representative plants.

It should be noted that this analysis makes no consideration of operational factors that might prevent or make difficult or time-consuming the implementation of venting arrangements considered. Such factors include the effects of radiological releases during venting, current technical specification requirements related to allowable valve lineups, and human factor considerations.

Section A-2.2 discusses steam venting capabilities for a range of vent sizes, Section A-2.3 discusses secondary side relieving capacities, and Section A-2.4 contains conclusions relative to the results in the preceding sections.

A-2.2 Steady-State Primary Venting Analysis

Heat removal through the steam generators or condensation on internal surfaces is not considered. Both large and small RCS venting configurations are included in this section. In general, steam discharge from relatively large RCS vents produces relatively small RCS pressure changes. Hence, the RWST gravity drain is still a possible option for maintaining core cooling. Several simplifying assumptions were made:

- Prior to reaching steady-state boiloff conditions, it is assumed any noncondensables initially in the primary system have been completely vented.

- It is assumed that the RCS is initially at mid-loop configuration, with the upper head on and the core liquid in a state of saturated boiling.

- There is a continuous replacement of boiled off liquid. It is assumed that either the ECCS, charging system, or gravity drainage from the RWST is available. For those situations where RWST/RCS gravity feed appears feasible, estimates are given for the amount of time before coolant is depleted.

- The containment pressure is maintained at atmospheric conditions.

A partial listing of possible vent paths for the Catawba, Waterford, and Davis-Besse plants is presented in Tables A-9 through A-11. Some of these mentioned vents are intermediate in size and could result in either choked or unchoked flow. There is also the possibility of venting from the RCS through ECCS lines to the auxiliary building. Because of radiological concerns, these path ways were not considered.

Table A-10. Summary of vent paths for the Catawba Four-Loop Westinghouse plant.

Vent type	Diameter (in.)	Comments
One pressurizer manway	19	Located near the top of the pressurizer steam dome.
Eight primary steam generator manways, two per steam generator	16	Venting possible if steam generator nozzle dams are not installed.
Three pressurizer code safety relief valve discharge lines	5	The removal of safety valves for maintenance opens a possible vent path to containment. However, removal of the code safety valves is an infrequent occurrence.
Two ECCS/ hot leg suction connections	8–12	These lines may be opened for service. However, these openings to the containment may be sealed
Vessel upper head vent valve	0.75–1	Found on most Westinghouse plants; small flow restriction orifices (0.375 inches) that limit possible loss-of-coolant accident events. Can be opened if vital power is lost.
Three pressurizer PORVs	1.25	Can be opened if vital power is lost under normal circumstances.[a]
RHR hot leg suction line containment vent valves (two vents off of two hot legs)	3/4 inch lines with 0.375 flow restriction orifices	Depending on RCS inventory, these valves may vent steam to containment. These are manual valves.
Hot and cold leg RTD bypass manifold (at least 8 vents)	3/4 inch lines with 0.375 orifices	Depending on RCS inventory, these vents may pass steam to containment. These are manual valves.
Pressurizer vent line	1/2—1 inch	Contain flow restriction orifices that limit flow in a loss-of-coolant accident event.
Ruptured Tygon hose	1 inch or less	Depending on the location, this break could vent either steam or liquid. [b]

a. Modes of activation vary from plant to plant. Most Westinghouse plants have only 2 PORVs. Some PORVs are solenoid operated and need a differential pressure threshold of 25–50 psid to open. It is assumed that if these valves are used, they are either discharging into containment or, if the PORV lines are still connected to the quench tank, the tank is open to containment. Such configurations would not normally be expected.

b. Tygon hose is used for level instrumentation readings during refueling and maintenance. These hoses are usually rated at 25 psig. One common connection is between the cold leg suction and top of the pressurizer.

Table A-11. Summary of vent paths for the Waterford 2 by 4 Combustion Engineering plant.[a]

Vent type	Diameter (in.)	Comments
One pressurizer manway	16	Located near top of pressurizer steam dome.
Four primary steam generator manways (two per steam generator)	16	There is potential for venting if steam generator nozzle dams not installed.
Three pressurizer safety relief lines	6	The removal of safety valves for maintenance opens a possible vent path to containment. However, removal of the code safety valves is an infrequent occurrence.
Vessel upper head vent valve	3/4	Can be manually opened to containment.
Ruptured Tygon hose	3/4	Depending on the location, this break could vent either steam or liquid.[b]
Pressurizer vent line	1	Can be manually opened to containment.

a. Waterford has no pressurizer PORVs.

b. Tygon hose connects from hot leg drain line to the top of the pressurizer differential pressure tap.

Table A-12. Summary of vent paths for the Davis-Besse 2 by 4 Babcock& Wilcox plant.

Vent type	Diameter (in.)	Comments
One pressurizer manway	16	Located near top of pressurizer steam dome.
Four primary steam generator manways (two per steam generator)	16	One manway each at the inlet plenum and outlet plenum. Steam must transit steam generator tubing to reach bottom manway.
Two core flood tank lines to upper vessel downcomer	14	Can be opened to containment for service. They are opened infrequently for maintenance, and if opened, they may be sealed to containment.
Two pressurizer safety relief valve discharge lines	4	The removal of safety valves for maintenance can open a vent path to containment. The removal of the valves is an infrequent occurrence.
Vessel upper head vent line	3	This line connects to the top of steam generator 2. Unless this line is opened to containment it is not a usable vent path.
One pressurizer PORV	2.5	Can be opened without vital ac power.[a]
Two Candy Cane high point vent lines	1	Contain flow restriction orifices that limit flow in a loca event. Can be opened to containment if vital power is lost.
Ruptured Tygon hose	1 or less	Depending on the location, this break could vent either steam or liquid.[b]

a. The long term use of the PORV requires that it vent to containment, which requires that either the quench tank be open to containment or the line down stream of the PORV be open containment. Such alignments are off normal configurations.

b. Tygon tubing connects from the cold leg to the upper pressurizer differential pressure tap.

Calculations were performed to determine vent size ranges that are adequate to accommodate core boiloff without significant RCS pressurization.[e] In this analysis, the steady-state Bernoulli equation was used for unchoked flow conditions, and the homogeneous equilibrium model (HEM) was used for choked conditions.[12,13] Generally, if choking occurs, the resultant RCS pressure is too high to allow significant RWST/RCS drainage; RWST/RCS drainage will cease under most circumstances. The HEM critical pressure ratio is approximately 0.58 for saturated steam flowing into the containment at 14.7 psia. Therefore, for RCS pressures above about 25 psia the discharge will be choked.

For unchoked flow the steam discharge rate is given by

$$m_{vent} = A_{eff}[2g_c 144\varrho(P_{RCS})\Delta P]^{1/2} \qquad \text{(A-6)}$$

where

A_{eff} = the effective flow area (ft^2)

ϱ = density of steam (lbm/ft^3)

P_{RCS} = primary system saturation pressure upstream of the vent opening (psia)

ΔP = $P_{RCS} - P_{con}$

P_{con} = the containment pressure (psia)

and the effective flow area is given as

$$A_{eff} = C_d A$$

where

C_d = equivalent discharge coefficient

A = geometric vent area (ft^2).

For choked flow the steam discharge rate is given by

$$m_{vent} = A_{eff} G_{choke}(P_{RCS}) \qquad \text{(A-7)}$$

where

$G_{choke}(P_{RCS})$ = choked mass flux (lbm/ft^2–s).

The mass flux function $G_{choke}(P_{RCS})$ was generated using the HEM model. In the above formula, C_d is a lumped parameter that is a function of a number of different variables including[14,15]

- Geometry effects and frictional losses that include expansion and contraction losses
- Compressibility effects, which are a function of vent geometry, specific heat ratios, and the ratio of down stream and upstream pressures
- Whether or not the flow is choked or unchoked.

In a conservative analysis, C_d would be estimated to produce the worst case (i.e. the lowest flow) and therefore the smallest possible discharge coefficient.

For steady-state venting conditions, the core boiloff rate $m_{boiloff}$ is equated to m_{steam} so

$$m_{boiloff} = m_{steam} = Q(t)/h_{fg}(P_{RCS}) \qquad \text{(A-8)}$$

where

A(t) = core decay power (Btu/s)

$h_{fg}(P_{RCS})$ = latent heat of vaporization (Btu/lbm).

Given a specific venting configuration, the steady-state RCS pressure that results from discharging steam into containment can be readily calculated as a function of decay time. If the flow is found to be unchoked, the pressure is calculated

e. The RCS pressurization is defined as significant if the vent discharge chokes, RCS pressurization significantly degrades gravity drain potential, or localized RCS pressurization generates differential hot/cold leg pressures that induce core level depression.

from combining Equations (A-6) and (A-8), giving

$$P_{RCS} = P_{con} + [Q(t)/h_{fg}]^2/2g_c\rho A_{eff}^2 \quad \text{(A-9)}$$

which must be solved iteratively for the primary system pressure, since h_{fg} and ρ are functions of P_{RCS}. If Equation (A-9) produces a pressure and the critical pressure ratio is 0.58, or lower ($P_{con}/P_{RCS} \leq 0.58$), Equations (A-7) and (A-8) are used, and the pressure is found from

$$G_{choke}\ (P_{RCS}) = Q(t)/(A_{eff}h_{fg}) \quad \text{(A-10)}$$

This indicates the pressure needed to produce a mass flux equal to the boiloff rate divided by the effective area.

Using the above methodology, tables were generated using steady-state RCS pressures for various venting configurations and times after reactor shutdown for the Catawba, Waterford, and Davis-Besse plants, respectively.

Tables A-13, A-14, and A-15 show estimated steady-state pressures for a number of both small and large vent configurations for these plants. The decay times correspond to the times used in Appendix B. In general, small vent paths using the pressurizer PORVs, code safeties, or HPVVs are not viable for RWST/RCS gravity drain. Even some large vent paths (such as in Waterford) are not adequate because the initial RWST/RCS differential pressure head is too low.

The tables also show gravity drain times for those venting configurations that do not "overpressurize" the RCS. These times were calculated assuming the drainage commences at 48 hours after reactor shutdown, the steaming rate remains at the 48 hour level, and the drain rate exactly matches the steaming rate until the differential head between the RWST and RCS is lost. It should be emphasized that these estimated drain times are theoretical limits, with no consideration given to how the drainage procedure could be implemented, controlled or monitored.

The venting results shown in Tables A-13 through A-16 indicate that open steam generator manways are the most desirable vents because they cause very little RCS pressurization and allow maximum use of RWST water. Indeed, for the Waterford plant, these are the only viable vents for a feed and steam procedure. For Catawba and Davis-Besse, the pressurizer manways are also viable feed-and steam vents, although their use results in a reduction in drain time. None of the smaller vent paths could be used in connection with feeding from the RWST because the elevated RCS pressure precludes gravity drainage into the RCS.

As indicated earlier, these results are based on assuming steady-state conditions. Prior to reaching a quasi-steady feed-and-steam condition, noncondensables in the RCS must be vented after boiling in the core begins. Because of the difference in density between air (or nitrogen) and steam, the pressure drop through a vent path differs for the two gases at a given volumetric flow rate. Since air is about twice as dense as steam for the same volumetric flow rate, the pressure drop for air is larger relative to the steam pressure drop. This will lead to a transient RCS pressure behavior during the period when noncondensables are being purged. This may temporarily cause the RCS pressure to rise above the values shown in Tables A-13 through A-16.

A-2.3 Secondary Side Venting Analysis

The steady-state methods for calculating relieving capacities are also applicable to secondary side systems. Numerical examples using representative plant data from the previous section are presented in this section. This is of relevance to conditions where one or more steam generators are functioning as heat sinks following a loss of RHR. As described in Appendix B, with a closed RCS, the primary pressure at steady-state is directly dependent on the secondary side saturation state.

Table A-13. Estimated RCS venting conditions after a loss of RHR for Catawba.[a]

Venting configuration	Hours after shutdown			Gravity drain time (h)[b]
	48	83	167	
	Corresponding RCS steady-state pressure (psia)[c]			
One SG manway opened	14.9	14.8	14.8	62.7
Four SG manways opened	14.7	14.7	14.7	63.6
Three code safety lines open to containment	23.8	21.9	20.2	29.6
Pressurizer manway through surge line open	18.6	17.7	16.9	49.0
Three PORVs open	753.1	623.0	507.6	None
Three PORVs, upper head vent and pressurizer vent (assume orifices are removed) opened	489.7	410.6	337.2	None

a. At 48 hours the saturated steaming rate is 13.2 lbm/s and initial gravity drain RCS shut off head is 43.5 psia.

b. Drain times calculated by conservatively assuming maximum steam flow at 48 hours with maximum back pressure at 48 hours.

c. All RCS steady-state pressures based on the assumption that there is no primary/secondary side heat sink, and that containment pressure remains at atmospheric conditions.

Table A-14. Estimated RCS venting conditions after a loss of RHR for Waterford.[a]

Venting configuration	Hours after shutdown			Gravity drain time (h)[b]
	48	83	167	
	Corresponding RCS steady-state pressure (psia)[c]			
One SG manway opened	15.1	15.0	14.9	10.0
Four SG manways opened	14.7	14.7	14.7	14.7
Pressurizer manway through surge line open	20.3	19.0	17.9	None
One pressurizer safety line (assume open to containment) open	79.3	68.4	57.9	None
Three pressurizer safety lines (assume open to containment) opened	29.0	25.6	22.3	None

a. At 48 hours the saturated steaming rate is 13.2 lbm/s and initial gravity drain RCS shut off head is 16.0 psia.

b. Drain times calculated by conservatively assuming maximum steam flow at 48 hours with maximum back pressure at 48 hours.

c. All RCS steady-state pressures based on the assumption that there is no primary/secondary side heat sink, and that containment pressure remains at atmospheric conditions.

Table A-15. Estimated RCS venting conditions after a loss of RHR for Davis-Besse.[a]

Venting configuration	Hours after shutdown			Gravity drain time (h)[b]
	48	83	167	
	Corresponding RCS steady-state pressure (psia)[c]			
One upper steam generator manway opened	16.7	15.2	15.8	87.7
Four upper steam generator manways opened	15.2	15.1	15.0	97.0
One pressurizer manway through surge line open	21.7	20.2	18.9	55.7
One PORV open	416.4	350.1	288.2	None
One PORV, high point vent valve (2) (assume orifices are removed) opened	303.8	256.4	212.0	None

a. At 48 hours the saturated steaming rate is 10.8 lbm/s and initial gravity drain RCS shut off head is 35.5 psia.

b. Drain times calculated by conservatively assuming maximum steam flow at 48 hours with maximum back pressure at 48 hours.

c. All RCS steady-state pressures based on the assumption that there is no primary/secondary side heat sink, and that containment pressure remains at atmospheric conditions.

Table A-16. Summary of secondary steam discharge paths for Catawba.

Vent description	Size diameter (in.)	Comments
At least one vent line per steam generator	2	It is assumed this line can be opened to containment or atmosphere if vital power is lost.
SG PORV one per steam line	3.6[a]	Can be opened if vital power is lost
Five spring loaded safeties per steam line	4.0[b]	Difficult to open manually.
Secondary steam generator manways	16	There are two per steam generator.

a. This is an effective diameter based on a HEM choked flow relieving capacity of 594,000 lbm/h at a pressure of 1,150 psia.

b. This is an effective diameter based on a HEM choked flow relieving capacity of 793,000 lbm/h at a pressure of 1,200 psia.

The principal difference between the primary and secondary venting schemes are differing hardware configurations. In performing the venting analysis for the secondary system the following assumptions were made:

- The boiler region was filled with saturated boiling liquid
- There is some source of make-up feedwater.[f]

Tables A-16 through A-18 indicate some of the possible secondary vent paths for the Catawba, Waterford, and Davis-Besse plants, respectively. Generally, the steam generator (SG) PORVs and safeties are effective discharge paths for removing decay energy. These vent paths are designed to handle decay power levels much higher than typical RHR decay levels. In most plants, the SG PORVs or atmospheric dump valves can be remotely opened without vital ac power. The steam dump system was not included in the tables because it was assumed that it becomes inoperable upon loss of vital ac power.

Using the same methodology as for RCS venting, tables were generated of steady-state SG pressures for various venting configurations and times after reactor shutdown for the Catawba, Waterford, and Davis-Besse plants. Tables A-19 through A-21 show estimated steady-state pressures for a number of both small and large vent configurations for these plants. Again these decay times correspond to the times used in Appendix D. As in the primary venting analysis, large vent paths yield relatively low steady-state SG pressures, while small vents produce corresponding higher pressures. The data in Tables A-19 through A-21 indicate that close to atmospheric secondary conditions can be established, if a steam generator manway is open or all steam generators are available with PORV or code safety vents. For low pressure boiling scenarios, possible sources of feedwater may include the fire protection system and possible gravity drain from the condensate storage tank. A positive differential head must exist between the steam generator inlet and condensate storage tank for this approach to

f. In general, turbine driven feedwater is operational only for SG pressures above 100 psia. Thus, at lower pressures, some other feed source must be used.

Table A-17. Summary of secondary steam discharge paths for Wat. 'ord.

Vent description	Size diameter (in.)	Comments
At least one vent line per steam generator	2	It is assumed this line can be opened to containment or atmosphere if vital power is lost.
Six main steam safety valves per line with variable settings	5.5[a]	Cannot be easily opened manually.
Atmospheric vent valves—one per line	3.0[b]	Cannot be easily opened on loss of vital power.
SG secondary manways	16	Two per steam generator.

a. This is an effective diameter based on a HEM choked flow relieving capacity of 1,307,000 lbm/h at a pressure of 1,085 psia.

b. This is an effective diameter based on a HEM choked flow relieving capacity of 378,000 lbm/h at a pressure of 1,065 psia.

Table A-18. Summary of secondary steam discharge paths for Davis-Besse.

Vent description	Size diameter (in.)	Comments
At least one vent line per steam generator	1.5	It is assumed this line can be opened to containment or atmosphere if vital power is lost.
Power operated atmospheric vent valves one per SG	3.2[a]	Can be manually opened if vital power is lost.
Nine spring loaded safeties per steam generator with variable settings	4.5[b]	Cannot be easily opened manually.
Secondary SG manway	16	

a. This is an effective diameter based on a PORV HEM choked flow relieving capacity of 459,000 lbm/h of full flow at a pressu. f 1,040 psia.

b. This is an effective diameter based on a PORV HEM choked flow relieving capacity 845,760 lbm/h at a pressure of 1,115 psia.

Table A-19. Estimated steady-state SG secondary pressures after a loss-of-RHR event for Catawba.

Venting configuration	Hours after shutdown		
	48	83	167
	Corresponding SG steady-state pressure (psia)		
One SG with one opened manway	15.1	15.0	14.9
Four SGs with each with one opened manway	14.7	14.7	14.7
One SG with one opened code safety	88.1	75.8	64.1
Four SGs each with one opened code safety	18.5	17.6	16.9
One SG with one opened PORV	112.7	96.6	81.3
Four SGs each with one opened PORV	20.4	19.1	18.0
One SG with one opened vent line	928.6	759.6	612.5
Four SGs each with one opened vent line	184.2	156.6	130.6

Table A-20. Estimated steady-state SG venting pressures after a loss-of-RHR event for Waterford.

Venting configuration	Hours after shutdown		
	48	83	167
	Corresponding SG steady-state pressure (psia)		
One SG with one opened manway	15.1	15.0	14.9
Two SGs with each with one opened manway	14.8	14.8	14.7
One SG with one opened code safety	48.9	42.6	36.5
Two SGs each with one opened code safety	16.0	15.7	15.4
One SG with an opened atmospheric vent valve	164.9	140.4	117.4
Two SGs each with an opened atmospheric vent valve	24.5	22.6	20.7
One SG with one opened vent line	920.9	753.6	607.9
Two SGs each with one opened line	395.2	332.5	273.9

Table A-21. Estimated steady-state SG venting pressures after a loss-of-RHR event for Davis-Besse.

Venting configuration	Hours after shutdown		
	48	83	167
	Corresponding SG steady-state pressure (psia)		
One SG with one opened manway	15.0	14.9	14.8
Two SGs with each with one opened manway	14.8	14.7	14.7
One SG with one opened code safety	58.4	50.6	43.2
Two SGs each with one opened code safety	20.6	19.3	18.2
One SG with an opened atmospheric dump valve (ADV)	114.8	98.3	82.7
Two SGs each with an opened ADV	30.7	27.7	24.8
One SG with one opened vent line	1,040[a]	1,040[a]	984.0
Two SGs each with one opened vent line	612.0	511.3	418.2

a. Dump valve will open at a set point at 1,040 psia.

work. Plant specific hardware modifications may be required to make a tie-in with the fire protection system.

A-2.4 Conclusions

A simplified analysis has been performed to evaluate the potential for feed-and-steam decay heat removal of the RCS, and to evaluate steam generator secondary side venting when one or more steam generators can be used as heat sinks. Conclusions from this study are as follows:

- Analysis of the three plant types shows the wide variability in the potential for feed-and-steam decay heat removal. Assuming a loss of RHR two days after shutdown under ideal conditions, the theoretical time period during which feed-and-steam could take place ranges from 15 hours for Waterford to 97 hours for Davis-Besse.
- Primary feed-and-steam decay heat removal is generally only possible when one or more manways are used as vent paths. Smaller vents cause system pressurization sufficient to preclude RWST/RCS gravity drainage.
- With respect to venting of the steam generator secondary side, maintaining a pressure close to that of containment requires that either a secondary manway is open or all steam generators are functioning with at least one code safety open in each.

A-3. ENVIRONMENTAL HEAT LOSS FOLLOWING LOSS OF RHR

A-3.1 Introduction

This section discusses environmental heat loss estimates for two possible plant configurations following a loss-of-RHR accident. The assumed heat sink is the reactor containment. The motivation for making such estimates is to determine if environmental heat losses are a significant fraction of the total decay power. The Catawba 4-loop Westinghouse plant is used as a plant specific example. Environmental losses were estimated for the RCS closed at mid-loop conditions; and for the RCS open with the upper head removed. An analysis of B&W and CE designs would be expected to produce results similar to the Westinghouse system.

Realistic decay power levels correspond to maintenance and refueling situations where the plant down times range from several days to months. Decay heat loads before refueling range from 0.5 to 0.1% of full power for the corresponding range of 1 to 120 days. For a 3411 MW plant such as Catawba, this translates into power levels in the range of 3.4 to 17 MW. If refueling has been completed, the above powers are reduced by roughly 1/3. For Catawba, the minimum decay power could be as low as 2 MW.

Radiation and free convection are the only assumed mechanisms for energy removal in the analysis. It is assumed that there is a loss of vital power and that the containment ventilation and spray systems are inoperative.[g] The containment volume is large (on the order of a million cubic feet or more); therefore, the containment heat up rate is relatively slow. In the initial order of magnitude analysis, the containment system temperature is assumed to remain at a constant value of 100°F. Of course, any heat up of the containment degrades the containment's heat sink potential.

Section A-3.2 addresses ambient heat losses at mid-loop operation with the RCS system closed, Section A-3.3 shows heat loss estimates with the RCS open and with an assumed loss of RCS liquid inventory, and Section A-3.4 contains conclusions.

A-3.2 RCS Heat Loss in a Closed Partially Filled Configuration

The steam generators are assumed to be unavailable for decay power removal and the RCS has reached a saturated boiling state. Ambient heat losses include losses via the RCS vessel and piping to the containment by conduction, convection, or radiation. Several simplifying assumptions are made in the heat loss approximation.

- The steam generators are isolated from the RCS with nozzle dams. This limits the RCS saturation temperature to not more than 300°F, because nozzle dams will fail for pressures in the range of 25–50 psig.

- The presence of piping insulation is ignored. Convective and radiation environmental losses from the RCS are approximated by assuming the vessel and associated piping are air cooled bare metal surfaces at isothermal conditions with the saturated primary liquid.

The RCS system is actually heavily insulated and some of the RCS outer regions are surrounded by pockets of stagnant air.[h] Therefore, the bare metal approximation will predict heat loss rates that are upper bounds on the actual

g. In other scenarios, the postulated use of containment ventilation or sprays requires analysis outside the scope of this Appendix. In particular, containment computer codes like HECTR are applicable to help provide detailed RCS/containment heat transfer analysis.[16,17,18]

h. Pockets of stagnant air in the vicinity of the RCS piping are the consequence of biological shields, missile barriers, etc.

ambient loss rates. Figure A-6 shows a schematic view of a Westinghouse reactor and surrounding containment structure.

The outer boundary of the reactor vessel was approximated as a vertical cylindrical surface and the loop piping as horizontal cylindrical surfaces that are exposed to free convection air cooling. For turbulent convection the heat transfer correlation is[19,20]

$$Nu = 0.13(PrGr)^{1/3} \qquad \text{(A-11)}$$

where

Nu = average surface value of the Nusselt Number

Pr = Prandtl number

Gr = Grashof number.

Figure A-7 is a plot of the estimated convection heat loss rates as a function of surface temperature for the temperature range 200–300°F. In the analysis, the vessel and piping bare metal surface areas were 2,050 ft^2 and 3,500 ft^2, respectively. From these results, it is clear that the convective heat losses are a small fraction of the minimum decay power.

The bare metal approximation was also used to obtain an order of magnitude value for radiative environmental heat losses. The same set of assumptions were made in doing the radiative energy loss approximation.

The radiant heat loss rate is estimated as follows[19,21]:

$$Q_r = A\delta\varepsilon(T_s^4 - T_c^4) \qquad \text{(A-12)}$$

where

A = the RCS surface area (ft^2)

δ = Stefan-Boltzmann constant 0.1714 $\times 10^{-8}$ Btu/(h-ft^2-R^4)

ε = is the emissivity of the surface

T_s = the RCS exterior piping surface temperature (R)

T_c = the containment temperature (R).

For mild steel, ε is about 0.3. The calculated radiative loss for an assumed containment temperature of 100°F is also shown in Figure A-7. The radiative loss rates are again significantly less than the expected minimum decay power.

A-3.3 RCS Environmental Heat Loss In an Open Configuration

It is of some interest to estimate the rate of heat transferred to the containment from an uncovered core. The assumption is made that the upper head and internals have been removed for refueling, and that the core has boiled dry following a loss-of-RHR event. Under this circumstance, both convection and radiation would be expected to transfer some decay heat to the containment.

In this simplified analysis, several assumptions are made.

- There are no other openings between the RCS and containment.
- The loops are blocked by nozzle dams so that air trapped in the loop regions is stagnant.
- Vital power is not available.
- The containment is maintained at a constant temperature of 100°F.
- The presence of vapor in the containment atmosphere is neglected in the free convection and radiant heat transfer calculations.
- Fuel damage effects are not considered during the process that resulted in core uncovery.
- The cross-sectional top of the vessel upper head mating surface is assumed to act like a horizontal radiating and convecting heater plate.

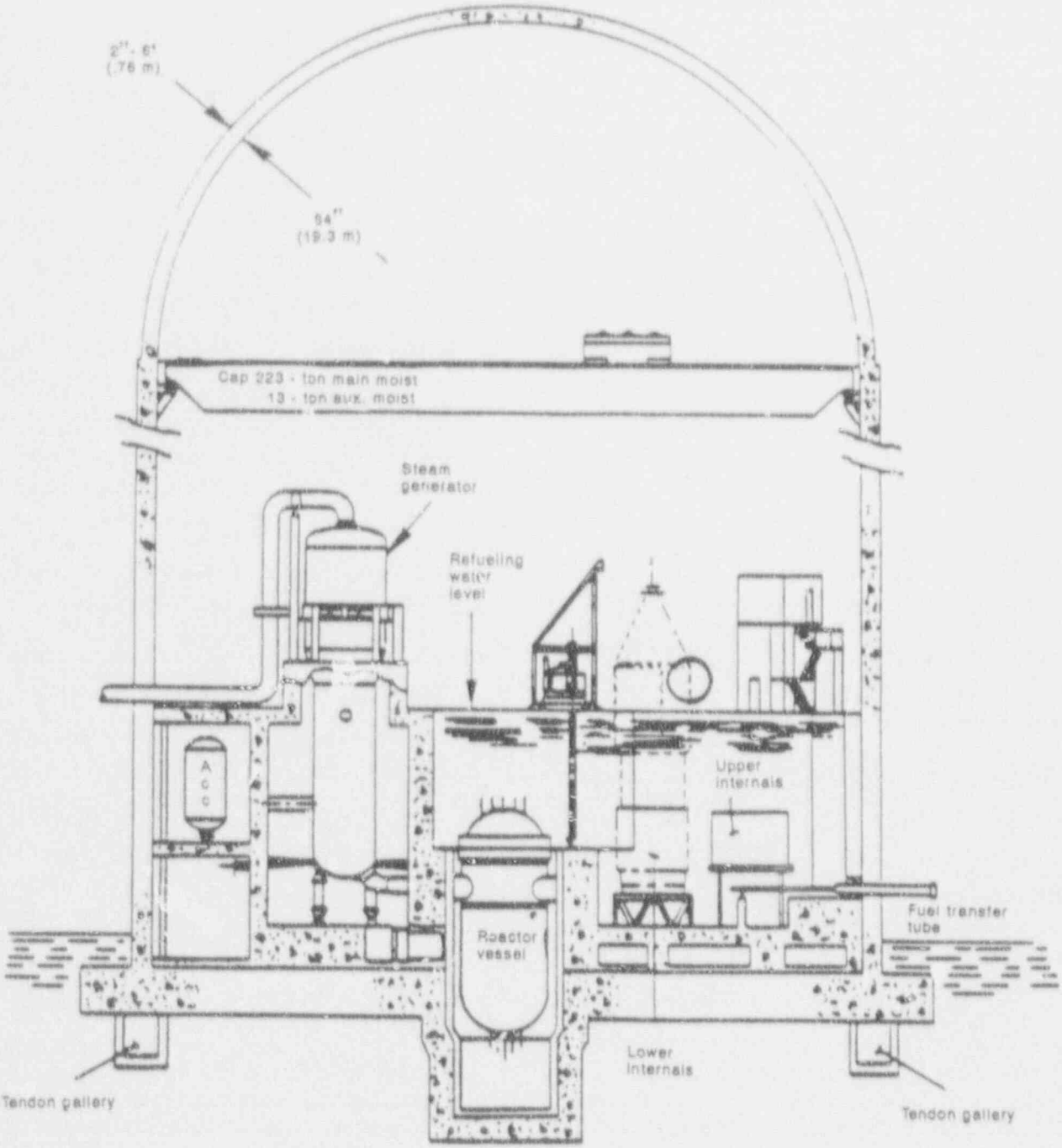

Figure A-6. Containment elevation view of a Westinghouse PWR.[9]

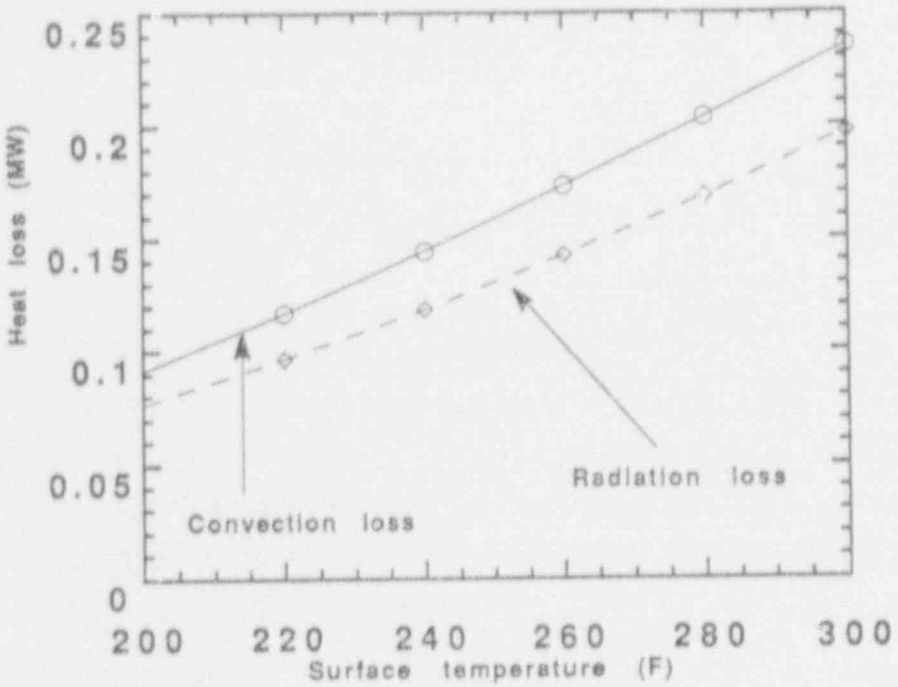

Figure A-7. Ambient convection and radiation losses.

- Fuel axial and radial temperature gradients are not considered. For convenience, it is assumed that the fuel clad and surrounding air temperatures are uniform.

The cross-sectional area at the core upper plenum/upper head interface is approximately 190 ft^2. This is used as the characteristic heat transfer area in the radiant and convective estimates. The surface temperature is set equal to the outer clad fuel temperatures at the top of the core. The free convection correlation for a horizontal flat surface is[19,21]:

$$Nu = 0.54(PrGr)^{1/4} \qquad \text{(A-13)}$$

Using Equation (A-13) with air property data, Figure A-8 was generated. This figure presents the estimated upper core/containment convective heat loss rate as a function of temperature for the range 200–2200°F.[i] As was the case with external RCS convection in a closed configuration, the above loss rates are well below the minimum decay power. Convective losses may be significantly enhanced if convective cells from the upper vessel regions penetrate deep into the fuel rod assembly regions. The analysis of such internal flow fields and corresponding heat transfer characteristics analysis is outside the scope of this appendix.

The corresponding radiant heat loss rates were estimated using Equation (A-12). Only radiation transport from the top of the core surface was considered. Transport losses in other directions are not significant because of internal radiative reflections off internal vessel metal structures. A more accurate calculation requires the use of actual emissivities and view factors for structures in containment and the upper region of the vessel. Figure A-9 shows the radiant heat losses as a function of the upper core surface temperature. The radiative losses were significantly larger than the corresponding convective losses. At 2,200°F the radiant losses were large but still below the minimum decay power level as discussed in

i. The upper limit of 2,200°F corresponds to the peak clad temperature used in most standard safety LOCA analysis. Above 2,200°F significant fuel damage begins.[22,23]

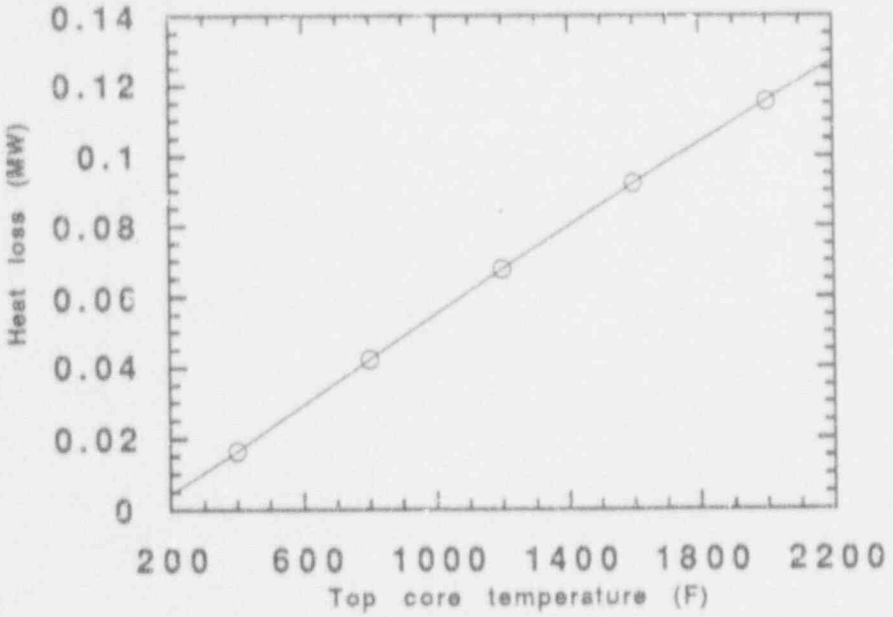

Figure A-8. Convective upper core/containment heat losses.

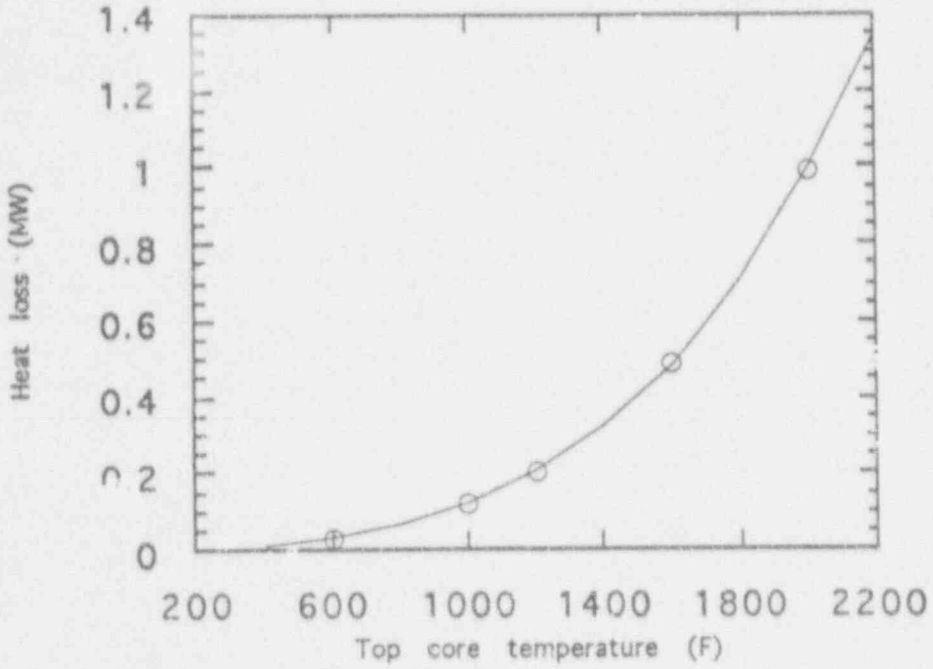

Figure A-9. Upper core radiant losses.

Section A-3.1. Relative to the upper core temperatures, the lower regions of the core are much hotter. If the top of the core reaches 2,200°F, lower core regions would be much hotter.[j] It is clear that radiant heat losses could not keep core temperatures below safe limits.

A-3.4 Conclusions

A simplified analysis has shown that for acceptable fuel temperatures, environmental heat losses to containment are a fraction of representative shutdown decay powers.

j. Clearly, for large enough fuel clad temperatures, containment radiant heat losses become significant. However, such large losses develop at temperatures where unacceptable collateral damage to the fuel and containment structures are highly probable.

A-4. REFERENCES

1. ANSI/ANS 5.1, "American National Standard for Decay Power in Light Water Reactors," American National Standards Institute, August 1979.

2. Jay R. Larson, *System Analysis Handbook*, NUREG/CR-4041, EGG-2354, December 1984.

3. T. S. Andreyched et. al., *Loss of RHRS Cooling While the RCS is Partially Filled*, Westinghouse Electric Cor oration, WCAP-11916, July 1988.

4. Toledo Edison Company, *Updated Safety Analysis Report, Davis-Besse Nuclear Power Station No. 1*, Docket Number 50-446, July 1982.

5. Louisiana Power & Light, *Final Safety Analysis Report, Waterford Steam Electric Station Unit No. 3*, Docket Number 50-382, January 1979.

6. Duke Power Company, *Catawba Nuclear Station Final Safety Anaiysis Report*, Docket Number 50-413, July 1980.

7. W. J. Galyean et. al., *Asse ment of ISLOCA Risks Methodology and Application: Babcock and Wilcox Nuclear Power Station*, NUREG/CR-5604, EGG-2608, February 1991.

8. NRC, *Loss of Vital AC Power and the Residual Heat Removal System During Mid-Loop Operations at Vogtle Unit 1 on March 20, 1990*, NUREG-1410, May 1990.

9. Westinghouse Electric Corporation, *The Westinghouse Pressurized Water Reactor Nuclear Power Plant*, 1984.

10. R. V. Giles, *Fluid Mechanics and Hydraulics*, New York: McGraw-Hill, 1962.

11. F. M. White, *Fluid Mechanics*, New York: McGraw-Hill, 1979.

12. D. G. Hall and L. S. Czapary, *Tables of Homogeneous Equilibrium Critical Flow Parameters for Water in SI Units*, EGG-2056, September 1980.

13. *Flow of Fluids Through Valves, Fittings, and Pipe*. Crane Technical Paper No. 410, 1979.

14. A. H. Shaprio, *The Dynamics and Thermodynamics of Compressible Fluid Flow*, Ronald Press Company, 1953.

15. J. R. Travis et. al., "Multidimensional Effects in Critical Two-Phase Flow," *Nuclear Science and Engineering*, *68*, 1978, pp. 338–348.

16. C. C. Lin et. al., *CONTEMPT4/MOD6 A Multicompartment Containment System Analysis Program*, NUREG/CR-4547, BNL-NUREG-51966, March 1986.

17. A. L. Camp, *HECTR Version 1.5 User's Manual*, NUREG/CR-4507, SAND86-0101, April 1986.

18. K. K. Murata et. al., *User's Manual for Contain 1.1: A Computer Code for Severe Nuclear Reactor Accident Containment Analysis*, NUREG/CR-5026, SAND87-2309, November 1989.

19. D. P. DeWitt and F. P. Incropera, *Fundamentals of Heat Transfer*, John Wiley & Sons, 1981.

20. W. J. Minkowycz et. al., "Local Nonsimiliar Solutions for Natural Convection on a Vertical Cylinder," *Journal of Heat Transfer*, 96, 178, 1974.

21. D. R. Pitts et. al., *Heat Transfer*, New York: McGraw-Hill, 1977.

22. Babcock and Wilcox Nuclear Power Group, *Study Guide Operator Training Degraded Core Recognition and Mitigation*, Volume 1, TRG-81-3, May 1981.

23. NRC, *Compendium of ECCS Research for Realistic LOCA Analysis*, NUREG-1230, April 1987.

Appendix B

Analysis of Plant Equilibrium States in Loss-of-RHR Incidents

CONTENTS

SUMMARY

This appendix investigates the thermal-hydraulic response of a nuclear steam supply system with a closed reactor coolant system (RCS) to loss of residual heat removal cooling capability. The specific processes investigated include boiling of the coolant in the core and reflux condensation in the steam generators, the corresponding pressure increase on the primary side, the heat transfer mechanisms on the primary and secondary sides of the steam generators, the effects of air or other noncondensable gas on the heat transfer processes, and void fraction distributions on the primary side of the system. Mathematical models of these physical processes are developed. The models are validated against available experimental data and are applied to analyses of two typical NSSS plants to estimate the response of the plant to a loss of residual heat removal incident.

Sensitivity studies show which thermal-hydraulic parameters are the most important relative to the critical aspects of the plant response. In the case of boiling in the core and reflux condensation in the steam generators, sensitivity studies show that the secondary side pressure/temperature, the heat transfer mode in the primary side, the number of nozzle dams installed, and the behavior of noncondensables in the pressurizer are the most important factors relative to RCS pressure increase. The decay heat level and number of active steam generators (as long as nozzle dams are not installed in others) has only a second-order effect. In addition, the analysis shows that pure reflux condensation in the steam generators provides the lower limit on the pressure increase. That is, the other possible heat transfer regimes are expected to give lower heat fluxes and subsequently higher primary side pressure than pure reflux condensation. The thermal-hydraulic models are validated against experimental data from the Semiscale and PKL facilities. The models predict the data with reasonable accuracy.

Appendix B

Analysis of Plant Equilibrium States in Loss-of-RHR Incidents

B-1. STATEMENT OF PROBLEM

B-1.1 Introduction

A study conducted at the Idaho National Engineering Laboratory (INEL) for the U.S. Nuclear Regulatory Commission (NRC) identified various natural circulation cooling modes that might be used in the removal of decay heat following loss of residual heat removal (RHR) during maintenance or refueling shutdown of U.S. pressurized water reactors (PWRs).[1] The study also identified the important thermal-hydraulic phenomena that could occur during such an event. One of the modes identified that required further investigation is reflux cooling, initiated during reduced inventory conditions with the upper regions of the reactor coolant system (RCS) filled with nitrogen or air. Of particular concern was the RCS pressure reached in establishing stable refluxing. If this pressure approached approximately 50 psig, it might be sufficient to cause failure of temporary closures, such as nozzle dams, and pressures as low as about 25 psig could threaten thimble tube seals.

A review of the various integral system thermal-hydraulic codes such as RELAP5 and TRAC-PF1 suggested that there are significant uncertainties with respect to treating the noncondensable phase. These uncertainties cast doubt on the codes' current ability to adequately model this situation. Accordingly, a new model was developed for calculating RCS pressure as a function of steam generator conditions, core power, and RCS water inventory.

The model makes some assumptions concerning the process leading to and during reflux condensation. Some of the assumptions are derived from the scenario itself on how the noncondensable gases are transported during the process of establishing steam generator heat removal. Others come from the physical processes occurring in the vessel, coolant system, and steam generators. Each assumption is discussed in the following two sections.

Section B-2 presents the model developed for all the dominant phenomena that would be expected to occur for a loss-of-RHR event in a closed system with reflux condensation cooling. The model is assessed against theoretical and experimental work related to natural circulation with noncondensable gases in Section B-3. Section B-4 discusses the results obtained using the model and Section B-5 shows the sensitivity of model calculations to changes in key parameters. The final section, B-6, discusses the conclusions that can be drawn from the analysis and what further work might be necessary to improve our understanding of the system responses to the assumed scenario.

B-1.2 Loss-of-RHR Scenario

The operating condition and configuration of the system assumed at the time of loss of RHR is mid-loop operation with all RCS openings secured (i.e., primary coolant system is closed from the containment). One or more of the steam generators is in wet layup, and nozzle dams may or may not be in place in one, but not all loops. Air or nitrogen fills all reactor coolant system internal space above the coolant level. Such a configuration can exist shortly after shutdown before refueling operations begin (within two or more days), or after refueling has been completed and preparations are underway to start up.

Following loss of RHR, core decay heat causes a rise in reactor coolant temperature until boiling begins. During this first phase, it is assumed that buoyancy-driven natural circulation causes all of the water above the bottom of the core to heat to the boiling point. A second phase begins after the core coolant begins to boil, during which the resulting steam expands into the primary coolant system and eventually reaches the steam generators. This might be referred to as the air compression phase.

In the third phase, steam inside the steam generator tubes condenses with the condensate draining back into the hot legs for U-tube steam generators or into the cold legs for once-through steam generators, and eventually to the reactor vessel. One or more steam generators may be available to condense the steam. The transfer of heat into the secondary coolant causes its temperature to gradually increase. Therefore, the primary vapor temperature and pressure also increase with time.

The fourth and final phase begins when the secondary coolant starts to boil. Here it is assumed that a secondary vent path can be established to relieve the steam. A pseudo-steady condition then prevails in which the primary pressure remains stable as long as sufficient secondary coolant exists to cover the condensing length of the tubes. Eventually, if the secondary coolant is not replenished, it would be boiled off. However, for most cases examined in this study, it is assumed that the steam generator tubes remained covered.

B-1.3 Physical Phenomena

There are several important physical phenomena that must be accounted for to perform an analysis of reflux cooling. The first is the heating of the water and metal mass in the reactor vessel and hot legs. Since the main concern is the final RCS pressure reached, the heatup is considered to have already been completed. Therefore, all of the decay heat goes to boiling the water in the vessel. The steam generated will eventually make its way to the steam generators. If the core decay heat level is high enough, and/or the initial water level is elevated above mid-loop, a two-phase mixture is produced, with the steam voids causing a swelling of the coolant volume. If the swelling is great enough, a two-phase nonannular mixture could enter the steam generator tubes. Thus, the heat transfer on the primary side of the steam generator tubes might take on a potentially wide range of values [from as low as 200 W/m^2-K to 15,000 W/m^2-K (35 Btu/h-ft^2-°F to 2650 Btu/h-ft^2-°F)].

Because of the high decay heat, the potential for a countercurrent flow limitation in the U-tube steam generators exists. This could flood the upper sections of the U-tubes with the condensate. On the secondary side of the steam generators, two possibilities exist: boiling or natural convection. Finally, the movement of noncondensable gases that fills the RCS above the water level is subject to some uncertainty. It is presumed that most of the gas will be swept out of the reactor vessel as the steam and/or steam and water mixture expands within the vessel. Some proportion of the gas may enter the pressurizer, which is already filled with noncondensable gas. The remainder will be compressed into the steam generator tubes and downstream spaces (i.e., the steam generator outlet plenum and cold legs) to a sufficient degree to create enough steam generator tube surface area to condense the steam.

B-2. MODEL DEVELOPMENT

B-2.1 Piston Model

A simplified, steady-state model was developed to calculate the state of the reactor coolant system for a long duration loss of RHR (long enough for boiling in the core to occur). It is well established that a balanced, pseudo-steady heat transfer condition can be reached after the loss of RHR if certain plant conditions exist.[2,3] The conditions necessary and the phases, or steps, to reach this pseudo-steady condition were described in

Section B-1. In this section, the models and associated assumptions used to calculate the conditions of the primary system are presented.

The principal assumption of the so-called Piston Model is that the noncondensable gas from almost every section of the RCS is transported into a noncondensing section (a "passive" region) of the steam generator(s) by the boiling of water in the core. This movement, or transport, of the noncondensable gas into a reduced volume by the steam is similar to the effect of a piston compressing a gas in a cylinder. Only two basic principles, with a few simple assumptions, are needed to determine the system conditions that will be reached. These principles are the Gibbs-Dalton Law of Partial Pressure and an energy balance across the steam generator tubes. The assumptions are

- The noncondensable gas originally occupying the upper plenum, upper head, and the hot legs is compressed by the steam into the steam generator tubes and cold legs.[a]
- An active steam generator is defined as one in a wet-layup condition without nozzle dams installed, allowing it to be a heat sink for the loss-of-RHR analysis. An inactive steam generator is one with the secondary side dry (filled with air or nitrogen) with or without installed nozzle dams.
- Noncondensable gas is compressed into any inactive steam generator without nozzle dams. The volume that the noncondensable gas occupies in the inactive steam generator(s) is the same as the volume the noncondensable gas occupies in the active steam generator(s). Therefore, the total amount of noncondensable gas to be compressed is equally split between the active and inactive steam generators.
- The temperature of the steam above the core, in the hot legs, and entering the steam generator equals the saturation temperature corresponding to the primary pressure.
- Condensation of the vapor entering the steam generator tubes begins at the top of the tube sheet and extends a distance through the tube bundle referred to as the condensing length.
- In the noncondensing region of the steam generator, steam and noncondensable gas are mixed together and have the same temperature as the secondary side of the steam generator.
- The steam generator tubes all behave identically.
- For condensation on the primary side of the steam generator tubes, a modified Nusselt-based thin film condensation model, a two-phase annular condensation correlation, or a two-phase nonannular condensation correlation may be applied.
- The heat transfer across the tube walls and at the outside surface of the tubes is calculated using a simple conduction calculation and natural convection correlations (boiling and non-boiling conditions), respectively.
- No credit is taken for heat transferred to the structure of the reactor coolant system.

The assumed behavior of the pressurizer during the pressurization of the RCS has a significant effect on the calculated end state. Three different cases were examined:

- Gas partitioning: The noncondensable gas originally occupying the upper plenum, upper head, and hot legs (up to the surge line connection) is compressed into all of the nonliquid filled downstream spaces.

a. The behavior of the pressurizer is treated as a variable and is subsequently discussed.

This includes the hot legs downstream of the surge line connection, pressurizer, steam generator, and cold legs. After the steam/gas "front" passes the surge line connection, only steam enters the pressurizer as the compression continues. This assumption fixes the relative amounts of noncondensable gas in the pressurizer and downstream areas.

- No gas exchange in the pressurizer: The amount of noncondensable gas initially in the pressurizer remains at its initial value for the whole duration of the compression process. Essentially, no noncondensable gas enters or leaves the pressurizer.

- Purging of gas in the pressurizer: Since heated steam is lighter than the noncondensable gas, steam rises to the top of the pressurizer, gradually fills the pressurizer, and forces all of the noncondensable gas in the pressurizer out into the rest of the RCS. The amount of the noncondensable gas added into the hot leg is known and can be added to the passive section of the steam generator tubes.

The important difference between each of these assumptions is the amount of noncondensable gas that ends up compressed into the steam generator and cold legs. As will become evident, the steady-state RCS pressure is very sensitive to this variable.

Application of the Gibbs-Dalton Law of Partial Pressures to the passive section of the steam generator gives the total RCS pressure

$$p_{Total} = p_{sat}(T_{sec}) + p_{NC} \tag{B-1}$$

where

p_{sat} = water vapor partial pressure

T_{sec} = secondary side fluid temperature

p_{NC} = pressure of the compressed noncondensable gas volume and p_{NC} is determined from the Ideal Gas Law

$$p_{NC} = \frac{m_a R T_{sec}}{V_{NC}} \tag{B-2}$$

where

m_a = mass of air/nitrogen

R = universal gas constant

V_{NC} = volume of the passive section

Now V_{NC} can be calculated from the relationship

$$V_{NC} = (N_L - N_{Dams}) \left[V_{OTS} + V_{OP} + V_{LSgas} + \frac{V_{Tubes}(L_{Tubes} - L_c)}{L_{Tubes}} \right] \tag{B-3}$$

where

N_L = number of primary loops

N_{Dams} = number of steam generators with a pair of nozzle dams installed

V_{OTS} = volume of the steam generator outlet tube sheet

V_{OP} = volume of the steam generator outlet plenum

V_{LSgas} = noncondensable gas volume in the cold leg loop seal

V_{Tubes} = volume of the steam generator tubes

L_{Tubes} = length of the steam generator tubes

L_c = condensing length

and L_c is the only unknown. By combining Equations (B-1) through (B-3), one forms an equation for the pressure necessary to compress the noncondensable gas into the steam generator

$$p_{Total} = p_{sat}(T_{sec}) + \frac{m_a R T_{sec}}{(N_L - N_{Dams})} \left[V_{OTS} + V_{OP} + V_{LSgas} + V_{Tubes}\left(1 - \frac{L_c}{L_{Tubes}}\right) \right]^{-1} \quad \text{(B-4)}$$

The heat transfer across the steam generator tubes can be expressed in each of three separate sections: primary, tube wall, and secondary. Thus,

$$Q_o \equiv Q_p = Q_w = Q_s \quad \text{(B-5)}$$

where

Q_o = power

Q_p = primary side heat transfer

$$= \bar{h}_p \pi D_{iSG} L_c N_T N_{act} (T_{sat} - T_{wp}) \quad \text{(B-6)}$$

where

$\bar{h}_p$ = average heat transfer coefficient on primary side

D_{iSG} = steam generator tube inner diameter

N_T = number of steam generator tubes per steam generator

N_{act} = number of active steam generators

T_{sat} = saturation temperature

T_{wp} = primary side wall temperature

Q_w = steam generator tube heat transfer

$$= \frac{k_w 2\pi L_c N_T N_{act}}{\ln(D_{oSG}/D_{iSG})}(T_{wp} - T_{ws}) \quad \text{(B-7)}$$

where

k_w = thermal conductivity of the steam generator tube wall

D_{oSG} = steam generator tube outer diameter

T_{ws} = secondary side wall temperature

Q_s = secondary side heat transfer

$$= \bar{h}_s \pi D_{oSG} L_c N_T N_{act} (T_{ws} - T_{sec}) \quad \text{(B-8)}$$

where

$\bar{h}_s$ = average heat transfer coefficient on secondary side.

These equations can be combined and rearranged to yield an equation with only T_{sat} and L_c as unknowns

$$T_{sat} = T_{sec} + \frac{Q_o}{2\pi L_c N_T N_{act}}\left[\frac{2}{\bar{h}_p D_{iSG}} + \frac{\ln(D_{oSG}/D_{iSG})}{k_w} + \frac{2}{\bar{h}_s D_{oSG}}\right] \quad \text{(B-9)}$$

This gives two equations [Equations (B-4) and (B-9)] and two unknowns (T_{sat} and L_c). A mathematical expression can easily be found for relating saturation temperature to saturation pressure (e.g., the Antoine equation or a similar correlation). This pair of equations and unknowns is easily solved by readily available numerical solution schemes. The Newton-Raphson method was selected because of its relative ease of use.

In Equation (B-9), the only variables that are not given by a property table or set constant are the primary and secondary heat transfer coefficients. Thus, correlations for these two variables must be developed for the particular flow regimes occurring inside and outside the steam generator tubes. These correlations are presented in the next section.

B-2.2 Heat Transfer Coefficient Correlations

Heat transfer coefficient correlations are needed for both the primary and secondary sides of the steam generator tubes. On the primary side, two types of heat transfer processes may occur: falling film condensation when only the vapor phase (and possibly noncondensable gas) enters, and condensation of a two-phase mixture when the froth level, because of mixture-level swelling, enters the steam generator. On the secondary side, heat transfer coefficient correlations for natural convection under both nonboiling and boiling conditions are needed. The heat transfer coefficient correlations used in the present analyses are given in the following subsections.

B-2.2.1 Falling Film Condensation. The heat transfer coefficient for condensation of a pure vapor onto the inner surface of a steam generator tube is obtained from the classical Nusselt analysis of this process.[4] In the Nusselt analysis, a boundary layer of liquid forms on a cooled solid surface and flows

downward because of gravity. The liquid boundary layer thickness increases in the direction of flow down the tube as the vapor condenses onto the liquid at the liquid-vapor interface. Conduction across the film resists heat transfer, and as the film thickness increases down the tube, the heat transfer coefficient decreases. The classical Nusselt analysis is based on the assumption of laminar flow in the liquid film. Although this seems to be a conservative assumption, it is quite applicable to the present case and is verified by calculation of the liquid-film Reynolds number

$$Re_f = 4W_f/(P_w \mu_{fs}) \tag{B-10}$$

where

W_f = mass flow rate of liquid condensate

P_v perimeter of the tubes

μ_{fs} = viscosity of the saturated liquid.

The liquid condensate mass flow rate is given by

$$W_f = Q_o/h_{fg} \tag{B-11}$$

where

Q_o = decay power

h_{fg} = latent heat of vaporization at the pressure of interest.

The perimeter of the tubes is expressed as

$$P_w = N_{act} N_T \pi D_{iSG} \tag{B-12}$$

where

N_{act} = number of active steam generators

N_T = number of tubes per generator

D_{iSG} = inside diameter of the tubes.

As an example, for the H. B. Robinson plant with one active steam generator, with $N_T = 3,214$ and $D_{iSG} = 0.01968$ m (0.775 in), at a pressure of 0.40 MPa (about 60.0 psia), and decay power of 20.0 MW, the liquid film Reynolds number is approximately 250 (below the transition-to-turbulence value of about 500).[4] The Reynolds number increases with diameter, pressure, and power and decreases with the number of active steam generators. The value of 20 MW is larger than is ever expected for reduced inventory conditions, and using one active steam generator results in the largest Reynolds number that will be encountered. The Nusselt analysis also assumes a constant thermodynamic state (density and latent heat), transport properties (viscosity and thermal conductivity), and steady-state conditions. With these assumptions, the local heat transfer coefficient is obtained as a function of distance, z, downward from the top of the liquid condensate film to be

$$h_p = \left[\frac{\varrho_{fs}(\varrho_{fs} - \varrho_{gs}) g h_{fg} k_{fg}^3}{z 4 \mu_{fs} (T_{sat} - T_{wp})} \right]^{1/4} \tag{B-13}$$

where

h_f = heat transfer coefficient on primary side

ρ_f = density of saturated liquid

ρ_g = density of saturated vapor

g = acceleration due to gravity

k_f = thermal conductivity of saturated liquid

z = elevation or direction of liquid condensate flow.

The average heat coefficient over the total condensate length, L_c, is

$$\bar{h}_p = \frac{1}{L_c}\int_0^{L_c} h_p(z)dz \tag{B-14}$$

which gives

$$\bar{h}_p = 1.943\left[\frac{\rho_f(\rho_f - \rho_g)gh_{fg}k_f^3}{L_c\mu_f(T_{sat} - T_{wp})}\right]^{1/4} \tag{B-15}$$

The average heat transfer coefficient on the primary side is therefore a function of the condensing length, L_c, which is one of the unknowns of the problem. The thermodynamic state and transport properties are functions of the pressure, which is also one of the unknowns of the problem.

The total energy transfer between the primary fluid and the inner wall surface is given by Equation (B-5). Putting Equation (B-15) into that equation for the heat transfer coefficient gives

$$Q_o = 0.943(N_{act}N_T\pi D_{iSG}L_c)\left[\frac{\rho_f(\rho_f - \rho_g)gh_{fg}k_f^3}{L_c4\mu_f(T_{sat} - T_{wp})}\right]^{1/4}(T_{sat} - T_{wp}) \tag{B-16}$$

B-2.2.2 Two-Phase Mixture Heat Transfer. Under some conditions of power and initial liquid level, a two-phase mixture may enter the steam generator tubes. The flow pattern in the tubes for this case is very complex. The mixture is entering the tubes, the vapor is condensing on the tube surface and flowing downward under the action of gravity, and the overall mixture flow rate is generally low. The flow may look somewhat like countercurrent, annular flow at low flow rates. There are no heat transfer coefficient correlations in the literature for these conditions. The correlation from Carpenter and Colburn as reported by Collier[4] is used as a preliminary estimate of the heat transfer coefficient under these conditions. For laminar flow of the vapor alone in the tubes, the heat transfer coefficient is

$$\bar{h}_p = 1.623\left(\frac{k_f\rho_f C_{pfs}}{\mu_{fs}}\right)^{1/2}\frac{G_{in}^3}{\rho_g\mu_{gs}A_{fp}} \tag{B-17}$$

where

C_{pfs} = liquid specific heat at constant pressure at saturation

G_{in} = mass flux in the steam generator tubes

μ_{gs} = viscosity of saturated vapor

A_{fp} = cross-sectional flow area for all the active steam generator tubes.

For turbulent flow of the vapor alone, the heat transfer coefficient is

$$\bar{h}_p = 0.002\left(\frac{k_{fs}\rho_{fs}C_{pfs}}{\mu_{fs}}\right)^{1/2}\frac{G_{in}^2}{\rho_{gs}}\left(\frac{\mu_{gs}A_{fp}}{0.58G_{in}}\right)^{-0.2} \quad \text{(B-18)}$$

The total energy transfer between the primary fluid and the inner wall surface is obtained by putting the appropriate heat transfer coefficient into Equation (B-5).

B-2.2.3 Secondary Side Natural Convection Heat Transfer. The heat transfer on the secondary side of the steam generator can be either single-phase natural convection or boiling two-phase heat transfer. The heat transfer coefficient for single-phase natural convection is obtained from a correlation based on heat transfer from heated vertical surfaces. On the steam generator secondary side, the natural convection heat transfer occurs on the outside of an array of tubes. The correlations available in the literature are primarily for natural convection adjacent to vertical flat plates and single cylinders. These correlations are assumed to be applicable to the process on the secondary side of the steam generator.

For natural convection adjacent to vertical plates and cylinders, the heat transfer coefficient is obtained from the Nusselt number given by[5]

$$\overline{Nu} = 0.0210(GrPr)^{0.40} \quad \text{(B-19)}$$

where

Gr = Grashof number

Pr = Prandtl number.

The average Nusselt number over the condensing length is

$$\overline{Nu} = \frac{\bar{h}_s L_c}{k_f} \quad \text{(B-20)}$$

where

k_f = thermal conductivity of subcooled liquid.

The product of the Grashof and Prandtl numbers is

$$GrPr = \frac{c_{pf}\beta_f \rho^2 \Delta T L_c^3}{\nu^2 k_f} \quad \text{(B-21)}$$

where

c_{pf} = liquid specific heat at constant pressure

β_f = coefficient of liquid thermal expansion

ΔT = change in temperature

ν = kinematic viscosity

and the temperature difference between the outer wall surface and the bulk liquid is

$$\Delta T = T_{ws} - T_{sec} \tag{B-22}$$

The total energy transfer between the outer surface and the bulk fluid is

$$Q_o = \bar{h}_o A_w \Delta T \tag{B-23}$$

where

A_w = wall heat transfer area

or

$$Q_o = 0.0210(N_{act} N_T \pi D_{oSG}) k_f \left[\frac{c_{pf} \beta_f g \Delta T L_c^3}{\nu^2 k_f} \right]^{0.40} (T_{ws} - T_{sec}) \tag{B-24}$$

For boiling conditions on the secondary side, the energy transfer is given by the Thom correlation[4] for fully developed subcooled boiling of water. The correlation gives the wall superheat required for the heat flux, q_w, as

$$(T_{ws} - T_{sat}) = 22.65 q_w^{0.5} e^{-p/87.0} \tag{B-25}$$

where q_w is measured in MW/m^2 and p = pressure (bar). In terms of the decay power, Q_o, and the heat transfer area on the secondary side of the steam generators, Equation (B-25) is

$$(T_{ws} - T_{sat}) = 22.65 \left(\frac{Q_o}{N_{act} N_T \pi D_{oSG} L_c} \right)^{0.5} e^{-p/87.0} \tag{B-26}$$

B-2.3 Level Swell from Boiling in the Core

Once boiling begins in the core, steam bubbles will rise into the upper plenum. Since the steam bubbles occupy more volume than a like quantity of liquid, the water level in the reactor vessel will swell into upward voids. The vapor will move by buoyancy upward through the core-outlet region, upper plenum, and into the hot leg pipes. If the rise in mixture level reaches the top of the hot legs, steam will begin collecting in the upper head. This will cause the upper head pressure to increase, forcing the mixture level in the reactor vessel downward until enough of a hot leg flow area is established to relieve the upper head pressure buildup. Under these conditions, a two-phase mixture will flow down the hot leg and into the steam generator. If this steam-water mixture reaches the steam generator tubes, the simplified Nusselt film condensation model for

heat transfer applied to the primary side of the steam generators is inappropriate and a heat transfer model appropriate for two-phase condensation must be used.

The drift flux model may be used to estimate the degree of level swell in the reactor vessel. The drift flux model uses continuity equations to describe the distribution of the liquid and vapor phases in a two-phase mixture. The continuity equations for the vapor and liquid are, respectively,

$$\frac{d}{dz} j_g = \frac{\Gamma_g}{\varrho_g} \tag{B-27}$$

and

$$\frac{d}{dz} j_f = -\frac{\Gamma_g}{\varrho_g} \tag{B-28}$$

where

j_g = superficial vapor velocity

j_f = superficial liquid velocity

Γ_g = vapor generation rate due to heat transfer in the core

ϱ_g = density of vapor.

At any axial location, the continuity equation for the mixture is

$$j = j_g + j_f \tag{B-29}$$

The void fraction from the drift flux model is[4]

$$\alpha_g = \frac{j_g}{C_o(j_g + j_f) + V_{gj}} \tag{B-30}$$

where

C_o = distribution coefficient

V_{gj} = vapor drift velocity.

Correlations are available for C_o and V_{gj}, and they are functions of the flow channel geometry and the two-phase flow regime. The local vapor generation rate is

$$\Gamma_g = -\frac{Q_o}{\varrho_g h_{fg} A_{fc}} \tag{B-31}$$

where

A_{fc} = flow area in the core.

For the case of saturated liquid at the inlet to the heated section, substituting Equation (B-31) into Equation (B-27) and performing the integration gives the vapor flux, j_g, as

$$j_g = \frac{Q_o z / L_{hc}}{\varrho_g h_{fg} A_{fc}} \tag{B-32}$$

where

L_{hc} = heated length of the core.

Putting Equation (B-32) into Equation (B-30) gives the local void fraction. The average void fraction is obtained by integrating the local fraction over the heated length of the fuel rods in the core

$$\bar{a}_{core} = \frac{1}{L_{hc}} \int_0^{L_{hc}} a_g(z) dz \tag{B-33}$$

and performing the integration gives

$$\bar{a}_{core} = \frac{1}{C_o} \left[1 - \frac{1}{Q_o^*} \ln(1 + Q_o^*) \right] \tag{B-34}$$

where

Q_o^* = nondimensional power

$$= \frac{C_o Q_o}{V_{gj} \varrho_g h_{fg} A_{fc}} \tag{B-35}$$

The vapor drift velocity, V_{gj}, is obtained from correlations of experimental data appropriate to the flow-channel geometry, two-phase flow regime, and operating conditions of interest. The situation of interest is the case of boiling in a stagnant pool of liquid. Kataoka and Ishii[6] have summarized the application of the drift flux model of two-phase flow to these situations. The vapor drift velocity for the churn-turbulent bubbly flow regime is

$$V_{gj} = 1.41 \left[\frac{\sigma g (\varrho_{ls} - \varrho_{gs})}{\varrho_{ls}^2} \right]^{1/4} \tag{B-36}$$

and for the slug flow regime

$$V_{gj} = 0.35 \left[\frac{g D_{hy} (\varrho_{ls} - \varrho_{gs})}{\varrho_{ls}} \right]^{1/2} \tag{B-37}$$

where

D_{hy} = hydraulic diameter

ϱ_{ls} = density of saturated liquid.

For the pressure range of interest in analyses of the loss-of-RHR incidents (0.1 to 0.4 MPa), these correlations give a drift velocity of about 0.2 m/s (0.6 ft/s).

The distribution coefficient, C_o, is given as a function of pressure by[4]

$$C_o = 1.2 - 0.2(\varrho_g/\varrho_f)^{1/2} \quad \text{(B-38)}$$

which gives a value of about 1.2 for the conditions of the loss-of-RHR incident. With V_{gj} from Equation (B-36) or (B-37), and C_o from Equation (B-38), the average void fraction of Equation (B-34) can be evaluated.

The voids generated in the core move upward by buoyancy into the core outlet and upper plenum. The void fraction in these regions can be evaluated by use of Equation (B-30) above with appropriate values of V_{gj} and C_o.

Void correlations give a wide range of void distributions in the core and the regions above the core. In many cases, a particular correlation combined with the initial liquid level and decay power will predict that the mixture will rise into the steam generator tubes and in some cases even go over the U-bend in U-tube steam generators. Some experimental confirmation of this possibility has been provided by experiments in the PKL system.[20] These tests, however, were conducted at power levels that are greater than those expected for loss-of-RHR incidents. This aspect of the response of PWR systems to loss-of-RHR incidents requires additional investigation.

If the froth level does enter the U-tubes, then a nonannular two-phase heat transfer coefficient must be calculated. From Reference 7, the following equation is used to determine the heat transfer coefficient during this situation:

$$\bar{h}_p = h_{2\phi}\gamma + h_{1\phi}(1 - \gamma) \quad \text{(B-39)}$$

where $h_{2\phi}$ is determined from either Equation (B-17) or (B-18), $h_{1\phi}$ is calculated using the Dittus-Boelter correlation for forced convection inside tubes

$$h_{1\phi} = 0.023 \frac{k_f}{D_{iSG}} \mathrm{Re}_f^{0.8} \mathrm{Pr}^{0.3} \quad \text{(B-40)}$$

and γ is calculated from the relationship

$$\gamma = \frac{\alpha_{UP}}{1 - \frac{2\delta}{D_{iSG}}} \quad \text{(B-41)}$$

where

α_{UP} = void fraction of the upper plenum

δ = liquid film thickness.

Correlations have been presented to determine the void fraction in the core and upper plenum and the effect on the primary heat transfer coefficient if a two-phase "froth" enters the steam generator U-tubes. Void fractions were calculated in the core region using the drift flux correlations and the results are shown as a function of decay power level in Figure B-1.

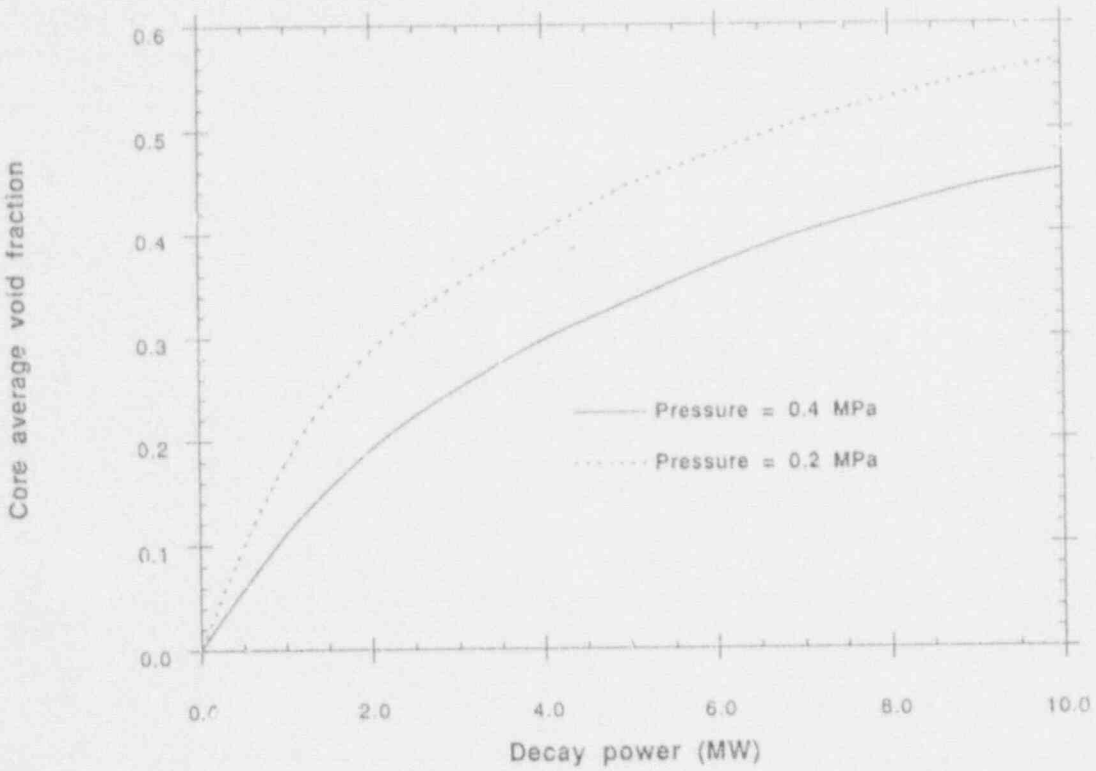

Figure B-1. Core average void fraction as a function of decay power for H. B. Robinson.

Because of the differences between drift flux correlations and the lack of experimental data for a froth level in the steam generator U-tubes, a large uncertainty exists for the proper values of C_o and V_{gj} to be used in Equation (B-33). Because of this uncertainty, it is important that a sensitivity study examines the effect of the primary heat transfer coefficient on RCS pressure. This study was performed and the results are reported in Section B-4.1.

B-2.4 Flooding of the Steam Generator U-Tubes

If the core decay heat power level is sufficiently high and only one steam generator is available for heat removal, the potential for flooding in the steam generator tubes exists. Under such a condition, the upward flow of steam into the tubes prevents a sufficient countercurrent flow of condensate to establish a mass flow balance. A liquid plug may then form in the tubes, leading to an unstable hydrostatic imbalance around the loop.

To evaluate the conditions under which flooding would occur, the Wallis correlation[8] was applied. The Wallis correlation is given by

$$\sqrt{j_g^*} + m\sqrt{j_f^*} = C \tag{B-42}$$

where

j_g^* = nondimensional superficial vapor velocity

$$= \frac{j_g\sqrt{\varrho_g}}{\sqrt{gD_{iSG}(\varrho_f - \varrho_g)}} \tag{B-43}$$

where

$$j_g = \frac{Q_c}{\varrho_g h_{fg} A_{SG} N_{act}} \tag{B-44}$$

where

A_{SG} = cross-sectional flow area per steam generator tube

j_f^* = nondimensional superficial liquid velocity

$$= \frac{j_f \sqrt{\varrho_f}}{\sqrt{g D_{iSG} (\varrho_f - \varrho_g)}} \tag{B-45}$$

where

ϱ_f = density of liquid.

For turbulent flow, m = 1, and for steam generator U-tubes, C = 0.8.[9]

Equations (B-42) through (B-45) can be used to determine j_f^* versus a reactor's power to obtain a curve of countercurrent flow limit (CCFL) for the desired system. Then, by using the mass balance between the liquid and vapor, a second curve can be obtained for the steady-state value of j_f^* versus reactor power. Therefore, the point where these two curves intersect is the maximum reactor power possible without exceeding a countercurrent limitation in the steam generator U-tubes. Experiments have also shown that CCFL occurs when j_g^* is greater than 0.5.[10,11,12,13,14,15] Figure B-2 shows this technique as applied to the H. B. Robinson Plant. For CCFL not to be a problem or area of concern with H. B. Robinson, the decay heat levels must be below 11 MW (shutdown for greater than 27 hours). Note that this point also has a j_g^* value just below 0.5.

B-2.5 Thermodynamic and Transport Properties

The model equations for the physical processes discussed in this appendix require thermodynamic equation-of-state properties and transport properties for water. Properties are needed for subcooled liquid, saturated liquid, and vapor states. For analysis of loss-of-RHR incidents, the properties are needed over a limited range of pressure.

High accuracy, high-order polynomials were fitted to tabulated thermodynamic and transport properties of water[16] over the ranges of pressure and temperature required for the analyses. The resulting polynomials, while accurate over the range of data from which they were obtained, cannot be extrapolated beyond the range of fitted data. For analyses of loss-of-RHR incidents in actual power plants, properties are needed over only very limited ranges of pressure. The experimental data from the Semiscale facility used to validate the models, however, required thermodynamic state and transport properties at a higher pressure and temperature. Additional polynomials were fitted for the pressure and temperature range of the Semiscale experiments.

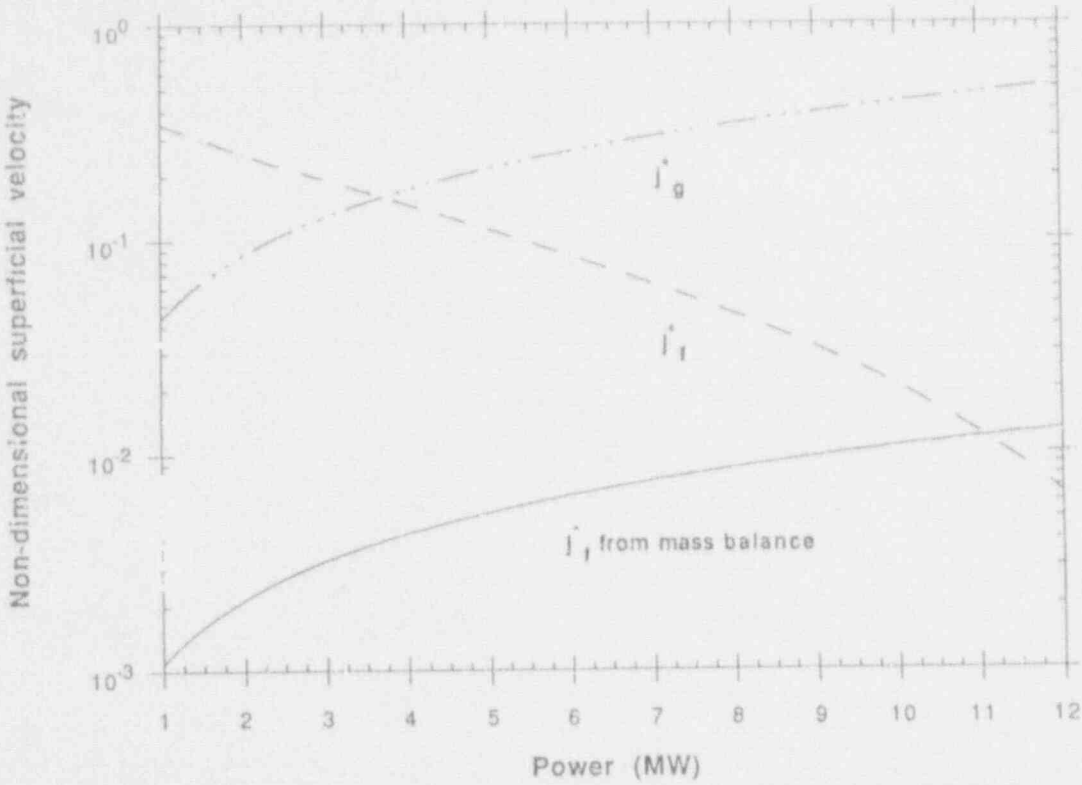

Figure B-2. Wallis flooding correlation for H. B. Robinson with one steam generator available as a heat sink (j_f^* from mass balance is calculated assuming all steam is condensed and flows downward as liquid).

B-2.6 Code Package Description

The appropriate equations from the previous sections were written into a FORTRAN77 computer program to solve for the RCS pressure and temperature, and the condensing length in the steam generator tubes. The program is broken into approximately 29 subroutines with each one performing a specific task. Table B-1 lists them by name with a description of each subroutine's computational task. Code compiling, debugging, and running are performed on a Macintosh IIci using Absoft's MacFortran/020™ software package in conjunction with the file editor QUED/M™ by Paragon Concepts.

A computational flow chart is given in Figure B-3 that shows the general order in which subroutines are executed. Four subroutines form the "Read input deck" section (RHRin, Build, Read1 and Read2). A good portion of the code is involved with the calculation of the equation constants, property values, size of the level swell, and in determining special volume sizes (DecHt, SubEOS, SatEOS, GasEOS, IntVol, HBRVol, OcoVol, Const, ConstO, Void, Root, and SysPro). Each flow chart block inside the iteration loop represents a single subroutine (from top to bottom: WalTem, WalThC, Hsys, Solver, Intout) and all are called from the HTC subroutine.

Two different methods exist to input the data needed for the calculations: reading two files or interacting on the terminal. The two input files are a control input file and a plant data file. An example of the control input file is given in Figure B-4 with appropriate comments on each input variable listed below the actual input data lines. The plant data files for H. B. Robinson and Oconee are given in Figures B-5 and B-6, respectively.

Table B-1. Subroutine listing.

Subroutine name	Description
RHRMain	Program driver
Zerout	Sets to zero all array and common block variables
RHRin	Reads the plant data file and control file or screen input
Build	Builds a plant data file
Read1 or 2	Reads the plant data file inside of RHRin
DecHt	Calculates the decay heat based on a shutdown time
SubEOS	Calculates subcooled water properties used by the code
SatEOS	Calculates saturated water properties used by the code
GasEOS	Calculates vapor and gas properties used by the code
Table	Prints the property values in a tabular form
Intvol	Determines water and gas volumes and dependent variables
HBRVol	H B Robinson's water and gas volumes
OcoVol	Oconee's water and gas volumes
HTC	Driver subroutine that contains the iteration loop
Const	Calculates parameters that do not change with each iteration
ConstO	Same as Const except especially applied to Oconee
SysPro	Calculates system wide parameters
Root	Calculates the angle between vertical and the water level in the hot leg during stratified flow
Void	Calculates the level swell
Psat	Calculates the saturation pressure and temperature
Hsys	Calculates the heat transfer coefficients
WalTem	Calculates the temperatures across the steam generator tubes
WalThC	Calculates the steam generator's wall thermal conductivity
Solver	The Newton-Raphson numerical solver subroutine
DrySol	Calculates the results if the condensing length exceeds the steam generator tube length
Intout	Prints the intermediate results at the end of each iteration
Conver	Checks to see if the iteration scheme has converged
RHRout	Prints the final results

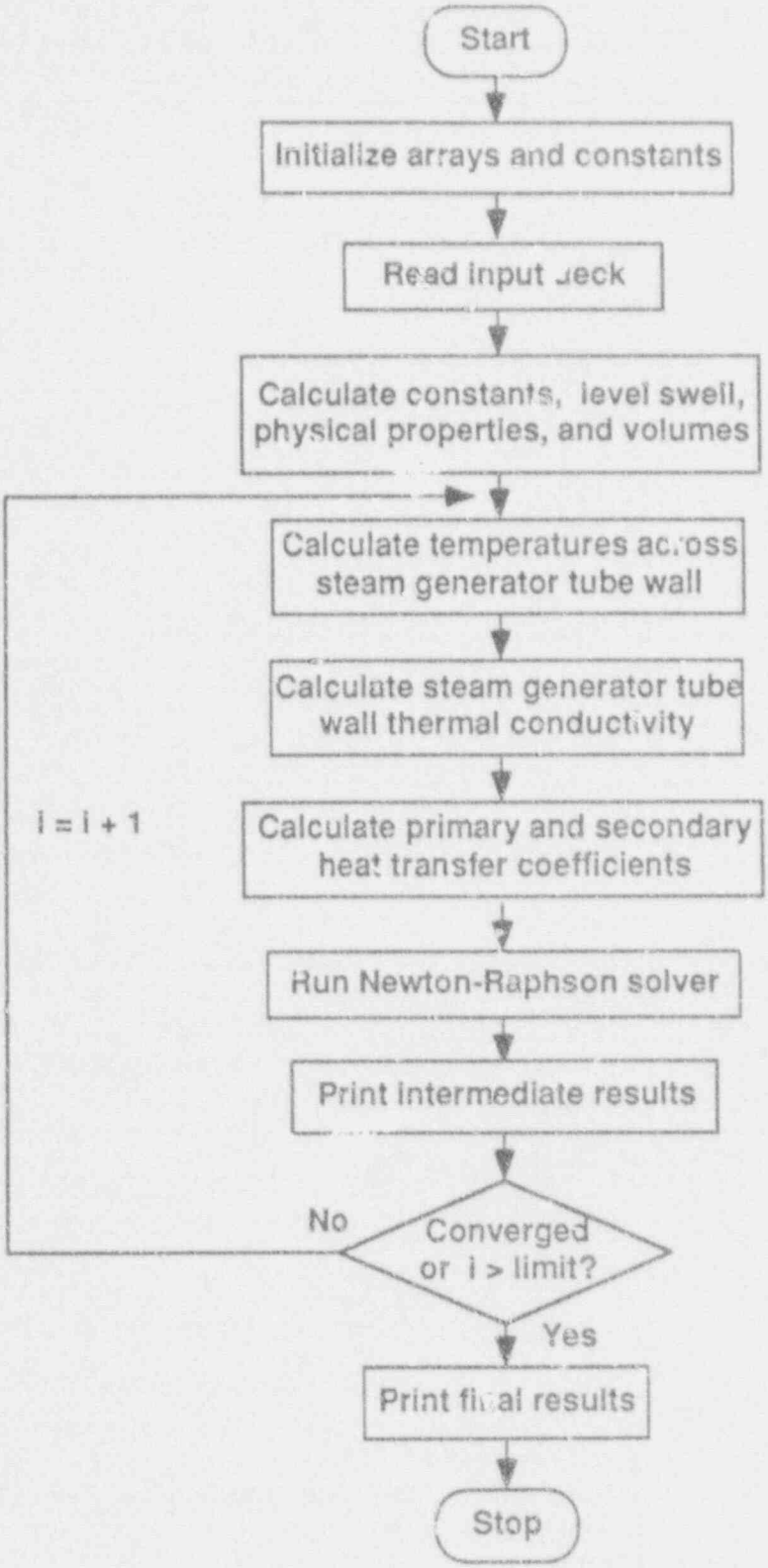

Figure B-3. Computational flow chart for the Piston Model code package.

```
3  1  2  0  2
48.0  0.101325  333.15  75.
374.15  0.101325  1  0
```

The above input is for the following variables

First Line:	Ielev0, Iedhs, Model, Irel, Iair
Second Line:	TimeSD, Pres0, Temp0, Pcta
Third Line:	TSGS0, PSGS0, ISGact, ISGdam

Variable Description:

Ielev0 Water level in the RCS
1. Top of core
2. Core outlet
3. Mid-loop operation.

Iedhs Heat Transfer Coefficient (HTC) input control:
1. Calculate the Primary HTC.
2. Input the Primary HTC as a constant.
3. Input the Secondary HTC as a constant.

Model Type of plant conditions to use:
1. No level swell in the RCS, no boiling in the SGs.
2. No level swell in the RCS, boiling in the SGs.
3. Level swell in the RCS, no boiling in the SGs.
4. Level swell in the RCS, boiling in the SGs.

Irel Type of correlation for the void fraction of the RCS coolant if level swell is taken into account:
0. Average of Sterman & Dimentiev and Wilson et al. correlations.
1. Sterman & Dimentiev correlation.
2. Wilson et al. correlation.

Iair Type of noncondensable gas displacement to be used:
1. Displace or mix everywhere.
2. Displace or mix only where steam flows + upper head.

TimeSD Time after shutdown in hours.
Pres0 Initial RCS pressure in MPa.
Temp0 Initial RCS temperature in degrees K.
Pcta Percent of air in the hot leg (ie 50.0 for 50%).
TSGS0 Final temperature of the steam generator in degrees K.
PSGS0 Final pressure in the steam generator in MPa.
ISGact The number of steam generators available as a heat sink.
ISGdam The number of loops with installed nozzle dams.

Figure B-4. An example of a control input file.

HBR Data (Section name, volume (m^3), and ref. height (m))		
Steady–State 100% Power	2300.0000	
Number of RCS Loops	3	
Lower Plenum	20.4068	2.9962
Core Region	20.4813	3.8606
Core Out Region	6.3747	0.7440
Upper Plenum (Lower)	0.9065	0.1227
Upper Plenum (Middle)	5.4407	0.7366
Upper Plenum (Upper)	14.9461	1.7257
Upper Head Region	14.8539	5.3777
Hot Outlet Pipe	3.0120	0.7370
SG Inlet Plenum	3.2600	1.0000
Inlet Tube Sheet	0.5420	0.5540
Hot Straight Section	9.3434	9.5512
U Bend Region	0.0000	0.0000
Cold Straight Section	9.3434	9.5512
Outlet Tube Sheet	0.5420	0.5540
SG Outlet Plenum	3.2600	1.0000
RCP Suction Leg Pipe	3.9190	2.1388
Reactor Coolant Pump	5.2046	1.2217
RCP Discharge/Cold Leg	2.4806	0.0000
Downcomer (Lower)	9.9392	5.1084
Downcomer (Low Middle)	1.6304	0.7440
Downcomer (Middle)	0.2640	0.1227
Downcomer (Up Middle)	1.5848	0.0684
Downcomer (Upper)	3.0334	1.7257
Pressurizer	36.8160	11.0060
Przr Surge Line	0.9960	2.7920
SG Secondary Side	93.6890	15.2590
Other Plant Data		
U–Tubes in a SG	3214	
U–Tubes Inner Diameter	0.019684	
U–Tubes Wall Thickness	0.01 368	
Total SG Flow Area	0.9780	
Hot Leg Pipe Diameter	0.736601	
Loop Seal Volume	3.688300	
Core X–Section Flow Area	3.871270	
Core SubChannel Hyd. Dia.	0.011278	

Figure B-5. Plant data file for the H. B. Robinson plant.

C nee.Data (Section name, volume (m^3), and ref. height (m))		
Steady-State 100% Power	2568.	
Number of RCS Loops	2	
Lower Plenum	0.1623E+02	0.2398E+01
Core Region	0.9709E+01	0.3658E+01
Core Out Region	0.3705E+01	0.6320E+00
Upper Plenum (Lower)	0.3463E+01	0.3493E+00
Upper Plenum (Middle)	0.9050E+01	0.9144E+00
Upper Plenum (Upper)	0.4907E+01	0.4967E+00
Upper Head Region	0.1380E+02	0.1748E+01
Hot Outlet Pipe	0.1501E+02	0.1127E+02
SG Inlet Plenum	0.6733E+01	0.1192E+01
Inlet Tube Sheet	0.1310E+01	0.6830E+00
Hot Straight Section	0.1939E+02	0.7942E+01
U Bend Region	0.0000E+00	0.0000E+00
Cold Straight Section	0.1939E+02	0.7942E+01
Outlet Tube Sheet	0.1489E+01	0.6100E+00
SG Outlet Plenum	0.7171E+01	0.1066E+01
RCP Suction Leg Pipe	0.8998E+01	0.9897E+01
Reactor Coolant Pump	0.3171E+01	0.1321E+01
RCP Discharge/Cold Leg	0.2567E+01	0.1036E+01
Downcomer (Lower)	0.1702E+02	0.4871E+01
Downcomer (Low Middle)	0.2206E+01	0.6314E+00
Downcomer (Middle)	0.6270E+00	0.3036E+00
Downcomer (Up Middle)	0.2095E+01	0.1006E+01
Downcomer (Upper)	0.3658E+01	0.1831E+01
Pressurizer	0.4306E+02	0.[illegible]8E+02
Przr Surge Line	0.5970E+00	0.[illegible]8E+01
SG Secondary Side	0.9704E+02	0.1589E+02
Steam Generator Data		
U-Tubes in the SG	15531	
U-Tube Inner Diameter	0.1408E-01	
U-Tube Wall Thickness	0.8640E-03	
Total SG Flow Area	0.2442E+01	
Hot Leg Pipe Diameter	0.9144E+00	
Loop Seal Volume	0.8998E+01	
Core Flow Area	0.4434E+01	

Figure B-6. Plant data file for Oconee.

Three types of output files are produced by the code. One is an output file with values of the major variables only, such as saturation temperature and pressure. A second type is a diagnostic file that virtually prints all variables that are calculated or used in each subroutine to aid in any type of code or run debugging. The last output file is one containing variable values produced in the iteration loop to evaluate the performance of the Newton-Raphson numerical method. This output file can be transferred easily to a Macintosh graphics package such as CricketGraph or KaleidaGraph for plotting.

B-3. MODEL ASSESSMENT

B-3.1 Theoretical and Experimental Support for the Piston Model

In the early 1980's, the effects of small break loss-of-coolant accidents (LOCAs) were the center of much attention in the nuclear industry. As part of the overall study of small break LOCAs, the limits of natural circulation heat removal were investigated; this included the reflux condensation mode. Several full-scale and individual component experiments were performed to characterize the reflux condensation heat transfer mode and to verify those thermal-hydraulic codes then in use by the industry. Appropriate experimental test data were obtained for assessment of the Piston Model to determine its accuracy in calculating system conditions.

The distribution of the noncondensable gases in the steam generator tubes is the crucial assumption in the Piston Model presented in this appendix. Reference 17 gives experimental results showing where the noncondensable gases go once they enter the steam generator tubes, and an analytical calculation to compare with these experimental results. It was determined, for the case when only steam enters the steam generator tubes, that three regions were established in an inverted U-tube along the length of the U-tube: an "active" zone, a very short transition zone, and a "passive" zone. The active zone contains only condensing water vapor at the temperature corresponding to the primary side saturation pressure. The passive zone contains a mixture of water vapor and noncondensable gases with no condensation occurring and a temperature equal to the secondary side temperature. The experiment also showed that the mixture of the steam-noncondensable gas in this passive zone is given by Dalton's Law so that the secondary temperature determines the partial pressure of the water vapor in the passive zone.

Reference 18, in part, examined the effect of noncondensable gases on the condensing length in an inverted U-tube. The Nusselt filmwise condensation theory and an energy balance across the U-tube was used to predict the condensing length. This analytical length was compared to experimentally measured condensing lengths. Their results showed the Nusselt theory to overpredict the true condensing length with the deviation becoming greater for higher steam flows. That is, a smaller length was measured than the condensing length determined using Nusselt's film condensation theory. The difference was attributed to two factors. The first is that Nusselt theory is for stagnant steam condensing on a vertical plate and not flowing steam condensing inside a vertical tube. The second factor is that dropwise condensation occurred locally in the upper portion of the condensing section. This was deemed to be the more dominant factor because of its much larger heat transfer rate.

The above experiments only examined the effects occurring in the steam generator's tubes. The code developed to evaluate the effects of loss of RHR must be applied to a complete RCS system. Thus, to truly validate the model, scaled system experiments needed to be found that examined the specific natural circulation regimes of concern to this report. Various closed system U-tube and thermosyphon experiments were examined and discarded because of a lack of information needed to accurately model or evaluate results with the Piston Model. Two scaled reactor system experiments were identified to have all of the necessary system information and experimental results. These are the Semiscale natural circulation experiment NC-6[19] and the PKL IIIB 4.5 test results for a loss-of-RHR event under reduced inventory conditions.[20]

B-3.2 Semiscale Natural Circulation Test NC-6

A series of natural circulation experiments was conducted in the Semiscale Mod-2A test facility to help verify codes that analyze the reactor system response to small break LOCAs. In one of these tests, NC-6, the test facility was placed in a reflux condensation mode under reduced coolant conditions. Then a series of nitrogen gas injections into the steam generator inlet plenum was performed to determine its effect on the condensation phenomena. This test was conducted at an operating system pressure of approximately 900 psia and at a decay heat level expected after a reactor scram. Reference 19 was used to provide an analytical method as a simple verification of the experiment results.

The Piston Model (using the Nusselt laminar film model) was evaluated for the conditions present during the NC-6 test run. The results from the model and the test runs are presented in Table B-2 and in Figure B-7. It is apparent that the code predicts the results from NC-6 reasonably well but tends to overpredict the pressure. This is consistent with the observation that the Nusselt laminar film condensing model will underpredict the average heat transfer coefficient, leading to a larger condensing length and greater noncondensable compression.

B-3.3 PKL Experiment Simulating a Failure-of-RHR Event Under Mid-loop Conditions

This experiment[20] closely approximates the reactor system conditions for a loss-of-RHR event during mid-loop operation. It was the only experiment found to specifically examine the system response during the low pressure, temperature, and power conditions existing when a plant is in cold shutdown with RHR cooling lost. Thus, this experiment should seemingly provide a good assessment of the Piston Model.

The system condition was shut down, at 323 K (122°F) and atmospheric pressure, with the RCS water level at mid-loop and nitrogen gas filling all RCS space above the water level. One steam generator was in wet-layup and the other three had their secondary sides drained but no dams installed. The reactor decay heat level was set to a value corresponding to 1% (0.25 MW) of full power and later lowered to 0.7% (0.175 MW). This power level is about twice as high as one would realistically expect because of the minimum of two days needed after shutdown to place the system in mid-loop operation.

This relatively high power level resulted in a large froth level being generated in the core, spread down the hot legs, and into the steam generator U-tubes. The resulting steam generation rate was high enough to be above a countercurrent flow limitation (Figure B-8), resulting in flooding of the steam generator U-tubes. The experimental results showed that a water slug formed on top of the condensing length. The water slug was at the temperature of the secondary side and remained for the duration of the experiment, even after the power was reduced to 0.7% (0.175 MW).

Table B-2. Semiscale analysis and experimental results.

Mass of N_2 injected (kg)	Predicted pressure (MPa)	Experimental pressure (MPa)	Error (%)
0.05614	6.410	6.1	5.08
0.19454	6.920	6.5	6.46
0.32641	7.415	7.1	4.44
0.41389	7.745	7.7	0.58

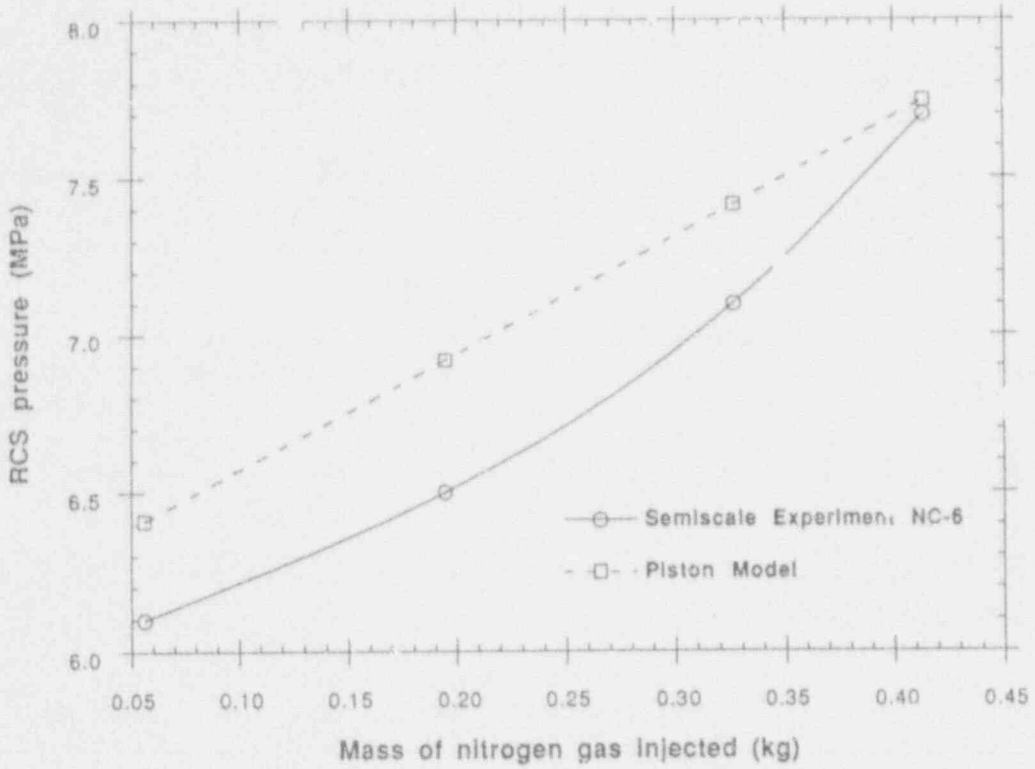

Figure B-7. Comparison of model and experimental results for Semiscale natural circulation test NC-6.

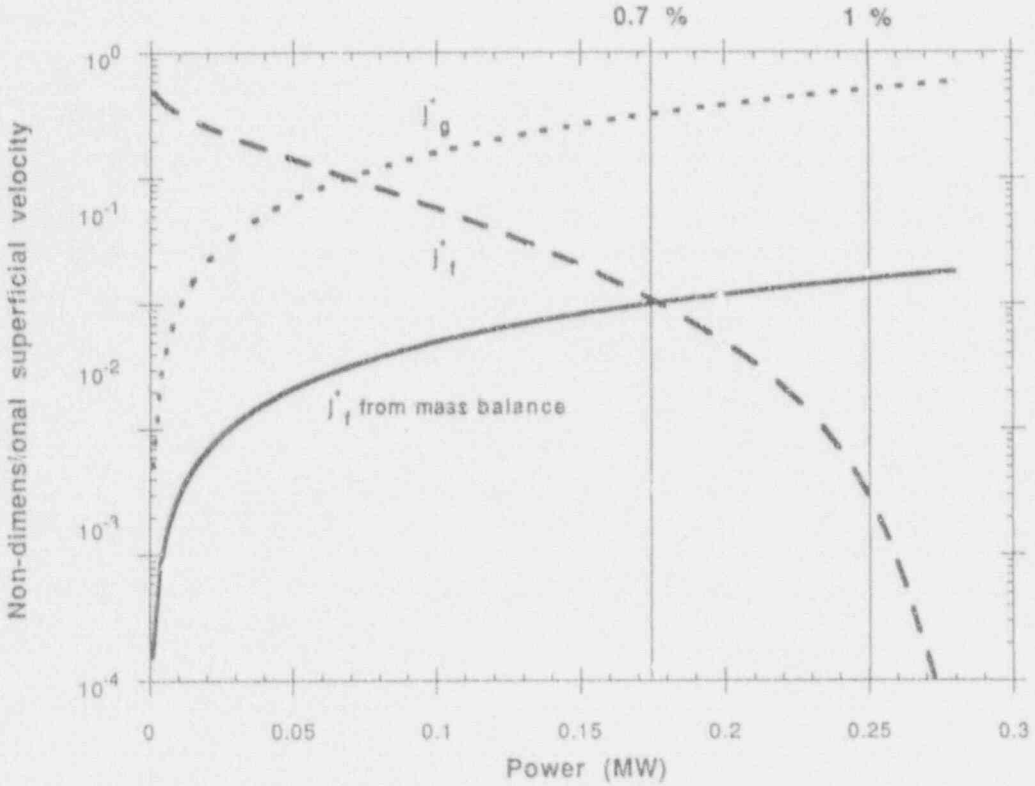

Figure B-8. Wallis flooding correlation for the PKL experimental facility for one steam generator available as a heat sink (j^*_f from mass balance is calculated assuming all steam condenses and flows downward).

The frothing phenomenon is an important effect with respect to the steady-state system conditions. If the Piston Model, as was verified by the Semiscale test, is used on this PKL experiment, the steady-state pressure is calculated to be significantly lower than the experiment's system pressure [4.3 bar (62 psia) vs. 6.6 bar (96 psia) at 1% power (0.25 MW) and 4.2 bar (61 psia) vs. 5.8 bar (84 psia) at 0.7% power (0.175 MW)]. This is not unexpected because the laminar film condensation model is no longer applicable when a two-phase mixture enters the steam generator tubes. Clearly, the void and volume growth in the core as a result of boiling impacts the final system conditions and needs to be taken into account in the model when such conditions occur.

The level swell model, as applied to the PKL Experiment IIIB 4.5 case at 1% power (0.25 MW), indicates that a froth level reaches the steam generators. When the two-phase nonannular heat transfer coefficient is used and compared to the analysis with the Nusselt heat transfer coefficient, the primary heat transfer coefficient decreases from 5329 to 3062 W/m^2-K (939 to 539 Btu/h-ft^2-°F) and the calculated RCS pressure increases only slightly from 4.3 to 4.8 bar (62 to 70 psia) [1.8 bar (26 psia) below the experiment's pressure at 1% power]. The results improve but clearly do not predict the conditions that occur during the experiment.

As a sensitivity study, the single-phase heat transfer correlation (Dittus-Boelter) was used in the Piston Model, and the PKL experiment analysis was repeated. The new results overpredict the RCS pressure by 0.9 bar (13 psia) [7.5 bar (109 psia) vs 6.6 bar (96 psia)]. The Dittus-Boelter correlation yields a primary heat transfer coefficient of about 250 W/m^2-K (44 Btu/h-ft^2-°F).

Therefore, the actual heat transfer coefficient for PKL Experiment IIIB 4.5 was between 250 and 3062 W/m^2-K (44 to 539 Btu/h-ft^2-°F). A back calculation of the experimental results yields a value of approximately 360 W/m^2-K (63 Btu/h-ft^2-°F), which falls between the previous two values.

One phenomenon not taken into account in the above analysis is the additional pressure needed to maintain a water slug above the condensing region in the steam generator U-tubes. If all of the up portions of the steam generator U-tubes were full of water from CCFL, the differential pressure across the water column would only be approximately 0.9 bar (13 psia). This means that in the situation of the PKL experiment, with two-phase nonannular flow and CCFL , the fluid entering the U-tube is mostly liquid (heat transfer coefficients around or below 500 W/m^2-K) and must support a water slug of 2 or more meters in height.

While neither of the correlations (two-phase nonannular or Dittus-Boelter) predict results within 10% of the experiment, the combination does set upper and lower limits that the RCS pressure should fall between. This means that one can determine a limit to the possible RCS pressure that could result from a loss-of-RHR event. Therefore, if one knows that the plant can withstand the upper limit, then it will also withstand the realistic situation with its lower RCS pressures, giving a conservative result.

B-4. PLANT CALCULATIONS

The Piston Model was applied to two classes of PWRs based on the type of steam generators used. The two classes are the inverted U-tube steam generator (UTSG) and the once-through steam generator (OTSG). The UTSGs are built by Westinghouse and Combustion Engineering and the OTSGs are built by Babcock and Wilcox. A representative plant of each type was studied based on the availability of the necessary plant data required by the model. The sources used for this information were existing RELAP5 input decks for the H. B. Robinson plant, a Westinghouse system, and the Oconee plant, a Babcock and Wilcox system. General system data are given for each of the plants in Table B-3.

Table B-3. System data.

Plant	Power [MW(Th)]	Number of RCS Loops	Comments
H. B. Robinson	2,300	3	—
Oconee	2,568	2	Lowered-loop plant, 2 reactor coolant pumps and cold legs per loop

Before the loss of RHR, each plant is assumed to be in its respective mid-loop operating condition. The system temperature is kept at or below 140°F (333 K) by the RHR system. A nitrogen purge blanket is also maintained above the water at atmospheric pressure. No manways are open; however, steam generator nozzle dams may have been installed in the case of the H. B. Robinson plant. The reactor vessel top head is in place and bolted down so the RCS can be considered a closed system.

B-4.1 Variations in Key Parameters

The time after shutdown is one of the key parameters that must be specified, since the decay heat level is dependent on time after shutdown. The decay heat level is calculated from the following relationship[21]:

$$P = 0.095P_o(3600\theta)^{-0.26} \qquad \text{(B-46)}$$

where

P_o = 100% steady-state power level (MW)

θ = time after shutdown (h).

It is known that certain operational procedures must be performed for a plant to be in the necessary cold shutdown condition and in a reduced inventory state.[22,23] Thus there exists a given time period from reactor shutdown to reaching reduced inventory, during which the decay heat level is decreasing. However, how quickly a plant can be cooled down and lined up for reduced inventory operation seems to depend on the type of plant shutdown maintenance to be performed. Three times were selected as being representative of the minimum time period to reach the conditions for mid-loop operations. Table B-4 lists these times with corresponding decay heat levels. In addition to these times, 30 days (720 hours) was also selected to give results for the long term.

Table B-4. Length of time to place RCS into mid-loop operation.

Time to mid-loop operation (h)	Decay heat (%)	Reference	Comments
48	0.413	23	Maximum cooldown and degas rates employed
83	0.358	22	No refueling
167	0.299	22	Shutdown for refueling

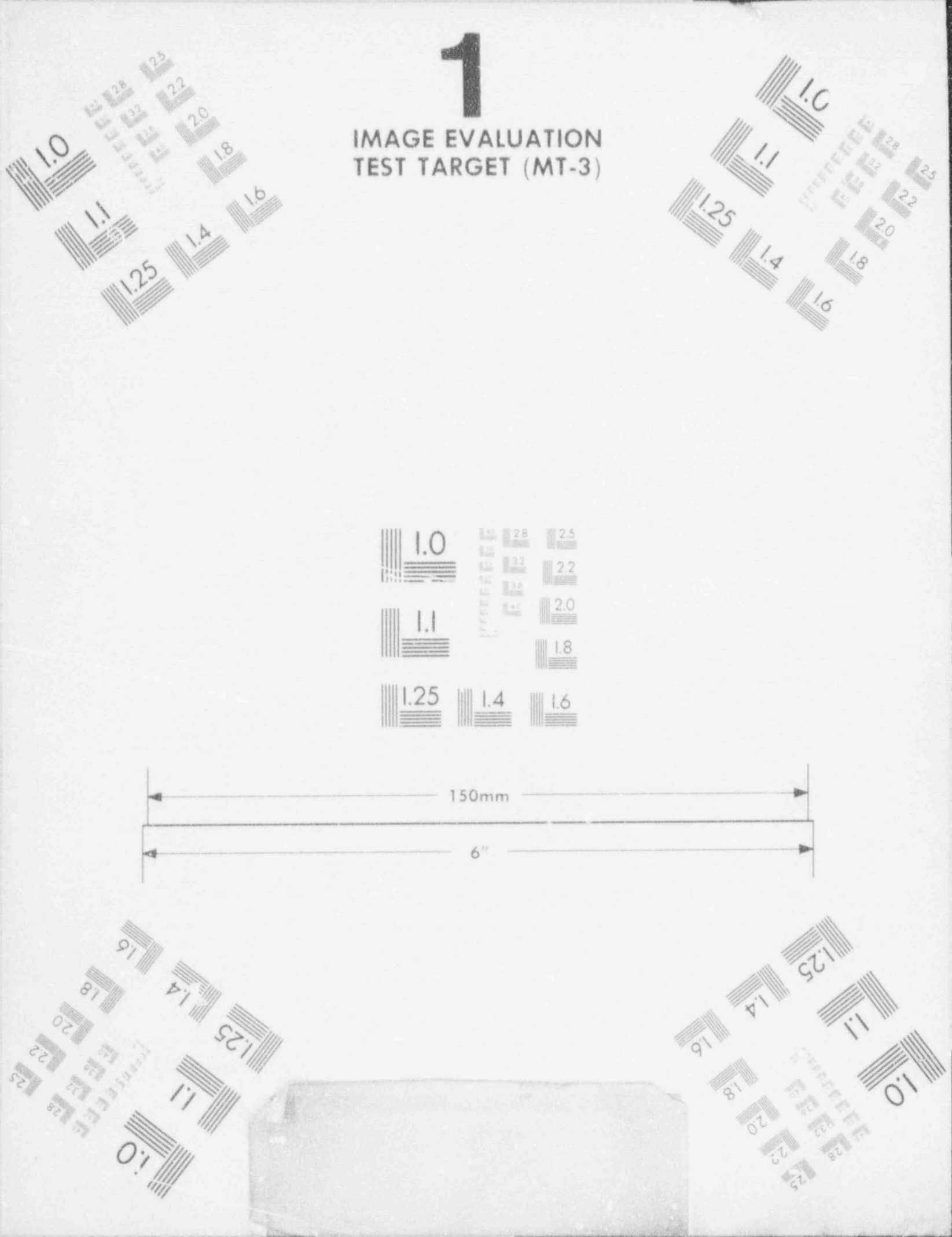
1
IMAGE EVALUATION
TEST TARGET (MT-3)
1.0
1.1
1.25
1.4
1.6
1.8
2.0
2.2
2.5
2.8
3.2
3.6
4.0
150mm
6"

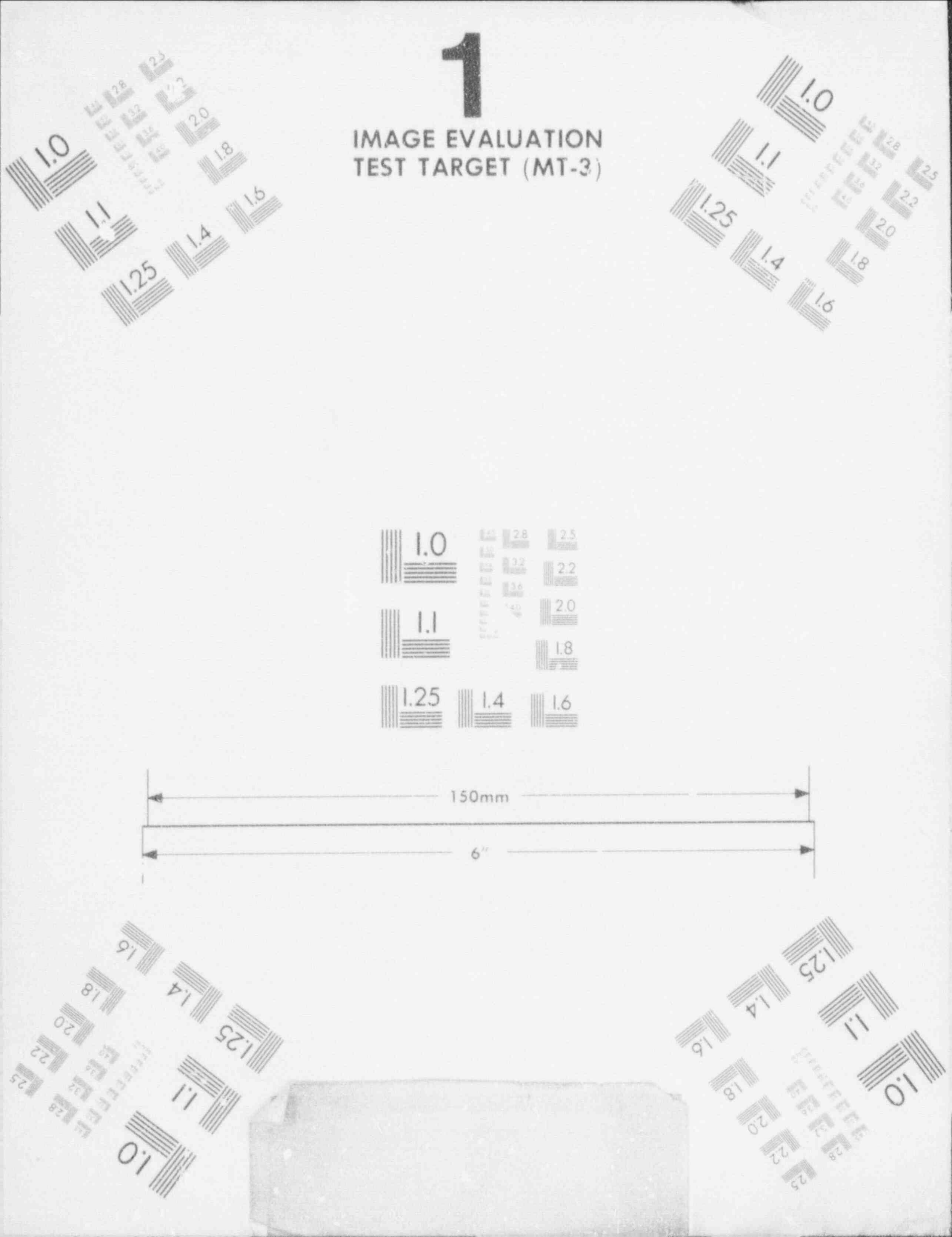
1
IMAGE EVALUATION
TEST TARGET (MT-3)
1.0
1.1
1.25
1.4
1.6
1.8
2.0
2.2
2.5
2.8
3.2
3.6
4.0
150mm
6"

1

IMAGE EVALUATION
TEST TARGET (MT-3)

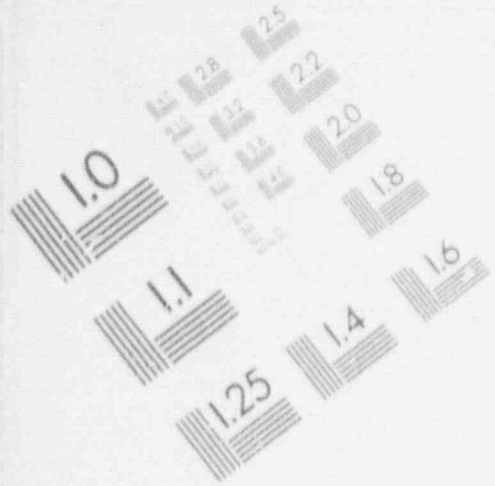

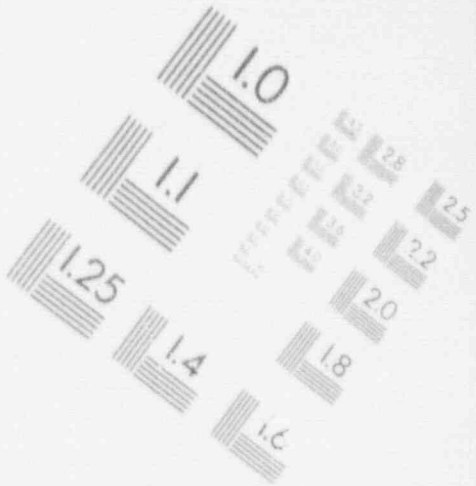

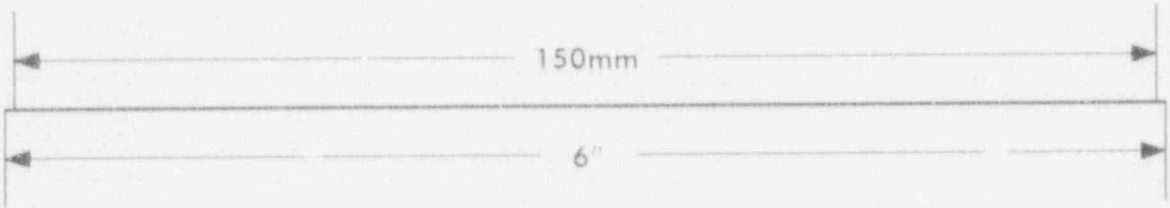

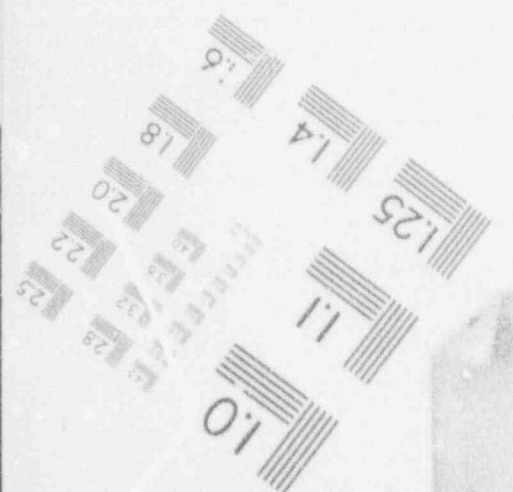

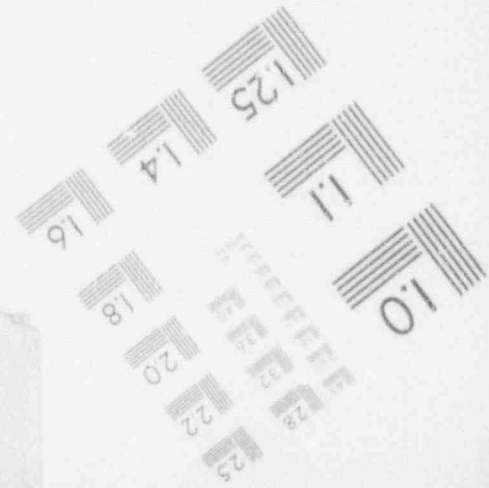

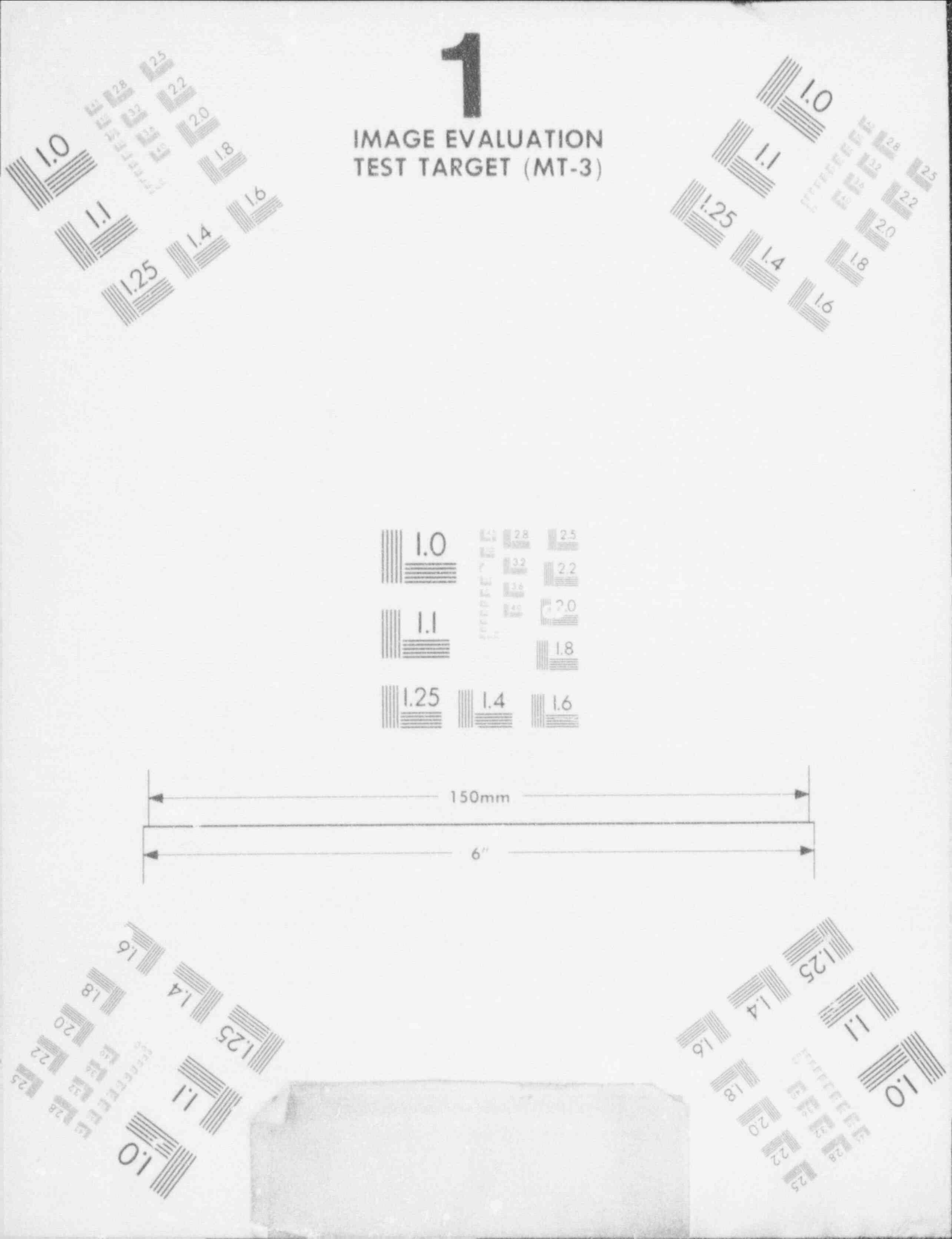
1
IMAGE EVALUATION
TEST TARGET (MT-3)
1.0
1.1
1.25
1.4
1.6
1.8
2.0
2.2
2.5
2.8
3.2
3.6
4.0
150mm
6"

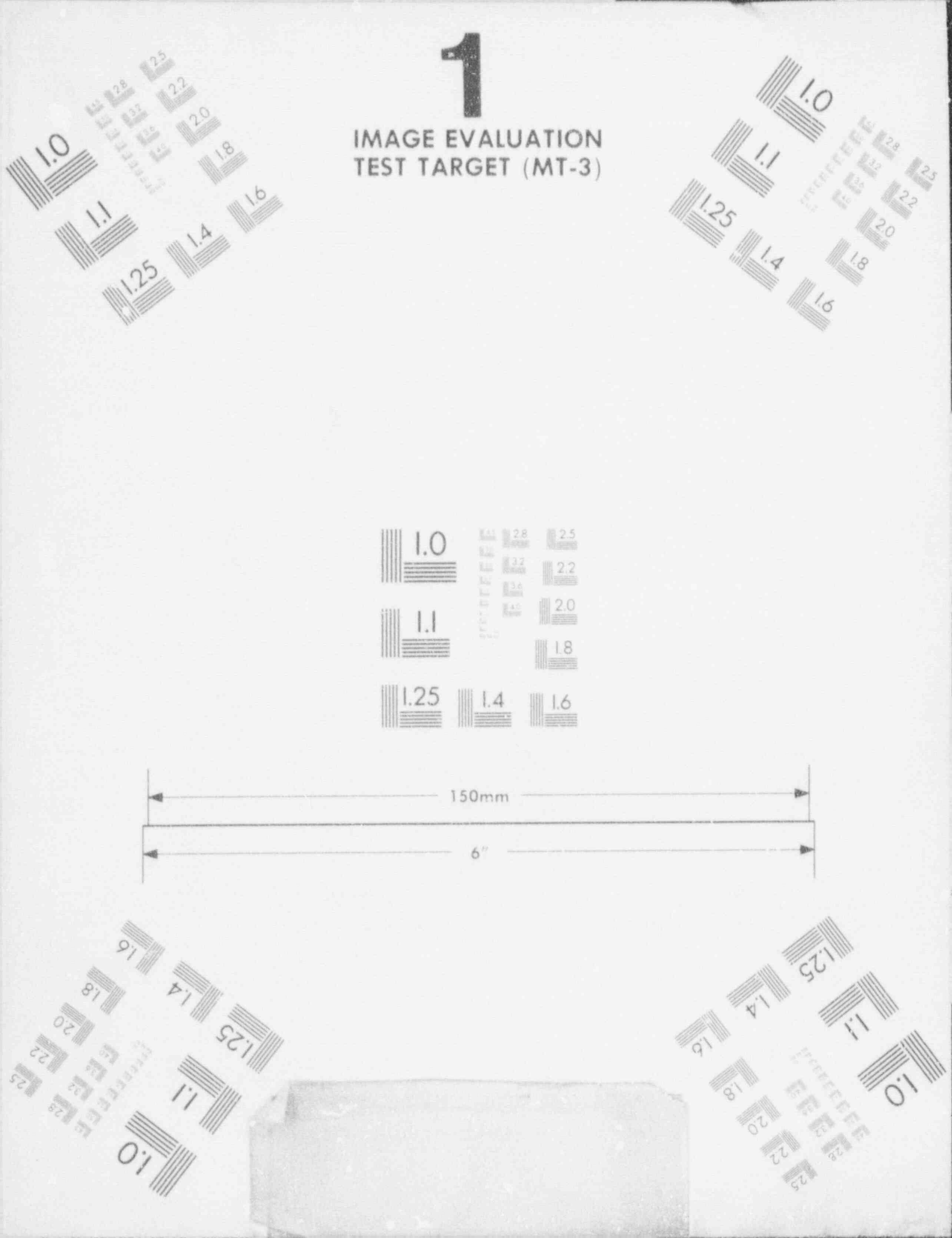
1
IMAGE EVALUATION
TEST TARGET (MT-3)
1.0
1.1
1.25
1.4
1.6
1.8
2.0
2.2
2.5
2.8
3.2
3.6
4.0
150mm
6"

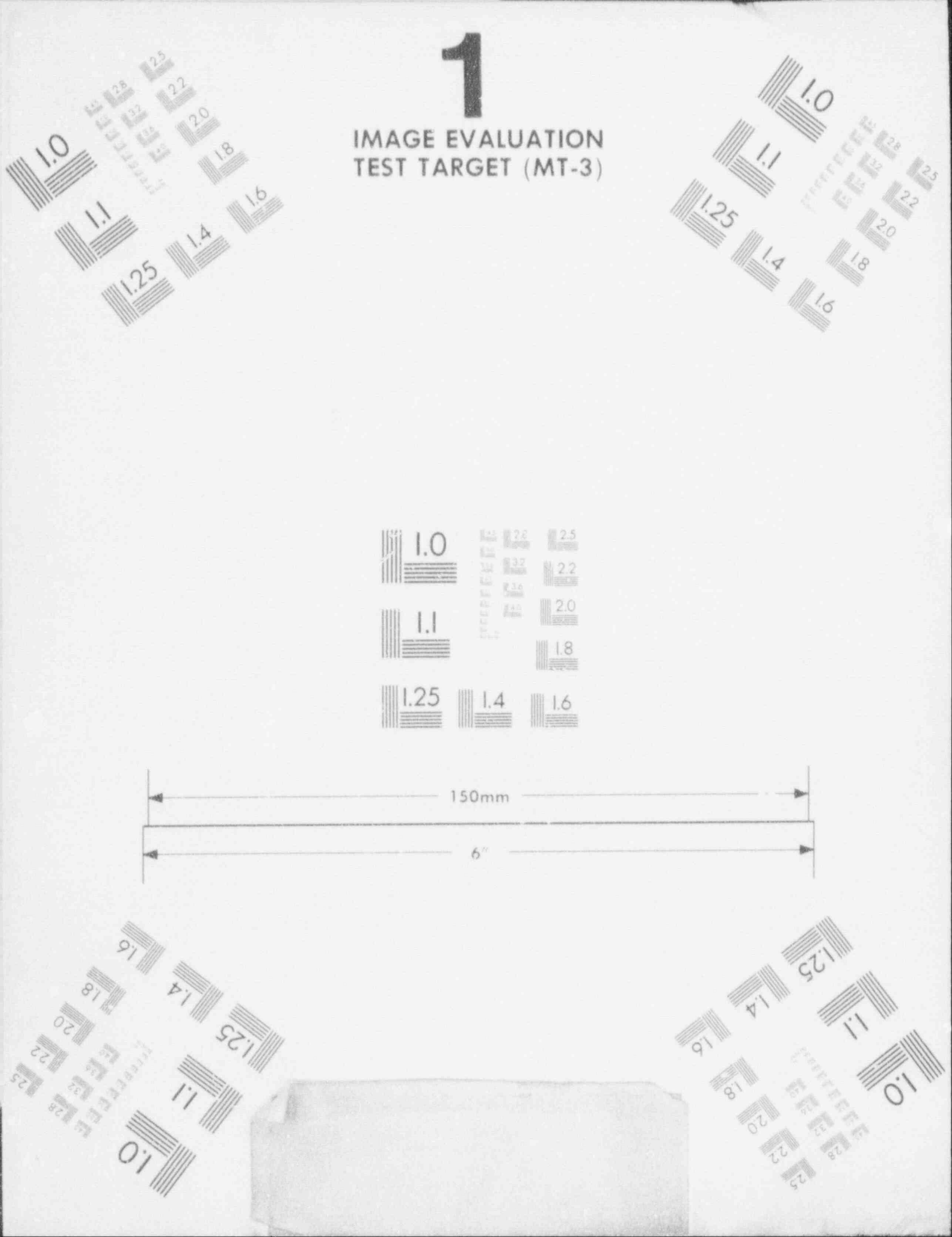
1
IMAGE EVALUATION
TEST TARGET (MT-3)
1.0
1.1
1.25
1.4
1.6
1.8
2.0
2.2
2.5
2.8
3.2
3.6
4.0
150mm
6"

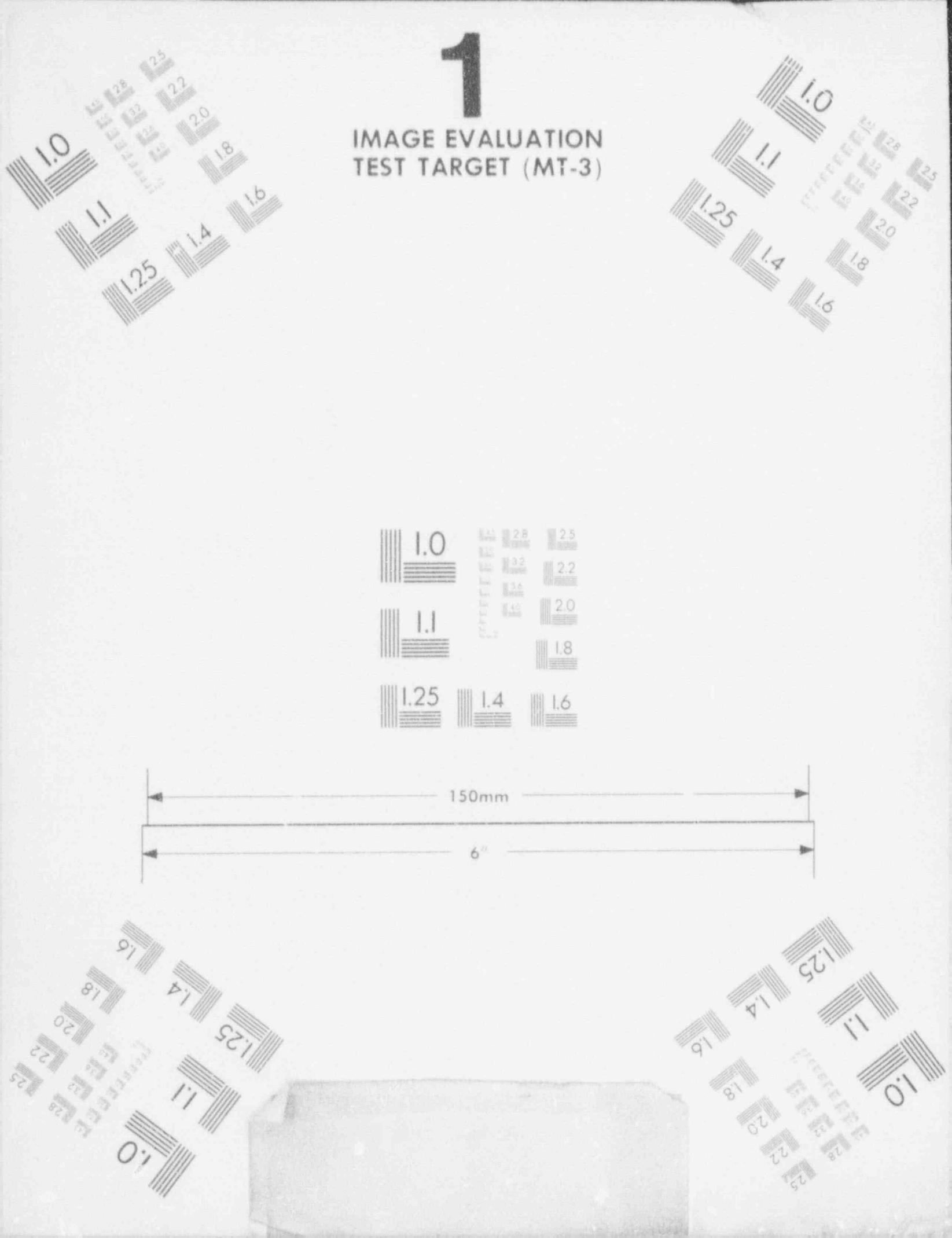
1
IMAGE EVALUATION
TEST TARGET (MT-3)
1.0
1.1
1.25
1.4
1.6
1.8
2.0
2.2
2.5
2.8
3.2
3.6
4.0
150mm
6"

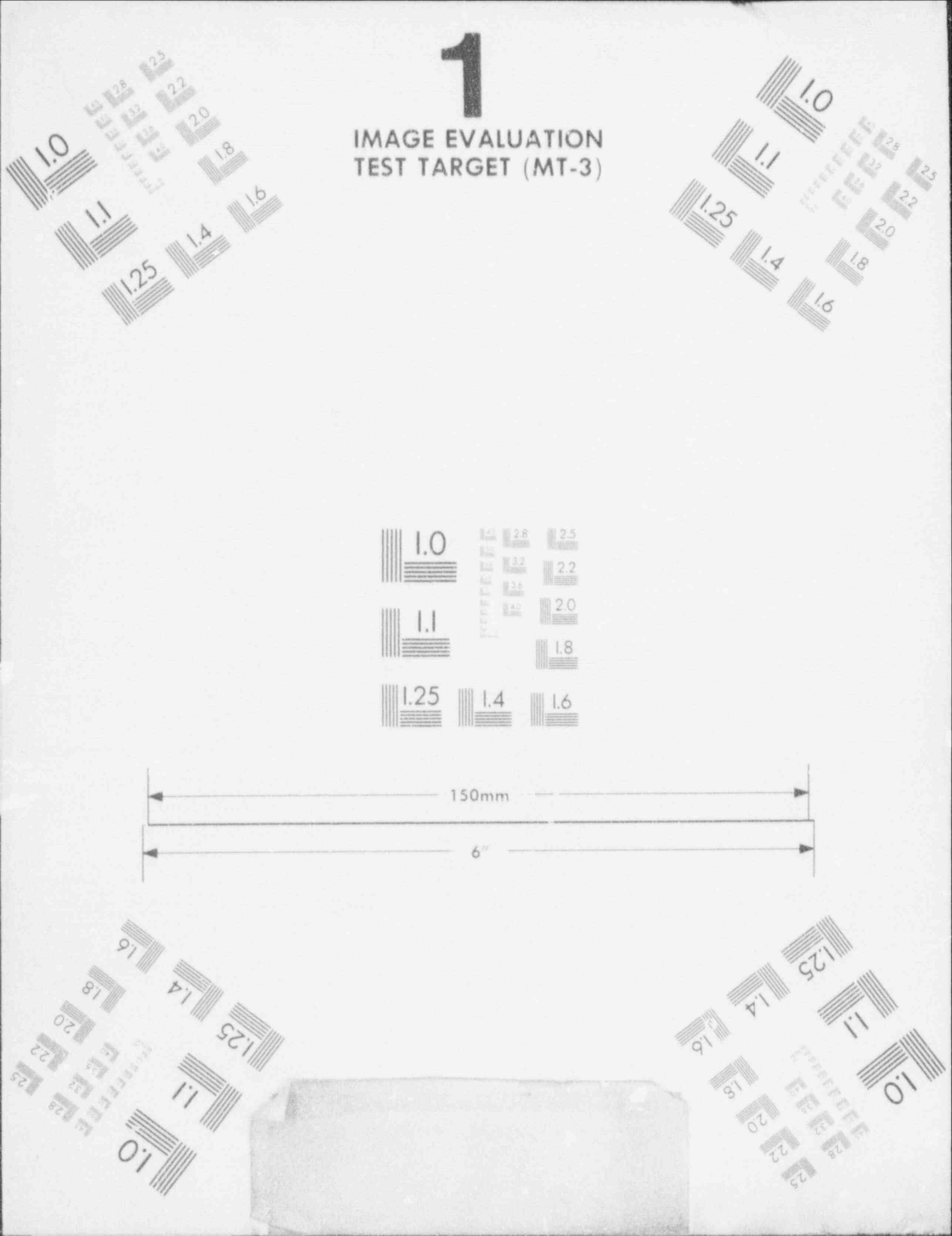
1
IMAGE EVALUATION
TEST TARGET (MT-3)
1.0
1.1
1.25
1.4
1.6
1.8
2.0
2.2
2.5
2.8
3.2
3.6
4.0
150mm
6"

1

IMAGE EVALUATION
TEST TARGET (MT-3)

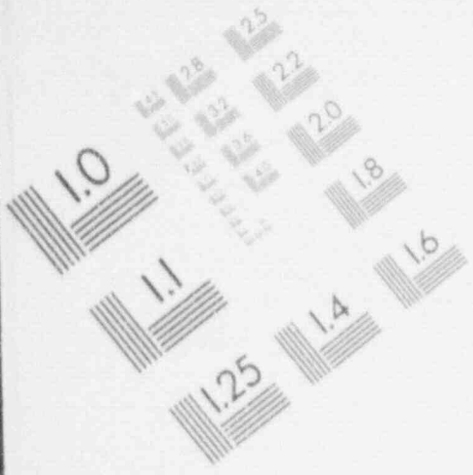

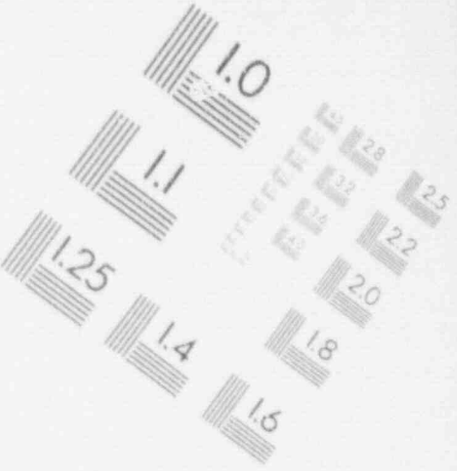

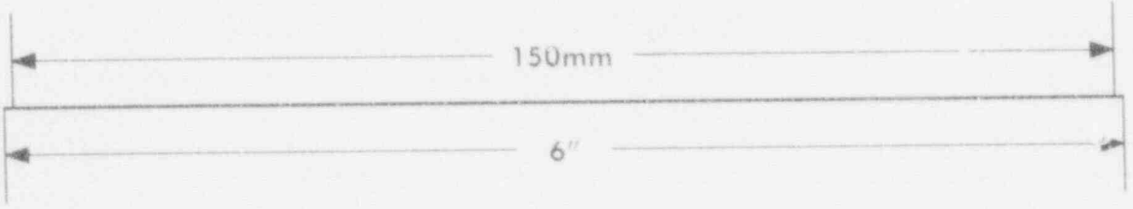

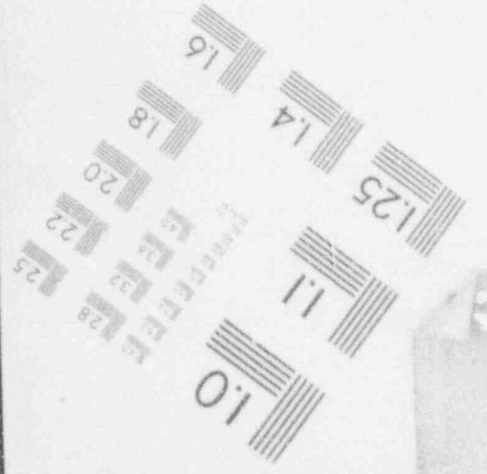

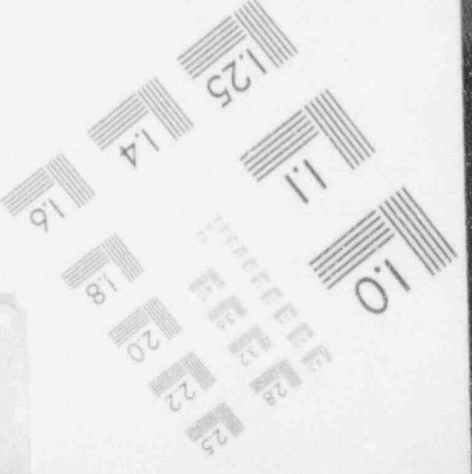

From Equation (B-4), the steam generator secondary side plays an important part in the RCS pressure. Basically, one would expect the RCS pressure to change in the same manner as a change in the secondary side temperature. Once boiling occurs on the secondary side, the saturation conditions that exist there will depend very heavily on adequately relieving steam from the secondary to the atmosphere. This capability to dump steam is determined by the size of the turbine bypass valve, the size of the secondary side relief valves, and the ability of these valves to be opened by the plant operators at the time RHR is lost. Because of the uncertainty in all three of these factors, one cannot completely be ensured that a steam dumping capacity will exist for all plant conditions to keep the secondary side at atmospheric pressure. For these reasons, three secondary side pressures (1, 2, and 3 atm) were selected to show the trend in RCS pressure versus a change in secondary side saturation conditions.

The mass of noncondensable gas is also in Equation (B-4). This value changes when the initial coolant level in the RCS varies. Besides the mid-loop operation level (50% of the hot leg occupied by coolant), three other coolant levels are selected to determine the trend of RCS pressure as a function of the quantity of noncondensable gas. The values selected are 75% of the hot leg with coolant, 25% of the hot leg with coolant, and at the core outlet level [height above the core is 0.774 m (2.54 ft) for H. B. Robinson and 0.807 m (2.65 ft) for Oconee]. These three values have no special significance with respect to plant operation, but do represent a range of values that are within the scope of the model.

From previous discussion (Sections B-2.3 and B-2.4), the value of decay heat has a large impact on water level swell in the reactor vessel and whether or not CCFL might occur in the steam generator U-tubes. If the level swell does enter the steam generator tubes, then a two-phase nonannular flow regime exists and the appropriate heat transfer coefficient must be used. However, as discussed in Sections B-2.3 and B-3.3, the heat transfer coefficient cannot be accurately determined when this condition exists. Thus, a single-phase and a best estimate two-phase nonannular heat transfer coefficient was used to analyze the response by H. B. Robinson. It was shown in Section B-2.4 (U-tube flooding) that after H. B. Robinson has been shut down for more than two days, a CCFL condition cannot occur, even if only one steam generator is available. For the Oconee plant with two OTSGs, level swell and CCFL are not a concern because there is a large volume of the candy-cane hot legs and no countercurrent flow exists (i.e., the steam flow and condensate flow is in the same direction). Therefore, the heat transfer coefficient was varied only for the H. B. Robinson plant.

Lastly, the assumed interaction of the pressurizer with the RCS during the noncondensable compression phase can have a significant impact. Three cases are examined involving different assumptions regarding pressurizer gas content, two of which are bounding cases.

These conditions set the scope of the analysis performed to bound the RCS pressure as a result of a loss-of-RHR event. The following two sections present these results, the first for H. B. Robinson and the second for Oconee.

B-4.2 H. B. Robinson Plant Results

Table B-5 lists the Piston Model calculations performed for H. B. Robinson. Each condition is analyzed for the four times after shutdown previously identified unless otherwise noted.

The calculated results for RCS pressure are shown in Figures B-9 through B-12 and Table B-6. The first figure shows the results for the three different steam generator availability cases (runs 1, 2, and 3). Figure B-10 groups the results when the steam generator reliefs or bypass valves cannot reduce the secondary side pressure to atmospheric pressure. Figure B-11 shows the effect of initial primary water mass inventory on RCS pressure. The last two figures for H. B. Robinson show how extremes in the flow regimes

Table B-5. Analysis for H. B. Robinson.

Run number	Number of SGs used as a heat sink	Number of SGs with dams installed	Secondary side pressure (psia)	Flow regime on SG tube primary side	RCS water level	Comments
1	1	0	14.7[a]	Two-phase annular	Mid-loop operation	—
2	1	2	14.7	Two-phase annular	Mid-loop operation	—
3	3	0	14.7	Two-phase annular	Mid-loop operation	—
4	1	0	29.4[b]	Two-phase annular	Mid-loop operation	—
5	1	0	44.1[c]	Two-phase annular	Mid-loop operation	—
6	1	0	14.7	Two-phase annular	Core outlet	Shutdown for 48 h
7	1	0	14.7	Two-phase annular	25% of hot leg volume	Shutdown for 48 h
8	1	0	14.7	Two-phase annular	75% of hot leg volume	Shutdown for 48 h
9	1	0	14.7	Two-phase nonannular	Mid-loop operation	—
10	1	0	14.7	Single-phase liquid	Mid-loop operation	—
11	1	2	14.7	Two-phase annular	Mid-loop operation	Pressurizer gas "partitioning," shutdown for 48 h
12	3	0	14.7	Two-phase annular	Mid-loop operation	Pressurizer gas "purging," shutdown for 48 h

a. 1 atm = 14.7 psia.

b. 2 atm = 29.4 psia.

c. 3 atm = 44.1 psia.

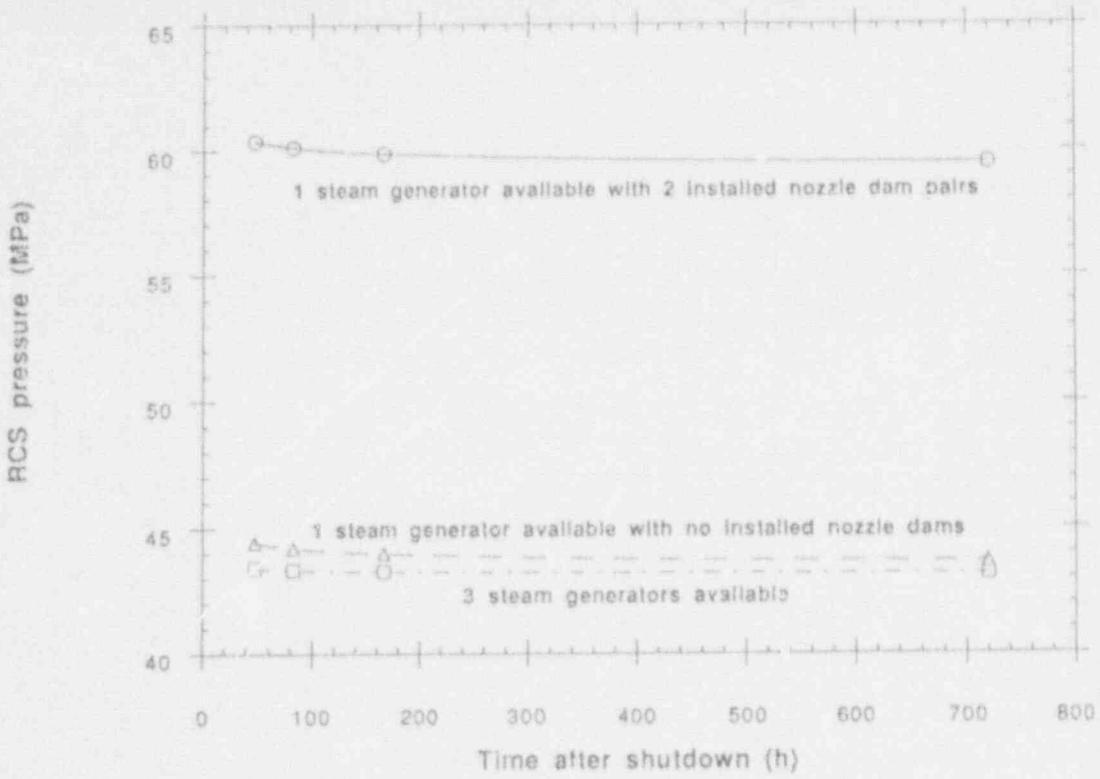

Figure B-9. H. B. Robinson's RCS pressure for various system configurations with the secondary at one atmosphere.

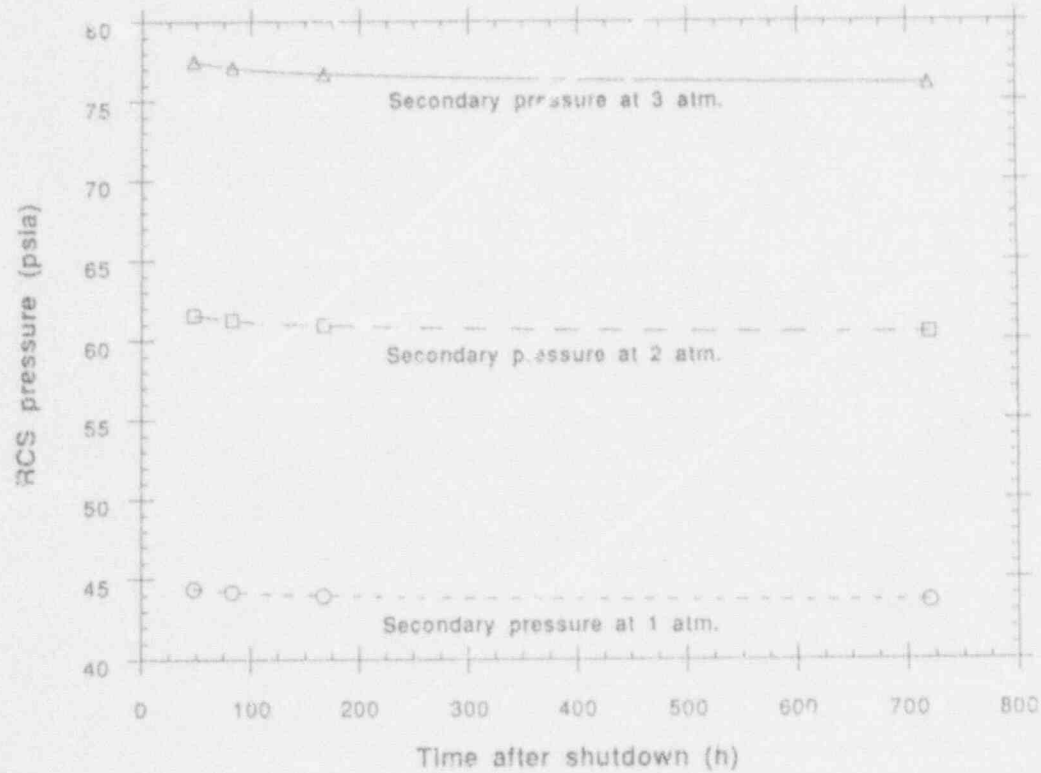

Figure B-10. H. B. Robinson's RCS pressure for various secondary pressures with one steam generator available and no installed nozzle dams.

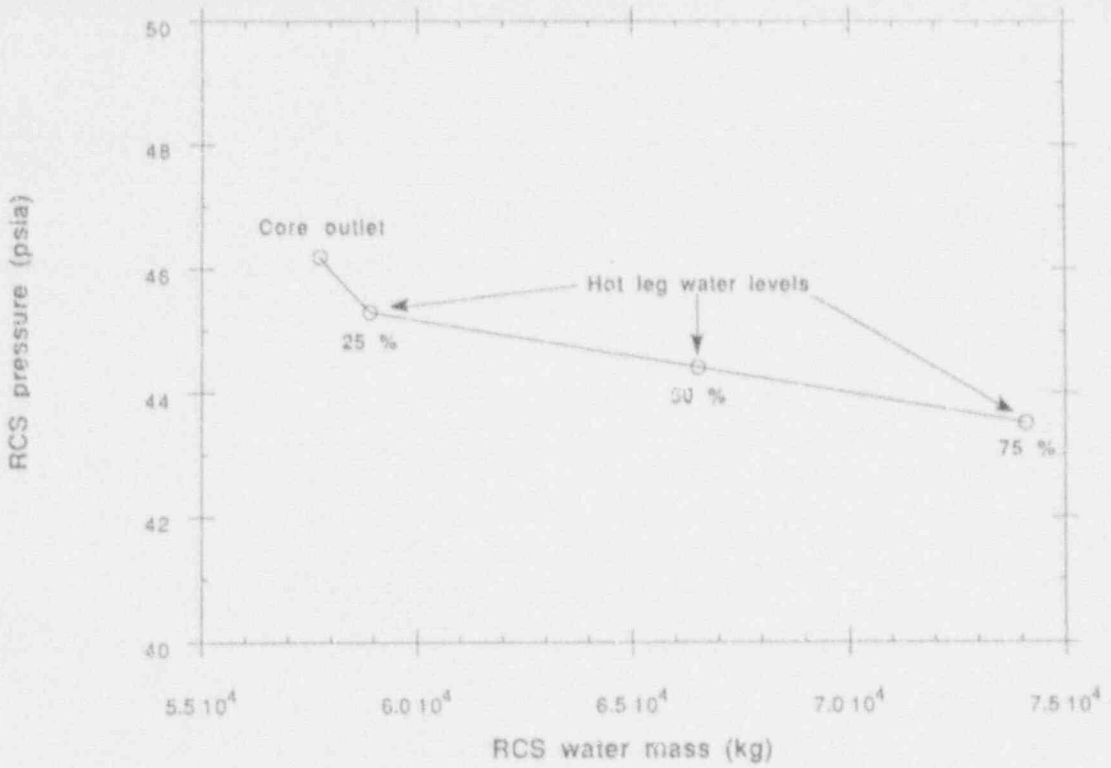

Figure B-11. H. B. Robinson's RCS pressure as a function of the RCS water inventory for one steam generator available with secondary pressure at atmospheric.

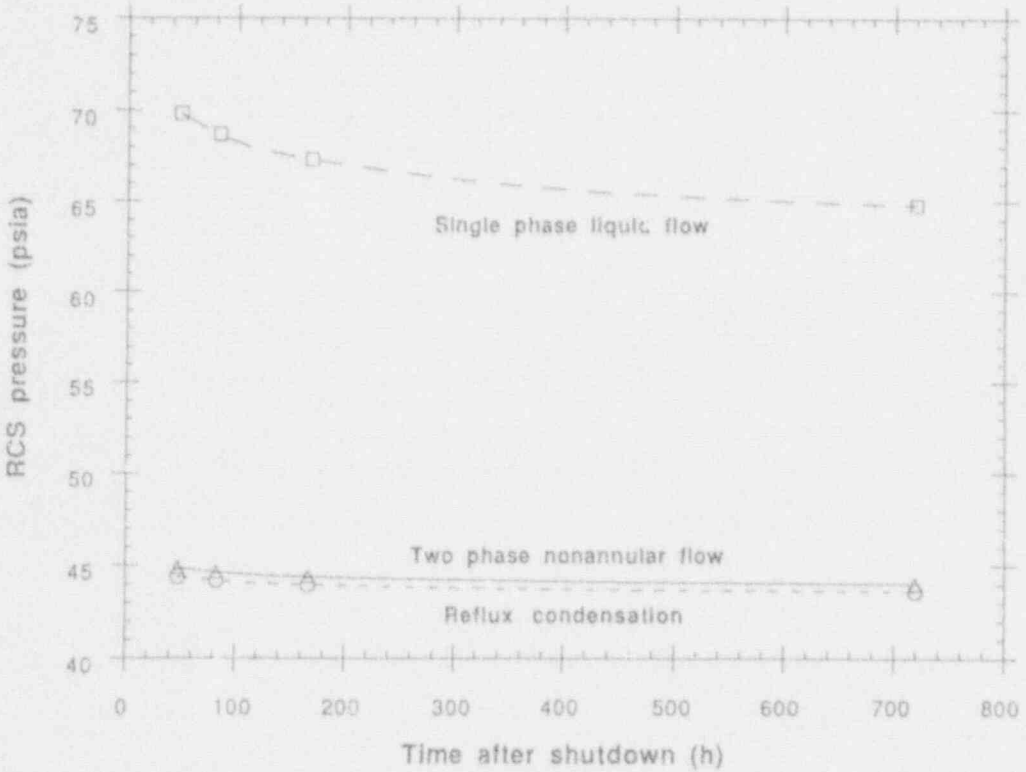

Figure B-12. Comparison of single phase flow and two phase nonannular flow to reflux condensation for H. B. Robinson with one steam generator available, no installed nozzled dams, and secondary pressure at atmospheric.

Table B-6. H. B. Robinson pressurizer sensitivity cases.

Pressurizer case	RCS pressure (psia)	
	One SG available with 2 dam pairs	3 SGs available
Gc partition	45.9	38.3
No gas exchange	60.4	43.4
Gas purge	90.4	52.6

from level swell could affect the RCS pressure (as exemplified in the PKL data). Finally, Table B-6 shows the effect of differing assumptions regarding pressurizer behavior.

Figures B-9 through B-13 show how little effect decay heat has on the final system pressure as long as only steam enters the steam generator tubes (at most, a 3 psia change over 30 days). Examining the physical processes occurring from the time core boiling begins to a steady-state pressure explains this relative insensitivity to decay heat. Regardless of decay heat level, a fixed amount of compression of the noncondensable gas is necessary to sweep the gas into the steam generator. In the case of H. B. Robinson, the volume of noncondensable gas must decrease by approximately 42% of its original volume. This equates to a pressure change of about 25 psia, raising RCS pressure from 14.7 to about 40 psia. The remaining rise in RCS pressure is that needed to uncover enough surface area to transfer the decay heat across the steam generator tubes.

Figure B-9 clearly shows how much the presence of nozzle dams can affect the system pressure. This is because the calculated primary system pressure is dominated by factors influencing the degree of compression of the noncondensable gas. In both the one (without dams) and three steam generator cases, the amount of noncondensable gas compression needed to introduce steam into the steam generators is virtually the same. The small difference in final pressure results from the marginal difference in the condensing length between the two cases needed to remove the decay heat from the primary system. In the case of two steam generators with nozzle dams, the removal of the steam generator and cold leg volumes as a final location for the noncondensable gas means that a larger mass of the gas must be compressed into the one active steam generator. Thus, the partial pressure of the gas is larger than the no dam case and the final total pressure clearly reflects the increase.

Figure B-10 shows the effect of a steam generator's steam relief system that cannot maintain secondary pressure at atmospheric pressure. The end result is to elevate the saturated steam and gas temperature in the passive section of the primary side steam generator tubes. Thus, the RCS pressure will be higher under this situation as compared to the case when the relief path can maintain atmospheric pressure in the steam generator.

Figure B-11 shows the change in H. B. Robinson's RCS pressure as a function of the initial water mass inventory (directly related to coolant level). Clearly, the figure shows a marked difference in changing the coolant level in the reactor vessel versus in the hot legs. The relative noncondensable gas and water mass inventories are directly related because of the initial conditions that exist before the loss of RHR. Thus, a change in the noncondensable gas inventory gives an accompanying change in water inventory. Using Equation (B-4), one can infer that an increase in noncondensable gas inventory (and therefore a decrease in water mass inventory) means an increase in RCS pressure. This can be seen in Figure B-11.

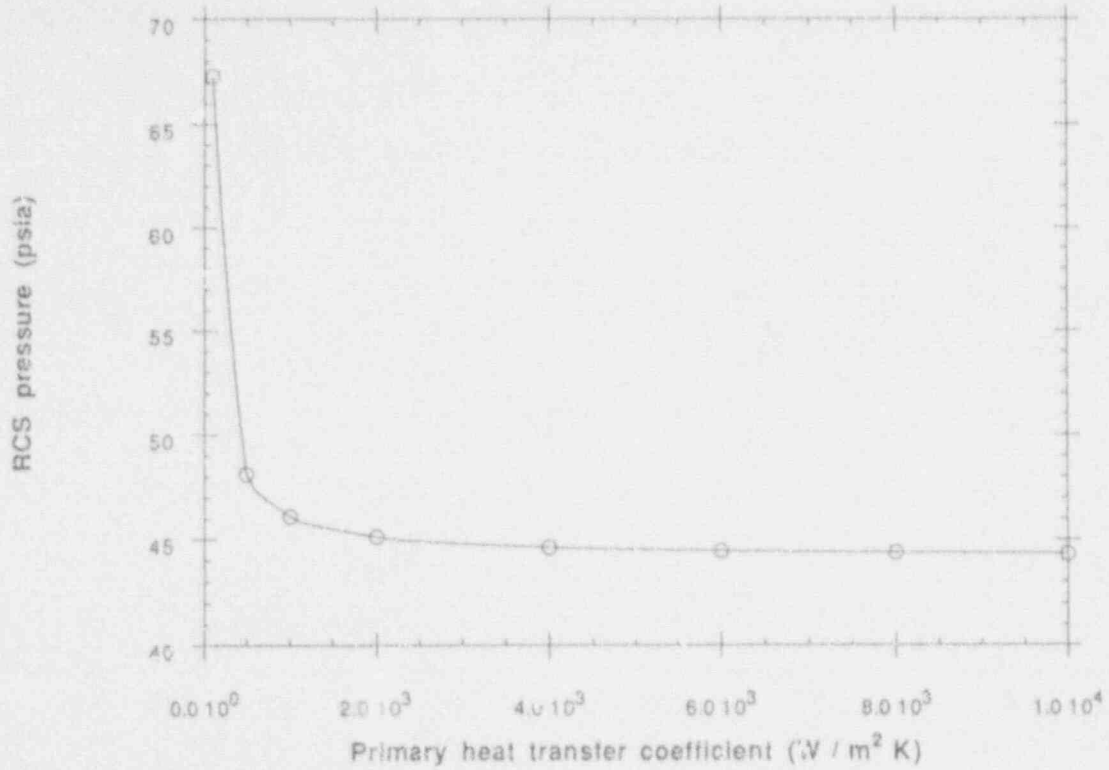

Figure B-13. RCS pressure as a function of the primary heat transfer coefficient for H. B. Robinson 48 hours after shutdown, one steam generator available, secondary pressure at atmospheric, and no installed nozzle dams.

As shown in Section B-3.3, the model could only bound the RCS pressure for PKL Experiment IIIB 4.5 when froth (or a two-phase nonannular flow) enters the steam generator tubes. To examine this effect for H. B. Robinson, the results from the two heat transfer correlations (two-phase nonannular and single-phase flow) are shown in Figure B-12. Along with the upper and lower bounds is the curve for Run 1 as a reference. The void fraction variation throughout the primary system can clearly cause a wide range in RCS pressure [a difference of over 0.138 MPa (20 psia)].

To examine the sensitivity to the primary side heat transfer coefficient in a more general way, Figure B-13 shows the calculated RCS pressure for H. B. Robinson as a function of the heat transfer coefficient. (In this set of calculations the shutdown time is assumed to be 48 hours, with one available steam generator and no nozzle dams.) Calculations were run for eight different values of the coefficient, ranging from 10,000 to 100 W/m^2-K (1760 to 17.6 Btu/h-ft^2-°F), corresponding to reflux condensation and single-phase liquid heat transfer, respectively. Only heat transfer coefficient values lower than 500 W/m^2-K (89 Btu/h-ft^2-°F) have a significant effect on pressure. Above 500 W/m^2-K, the change in condensing length is not great enough to have a significant effect on the passive length containing the noncondensable gas. Therefore, it is only with low heat transfer coefficients that the volume needed to remove all of the decay heat from the primary compresses the noncondensable gas enough to yield a significant pressure increase.

Finally, there is a sensitivity in the results relating to the assumed behavior of the pressurizer during the noncondensable compression phase. The "base case" Piston Model assumes that the original mass of noncondensable in the pressurizer remains constant. This might be referred to as the "no gas exchange case." Two other bounding assumptions can be made. The first, referred to as the "gas partition" case, assumes that the noncondensable gas originally in the reactor vessel above the core, plus that in the hot legs

between the vessel and the pressurizer surge line, is compressed into the steam generator and the pressurizer. This case assumes that only noncondensable gas enters the pressurizer until a steam/gas front passes the surge line. The second case, called the "purge" case, has all of the original pressurizer noncondensable gas empty into the hot leg and then be compressed into the steam generator. In this bounding case, steam is assumed to replace all the noncondensable in the pressurizer.

These three variations in the assumed movement of noncondensable gas in the pressurizer produce significantly different final RCS pressures. Table B-6 shows the calculated RCS pressures for H. B. Robinson for the three cases, including the effects of the number of steam generators available. The differences in pressure are as one might expect, with the lowest value occurring when the pressurizer "absorbs" some of the noncondensable from the vessel and hot legs, and the highest when the pressurizer is emptied of all noncondensable gas (which must be compressed into the steam generator). The intermediate pressure is produced by the "no gas exchange" case.

The cases that represent a scenario closest to reality might be arguable. On the one hand, it seems likely that some additional noncondensable gas would be compressed into the pressurizer (as in the gas partition case). On the other hand, since steam entering the surge line is considerably lighter than the noncondensable gas in the pressurizer, it is conceivable some gas might be expelled. The "no gas exchange" case is therefore an intermediate scenario between the two extremes.

B-4.3 Oconee Plant Results

Since Oconee has one less RCS loop and hot leg nozzle dams are not used, the number and type of analyses necessary are fewer in number than for H. B. Robinson. The runs performed for Oconee are shown in Table B-7. The first seven runs are similar in nature to runs 1 through 8 for H. B. Robinson, with the nozzle dam case omitted. The results are shown in Figures B-14, B-15, and B-16, and in Table B-8. Oconee exhibits the same trends as H. B. Robinson (a slight drop in pressure with lower decay heat levels or having all steam generators available as the heat sink; and a pressure increase if the secondary side vent path is restricted). However, there are noticeable differences between the plants for the steady-state pressures obtained.

The same phenomena that affect the shape of the curves of Figures B-9 and B-10 for H. B. Robinson also occur for the Oconee plant as shown in Figure B-14. The difference between the H. B. Robinson and Oconee results stems from the differences between the UTSG and OTSG, and the differences in their hot leg volumes. The drop in RCS pressure as decay heat decreases is still fairly small. However, there is a more noticeable drop in RCS pressure for Oconee because of the greater compression of the "passive" tube length per available condensing length. For Oconee, with its larger hot leg, the drop in noncondensable volume to compress the gas into the steam generator is at most 37% of the original volume, as compared to 58% for H. B. Robinson.

Figure B-15 shows the change in Oconee's RCS pressure as a function of the initial water mass inventory. Oconee's results differ from H. B. Robinson in that the slope of the data points is lower. This is due to the smaller change in noncondensable gas mass for a given change in coolant level in Oconee.

For wet layup conditions in OTSGs, the secondary side is nearly water-full. Therefore, once boiling begins on the secondary side with no make-up feedwater available, the secondary side water level will begin to decrease. Hence, the tube length available for heat rejection begins to decrease. As the possible condensing length and tube volume decreases, the volume available for the passive length containing noncondensable gas also decreases. The result of this is that the system pressure increases. Run 8 investigated this phenomena and the results are shown in Figure B-16. Note the rapid rise in system pressure once the steam generator has been allowed to boil for three hours without make-up feedwater. This behavior

Table B-7. Analysis for Oconee.

Run number	Number of SGs used as a heat sink	Secondary side pressure (psia)	RCS water level	Secondary boiling time (h)	Comments
1	1	14.7[a]	Mid-loop operation	0	Make-up feedwater available
2	2	14.7	Mid-loop operation	0	Make-up feedwater available
3	1	29.4[b]	Mid-loop operation	0	Make-up feedwater available
4	1	44.1[c]	Mid-loop operation	0	Make-up feedwater available
5	1	14.7	Core outlet	0	Shutdown for 48 h
6	1	14.7	25% of hot leg volume	0	Shutdown for 48 h
7	1	14.7	75% of hot leg volume	0	Shutdown for 48 h
8–12	1	14.7	Mid-loop operation	1, 2, 2.5, 3, and 3.25	Shutdown for 48 h, no make-up feedwater available
13	1	14.7	Mid-loop operation	0	Pressurizer gas "partitioning," shutdown for 48 h
14	2	14.7	Mid-loop operation	0	Pressurizer gas "purging," shutdown for 48 h

a. 1 atm = 14.7 psia.

b. 2 atm = 29.4 psia.

c. 3 atm = 44.1 psia.

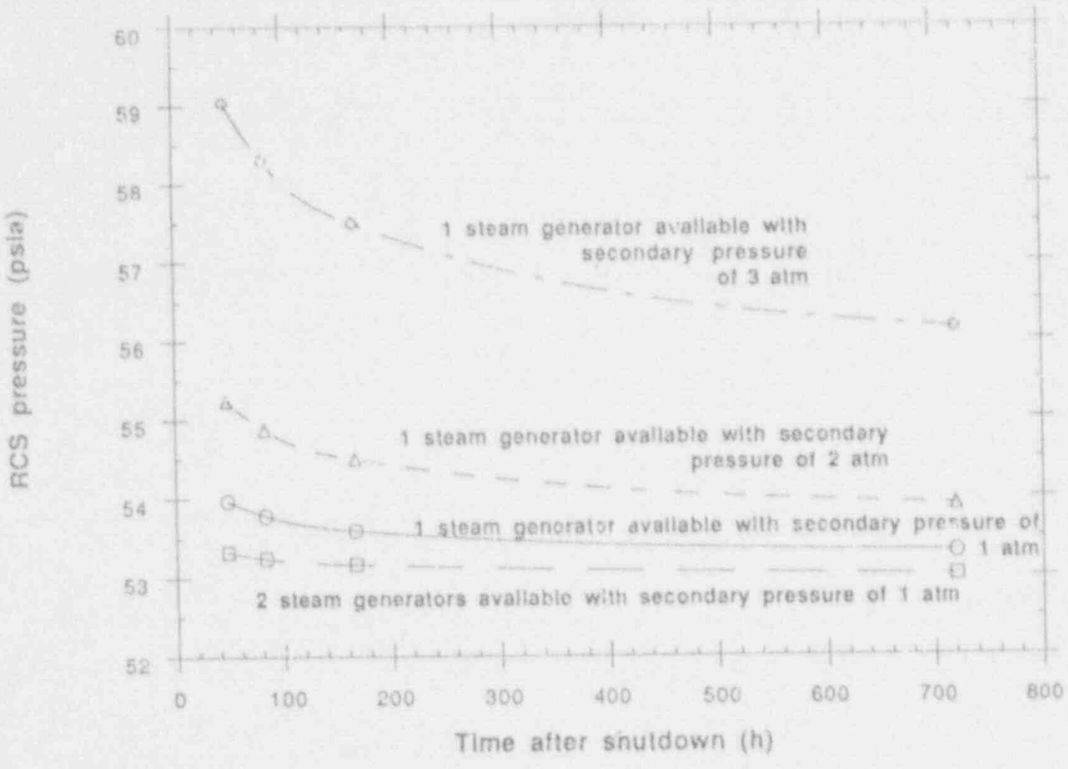

Figure B-14. Oconee's RCS pressure for various steam generator availabilities and secondary pressures.

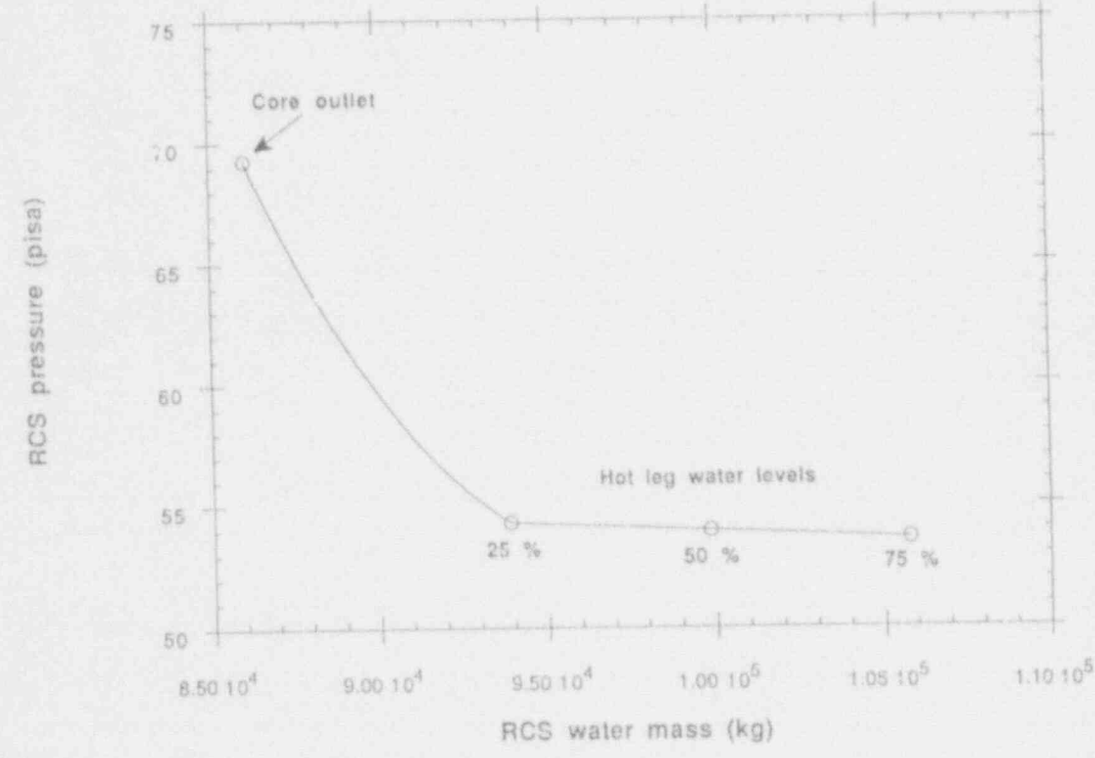

Figure B-15. Oconee's RCS pressure as a function of the RCS water mass inventory for one steam generator available with secondary pressure at atmospheric.

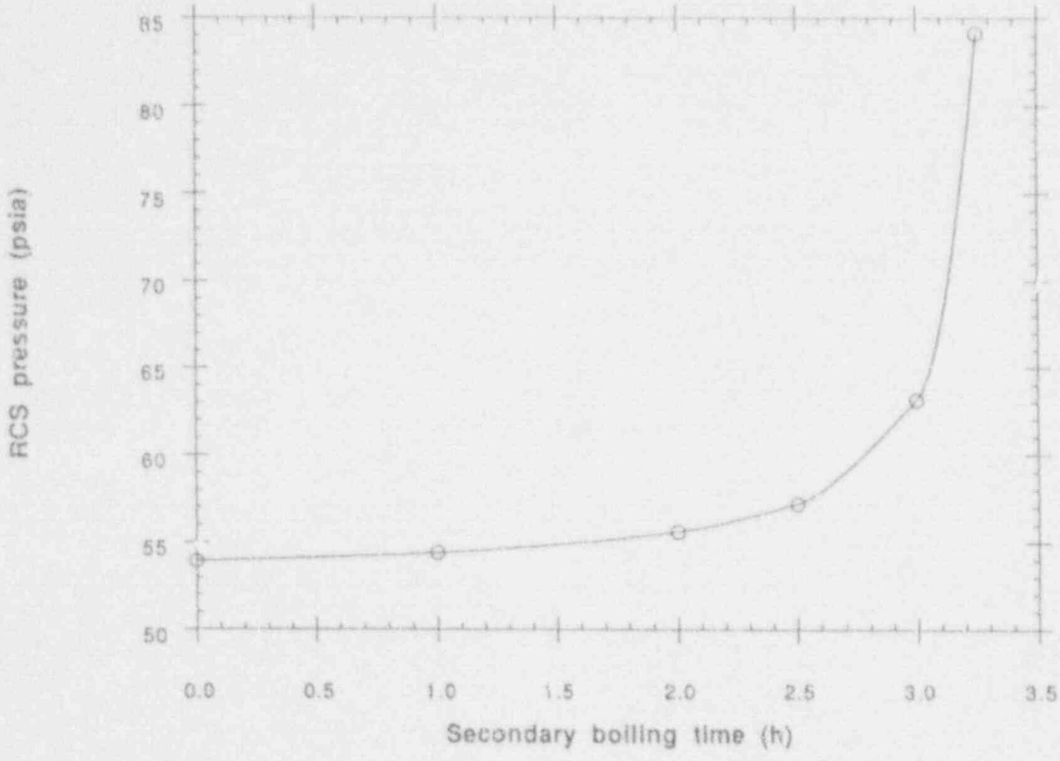

Figure B-16. Oconee's RCS pressure as a function of the secondary boiling time without water resupply for one steam generator available with secondary pressure at atmospheric.

Table B-8. Oconee pressurizer sensitivity cases.

	RCS pressure (psia)	
Pressurizer case	One SG available	Two SGs available
Gas partition	48.8	48.5
No gas exchange	54.0	53.3
Gas purge	71.4	70.6

differs from what would occur in H. B. Robinson because condensation takes place very low in the tube bundle in the UTSG design, relative to the secondary water level. Moreover, in the UTSG design, buoyancy forces will keep the secondary coolant well-mixed, whereas in the OTSG design, buoyancy forces work against mixing (i. e., secondary water heats near the top of the steam generator).

Table B-8 shows the Oconee results for sensitivity to pressurizer gas behavior, analogous to those for H. B. Robinson in Table B-6. The trends are the same as for H. B. Robinson, but the differences in pressure levels are not as pronounced.

B-5. CONCLUSIONS

A model has been developed to determine the steady-state RCS pressure after a loss-of-RHR during mid-loop operations, with cooling by one or more steam generators. The model was assessed against two experiments and then applied to two types of PWRs (H. B. Robinson and Oconee). The significant results from the analysis are

- The final RCS pressure is relatively insensitive to the number of steam generators available (when nozzle dams are not installed), the time after shutdown when the loss-of-RHR begins, and a wide range of heat transfer coefficients [above about 500 W/m^2-K (88 Btu/h-ft^2-°F)] assumed for the condensing region of the steam generator tubes.

- The pressure is strongly affected by the number of steam generator nozzle dams present, the venting and feedwater supply capacities available to the steam generators, and the behavior of the pressurizer during the noncondensable compression phase.

It is apparent that for a closed RCS, condensation will provide adequate heat removal at some RCS pressure level indefinitely, as long as feedwater is available. Depending on the situational and phenomenological assumptions made, the Piston Model predicted pressures ranging from 0.262 to 0.620 MPa (38 to 90 psia) for H. B. Robinson and 0.338 to 0.489 MPa (49 to 71 psia) for Oconee, using decay heat at 48 hours after shutdown and assuming the secondary pressure remains at atmospheric pressure. For H. B. Robinson, the greatest impact on pressure is the presence or absence of nozzle dams. The pressures calculated for Oconee were relatively unaffected by either of the situational variables examined (i. e., time after shutdown or number of steam generators available). For both plants, pressurizer behavior produced the greatest impact on RCS pressure of all the variables examined.

Although a wide range of effects has been examined, the results should not be interpreted as being all encompassing. Care must be exercised when interpreting the calculations presented in this study. There are potential conditions that could have a significant effect on RCS pressure (e. g., water level above the top of the hot legs or a cold pressurizer) that were not covered in this study. If the consequences of pressures higher than those calculated warrant, further analysis and/or experimentation could be undertaken to predict the effects of such conditions.

B-6. REFERENCES

1. P. R. McHugh and R. D. Hentzen, *Natural Circulation Cooling in U. S. Pressurized Water Reactors*, NUREG/CR-5769, EGG-2653, January 1992.

2. J. L. Crew et al., *Loss of Residual Heat Removal System, Diablo Canyon, Unit 2, April 10, 1987 (Augmented Inspection Team Report April 15–21, 29, and 1 May 87)*, NUREG-1269, June 1987.

3. NRC, *Loss of Vital AC Power and the Residual Heat Removal System During Mid-Loop Operations at Vogtle Unit 1 on March 20, 1990*, NUREG-1410, June 1990.

4. J. G. Collier, *Convective Boiling and Condensation*, New York: McGraw Hill, 1972.

5. V. S. Arpaci and P. S. Larsen, *Convection Heat Transfer*, Englewood Cliffs, New Jersey: Prentice-Hall, Inc., 1984.

6. Isao Kataoka and Mamoru Ishii, *Prediction of Pool Void Fraction by New Drift Flux Correlation*, ANL-86-29, 1986.

7. C. L. Tien, S. L. Chen, P. F. Peterson, *Condensation Inside Tubes*, EPRI-NP-5700, January 1988.

8. G. B. Wallis, *One-Dimensional Two-Phase Flow*, New York: McGraw Hill, 1969, pp. 336–341.

9. Q. T. Nguyen, *Condensation in Inverted U-Tube Heat Exchangers*, Ph. D. dissertation, University of California at Santa Barbara, August 1988.

10. C. D. Fletcher, P. R. McHugh, S. A. Naff, and G. W. Johnsen, *Thermal-Hydraulic Processes Involved in Loss of Residual Heat Removal During Mid-Loop Operation, Rev. 1*, EGG-EAST-9337, February 1991.

11. G. Loomis, *Summary of the Semiscale Program (1965–1986)*, NUREG/CR-4945, EGG-2509, July 1987.

12. Y. Kukita et al., "Flooding at Steam Generator Inlet and Its Impact on Simulated PWR Natural Circulation," *ASME Winter Meeting, Boston, Massachusetts, December 13–18, 1987*, FED-Vol. 61, HTD-Vol. 92.

13. Y. Kukita et al., "Nonuniform Steam Generator U-tube Flow Distribution during Natural Circulation Tests in ROSA-IV Large Scale Test Facility," *24th ASME/AIChE National Heat Transfer Conference, Pittsburg, Pennsylvania, August 9–12, 1987*.

14. P. Bazin et al., "Natural Circulation Under Variable Primary Mass Inventories at BETHSY Facility," *Fourth International Meeting on Nuclear Reactor Thermal-Hydraulics, NURETH-4, Karlsruhe Federal Republic of Germany, October 10–13, 1989*, p. 504.

15. Q. T. Nguyen and S. Banerjee, "Flow Regimes and Heat Removal Mechanisms in a Single Inverted U-Tube Steam Condenser," *American Nuclear Society Transactions, 43*, 1982, pp. 788–789.

16. K. Raznjevic, *Handbook of Thermodynamic Tables and Charts*, Washington, D.C.: Hemisphere Publishing Corp., 1976.

17. D. Hein, R. Rippel, P. Weiss, "The Distribution of Gas in a U-Tube Heat Exchanger and Its Influence on the Condensation Process," *International Heat Transfer Conference, Munich, Germany, September 1982.*

18. M-H. Chun and J-W. Park, "Reflux Condensation Phenomena in Vertical U-Tubes With and Without Noncondensable Gas," *ASME Winter Meeting, New Orleans, Louisiana, December 13–19, 1984.*

19. G. Loomis and K. Soda, *Results of the Semiscale MOD-2A Natural Circulation Experiments*, NUREG/CR-2335, EGG-2200, September 1982.

20. R. M. Mandl, K. J. Umminger, J. v.d. Logt, "Failure of PWR-RHRS Under Cold Shutdown Conditions Experimental Results from the PKL Test Facility," *18th Water Reactor Safety Research Information Meeting, Rockville, Maryland, October 22–24, 1990.*

21. M. M. El-Wakil, *Nuclear Heat Transport*, New York: International Textbook Co., 1971.

22. T. L. Chu, R. Fitzpatrick, W. H. Yoon, A. Tingle, *Improved Reliability of Residual Heat Removal Capability in PWRs as Related to Resolution of Generic Issue 99*, NUREG/CR-5015, BNL-NUREG-52121, May 1988.

23. D. C. Bley and J. W. Stetkar, *Zion Nuclear Plant Residual Heat Removal PRA*, NSAC/84, July 1985.

Appendix C

RELAP5/MOD3 Analysis of Reflux Condensation Behavior in a Steam Generator During Reduced Inventory Operation

Appendix C

RELAP5/MOD3 Analysis of Reflux Condensation Behavior in a Steam Generator During Reduced Inventory Operation

This appendix presents the results of the RELAP5/MOD3 analyses of the consequences of a loss of the residual heat removal (RHR) in pressurized water reactor (PWR) systems with U-tube steam generator designs. Preparation of the RELAP5/MOD3 model and the results of four analyses performed using this model are discussed in this section.

C-1. BACKGROUND

Transient thermal-hydraulic analyses of the consequences of the loss of RHR were performed using the RELAP5/MOD3 code. The analyses assessed (a) the primary and secondary system thermal and hydraulic performance following a failure of RHR and (b) the capability of the RELAP5/MOD3 program to perform transient analysis under near atmospheric pressure conditions with noncondensable gas in the reactor coolant system.

The analyses presented in this appendix focus on assessing the reactor coolant system (RCS) pressure and temperature response if the steam generators are used as an alternate means of decay heat removal. The principal heat removal mechanism in the steam generator is expected to be reflux condensation. During reflux condensation, steam enters the steam generator tubes where it condenses and drains back to the hot leg. Reflux condensation is of interest because the RCS may contain air above the liquid level located at the midplane of the hot and cold legs. The air would probably prevent natural circulation through the steam generator tubes to the cold leg. As a result, RCS temperature and pressure will be determined by the efficiency of the reflux condensation process.

C-2. METHOD OF ANALYSIS

C-2.1 RELAP5/MOD3 Computer Program

Transient thermal hydraulic analyses of the loss of RHR were performed using the RELAP5/MOD3 (Version 5m5) computer program[1] executed on a DECstation 5000/Model 200 RISC Workstation. The RELAP5 code was used to assess the performance of the H. B. Robinson plant (HBR-2), which is a three loop Westinghouse PWR with a thermal power rating of 2,300 MW(Th). The initial HBR-2 model was first developed in 1983 for pressurized thermal shock analyses[2] using previous versions of RELAP5 (RELAP5/MOD1 and RELAP5/MOD2). This initial model consisted of a detailed representation of the HBR-2 plant describing the primary and secondary systems, including the main steam and feed systems. Conversion of the original HBR-2 model to RELAP5/MOD3 was completed in December 1990.[a] This model is the basis for the RELAP models used in this appendix.

The HBR-2 plant has three primary coolant loops that are explicitly represented in the base RELAP5 model. These loops are designated as A, B, and C. Each loop consists of a hot leg, U-tube steam generator, reactor coolant pump suction leg, reactor coolant pump, and a discharge leg. The pressurizer is attached to Loop C. Heat structures were included to represent the metal mass of the reactor coolant system piping, steam

a. Private communication from Paul Roth, EG&G Idaho, Inc., Idaho Falls, Idaho, to Leonard Ward, EG&G Idaho, Inc., Idaho Falls, Idaho, January 4, 1991.

generator tubes, reactor vessel and the pressurizer.

Modifications were made to the RELAP5/MOD3 HBR-2 plant model for use in PWR analyses during loss-of-RHR events. These modifications consisted of removing the control systems, secondary side components, and emergency core coding (ECC) components that do not have a role in the loss-of-RHR event. The RELAP5 nodalization of the reactor pressure vessel includes the downcomer, downcomer bypass, lower plenum, core, upper plenum and upper head. Figure C-1 shows this nodalization. The nodalization of the primary coolant loops is shown in Figure C-2. Loop C, which includes the pressurizer and hot leg, is also shown. The nodalization of the primary side of the steam generator is shown as Component 408 in Figure C-2 while the secondary side of the steam generator is shown in Figure C-3.

A one-loop model was developed from the HBR-2 three-loop model by eliminating two of the three loops to simulate isolation of these components through the use of nozzle dams in the hot and cold leg piping. The pressurizer and surge line are retained in this one loop model. These changes are made on the premise that only one steam generator is available for decay heat removal and the other two steam generators are effectively removed from the system by nozzle dams.

Further changes were made to the vessel nodalization to improve computer execution time and characteristics. The changes are summarized below.

- The flow connection between the downcomer (Component 102) and the upper plenum (Component 120) is eliminated. The loss coefficient in the junction connecting these components is high (1.37×10^5) because of the minimal flow area for this leakage path.

- The flow connection between the downcomer (Component 104) and the core bypass (Component 116) is eliminated. The loss coefficients in the junction between these components is also high (21,169 in the forward direction and 3,169 in the reverse direction), implying minimal flow.

- The reactor coolant pump is replaced by a branch component using two junctions corresponding to the pump inlet and outlet. A forward and reverse loss coefficient of 10 is assumed, which represents a locked rotor condition. The length, volume, vertical angle, elevation, and junction flow area are the same as the original component.

- The number of volumes in the pressurizer body is reduced from seven to two. The main body of the pressurizer is lumped into one volume. The bottom volume is not changed.

- The component connecting the upper plenum with the upper head (Component 129) is eliminated from the model. The volume of this component (10.922 ft^3) is judged to be negligible.

- A vent path was added to the steam generator to allow venting of the steam when boiling develops on the secondary side.

The one-loop model was initialized at an initial water temperature of 90°F and a initial water level at the hot leg centerline elevation. Air at 90°F and 100% relative humidity is present in all volumes above the centerline of the hot and cold legs. To check the ability of the model to hold steady-state conditions, a null transient was executed. Review of the results of the null transient showed that oscillations occurred in the predicted void fraction and mass flow rates in the hot and cold legs that did not damp out over a period of time. The cause of these oscillations was never established and the RELAP5/MOD3 development group has been apprised of the problem.

Several analyses were executed with the nodalization shown in Figures C-1 to C-3 using the decay heat power level corresponding to one day after shutdown (0.5% power or 11.5 MW). The results of these calculations showed continued pressurization of the RCS in excess of 100 psia,

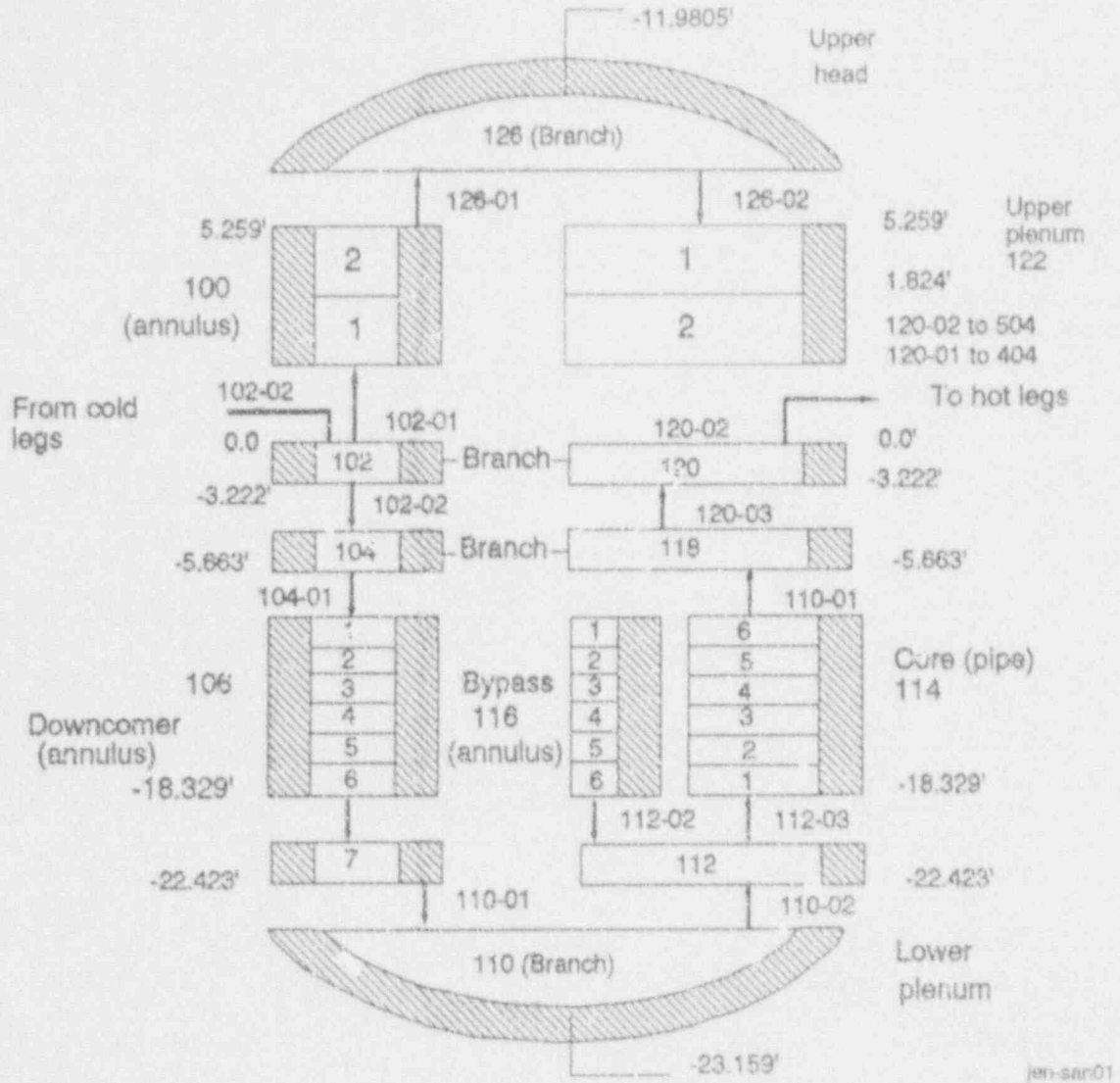

Figure C-1. Nodalization of the reactor vessel for the H. B. Robinson one-loop model.

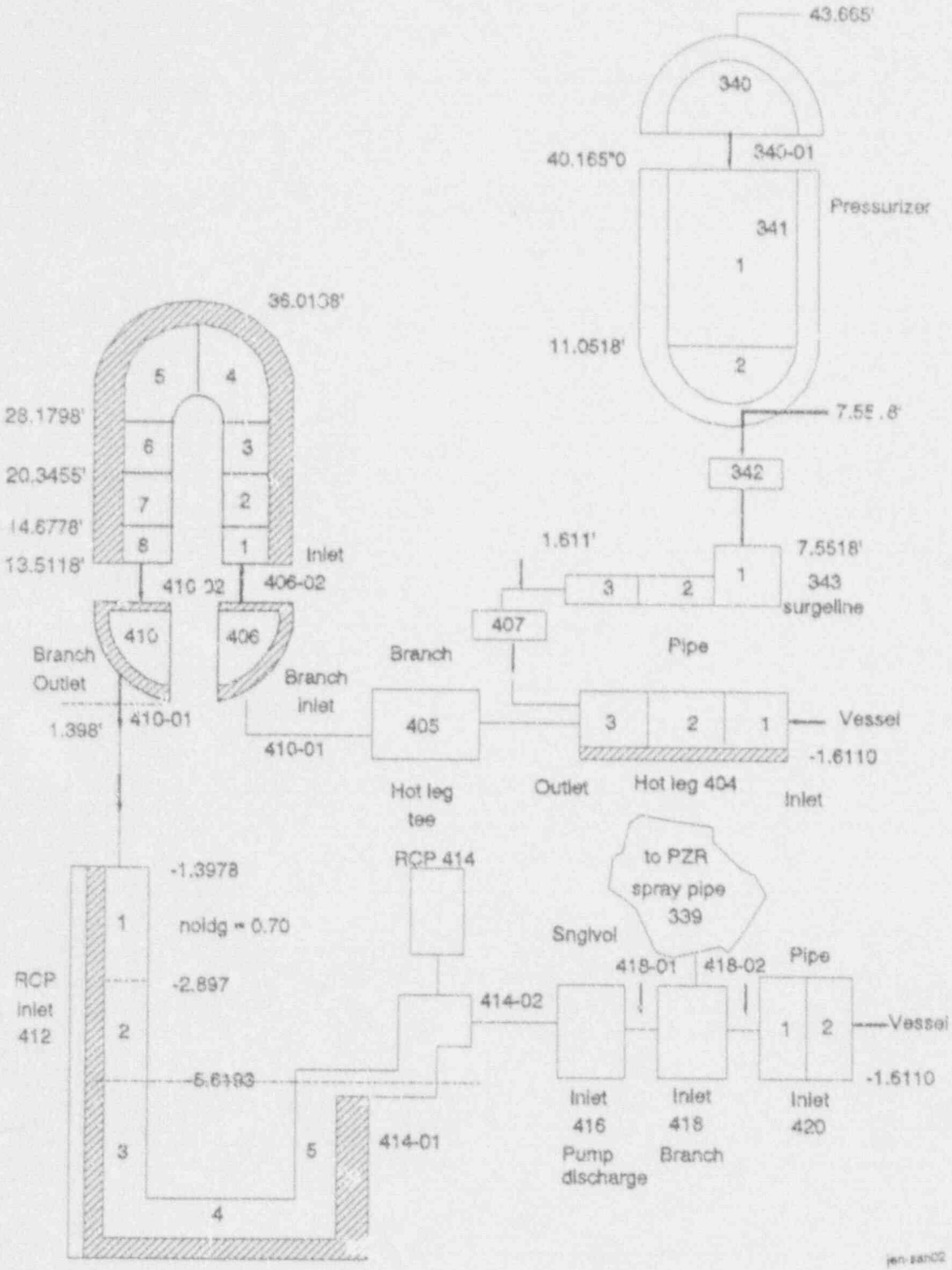

Figure C-2. Nodalization of primary Loop C for the H. B. Robinson one-loop model.

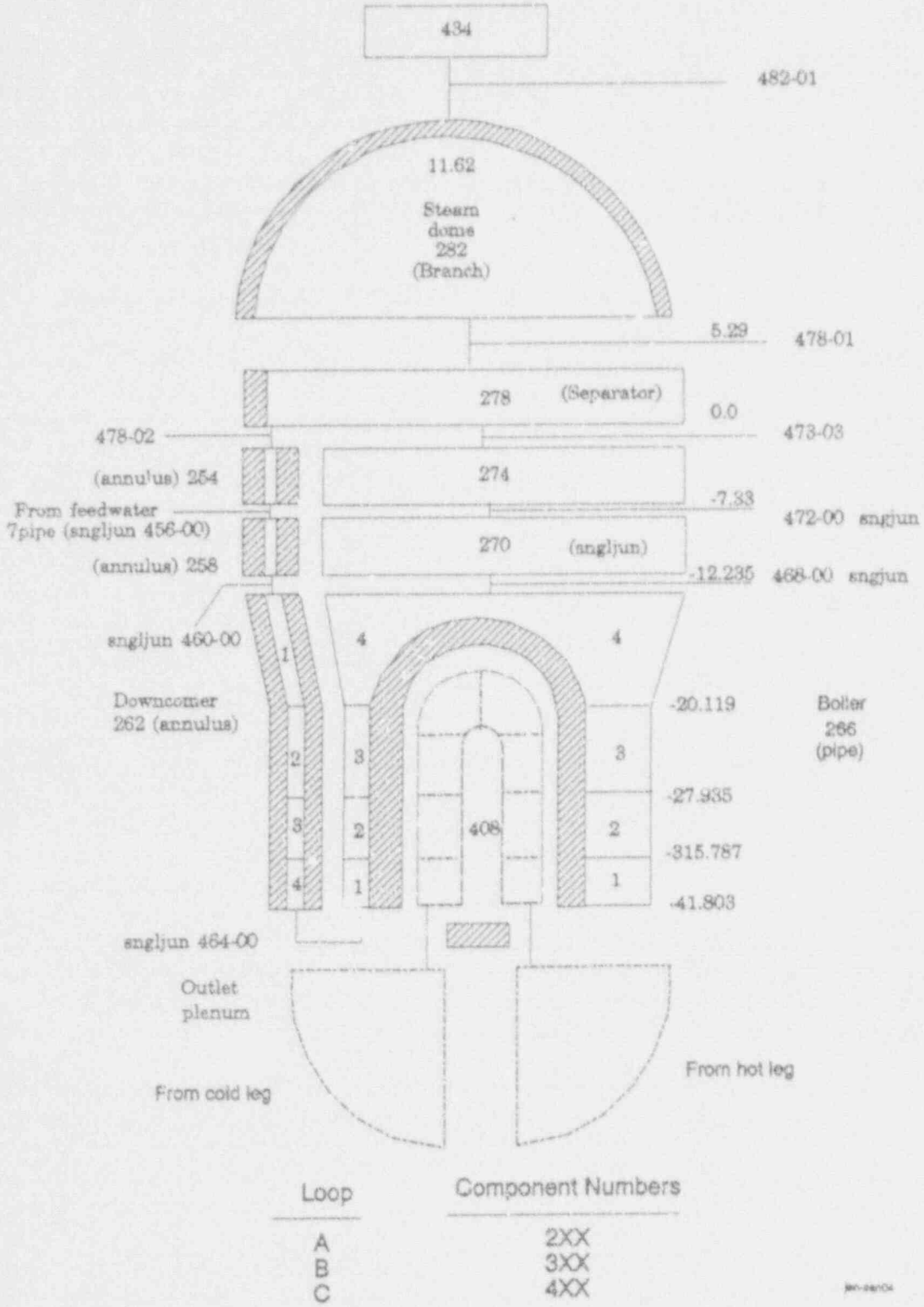

Figure C-3. Nodalization of steam generator secondary for the H. B. Robinson one-loop model.

which is far higher than the pressure expected if reflux condensation in the steam generator is removing heat from the RCS. The principal reason for the high-pressure prediction is the calculated accumulation of water in the steam generator active tube region. The water was entrained by the steam penetrating the hot leg from the reactor vessel. With the accumulation of water at the inlet to the steam generator active tube region, the two-phase flow rates at the entrance to the tubes were calculated to be too low to provide sufficient condensation heat transfer to establish a steady-state heat removal capability that matched decay heat generation. The high interfacial drag between steam and water predicted by RELAP5 in the hot leg expelled unrealistically high amounts of water from the hot leg piping in the intact loop while also limiting the drainage of condensed and deentrained water toward the vessel from the steam generator tubes and inlet plenum.

To circumvent this problem, the hot leg and inlet plenum to the steam generator were divided into two parallel components to allow drainage of the liquid from the steam generator and inlet plenum to the vessel upper plenum in the lower half of the hot leg. At the same time, steam can exit the vessel toward the steam generator along the upper half. The volume of the original hot leg components (pipe and steam generator inlet plenum) is divided equally between the upper and lower portion of the divided hot leg components. In addition, the option to not use the choking model in the one-loop model was selected for all junctions on the primary side of the reactor coolant system. This option was selected because RELAP5/MOD3 was predicting unrealistically low sound velocities (10 ft/s or less), which would result in the prediction of choking under conditions where choking should not occur.

Figure C-4 presents the revised nodalization of the hot leg and inlet plenum. The hot leg is split equally into two parallel sections with an elevation difference of 1.611 feet. The inlet plenum is also modeled as two separate components designated as 406 and 506. Components 406 and 506 connect the lower and upper portions of the hot leg to the steam generator inlet plenum, respectively.

The split hot leg nodalization allows steam to exit the vessel along the upper hot leg segment while condensed and deentrained liquid can return to the vessel along the lower portion of the pipe. This type of flow behavior is expected during reflux condensation.

C-2.2 Analysis Results

The four cases analyzed are listed below.

- Case 1—The RCS is at mid-loop operation with an initial water temperature of 90°F and a initial water level at the hot leg centerline elevation. Air at 90°F and 100% relative humidity are present in all volumes above the centerline of the hot and cold legs. The decay heat power level assumed corresponds to one day after shutdown (0.5% power or 11.5 MW).

- Case 2—This case is the same as Case 1 except that the decay heat power level assumed corresponds to one week after shutdown (0.3% power or 7.13 MW).

- Case 3—This case is the same as Case 1 except that the initial RCS liquid level is at the top elevation of the hot and cold legs.

- Case 4—This case is the same as Case 1 except the initial RCS level is at the elevation of the reactor vessel flange.

For all cases, the secondary side of the steam generator was initialized with water at a temperature of 90°F. When secondary boiling started, a vent path was assumed to be available to maintain secondary pressure and temperature near atmospheric conditions. Also, after secondary boiling began, the addition of auxiliary or emergency feedwater was necessary to prevent loss of the secondary as a heat sink.

In comparing Cases 1 and 2, the sensitivity of RCS peak pressure to the time of loss of RHR following shutdown is illustrated.

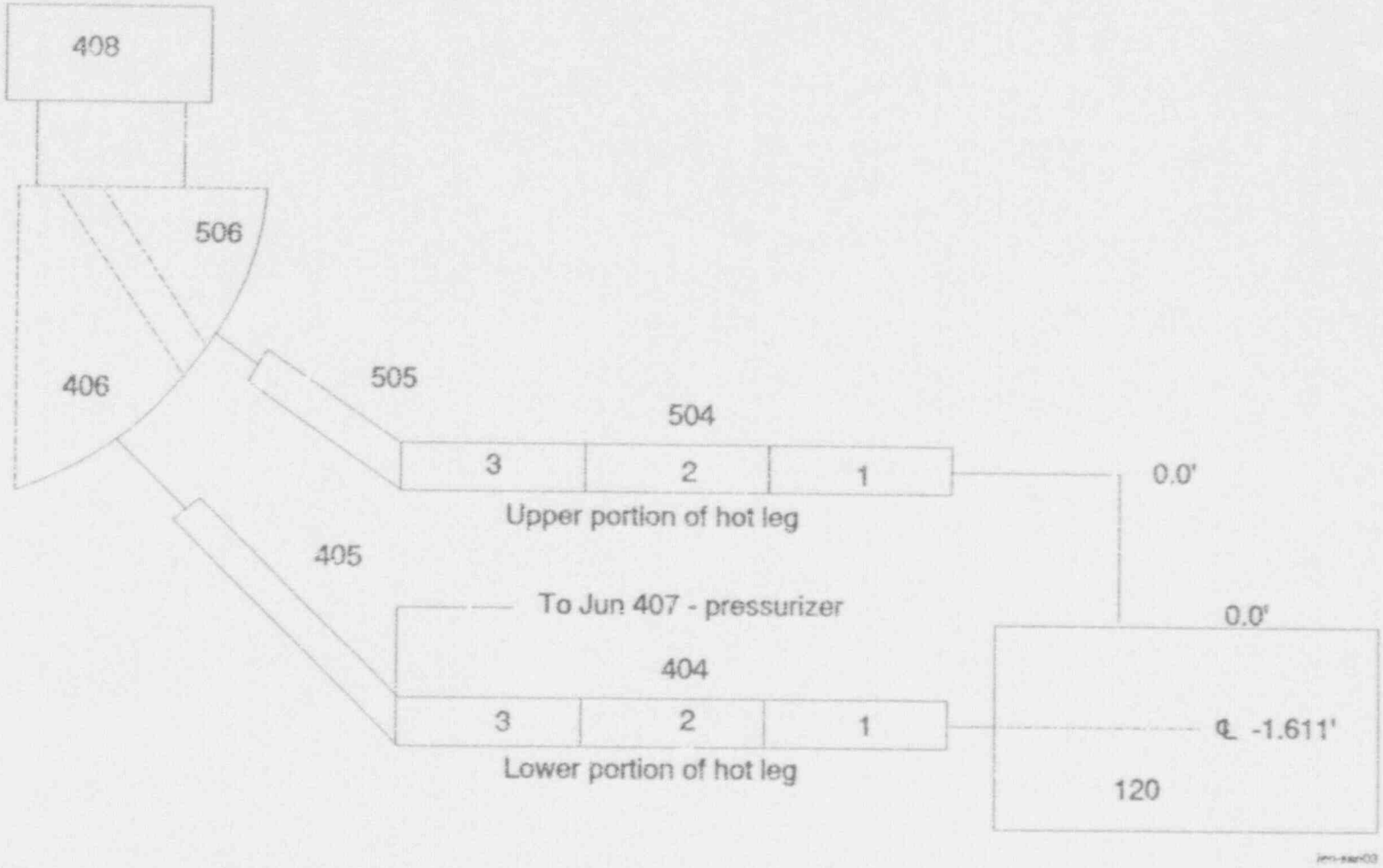

Figure C-4. Hot leg nodalization for the H. B. Robinson one-loop model.

Cases 1, 3, and 4 reflect the sensitivity of peak RCS pressure to the initial RCS water level. The results of the four cases are discussed below.

C-2.2.1 Case 1—Loss of RHR at One Day.

Figure C-5 shows the pressure transient in the primary side of the steam generator when the RHR is lost one day after shutdown. The peak pressure of about 41 psia (28.5×10^4 Pa) was achieved about 7,000 seconds after the loss of RHR. The peak pressure is reached at the time that the water in the steam generator secondary reaches saturation (satemp), which is reflected in the behavior of the primary and secondary water temperatures (tempf) and the vapor void fraction on the steam generator secondary side (see Figures C-6 and C-7).

Table C-1 presents the Case 1 distribution of air in the RCS as a function of time. These results show that the air is predicted to be removed from the vessel, hot leg piping, and steam generator inlet plenum and accumulated in the steam generator active tubes and outlet plenum volumes, pressurizer, and suction leg piping. Boiling in the core region is initiated about 1,250 seconds after loss of RHR as shown in Figure C-8, or when the liquid in the vessel above the core reaches saturation. Saturation is indicated by the water temperature in the uppermost core volume (114-06).

After the initiation of bulk boiling in the vessel and once the steam has compressed the air in the RCS to a volume less than that of the steam generator active tube region, a condensing surface is formed. As a result, the primary heat transfer rate increases and secondary side boiling is soon achieved. Once secondary side boiling occurs and the secondary temperature stabilizes, the primary system pressure then achieves a maximum. At this time, condensation in the generator occurs primarily in the first tube volume above the tube sheet, with some condensation also occurring in the next active tube volume. Figure C-9 shows the vapor void fraction in the first two volumes of the steam generator primary tubes (408 01 and 408 02) while Figures C-10 and C-11 show the heat flux in the steam generator primary tubes in these regions. The primary side heat transfer coefficients for these volumes are presented in Figures C-12 and C-13.

Because of the low decay heat fraction and the limited mixing of the air and steam in these first two steam generator active tube volumes above the tube sheet, primary pressure stabilizes. The condensation coefficient of about 3,000 W/M^2-K or 528 Btu/h-ft^2-°F after 7,000 seconds is sufficient to remove decay heat at the primary to secondary temperature difference of about 35°F, which develops during the later portion of the transient (see Figure C-12). The primary to secondary temperature difference is illustrated in Figure C-14. After 7,000 seconds, the mass flow toward the steam generator in the upper portion of the hot leg pipe is balanced by an equal amount of downflow from the steam generator toward the vessel in the lower part of the hot leg. Figure C-15 illustrates the establishment of this quasisteady-state mass flow in the upper and lower portions of the hot leg. The high mass flow rates are due to the high hot leg steam velocities that entrain the water in the upper portion of the pipe. Deentrained and condensed water accumulated in the steam generator inlet plenum and tubes flows back toward the vessel in the lower section.

Figure C-16 shows the noncondensable mass fraction in the U-bend of the steam generator active tubes. Figure C-17 presents the vapor temperature for this case. The secondary side temperature is also shown in Figure C-17. The decreasing mass fraction in the air region indicates that some steam has entered the cold side of the steam generator active tube region.

It is also of particular importance to note that the RELAP5 transient pressure response displays an oscillatory behavior once the peak pressure of about 41 psia is achieved after about 7,000 seconds (Figure C-5). These oscillations are a result of the changes in steam velocity at the entrance to the steam generator tubes, and affect the condensation coefficient and void fraction in the first tube region above the tube sheet. The transition from countercurrent two-phase flow to slug flow as liquid

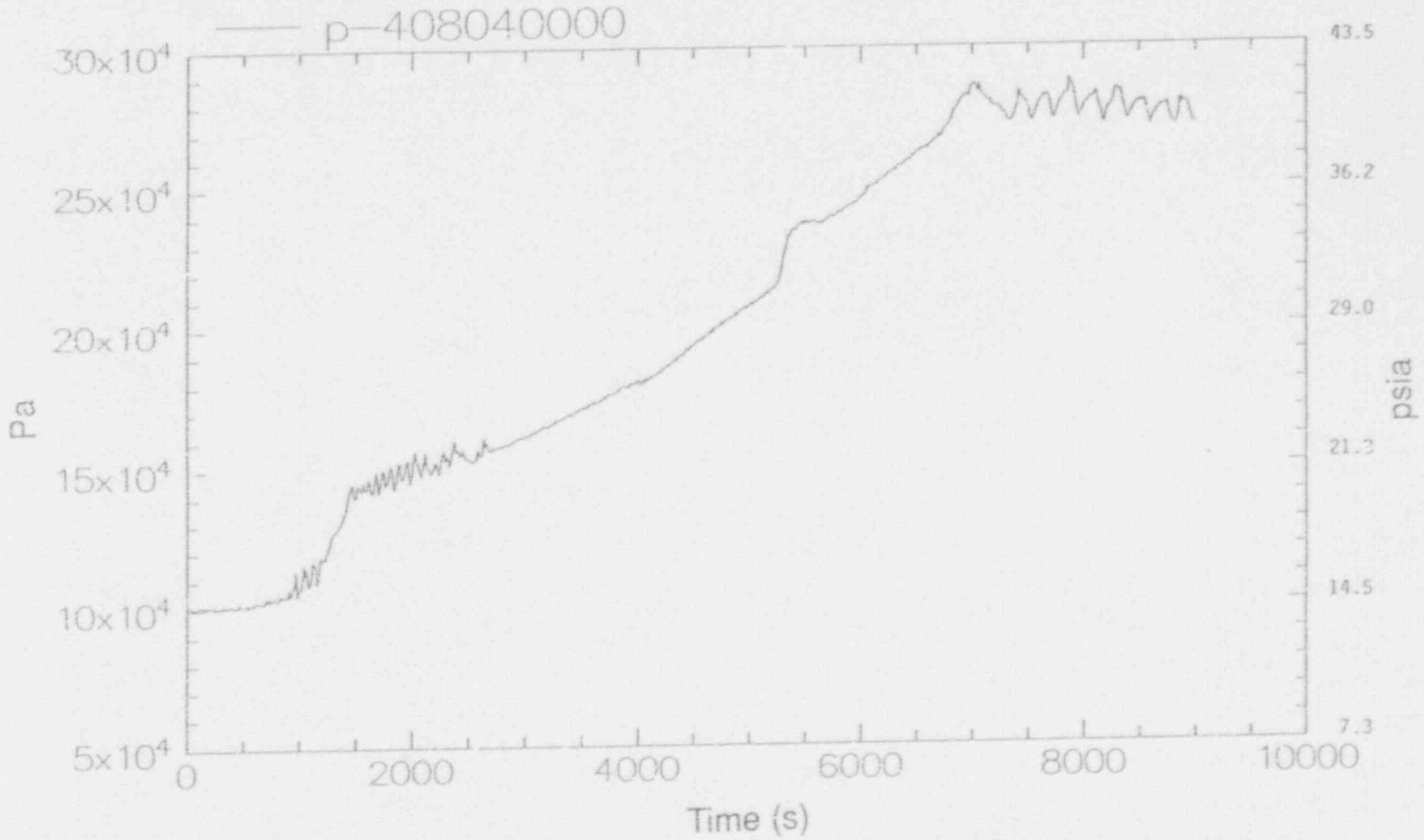

Figure C-5. Steam generator primary pressure for Case 1.

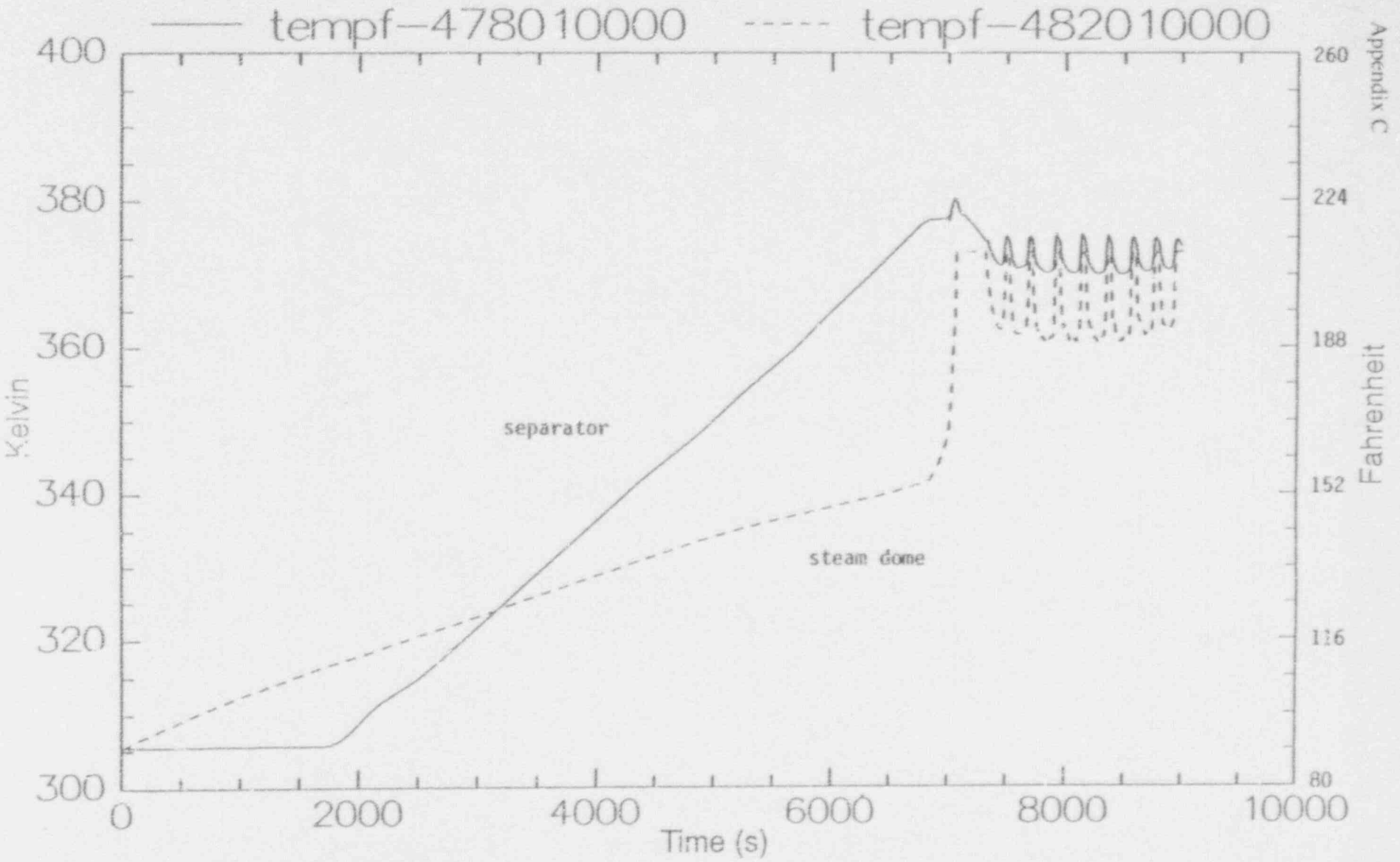

Figure C-6. Water temperature in the steam generator secondary for Case 1.

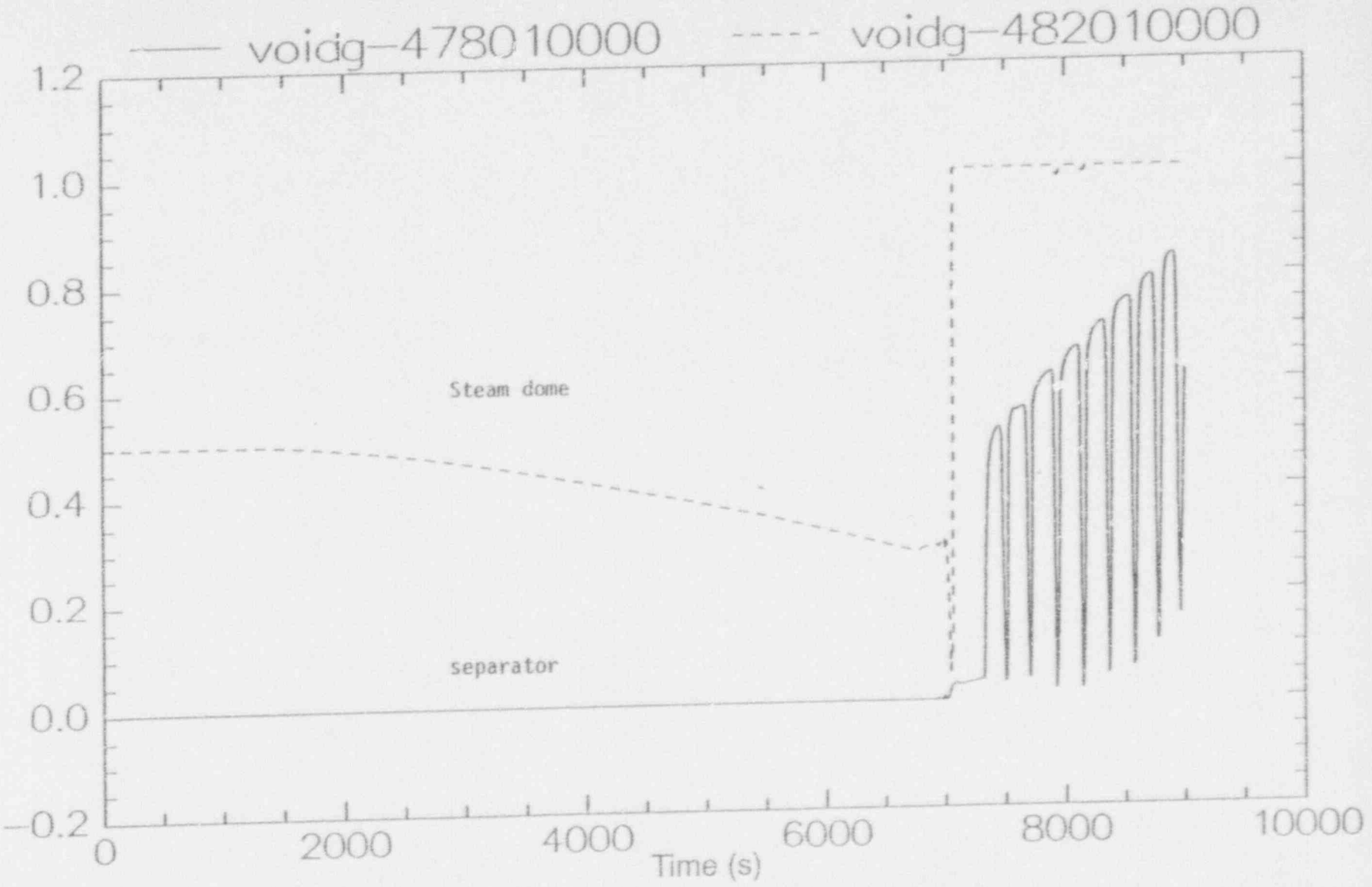

Figure C-7. Void fraction in the steam generator secondary for Case 1.

Table 1. Distribution of air in the RCS for RELAP5/MOD3 Case 1 (use of steam generators for decay heat removal).

	Mass of air (lb)			
Component (component number)	Initial	3,600 s	7,200 s	9,000 s
Downcomer (100)	7.7	12.4	10.7	10.3
Downcomer (102)	2.6	8.5	13.7	13.4
Downcomer (104)	0.0	6.6	10.5	10.4
Downcomer (106)	0.0	4.8	12.4	14.7
Upper plenum (120)	8.8	$<10^{-2}$	$<10^{-2}$	$<10^{-2}$
Upper plenum (122)	34.0	1.9	$<10^{-2}$	$<10^{-2}$
Upper head (126)	35.2	44.2	0.05	0.03
Hot leg (404, 405, 504, 505)	6.0	0.03	$<10^{-2}$	$<10^{-2}$
Steam generator inlet plenum (406, 506)	7.8	$<10^{-2}$	$<10^{-2}$	$<10^{-2}$
Steam generator tubes (408-01)	5.6	1.1	$<10^{-2}$	$<10^{-2}$
Steam generator tubes (408-02)	5.6	7.7	5.9	6.7
Steam generator tubes (408-03 to 408-08)	33.9	50.4	61.4	62.5
Steam generator outlet plenum (410)	7.9	13.0	7.1	6.7
Pressurizer/surge line (340, 341, 343)	91.4	87.9	85.5	63.9
Cold leg (412, 414, 416, 418, 420)	16.8	25.5	58.4	56.9

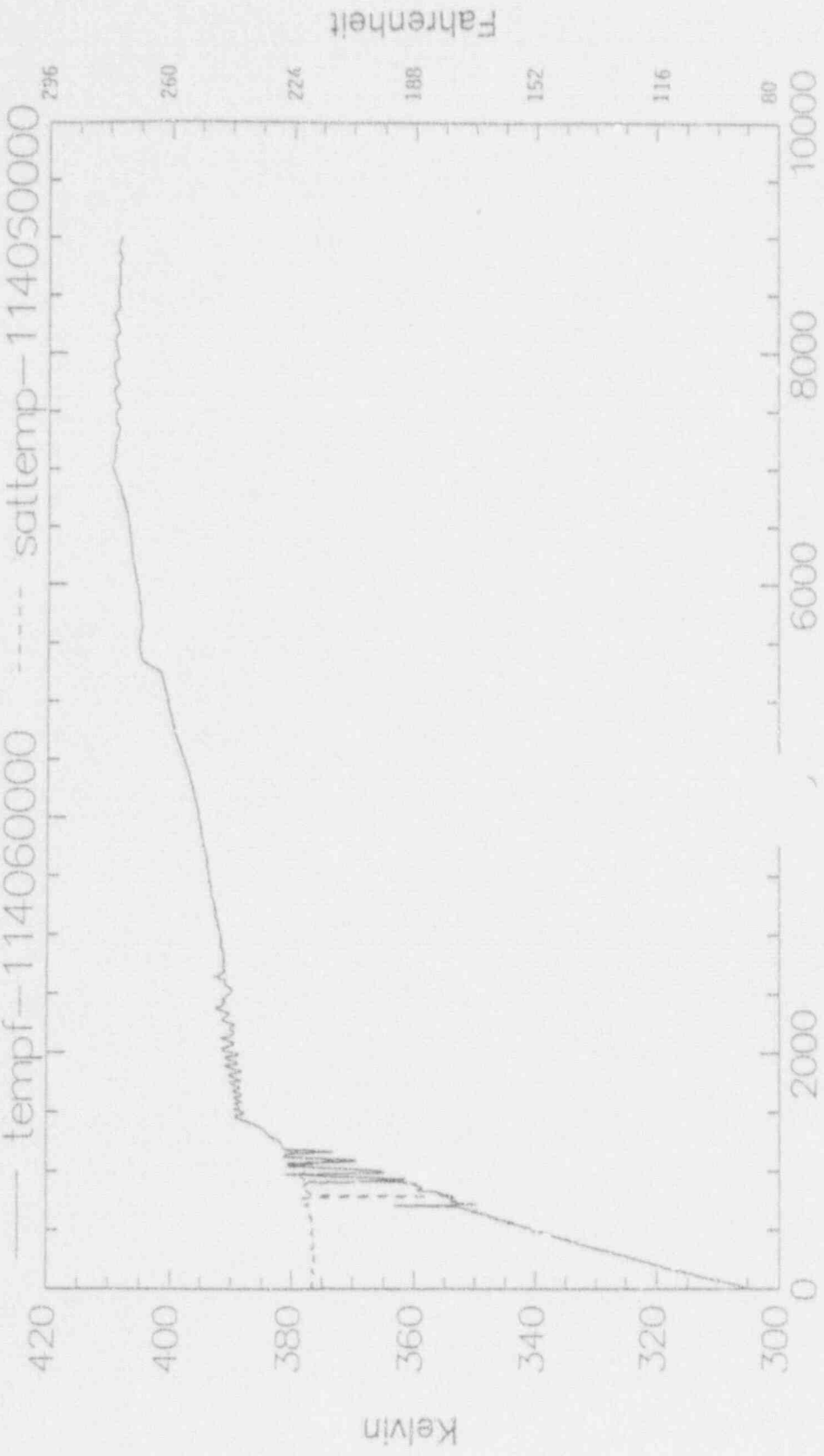

Figure C-8. Water temperature in the upper core volume (114-06) for Case 1.

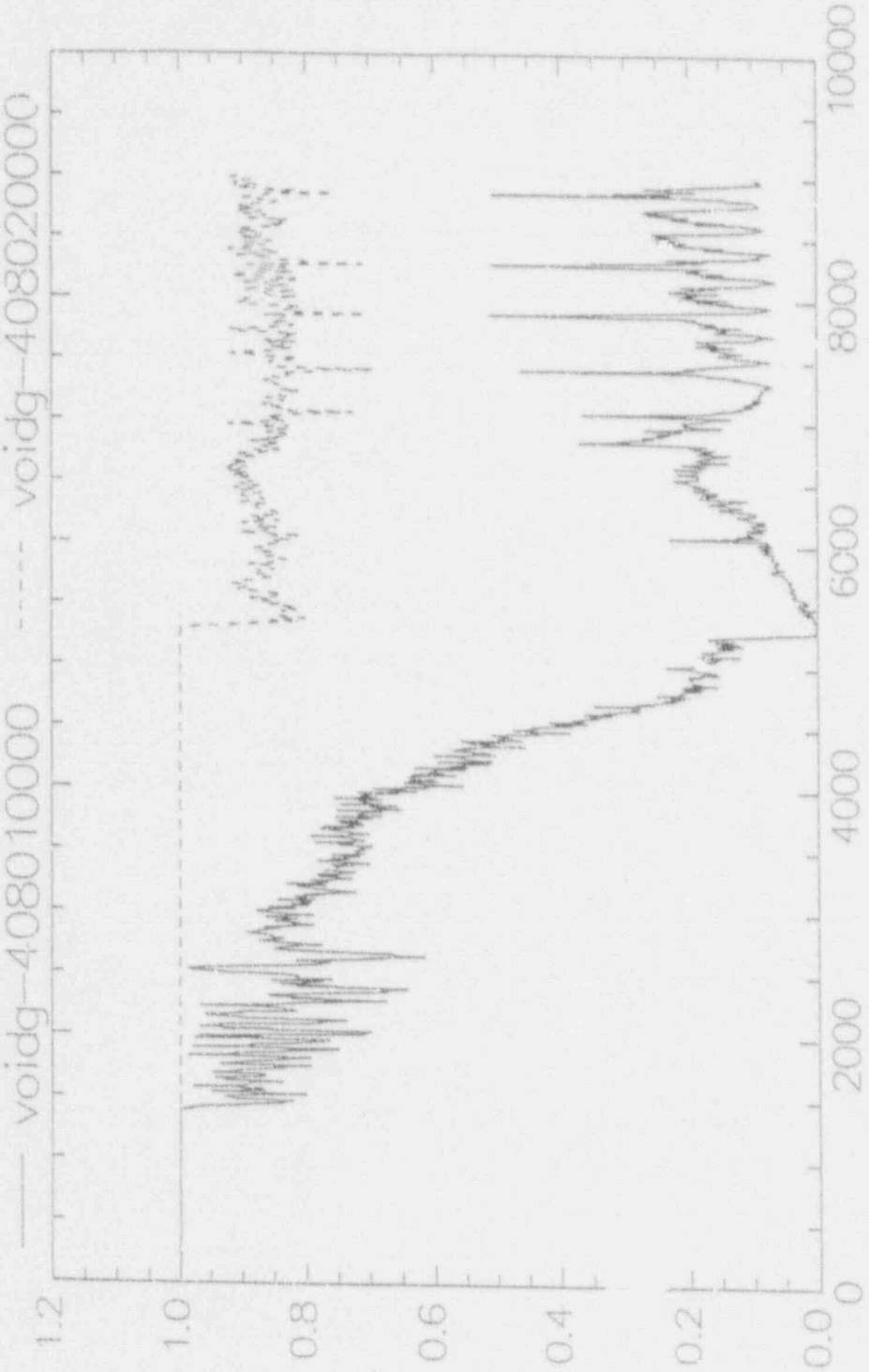

Figure C-9. Void fraction in the first two volumes of the steam generator tubes for Case 1.

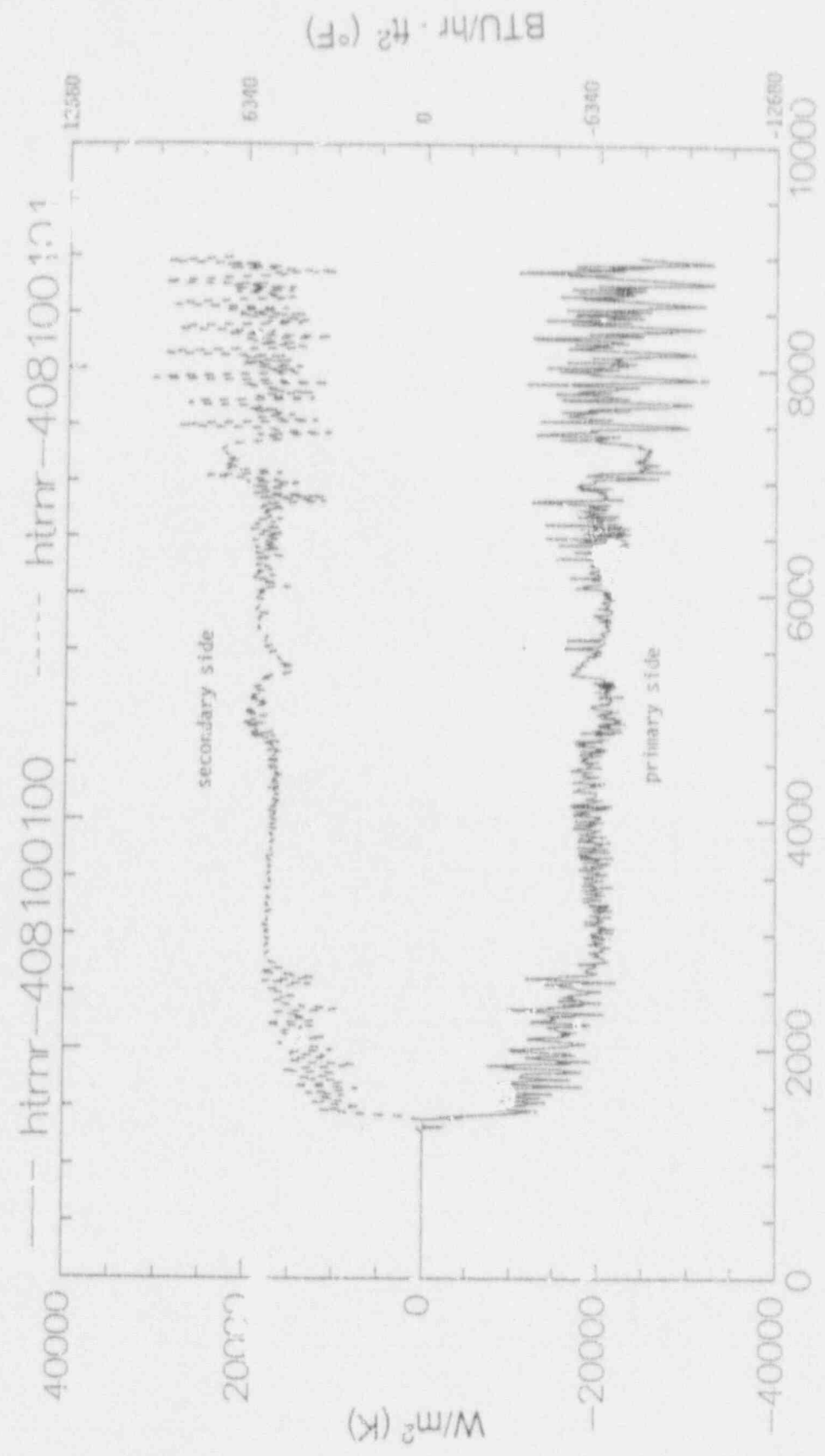

Figure C-10. Heat flux through the tubes in the first steam generator volume for Case 1.

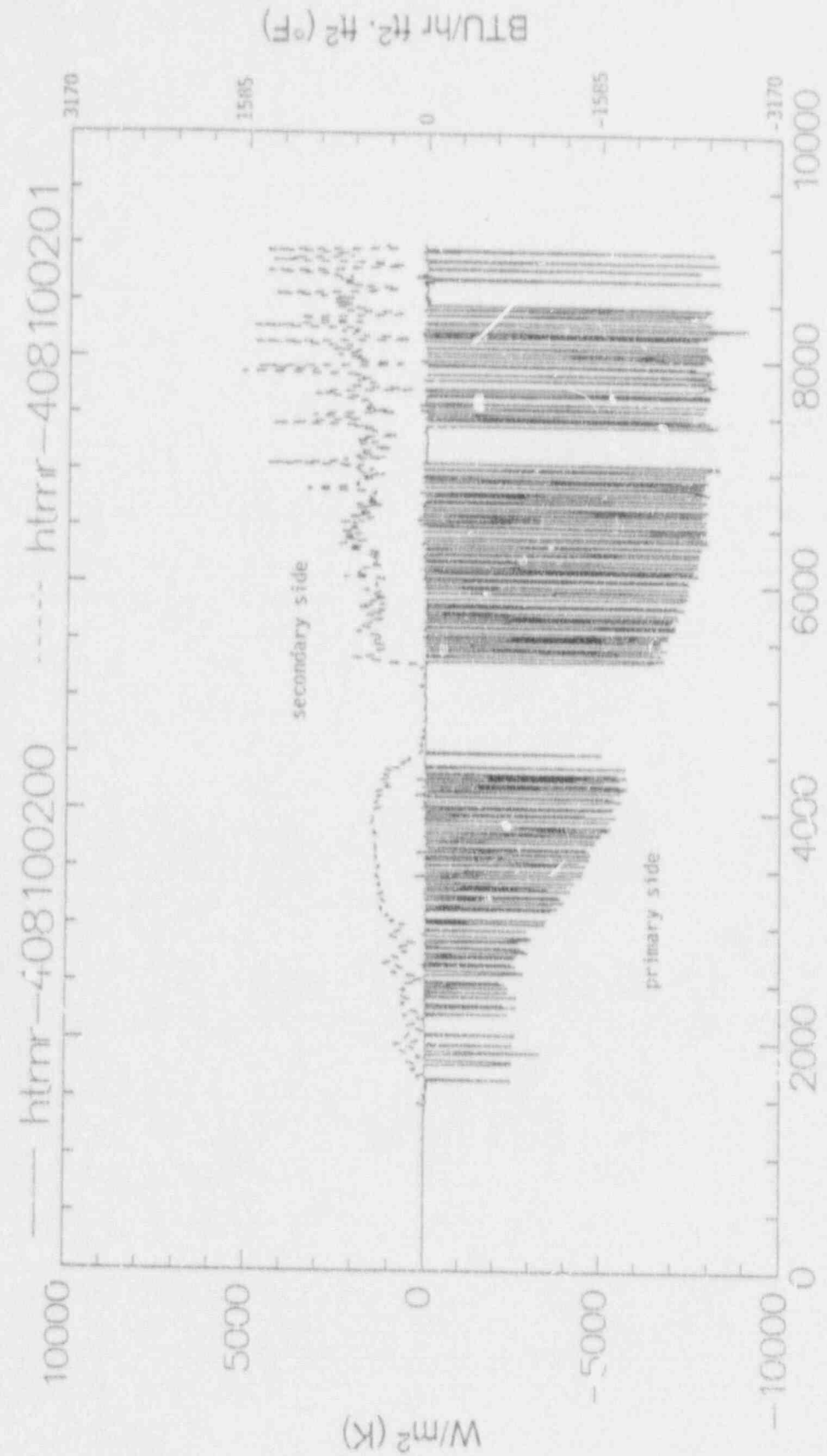

Figure C-11. Heat flux through the tubes in the second steam generator volume for Case 1.

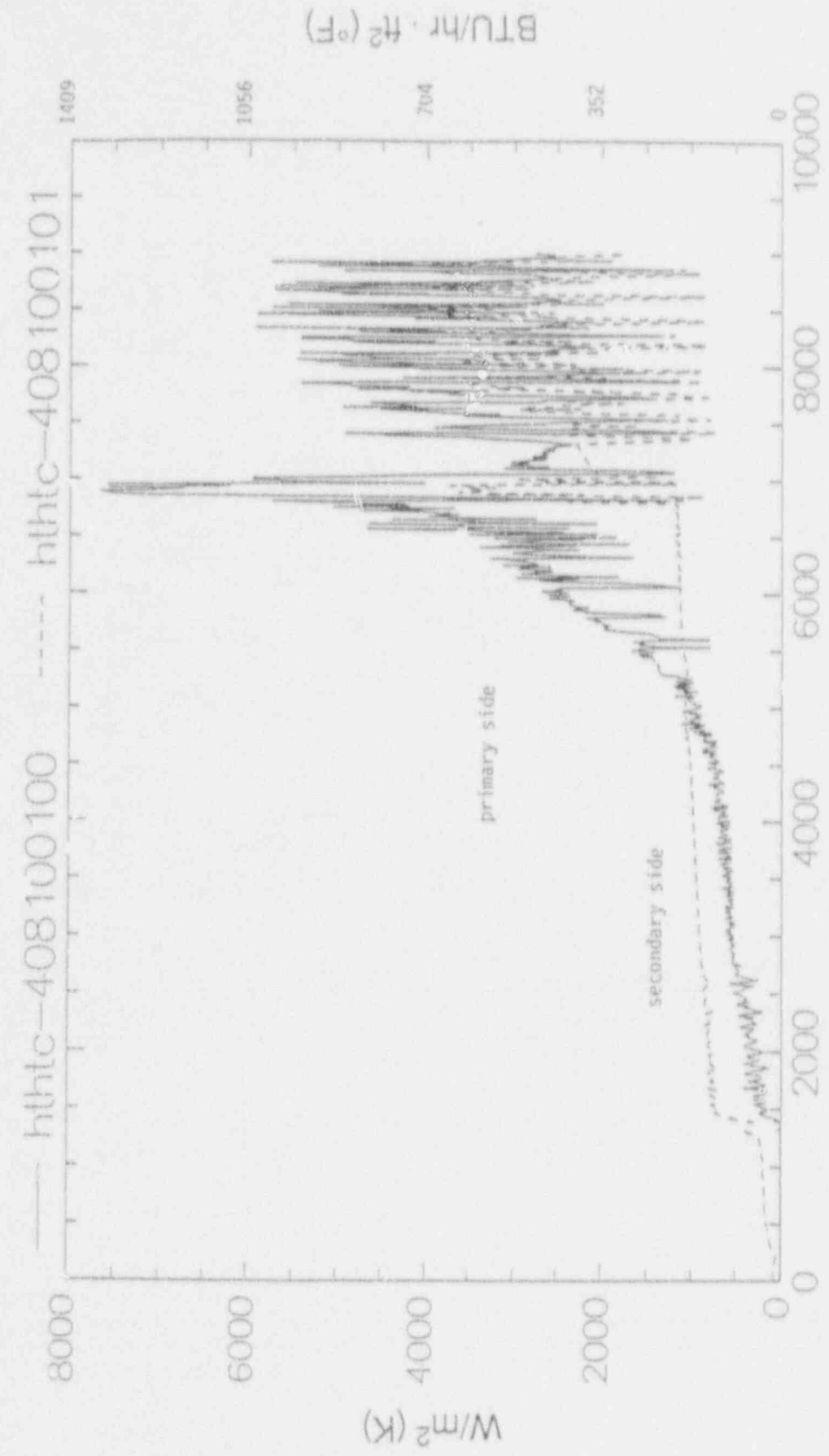

Figure C-12. Heat transfer coefficients in the first volume of the steam generator primary tubes for Case 1.

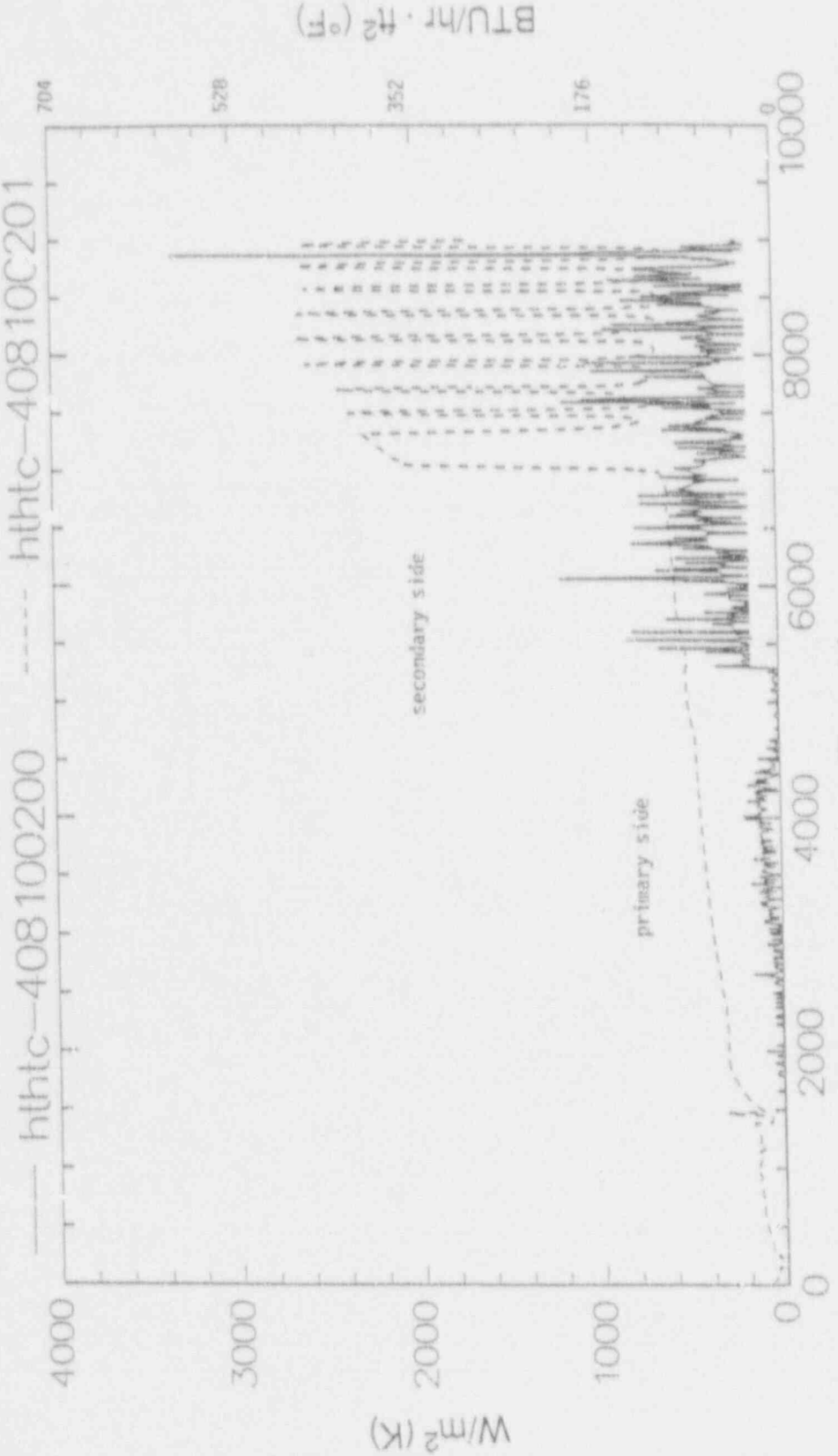

Figure C-13. Heat transfer coefficients in the second volume of the steam generator primary tubes for Case 1.

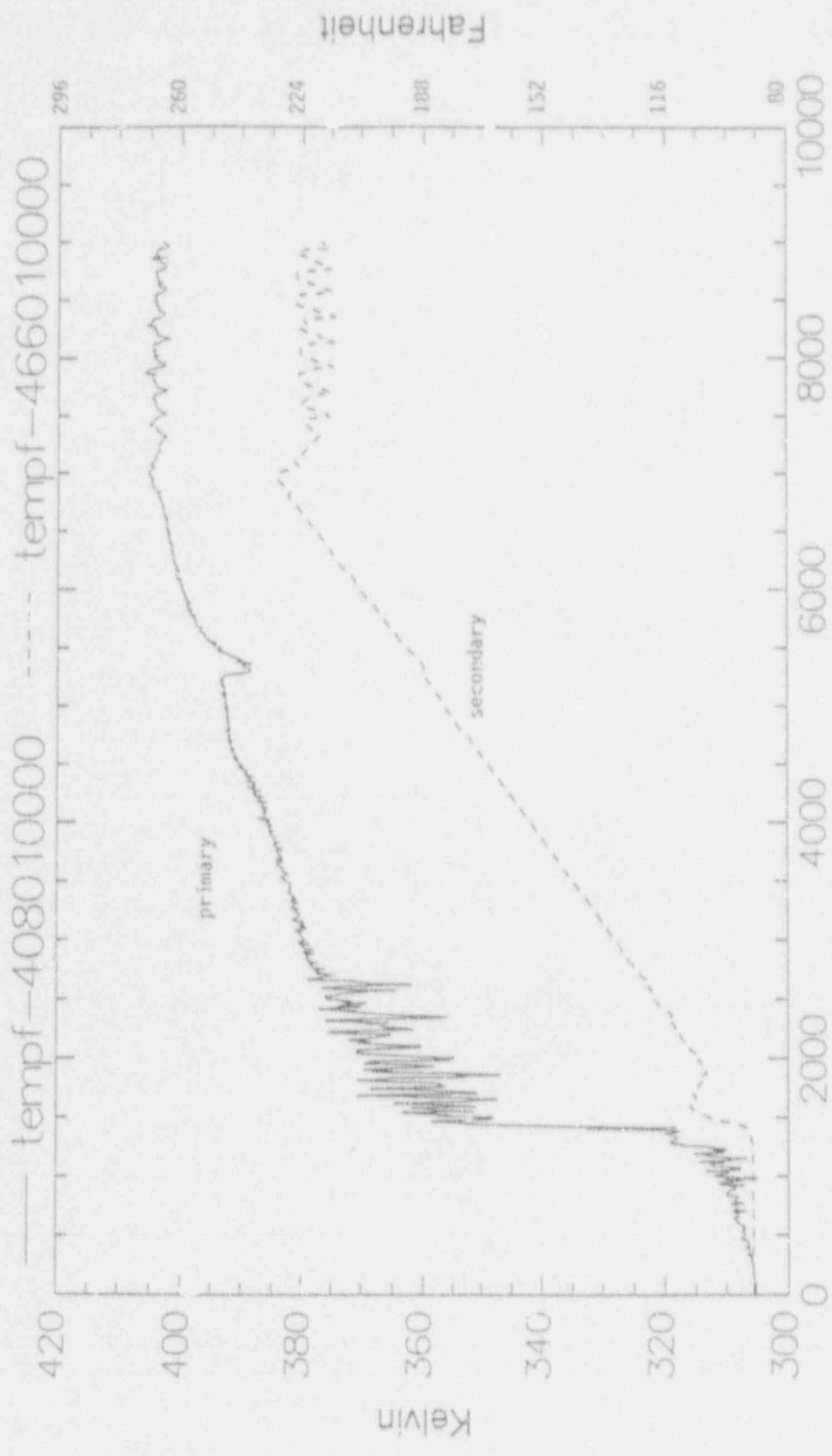

Figure C-14. Primary and secondary temperatures in first steam generator volume for Case 1.

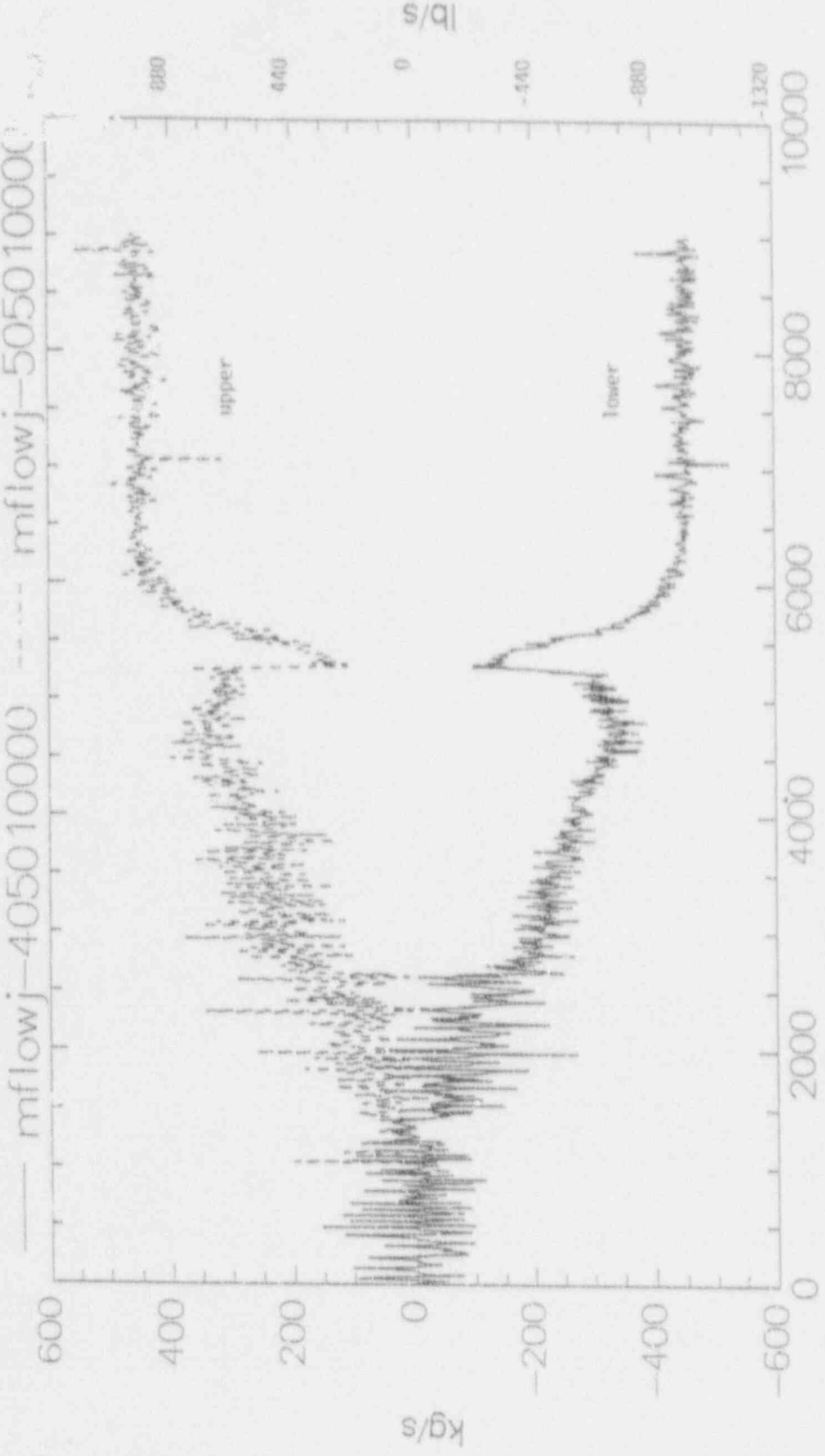

Figure C-15. Mass flow in the upper and lower parts of the hot leg for Case 1.

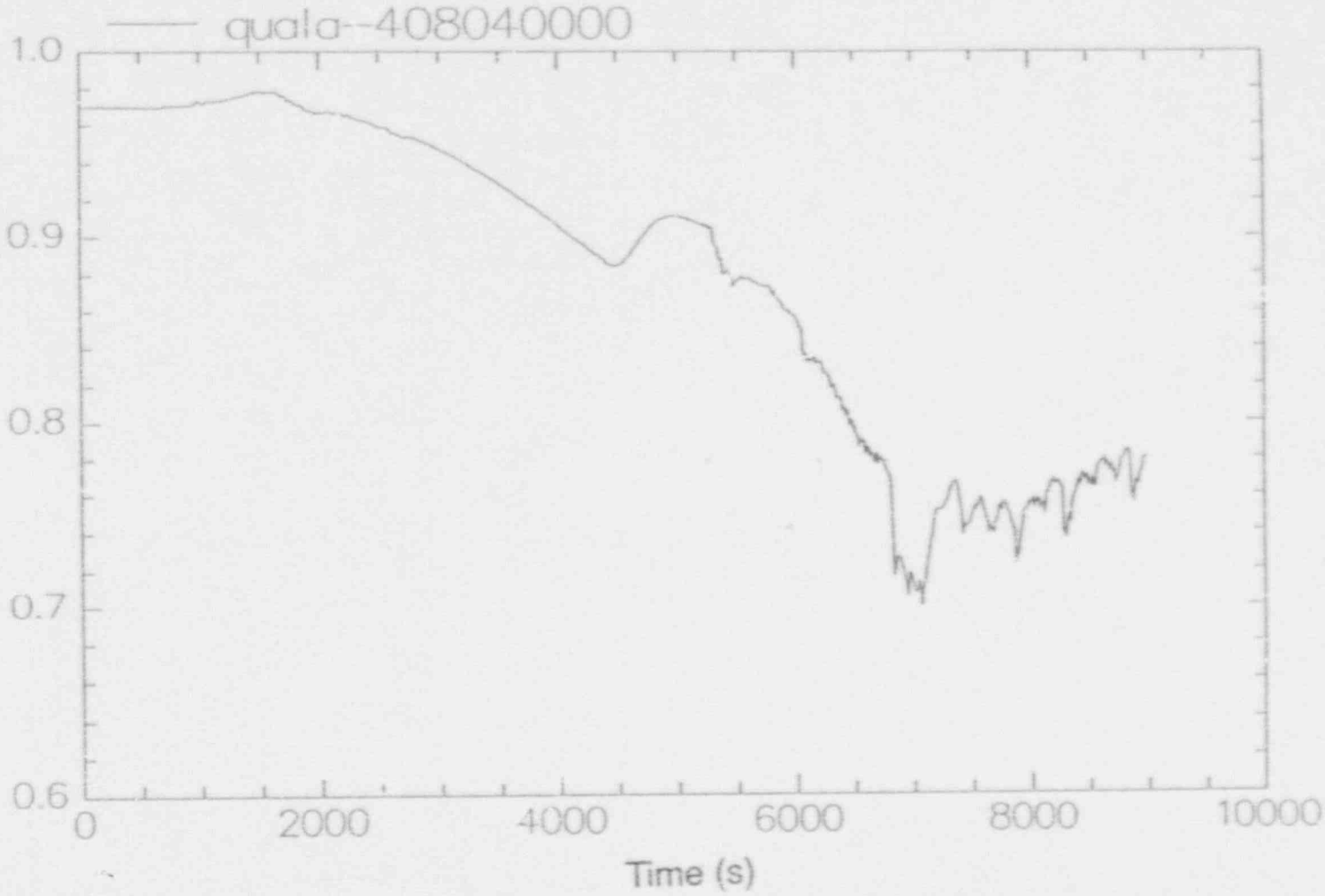

Figure C-16. Noncondensable mass fraction in the U-bend of the steam generator tubes for Case 1.

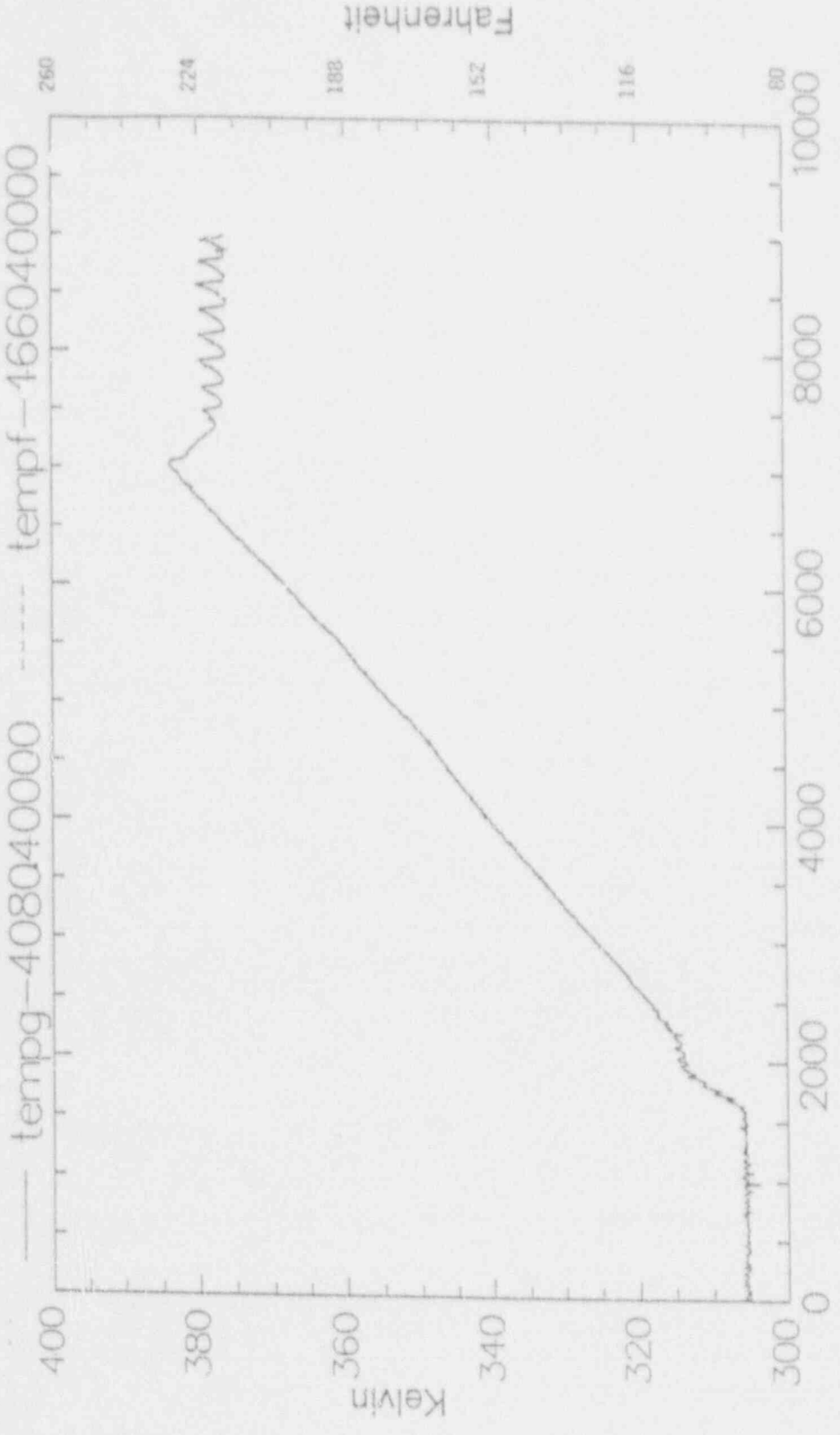

Figure C-17. Primary and secondary temperatures at the U-bend of the steam generator tubes for Case 1.

builds up and drains affects the pressure drop at the tube entrance. The subsequent effect on the steam velocities in the active tubes causes the heat transfer coefficient and void fraction to vary, producing the oscillations in RCS pressure (Figure C-5).

These results may be particularly important. The results suggest that while RCS peak pressure for the above reflux boiling conditions may not exceed nozzle dam failure conditions, if the oscillatory pressure behavior persists, in time it alone may be sufficient to dislocate a dam. If such conditions are realistic, the success of reflux boiling in mitigating the consequences of a loss of RHR depends not only on the peak RCS pressure but also the amplitude and period of the peak pressure oscillations that result later in the event.

C-2.2.2 Case 2—Loss of RHR at Seven Days. Figure C-18 shows the pressure response in the RCS when the RHR is lost seven days after shutdown. The peak pressure of about 38 psia (26.5×10^4 Pa) is reached approximately 12,000 seconds after the loss of RHR occurs. The peak pressure for this case is also reached at the time that the steam generator secondary reaches saturation as indicated by the behavior of the secondary water temperature (tempf) (Figure C-19).

Table C-2 presents the Case 2 distribution of air in the RCS as a function of time. These results again show that most of the air is predicted to be purged from the vessel, hot leg piping, and steam generator inlet plenum once core boiling begins. In general, the steam carries the air into the high points of the RCS or steam generator and pressurizer regions. Unlike Case 1, some air remains in the upper head because of the lower steam velocity in this region. The lower steam velocity is caused by the much lower decay heat level. Boiling in the core region begins about 2,600 seconds after loss of RHR as shown in Figure C-20. Boiling occurs when the water temperature in the uppermost core volume (114-06) reaches the saturation temperature.

Figure C-21 illustrates the vapor void fraction in the first two volumes of the steam generator primary tubes (408-01 and 408-02) and again shows that condensation in this portion of the steam generator develops sufficiently to remove decay heat when primary pressure reaches 38 psia. Figures C-22 and C-23 are plots of the heat flux through the steam generator primary tubes in the first two volumes. The heat transfer coefficients for these volumes are shown in Figures C-24 and C-25, while the primary to secondary temperature difference in the volume just above the tube sheet is given in Figure C-26.

These results are very similar to those for Case 1 above except the magnitude of the heat flux is lower for this case because of the lower decay heat power. Based on the Case 1 and 2 results, the peak pressure achieved after the loss of RHR is relatively insensitive to decay power since the bulk of the RCS pressurization is a direct result of the need to compress the air volume to a value that allows steam to reach the first steam generator active volume creating a condensing surface. The pressure required to compress the air to this condition is independent of power because the bulk of the pressurization of the RCS is needed to compress the air to the volume of the steam generator and outlet plenum volumes. Lower decay heat power levels simply delay the initiation of boiling and consequently delay the time the peak pressure (38–41 psia) is achieved. The mass flow characteristics in the upper and lower portions of the hot leg are similar to Case 1, as shown in Figure C-27. The noncondensable mass fraction and vapor temperature characteristics are also similar to Case 1 as shown in Figures C-28 and C-29, respectively. The analyses using the alternate methods of Appendix B also confirm these RELAP5 results.

C-2.2.3 Case 3—Loss of RHR at One Day with the Liquid Level at the Top of the Hot Leg. Figure C-30 shows the transient pressure in the RCS when decay heat is lost one day after shutdown. Unlike Case 1 with the initial level at the hot leg centerline, the initial RCS water level for Case 3 is increased to the top elevation of the hot leg piping. Following the loss of RHR and initiation of bulk boiling in the RCS, the peak pressure of about 40 psia (28.5×10^4 Pa) is reached

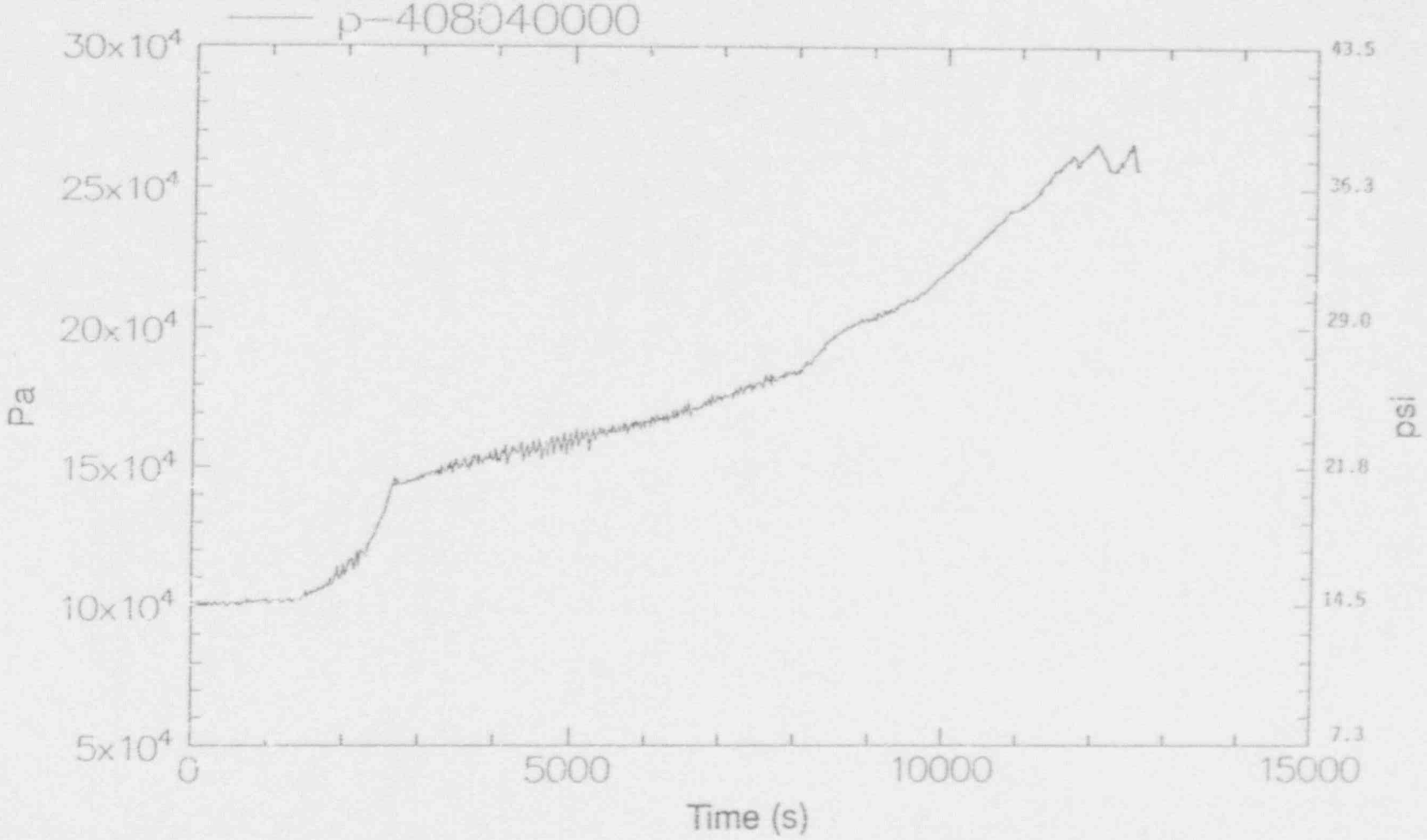

Figure C-18. Steam generator primary pressure for Case 2.

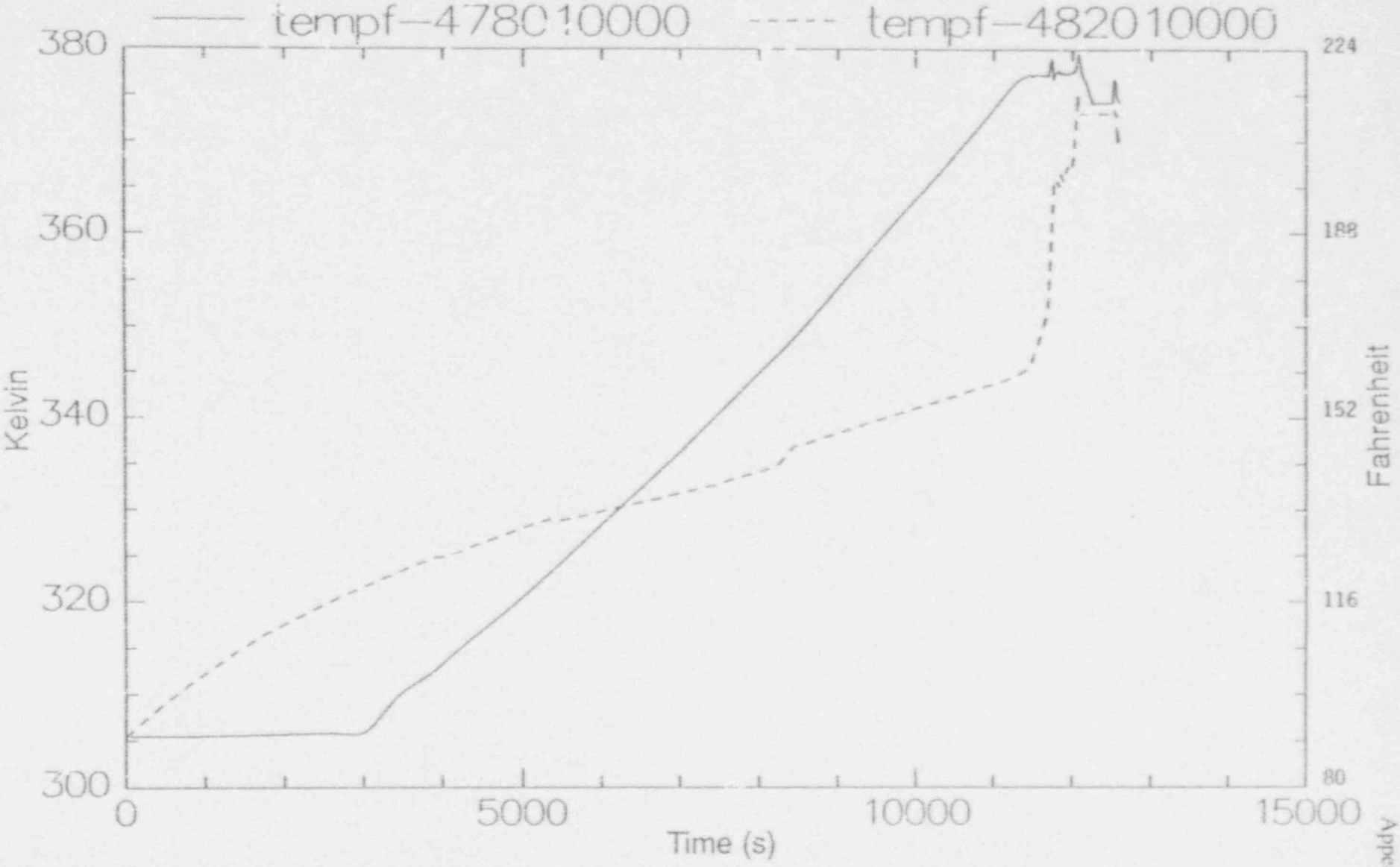

Figure C-19. Water temperature in the steam generator secondary for Case 2.

Table 2. Distribution of air in the RCS for RELAP5/MOD3 Case 2 (use of steam generators for decay heat removal).

	Mass of air (lb)				
Component (component number)	Initial	3,600 s	7,200 s	10,800 s	12,600 s
Downcomer (100)	7.7	11.5	13.2	17.2	16.6
Downcomer (102)	2.6	7.7	8.7	11.2	12.3
Downcomer (104)	0.0	5.9	6.4	8.4	9.2
Downcomer (106)	0.0	3.1	3.1	8.9	9.4
Upper plenum (120)	8.8	$<10^{-2}$	$<10^{-2}$	$<10^{-2}$	$<10^{-2}$
Upper plenum (122)	34.0	2.9	4.4	$<10^{-2}$	0.02
Upper head (126)	35.2	37.6	33.2	16.0	8.7
Hot leg (404, 405, 504, 505)	6.0	0.03	$<10^{-2}$	$<10^{-2}$	$<10^{-2}$
Steam generator inlet plenum (406, 506)	7.8	0.06	0.05	$<10^{-2}$	0.01
Steam generator tubes (408-01)	5.6	4.9	3.8	0.03	0.2
Steam generator tubes (408-02)	5.6	8.1	7.7	5.7	6.7
Steam generator tubes (408-03 to 408-08)	33.9	49.7	49.9	49.9	48.9
Steam generator outlet plenum (410)	7.9	11.7	13.5	17.2	18.2
Pressurizer/surge line (340, 341, 343)	91.4	89.7	87.6	88.6	88.9
Cold leg (412, 414, 416, 418, 420)	16.8	22.2	25.5	32.7	37.7

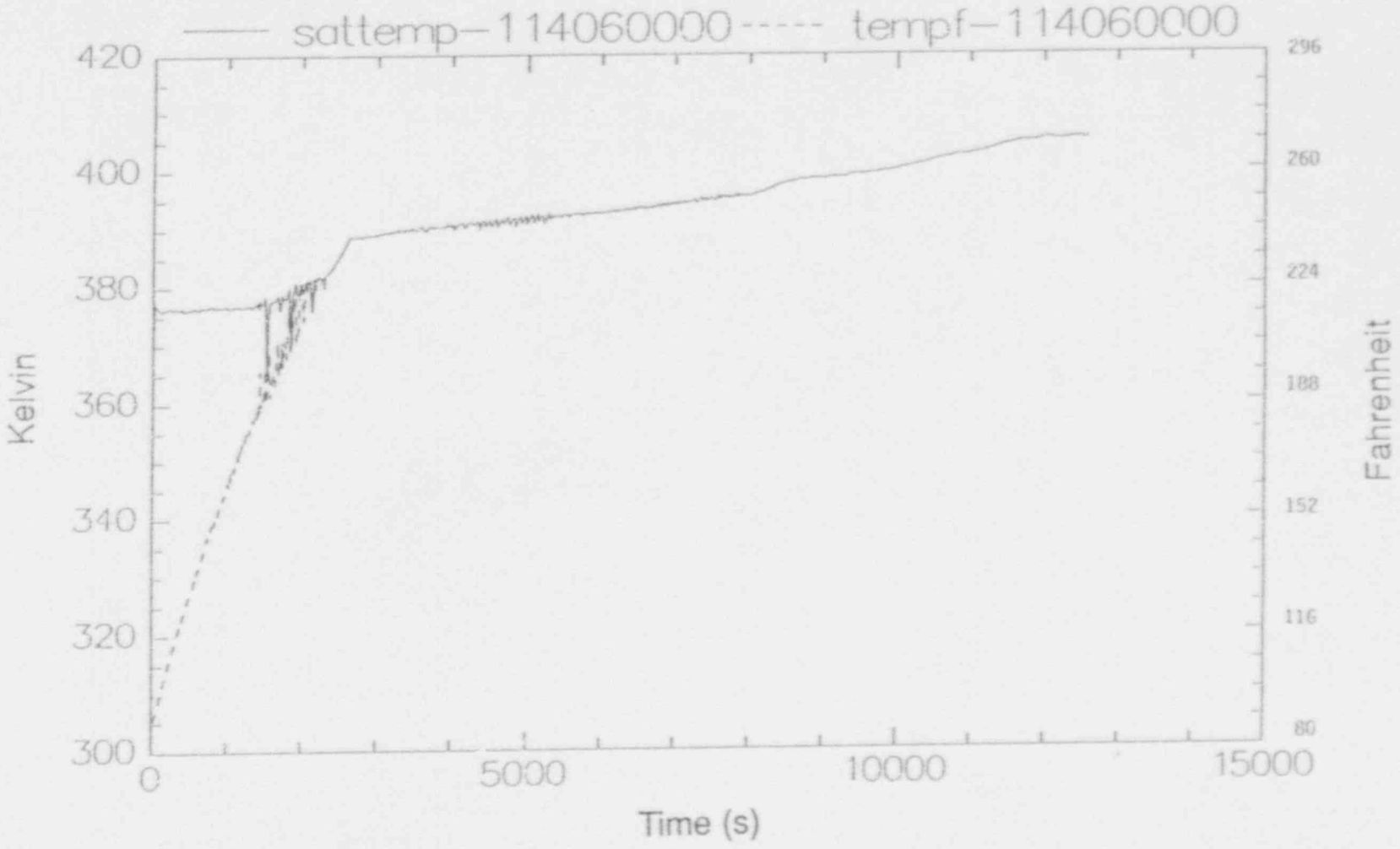

Figure C-20. Water temperature in the upper core volume (114-06) for Case 2.

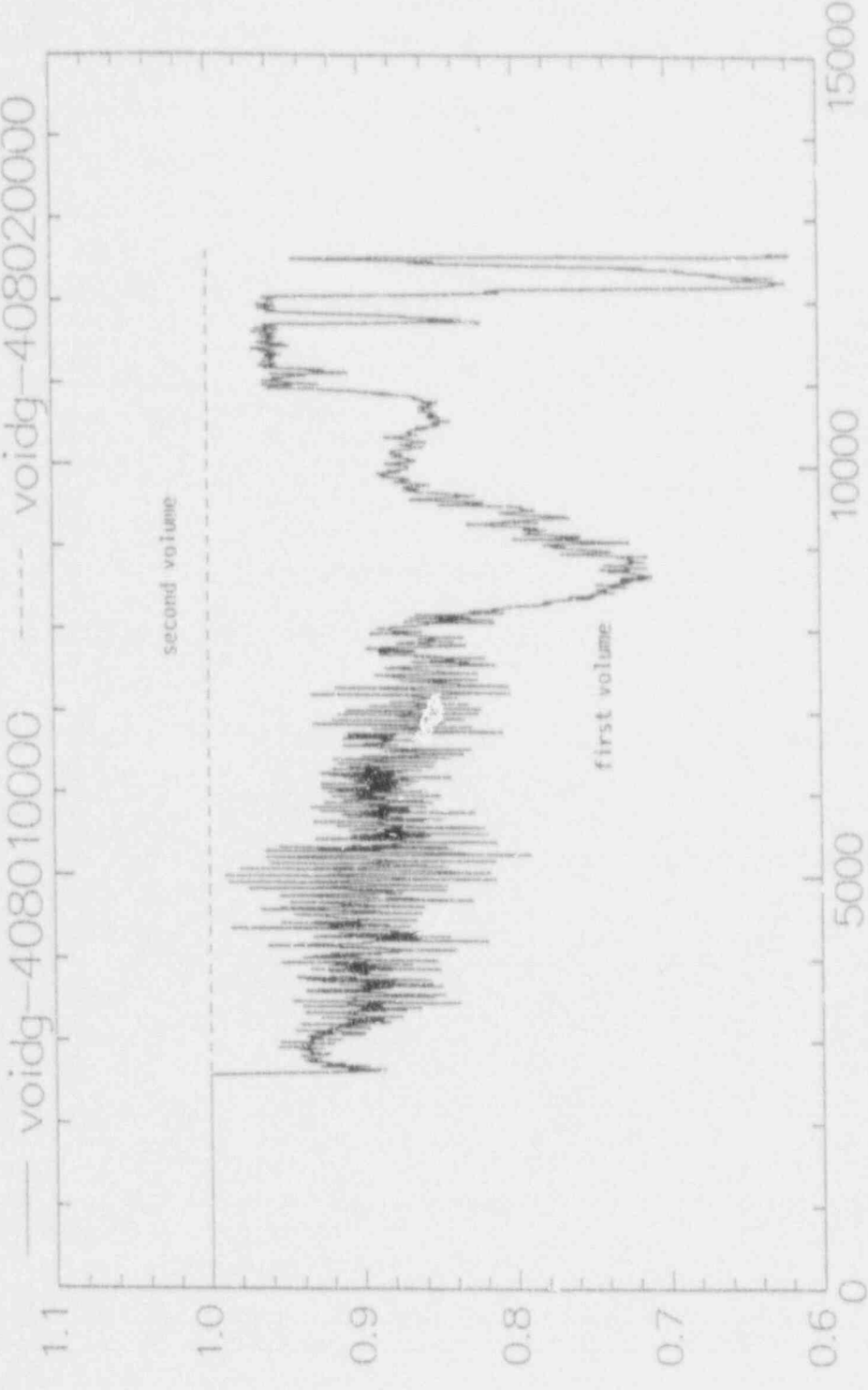

Figure C-21. Void fraction in the first two volumes of the steam generator for Case 2.

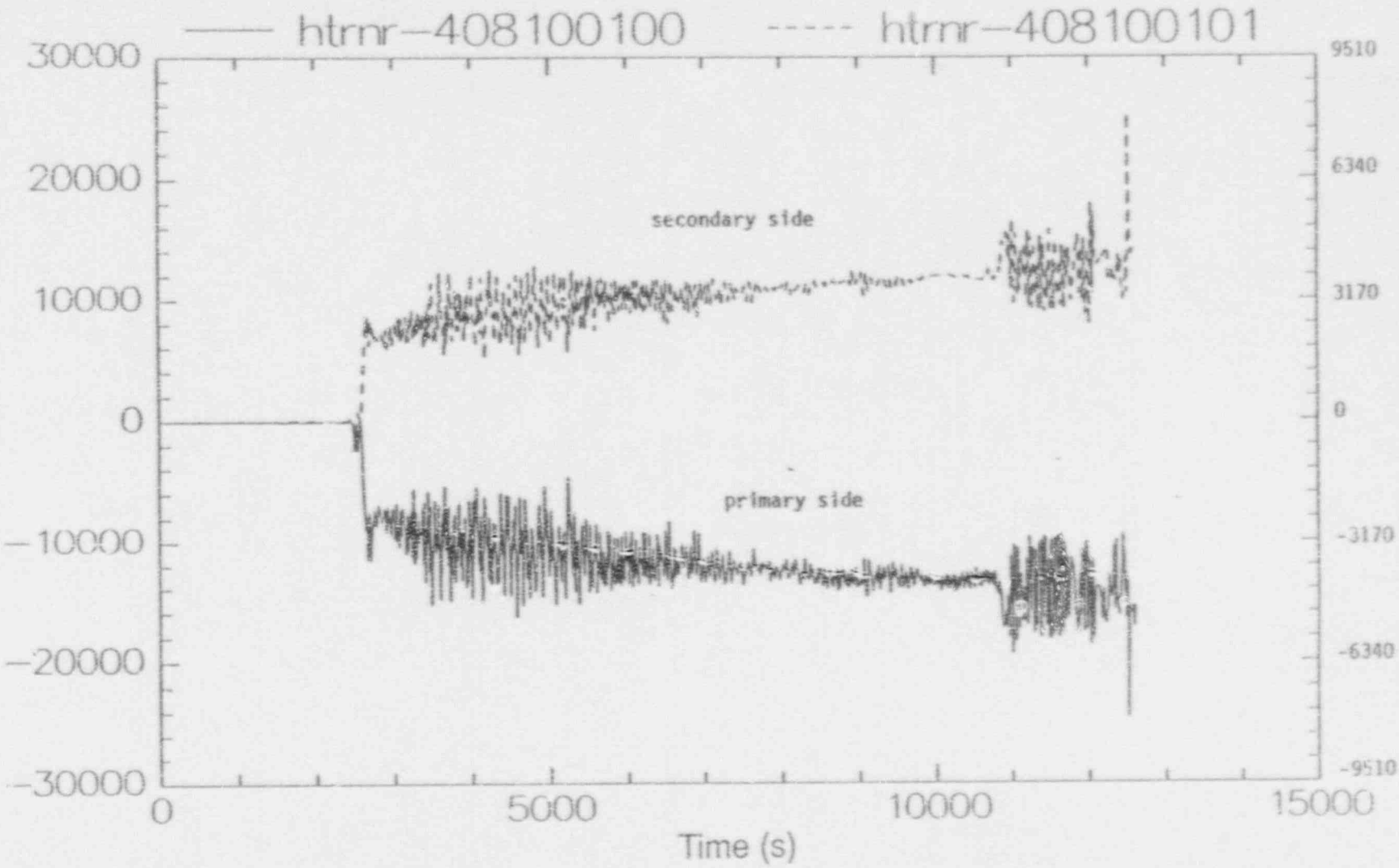

Figure C-22. Heat flux through the tubes in the first steam generator volume for Case 2.

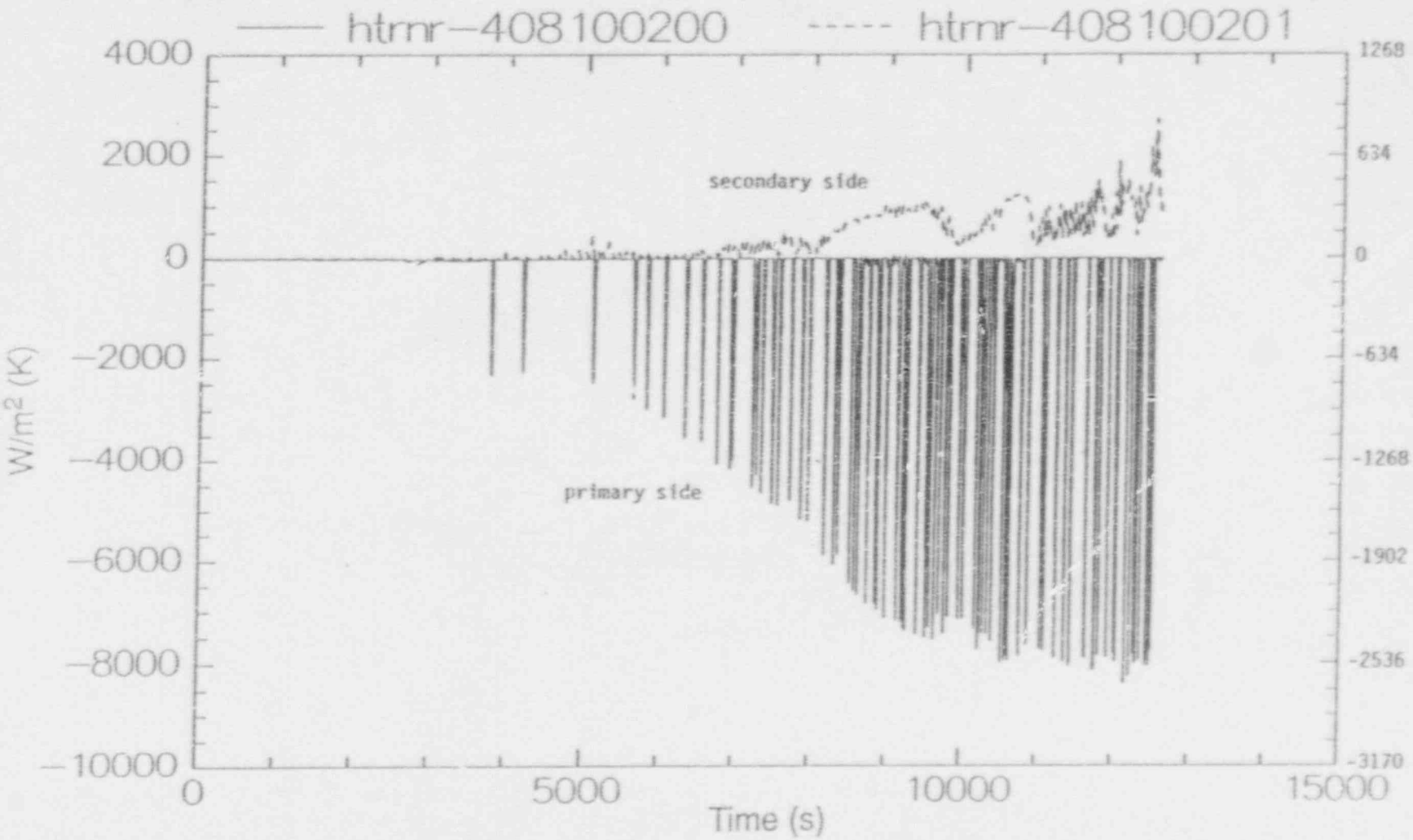

Figure C-23. Heat flux through the tubes in the second steam generator volume for Case 2.

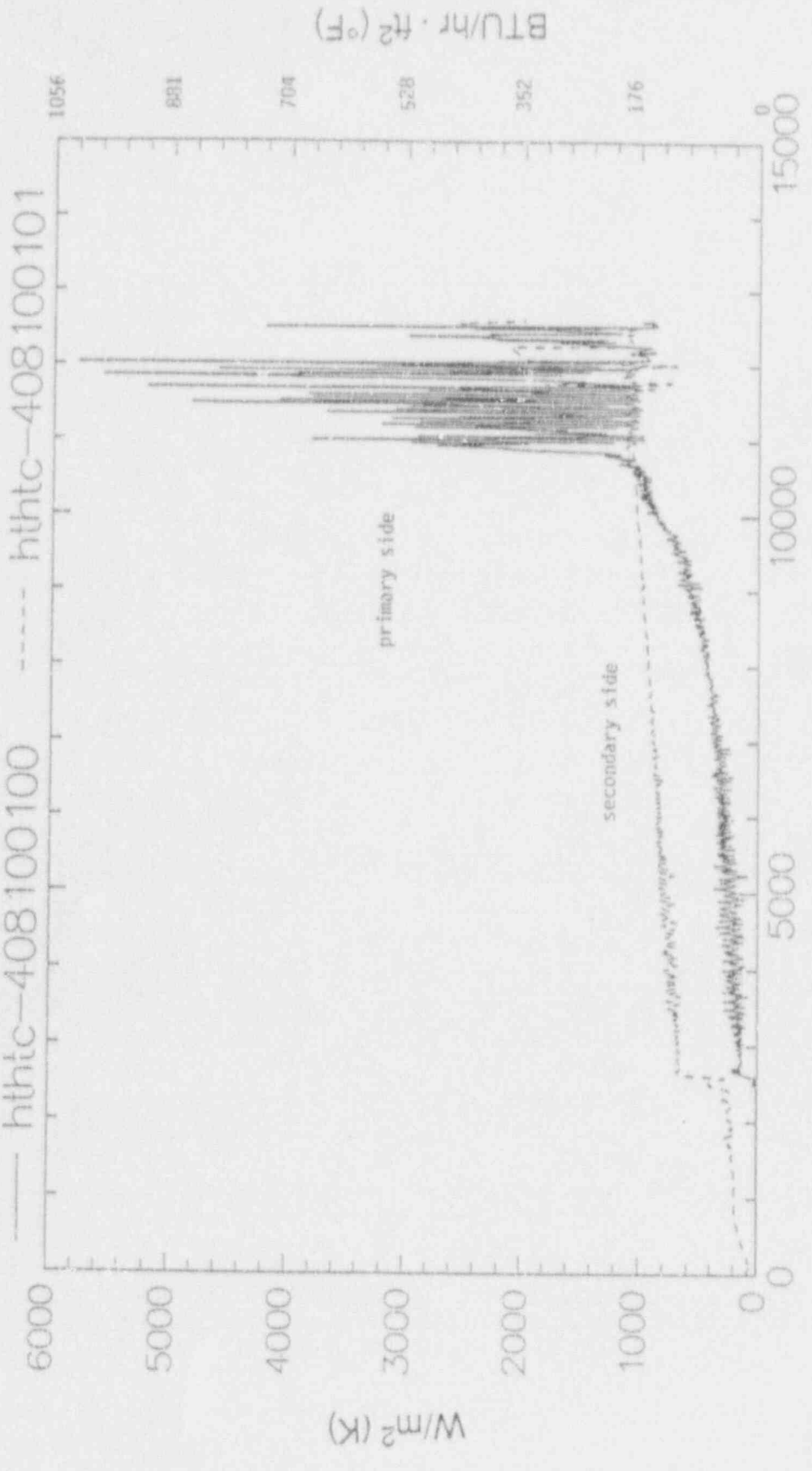

Figure C-24. Heat transfer coefficients in the first volume of the steam generator primary tubes for Case 2.

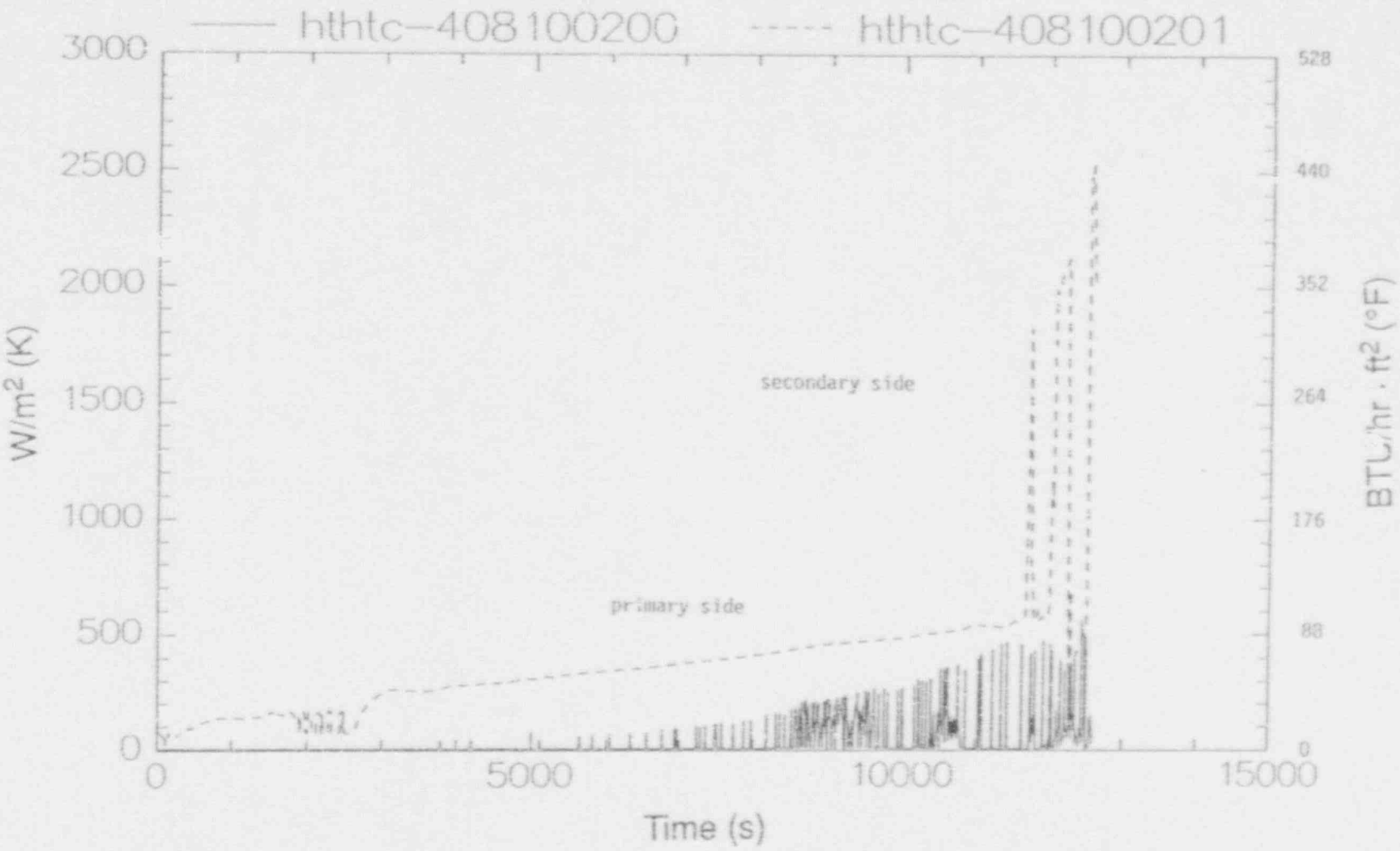

Figure C-25. Heat transfer coefficients in the second volume of the steam generator primary tubes for Case 2.

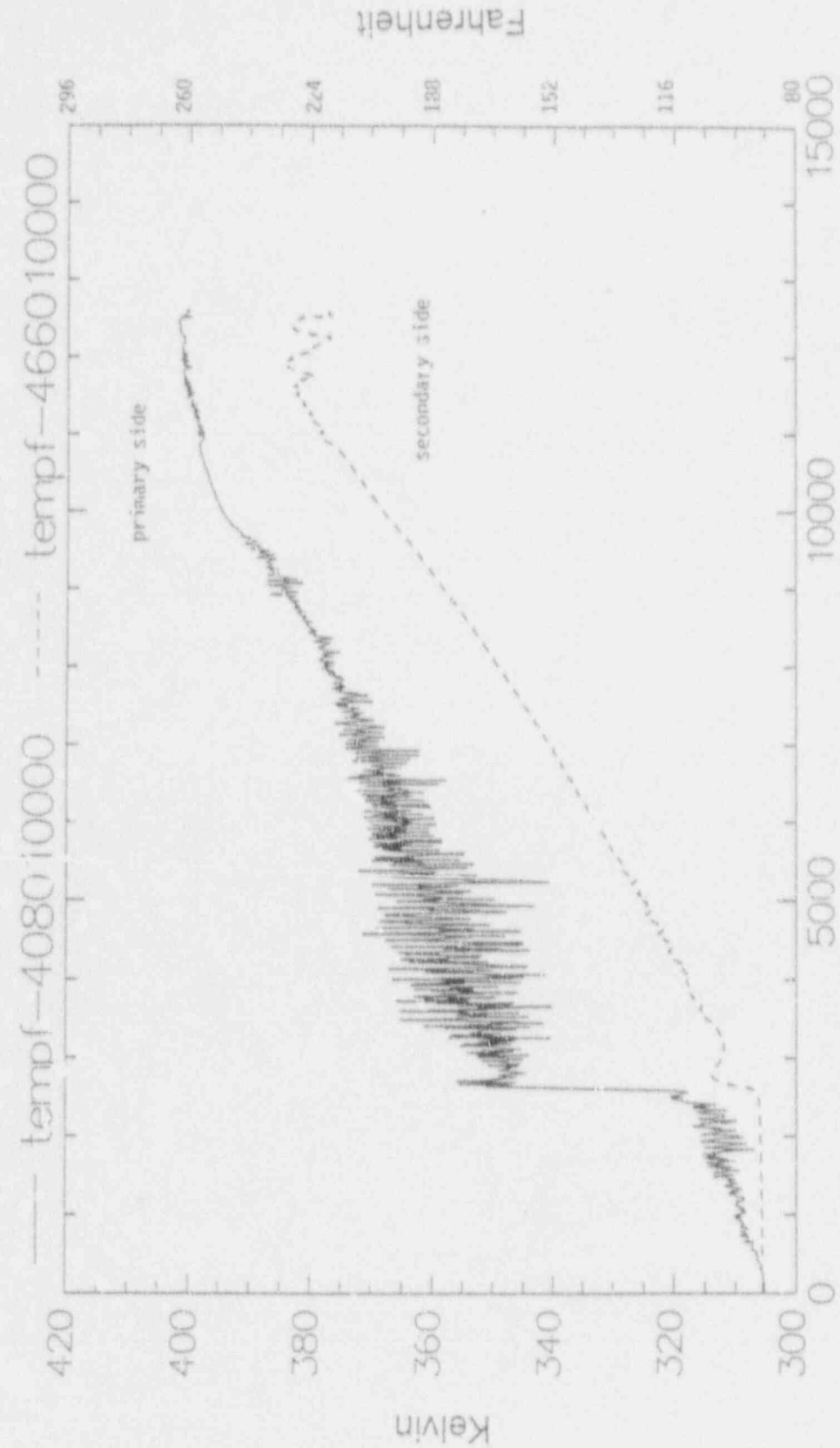

Figure C-26. Primary and secondary temperature in the first steam generator volume for Case 2.

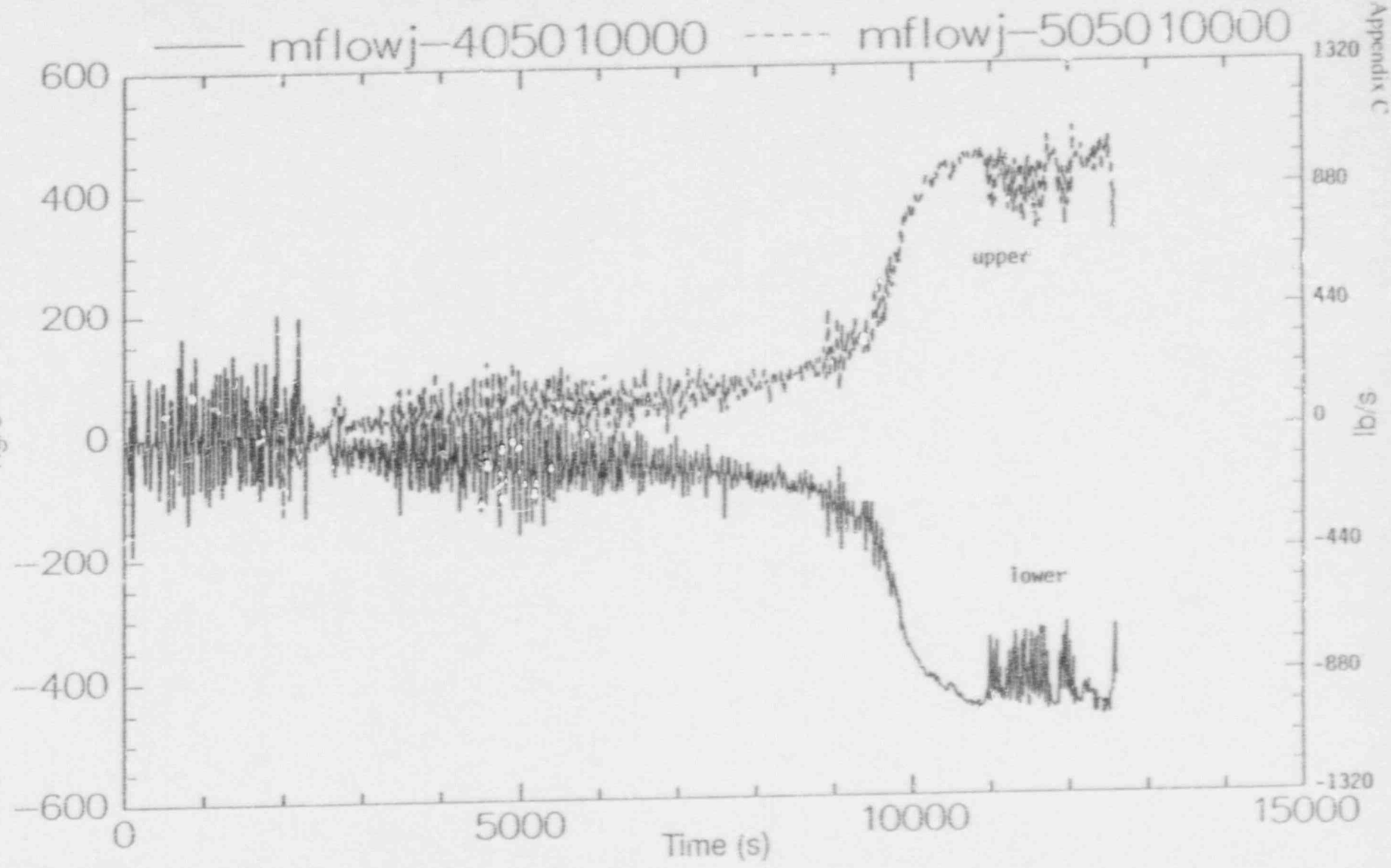

Figure C-27. Mass flow in the upper and lower parts of the hot leg for Case 2.

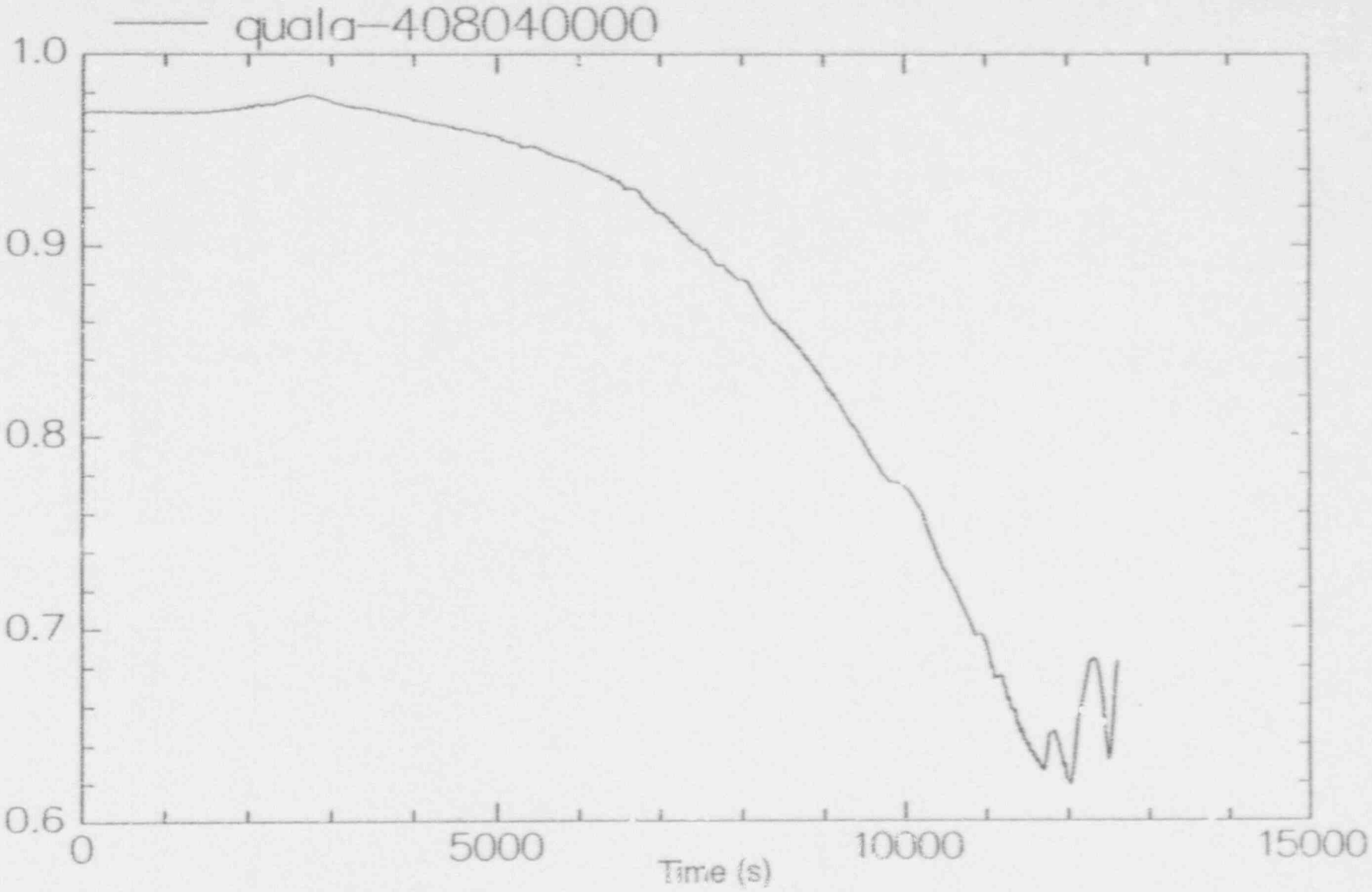

Figure C-28. Noncondensable mass fraction in the U-bend of the steam generator tubes for Case 2.

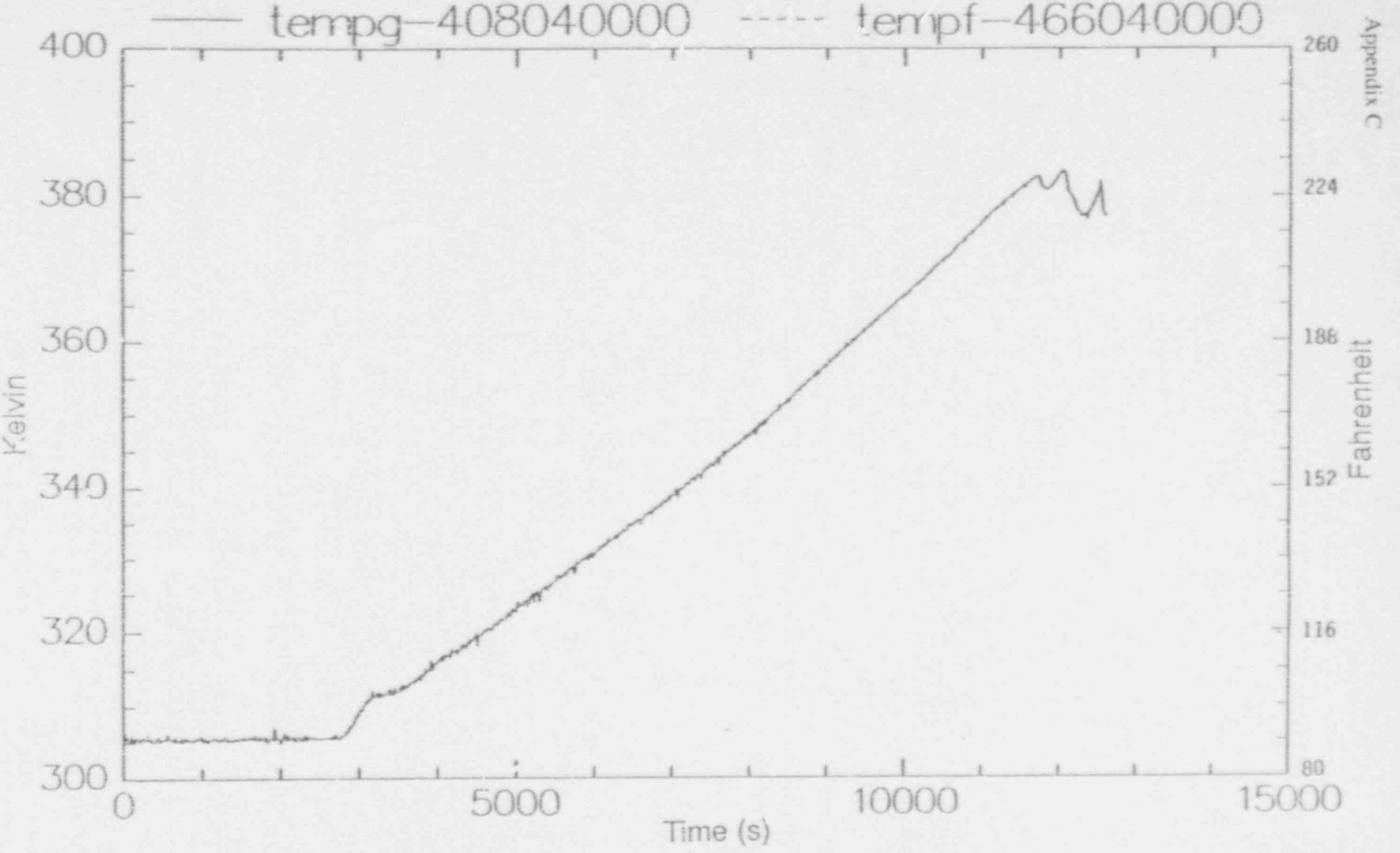

Figure C-29. Primary and secondary temperatures at the U-bend of the steam generator tubes for Case 2.

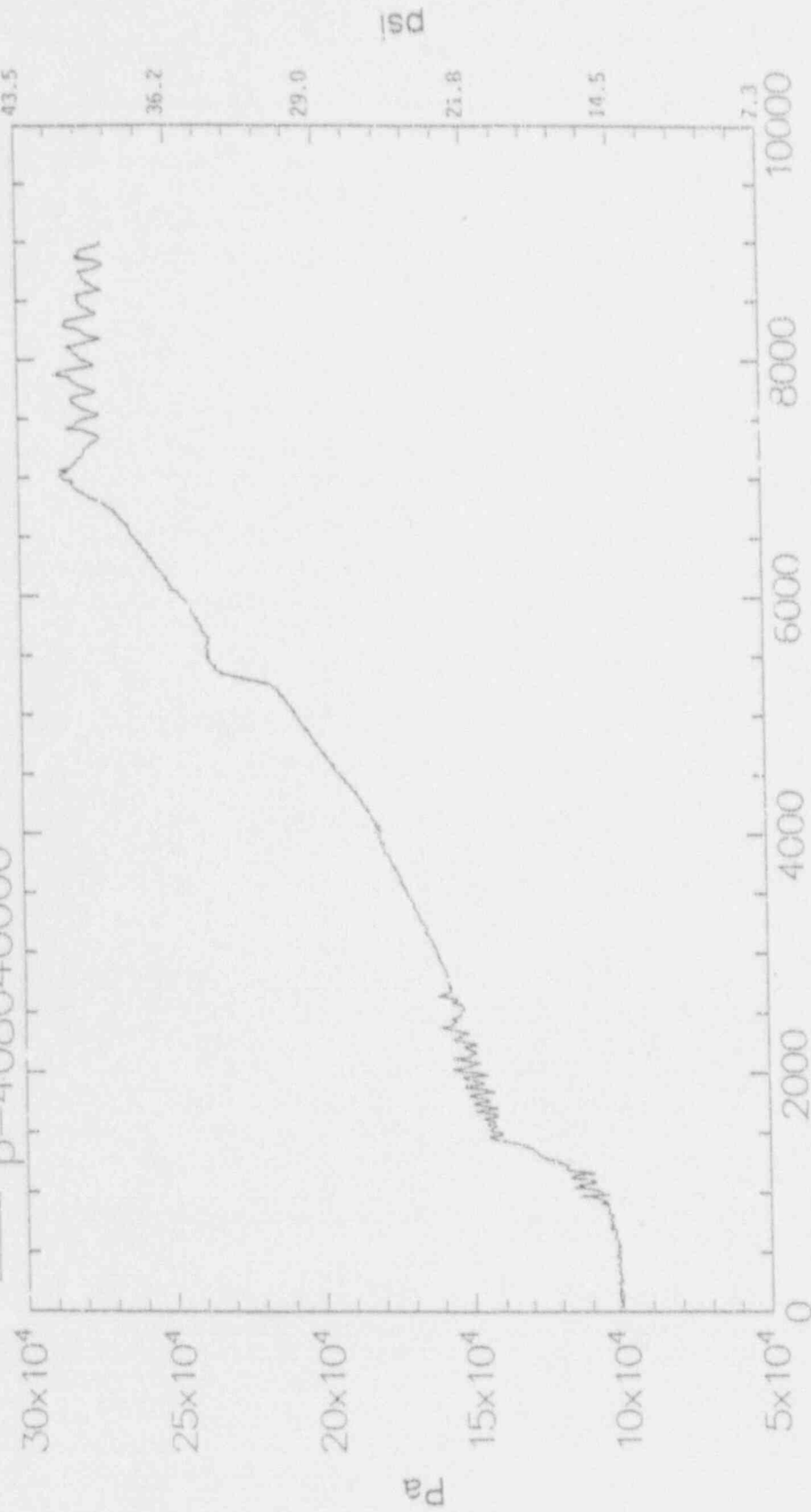

Figure C-30. Steam generator primary pressure for Case 3.

at approximately 7,500 seconds, as shown in Figure C-30. The peak pressure again is reached after the time the water in the steam generator secondary reaches saturation, as shown by the secondary behavior of the water temperature (tempf) in Figure C-31. Comparison with Case 1, where the initial water level was at mid-loop operation, demonstrates that the peak pressure is not sensitive to initial water levels between the hot leg midplane and top elevations. This is not surprising because with this initial water level, fluid expansion and the entrainment of water from the hot legs is still insufficient to plug the entrance into the steam generators to prevent the development of a condensing surface.

Table C-3 presents the Case 3 distribution of air in the RCS as a function of time. These results show that most of the air is predicted to be swept by the steam into the steam generator from the reactor vessel, hot leg, and inlet plenum once core boiling begins. Boiling in the core region begins about 1,500 seconds after loss of RHR as shown in Figure C-32, based on the water temperature in the uppermost core volume (114-06).

Figure C-33 shows the vapor void fraction in the first two volumes of the steam generator primary tubes (408-01 and 408-02) where condensation of the steam occurs. Figures C-34 and C-35 show the heat flux through the steam generator primary tubes in the first two volumes. The heat transfer coefficients for these volumes are presented in Figures C-36 and C-37, while the primary and secondary water temperatures for the first tube volume above the tube sheet are presented in Figure C-38.

C-2.2.4 Case 4—Loss of RHR at One Day with the Liquid Level at the Vessel Flange. Figure C-39 shows the transient pressure in the RCS when RHR is lost one day after shutdown with an initial RCS water level at the elevation of the reactor vessel flange. The Case 1 initial water level was assumed to be at the elevation of the centerline of the hot leg, while Case 3 assumed the level was located at the top of the hot leg. With the level at the vessel flange, a peak pressure of about 95 psia (28.5×10^4 Pa) was achieved about 25,000 seconds after the loss of RHR (see Figure C-39). The peak pressure again is reached well after the water in the steam generator secondary reaches saturation, as shown by the behavior of the water temperature in Figure C-40 and the secondary void fraction in Figure C-41. Boiling in the RCS initiates at about 2,000 seconds, as shown in Figure C-42 when the water temperature reaches saturation in the uppermost core volume.

Comparison with Cases 1 and 3, where the initial water levels were at mid-loop and the top of the hot leg, demonstrates that for water levels above the top of the hot leg, the peak pressure could result in pressures well above the nozzle dam and other temporary boundary design conditions. With the much higher initial water level, fluid expansion and level swell during the transient is sufficient alone to fill the entrance to the steam generator active tube region well above the tube sheet elevation.

Figures C-43 and C-44 display the void fractions in the steam generator active tube region and show that all of the tube volume excluding the U-bend volumes (volumes 4 and 5) accumulates liquid after about 17,000 seconds into the event. In fact, as the RCS liquid heats up and expands, the flow rates through the hot leg to the entrance to the steam generator tube region initially is too low for steam generator heat removal to develop sufficiently to match decay heat generation. As a consequence, the RCS continues to pressurize until sufficient RCS pressure (and hence primary to secondary temperature difference) and flow in the steam generator establish a heat removal rate that can accommodate the core decay heat generation. As shown in Figure C-45, with the expanded time scale during the latter portion of this transient, the RCS has nearly ceased pressurizing. Also, sufficient primary to secondary temperature difference and flow into the active tube region develops to match decay heat and to slowly stabilize pressure near 95 psia.

The results of these analyses suggest that increasing the RCS liquid level above the top elevation of the hot legs (to ensure that vortices

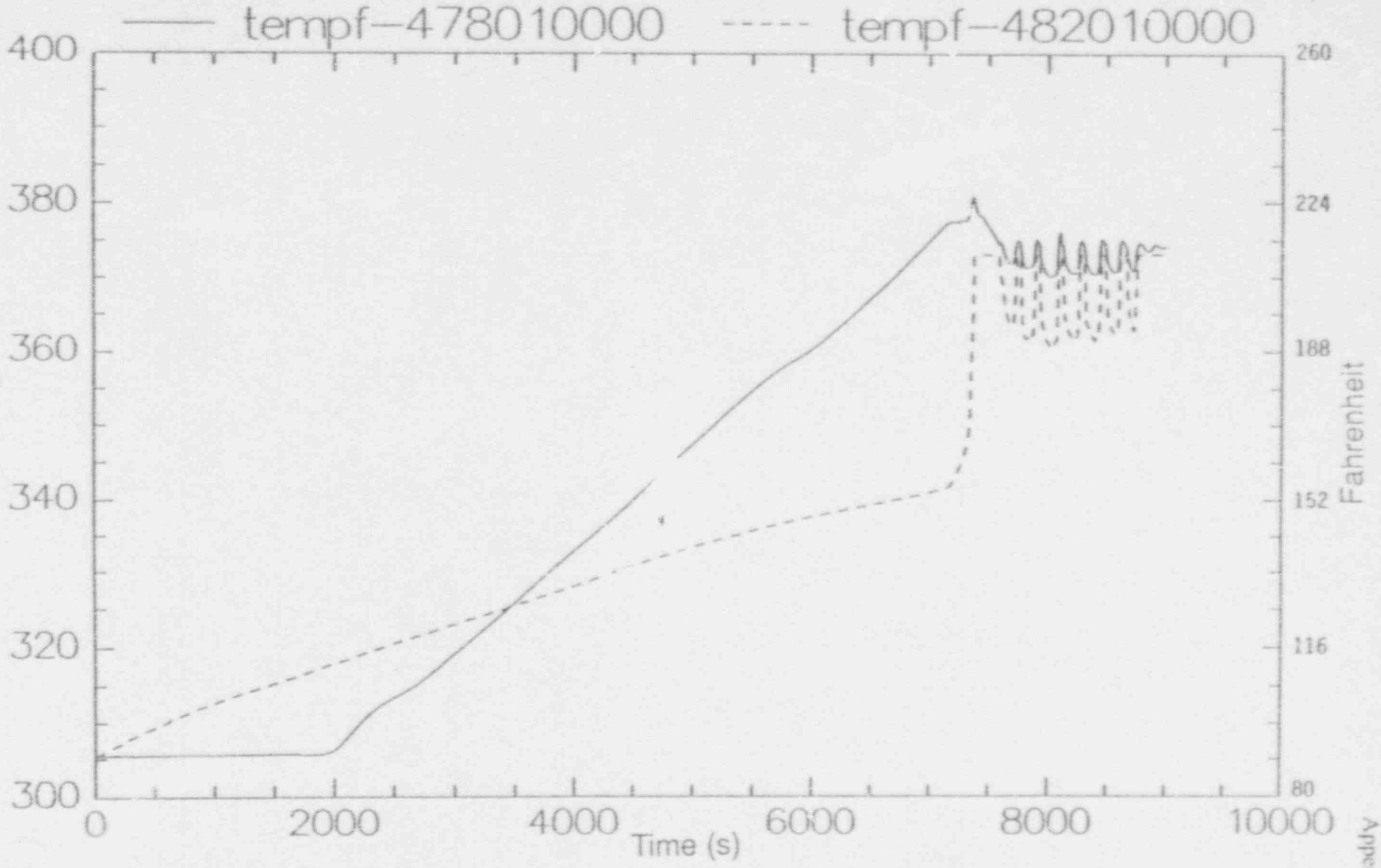

Figure C-31. Water temperature in the steam generator secondary for Case 3.

Table 3. Distribution of air in the RCS for RELAP5/MOD3 Case 3 (use of steam generators for decay heat removal).

Component (component number)	Mass of air (lb)			
	Initial	3,600 s	7,000 s	9,000 s
Downcomer (100)	7.7	12.3	5.9	12.7
Downcomer (102)	0.0	8.7	12.6	12.3
Downcomer (104)	0.0	6.7	10.3	9.5
Downcomer (106)	0.0	2.4	9.3	17.6
Upper plenum (120)	0.0	0.0	$<10^{-2}$	0.01
Upper plenum (122)	34.0	4.4	$<10^{-2}$	0.6
Upper head (126)	35.2	23.3	0.01	1.6
Hot leg (404, 405, 504, 505)	4.8	0.0	$<10^{-2}$	$<10^{-2}$
Steam generator inlet plenum (406, 506)	7.8	0.0	$<10^{-2}$	$<10^{-2}$
Steam generator tubes (408-01)	5.6	0.9	$<10^{-2}$	0.05
Steam generator tubes (408-02)	5.6	8.3	5.5	6.4
Steam generator tubes (408-03 to 408-08)	33.9	57.7	60.5	50.6
Steam generator outlet plenum (410)	7.9	9.4	4.7	18.5
Pressurizer/surge line (340, 341, 343)	91.4	83.4	63.2	63.9
Cold leg (412, 414, 416, 418, 420)	0.6	21.2	41.9	21.6

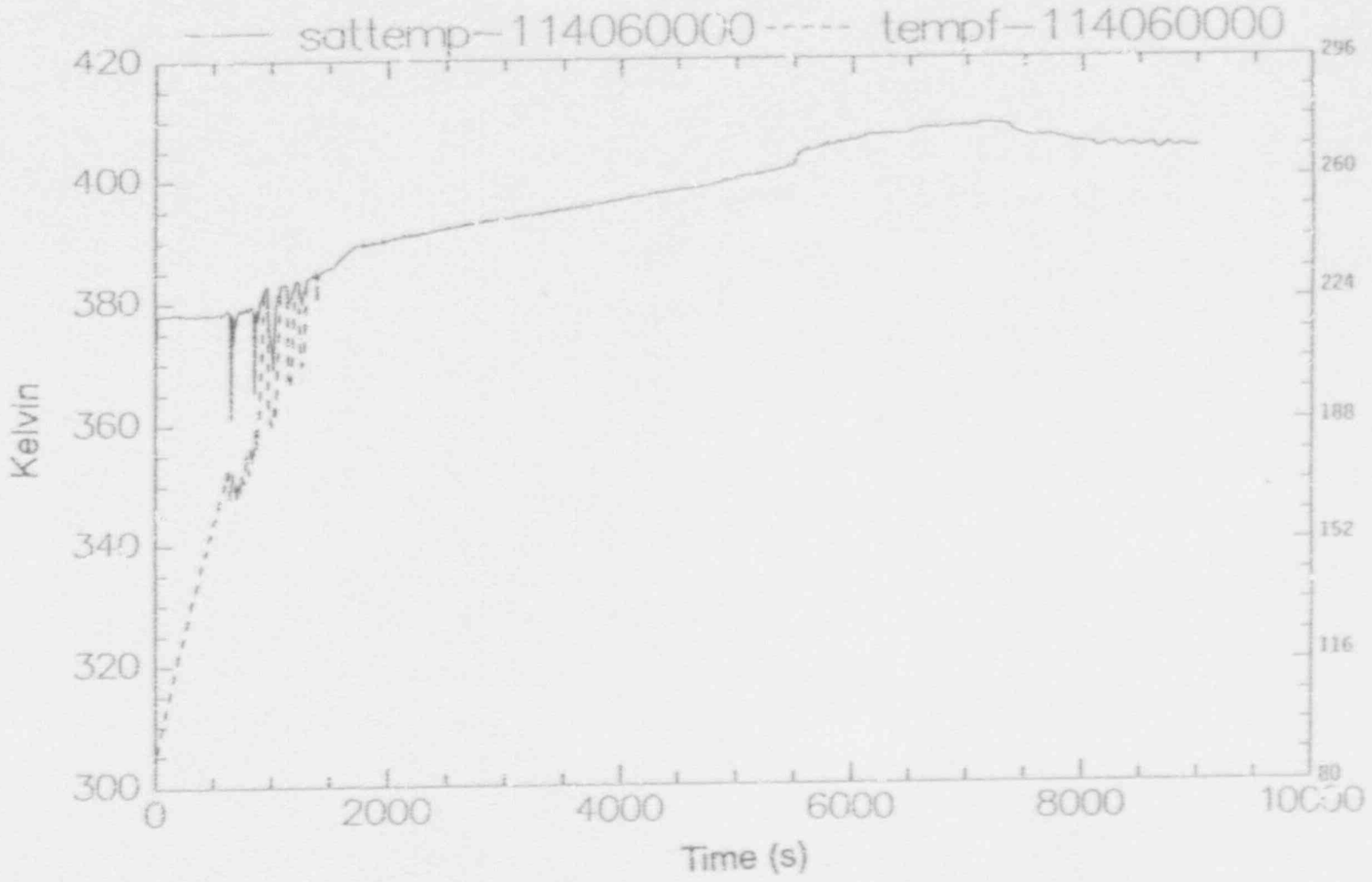

Figure C-32. Water temperature in the upper core volume (114-06) for Case 3.

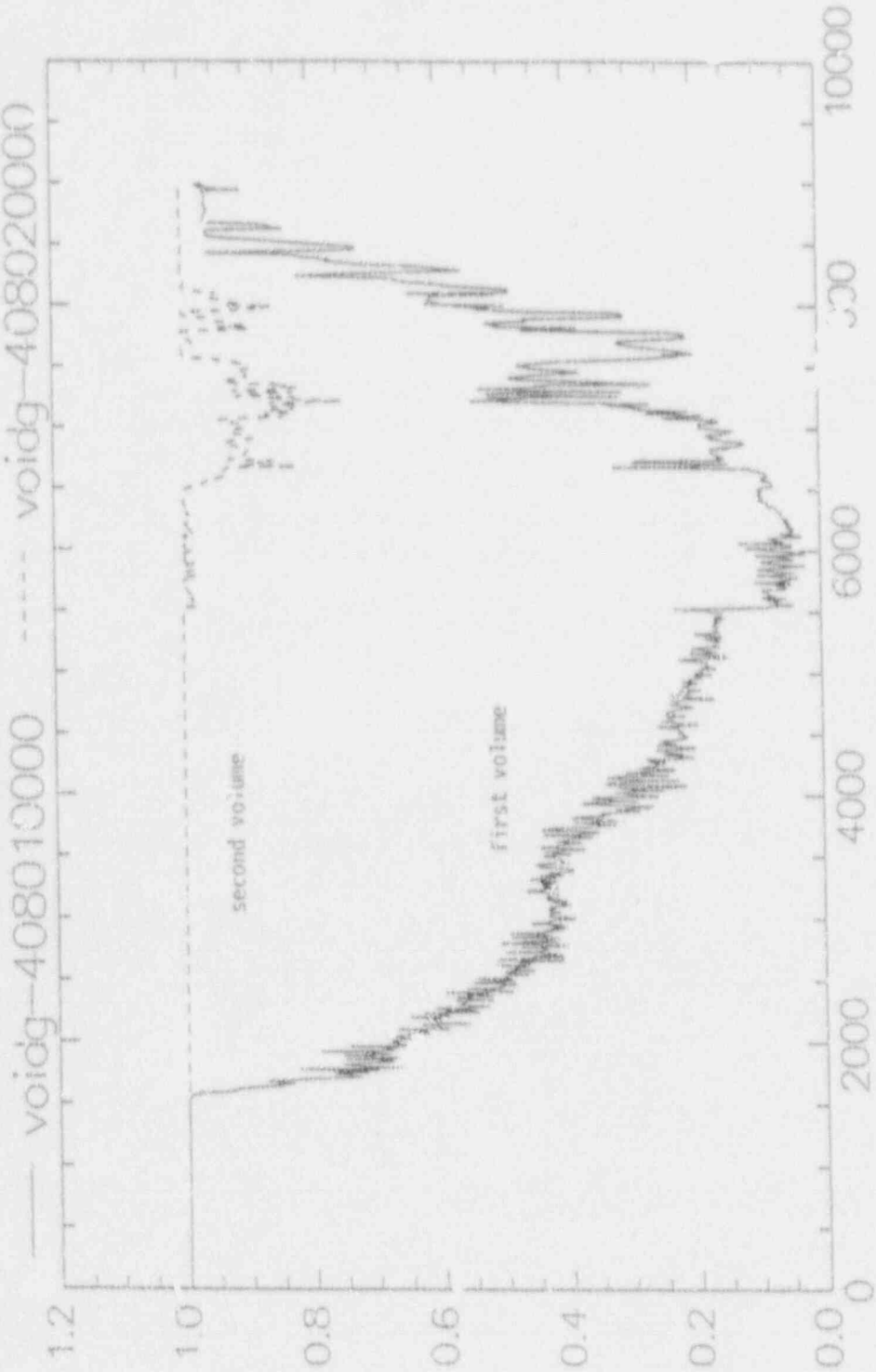

Figure C-33. Vapor void fraction in the first two volumes of the steam generator tubes for Case 3.

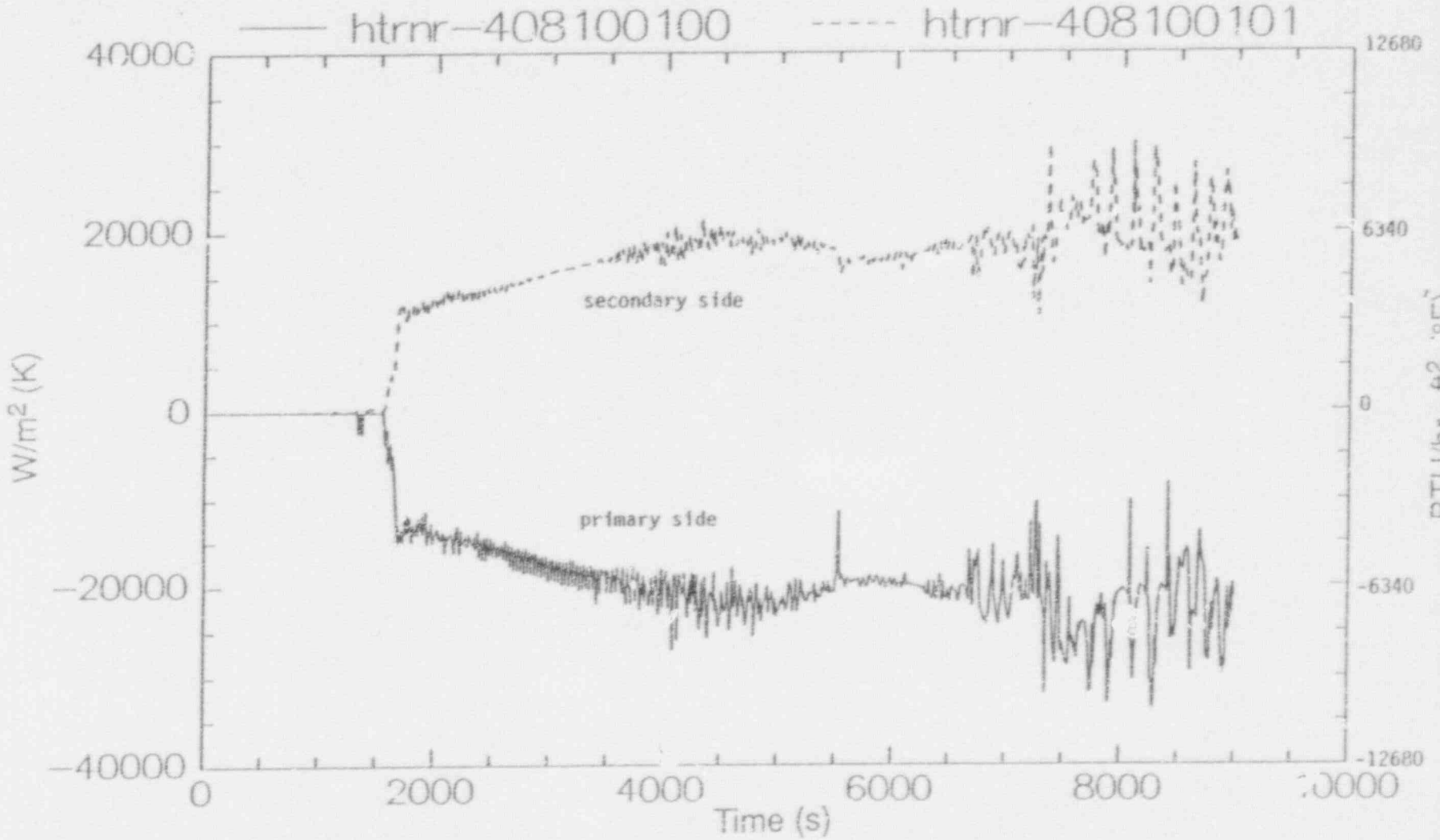

Figure C-34. Heat flux through the tubes in the first steam generator volume for Case 3.

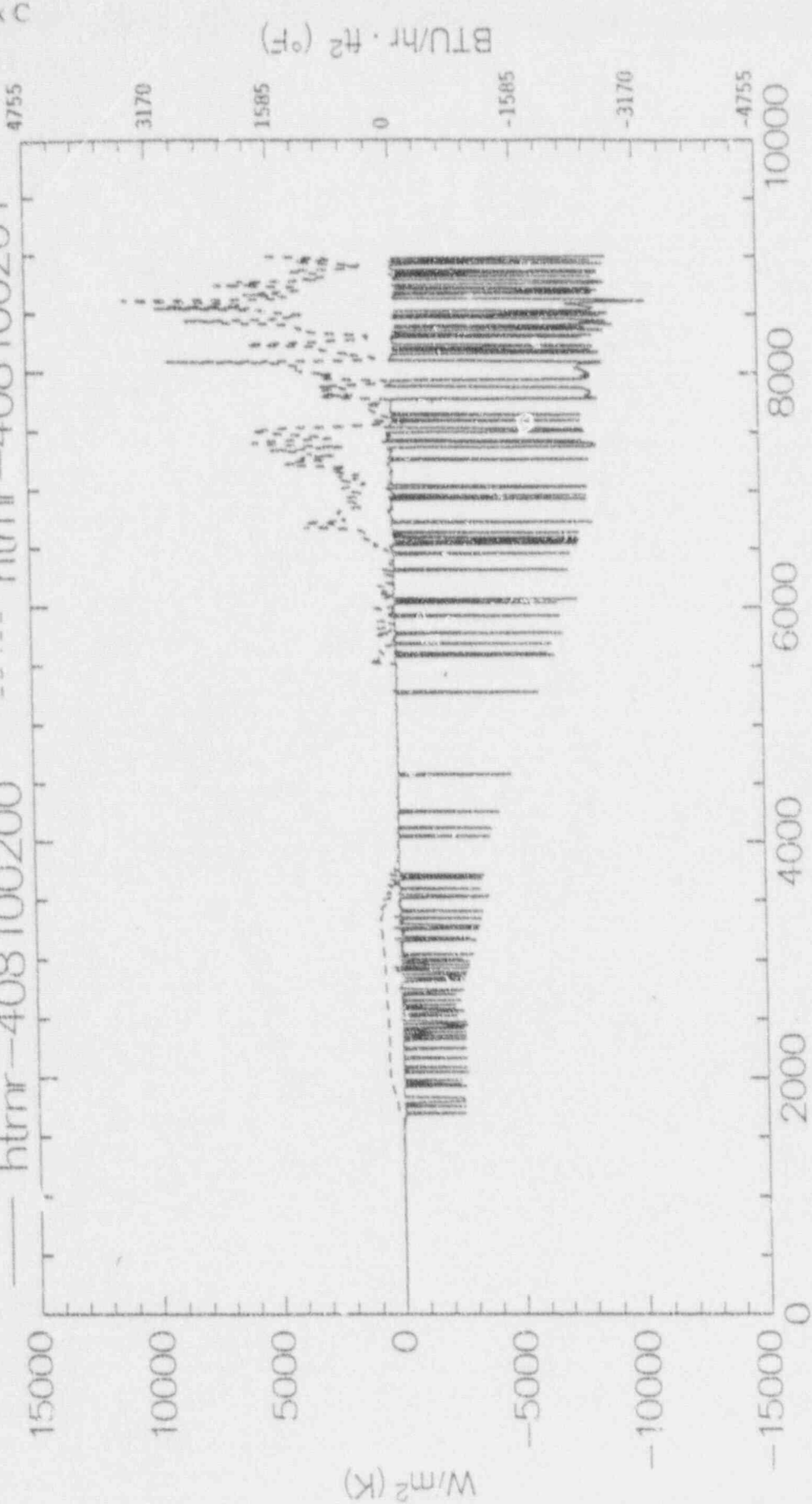

Figure C-35. Heat flux through the tubes in the second steam generator volume for Case 3.

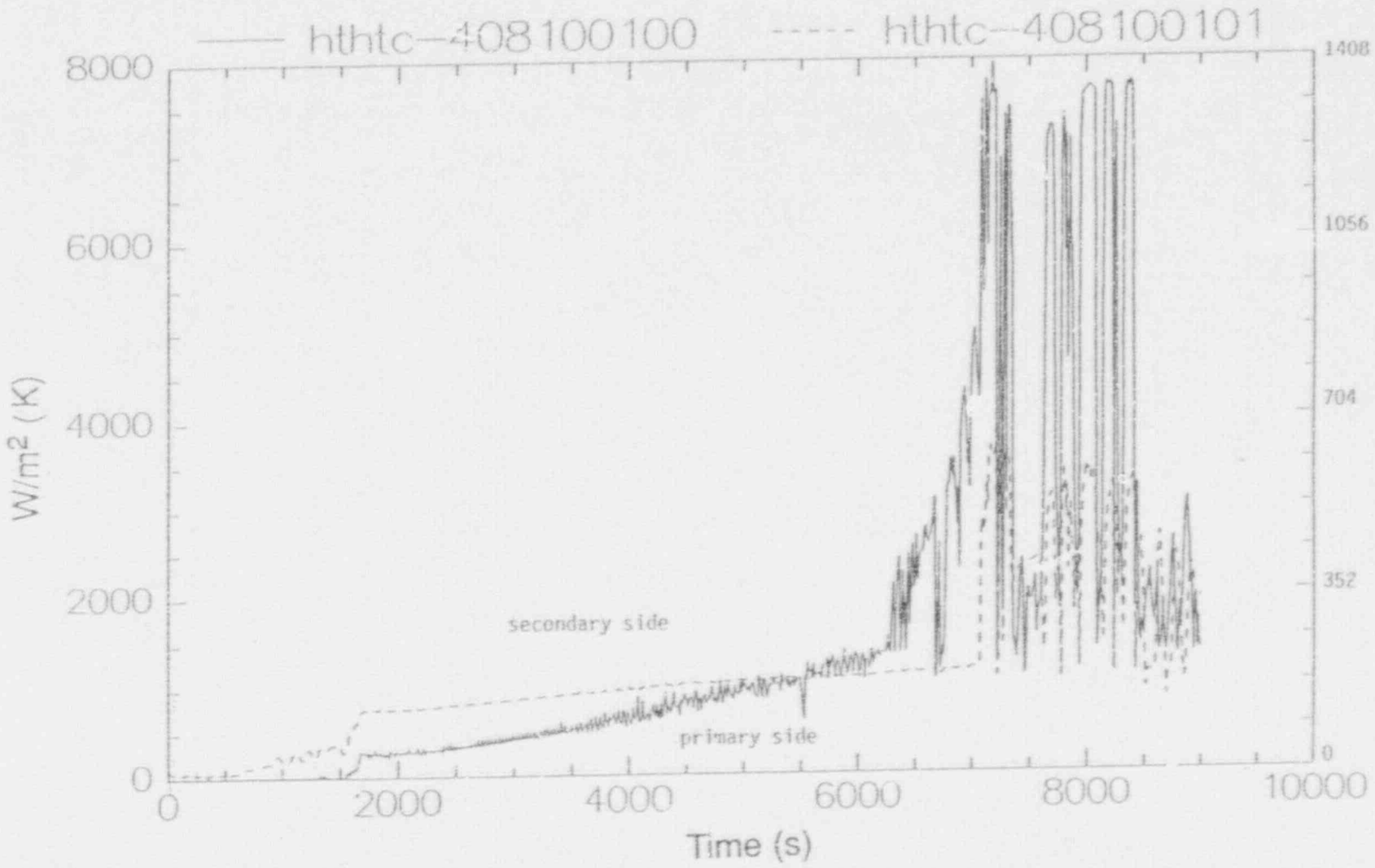

Figure C-36. Heat transfer coefficients in the first volume of the steam generator primary tubes for Case 3.

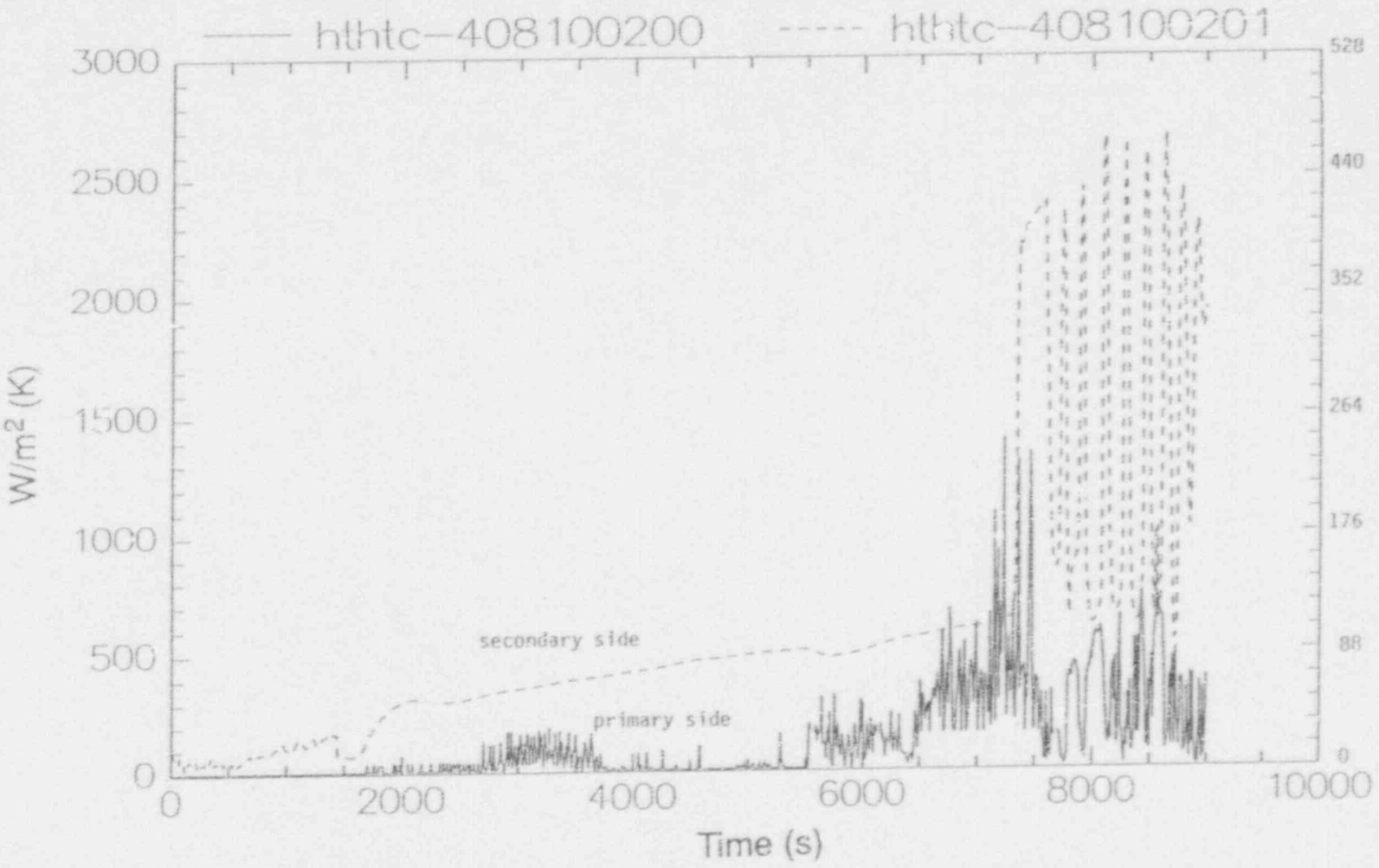

Figure C-37. Heat transfer coefficients in the second volume of the steam generator primary tubes for Case 3.

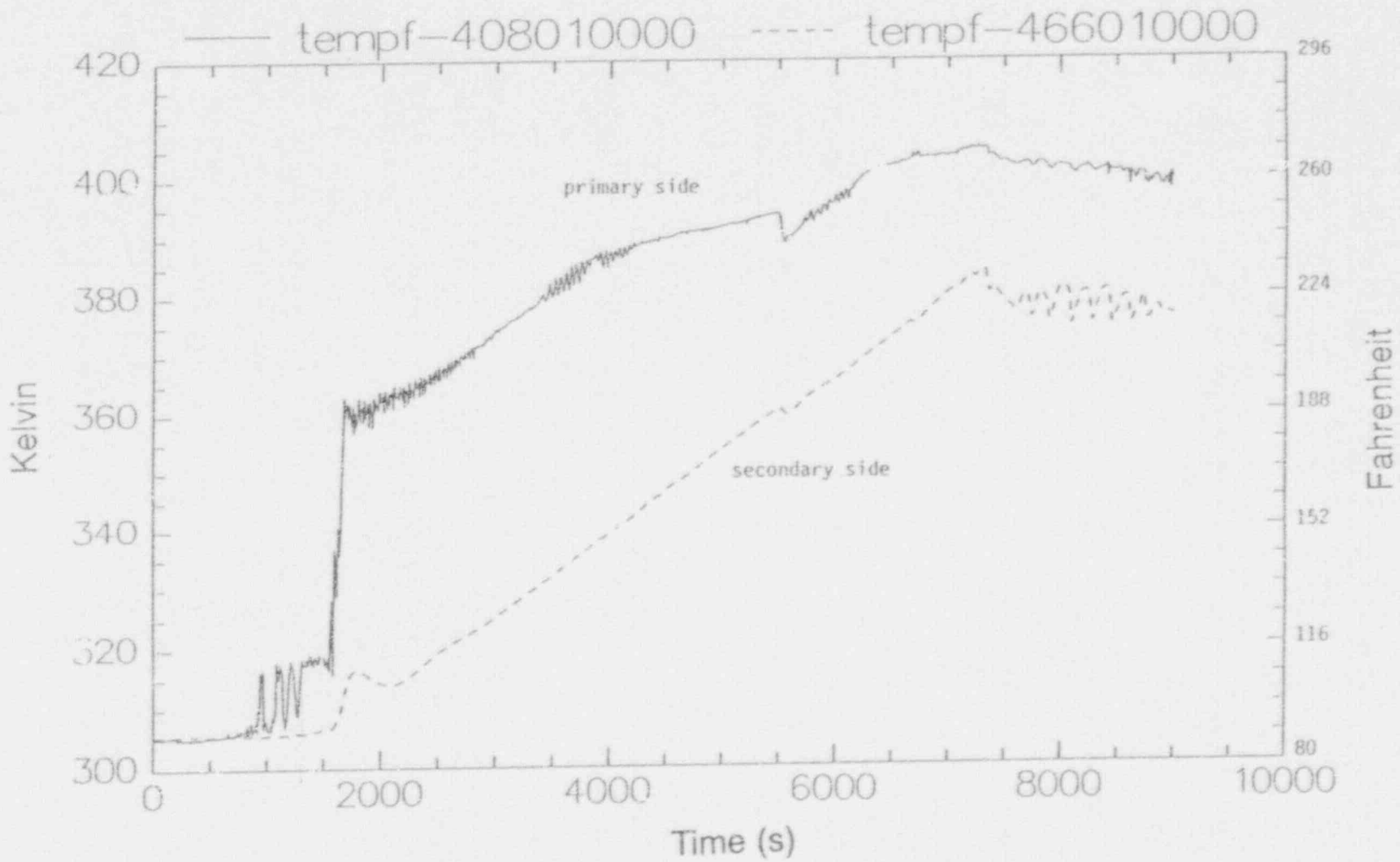

Figure C-38. Primary and secondary temperature in the first steam generator volume for Case 3.

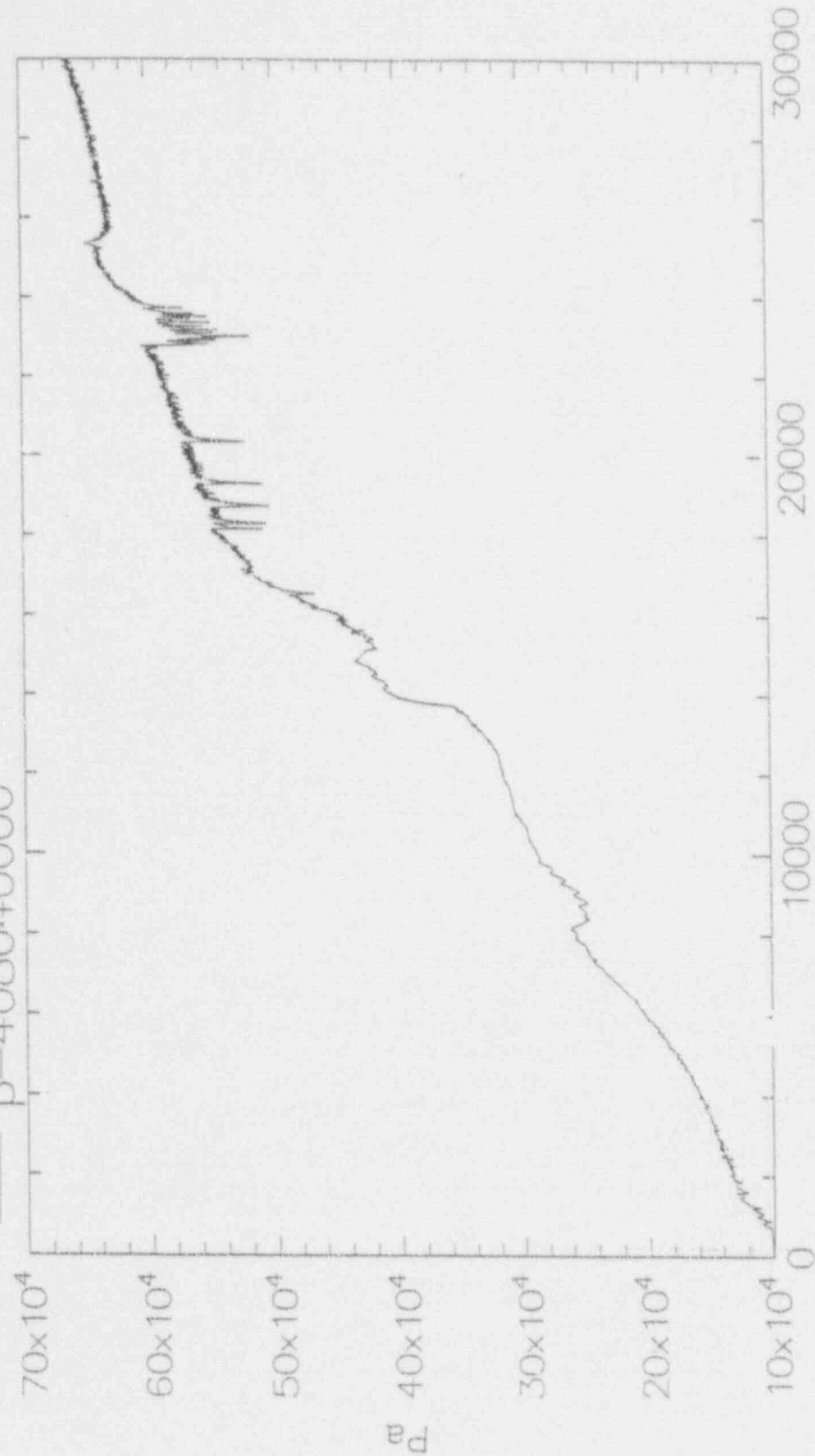

Figure C-39. Steam generator primary pressure for Case 4.

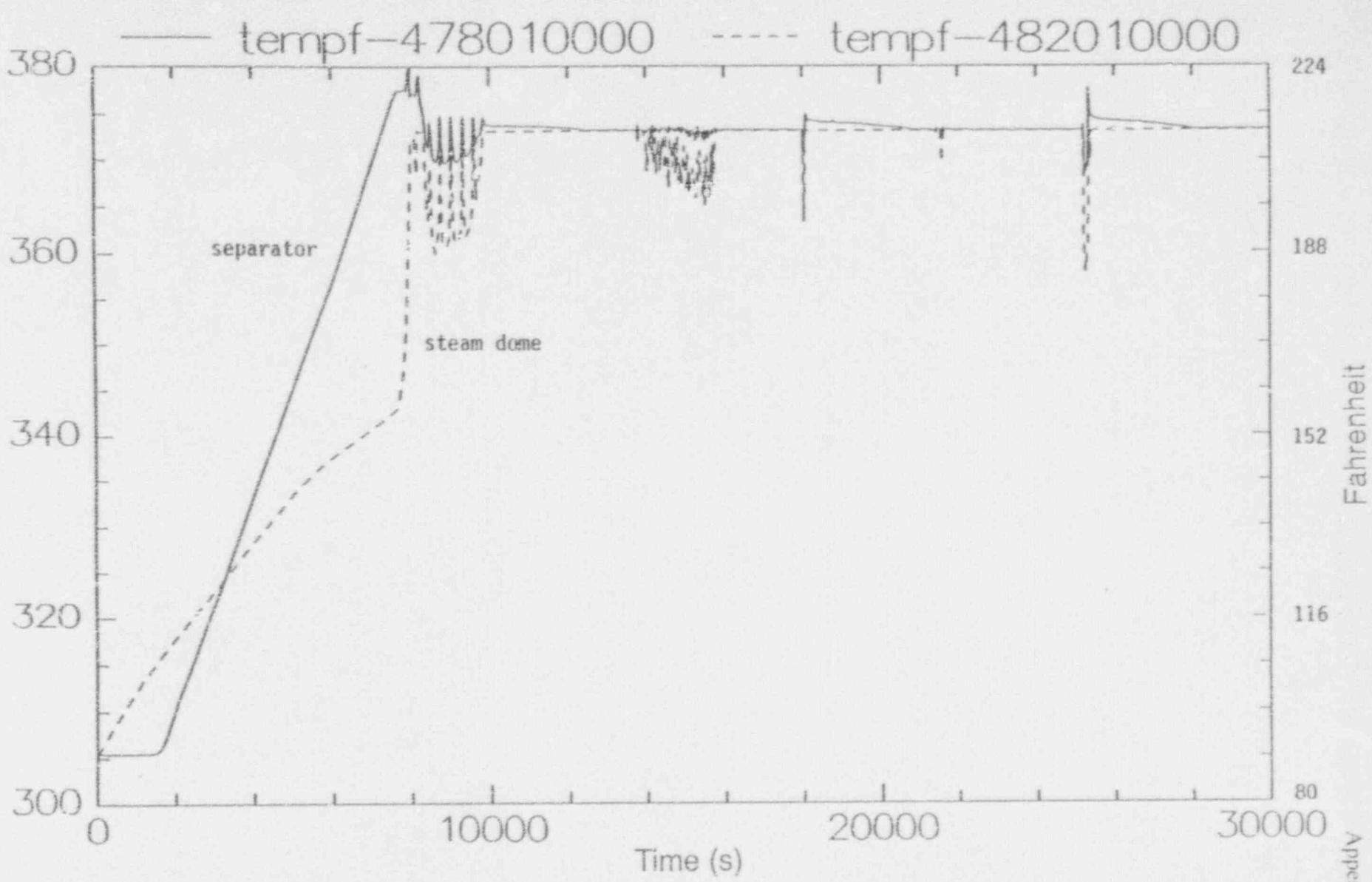

Figure C-40. Water temperature in the steam generator secondary for Case 4.

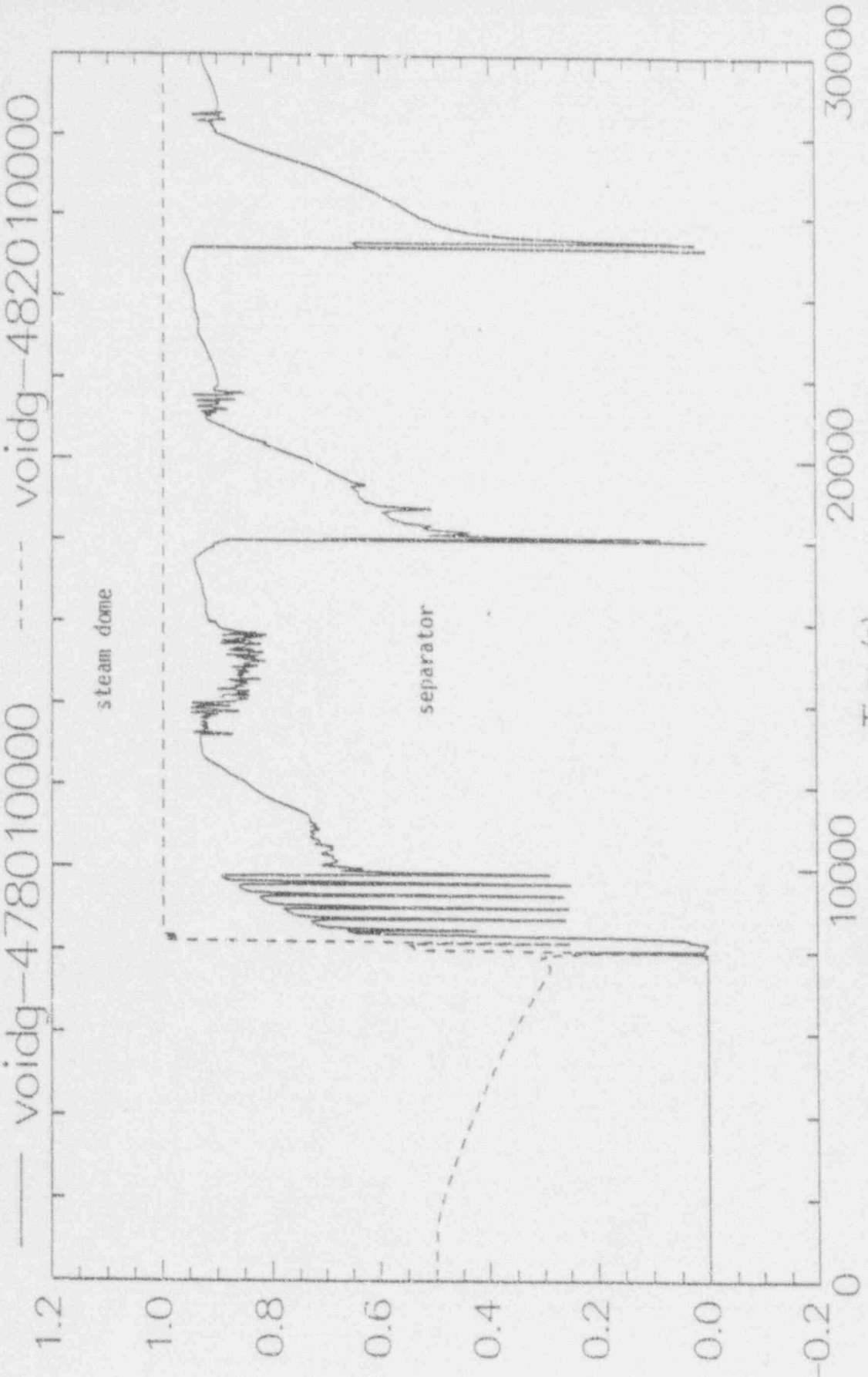

Figure C-41. Void fraction ion the steam generator secondary for Case 4.

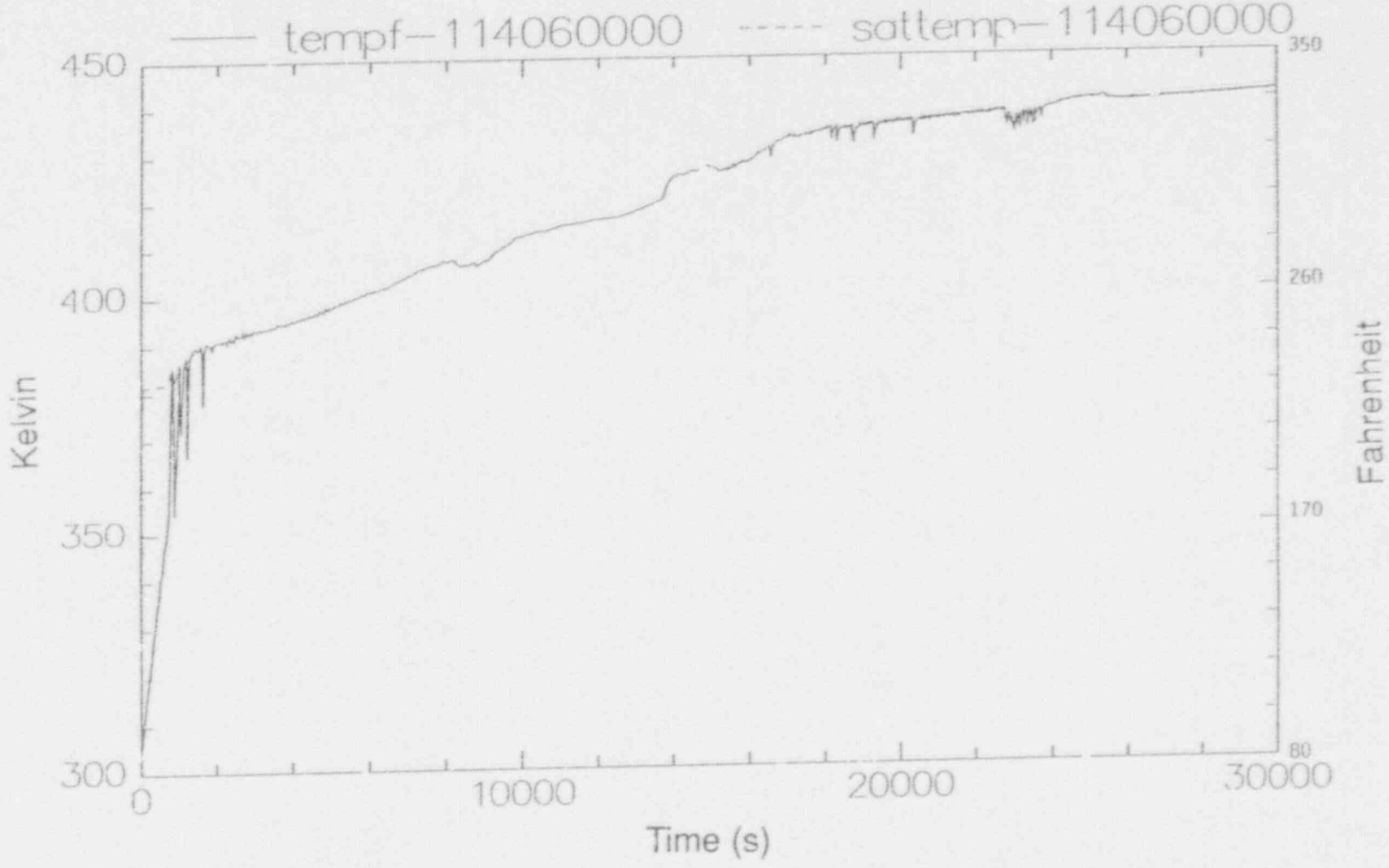

Figure C-42. Water temperature in the upper core volume (114-06) for Case 4.

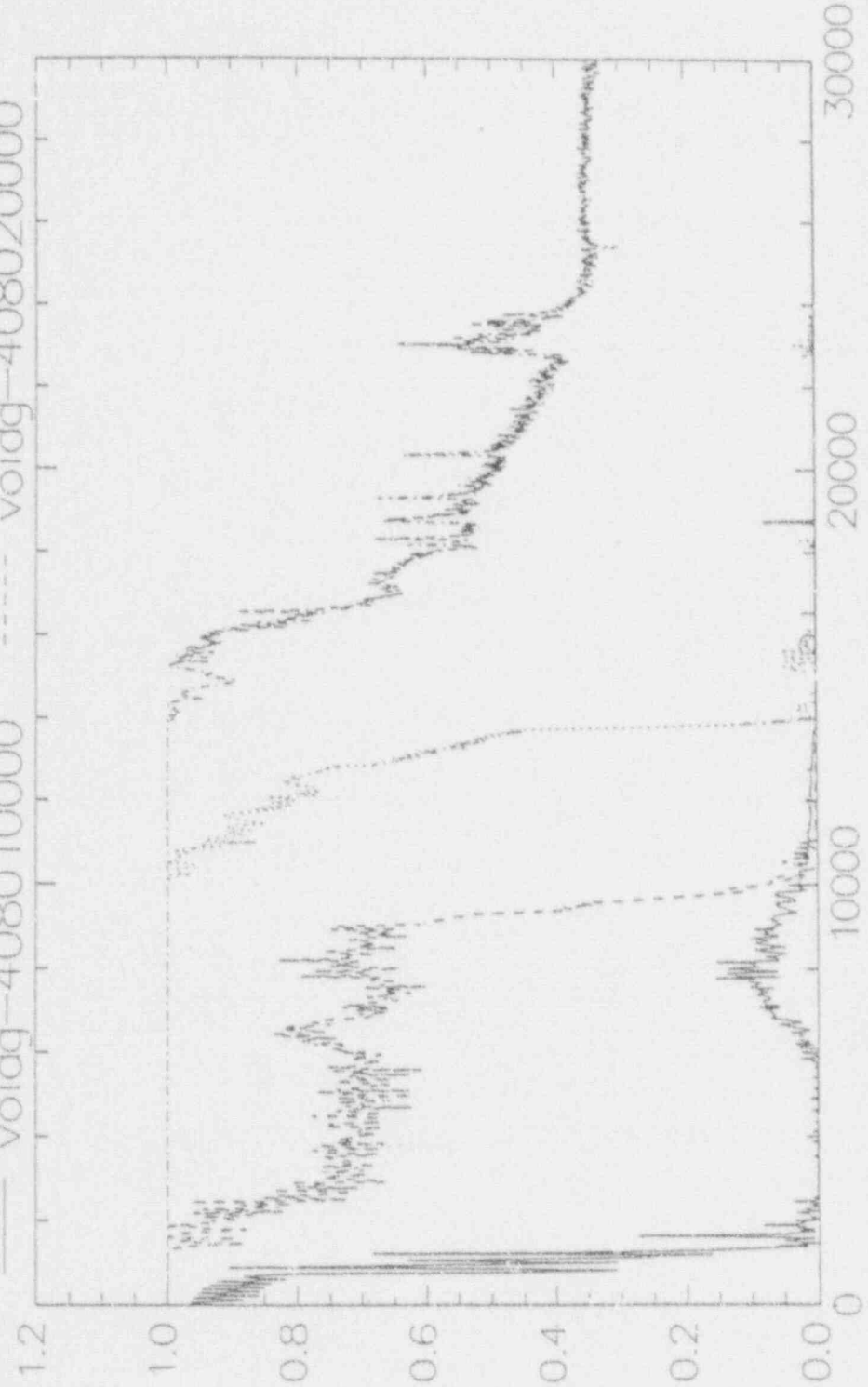

Figure C-43. Void fraction in the steam generator tube volumes for the inlet plenum to the U-bend for Case 4.

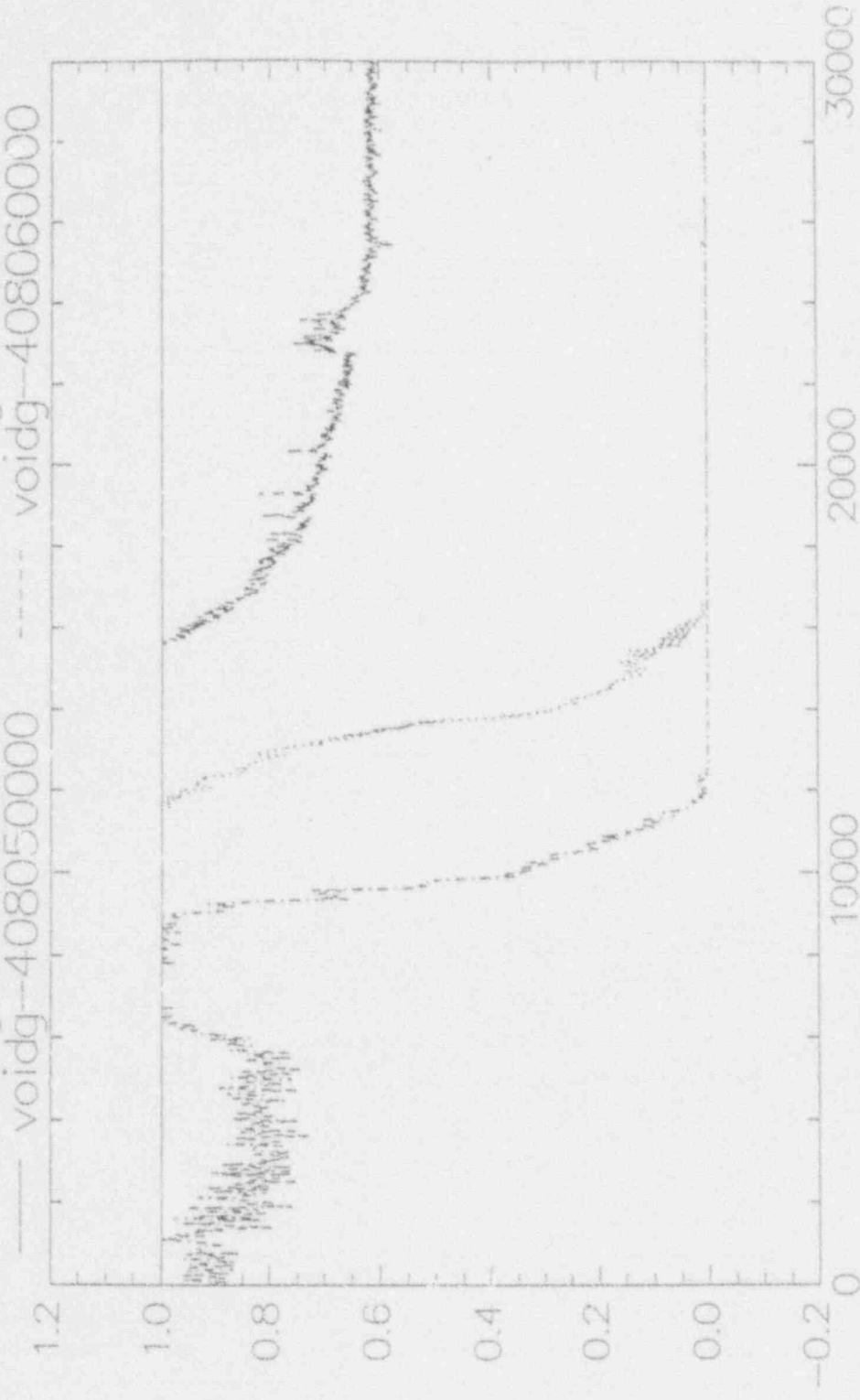

Figure C-44. Void fraction in the steam generator tube volumes from the U-bend to the outlet plenum for Case 4.

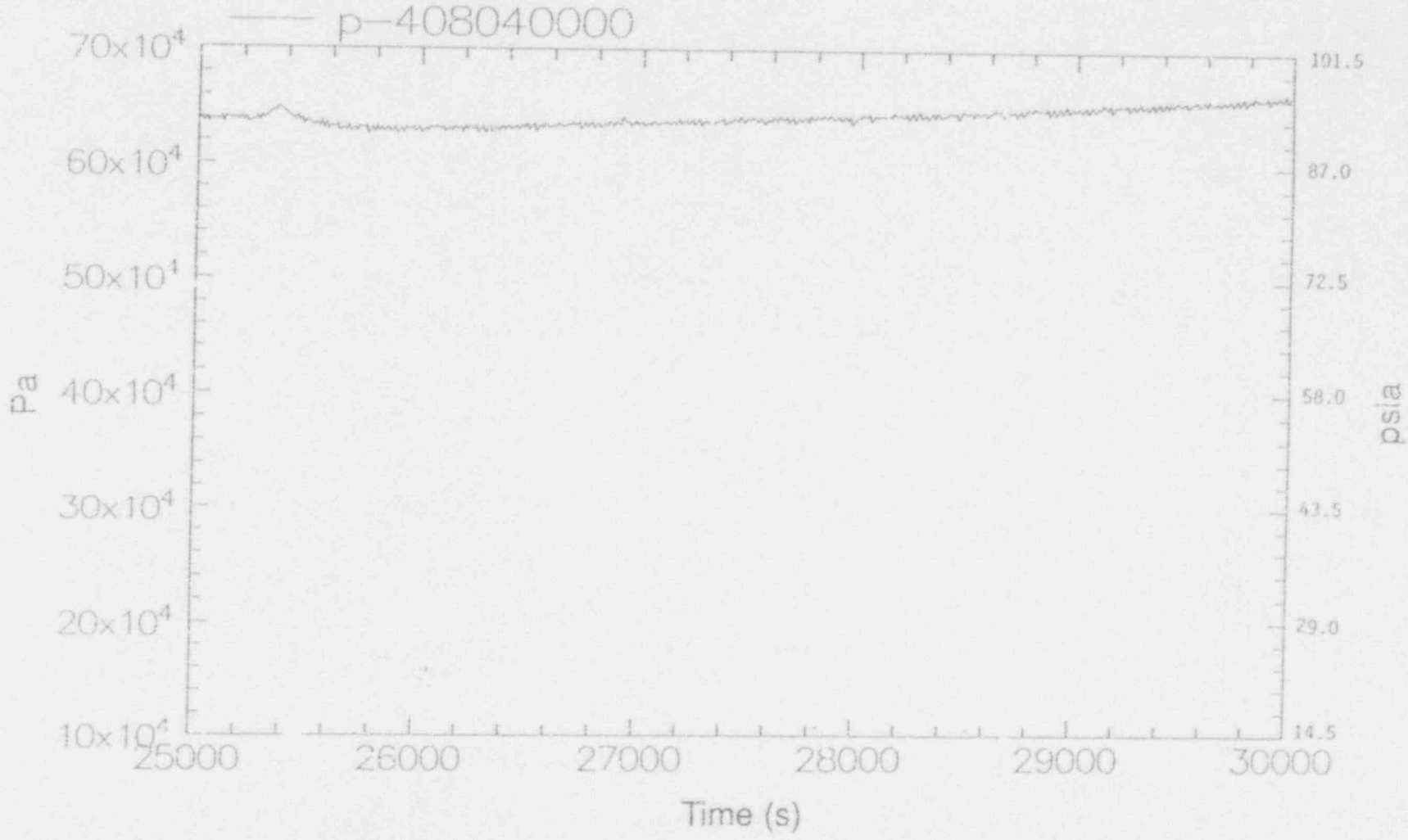

Figure C-45. Steam generator primary pressure from 25,000 to 30,000 seconds for Case 4.

are not created in the hot leg that could cause pump cavitation and failure) could inhibit reflux boiling at pressures below the failure limits of the temporary RCS boundaries.

Table C-4 presents the Case 4 distribution of air in the RCS as a function of time. For the earlier cases with the lower initial water levels, the higher air inventory in the RCS did not inhibit reflux boiling, and peak RCS pressures remained from 38 to 41 psia. For Case 4, where the initial water level is at the reactor vessel flange (well above the hot leg elevation), peak RCS pressures of 95 psia or more are predicted. The higher pressures are caused by the large inventory of subcooled liquid, which results in sufficient fluid expansion following a loss of the RHRS to plug the steam generators with liquid.

Figures C-46 and C-47 are plots of the heat flux through the steam generator primary tubes in the first two volumes. The heat transfer coefficients for these volumes are presented in Figures C-48 and C-49. After about 20,000 seconds into the event with the flow rate and resulting primary heat transfer coefficient established, the slowly increasing primary to secondary temperature difference gradually establishes a primary heat removal rate that can match the core decay heat generation rate. The primary and secondary temperatures are illustrated in Figure C-50. The inlet and outlet mass flow to the inlet plenum are shown in Figure C-51. Figures C-52 and C-53 display the steam generator noncondensable mass fraction and temperature, respectively.

Although a natural circulation flow through the steam generators U-bend region to the cold side is not established during this event, the primary to secondary temperature difference, flow, and hence heat transfer coefficient in the first volume of the steam generator active tube region develops sufficiently to nearly stabilize RCS pressure at about 95 psia. Note that RCS pressure has not yet stabilized completely and displays about a 1 psi increase over the last 5,000 seconds of the event.

Table 4. Distribution of air in the RCS for RELAP5/MOD3 Case 4 (use of steam generators for decay heat removal).

Component (component number)	Mass of air (lb)			
	Initial	10,800 s	18,000 s	30,000 s
Downcomer (100)	0.0	1.3	$<10^{-2}$	2.2
Downcomer (102)	0.0	9.3	3.6	5.7
Downcomer (104)	0.0	5.3	7.2	5.6
Downcomer (106)	0.0	0.0	8.1	5.0
Upper plenum (120)	0.0	$<10^{-2}$	$<10^{-2}$	0.01
Upper plenum (122)	0.0	0.03	$<10^{-2}$	0.9
Upper head (126)	35.2	0.2	0.01	1.6
Hot leg (404, 405, 504, 505)	0.0	$<10^{-2}$	$<10^{-2}$	$<10^{-2}$
Steam generator inlet plenum (406, 506)	0.0	$<10^{-2}$	$<10^{-2}$	$<10^{-2}$
Steam generator tubes (408-01)	5.3	$<10^{-2}$	$<10^{-2}$	0.01
Steam generator tubes (408-02)	5.6	0.1	$<10^{-2}$	0.02
Steam generator tubes (408-03 to 408-08)	33.5	46.7	46.3	50.5
Steam generator outlet plenum (410)	0.0	0.0	0.0	0.03
Pressurizer/surge line (340, 341, 343)	89.6	19.4	15.4	14.9
Cold leg (412, 414, 416, 418, 420)	0.0	33.4	39.9	45.8

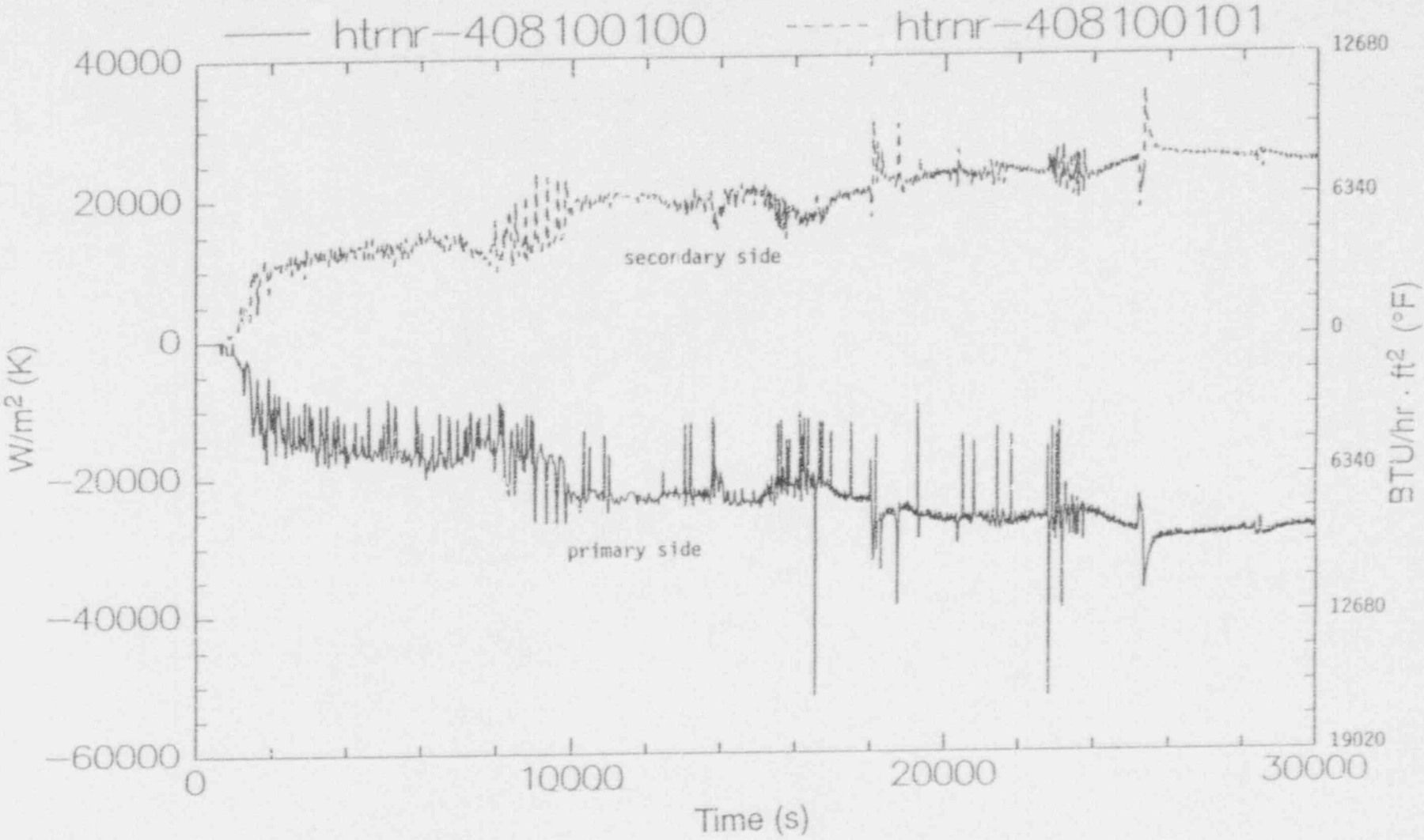

Figure C-46. Heat flux through the tubes in the first steam generator volume for Case 4.

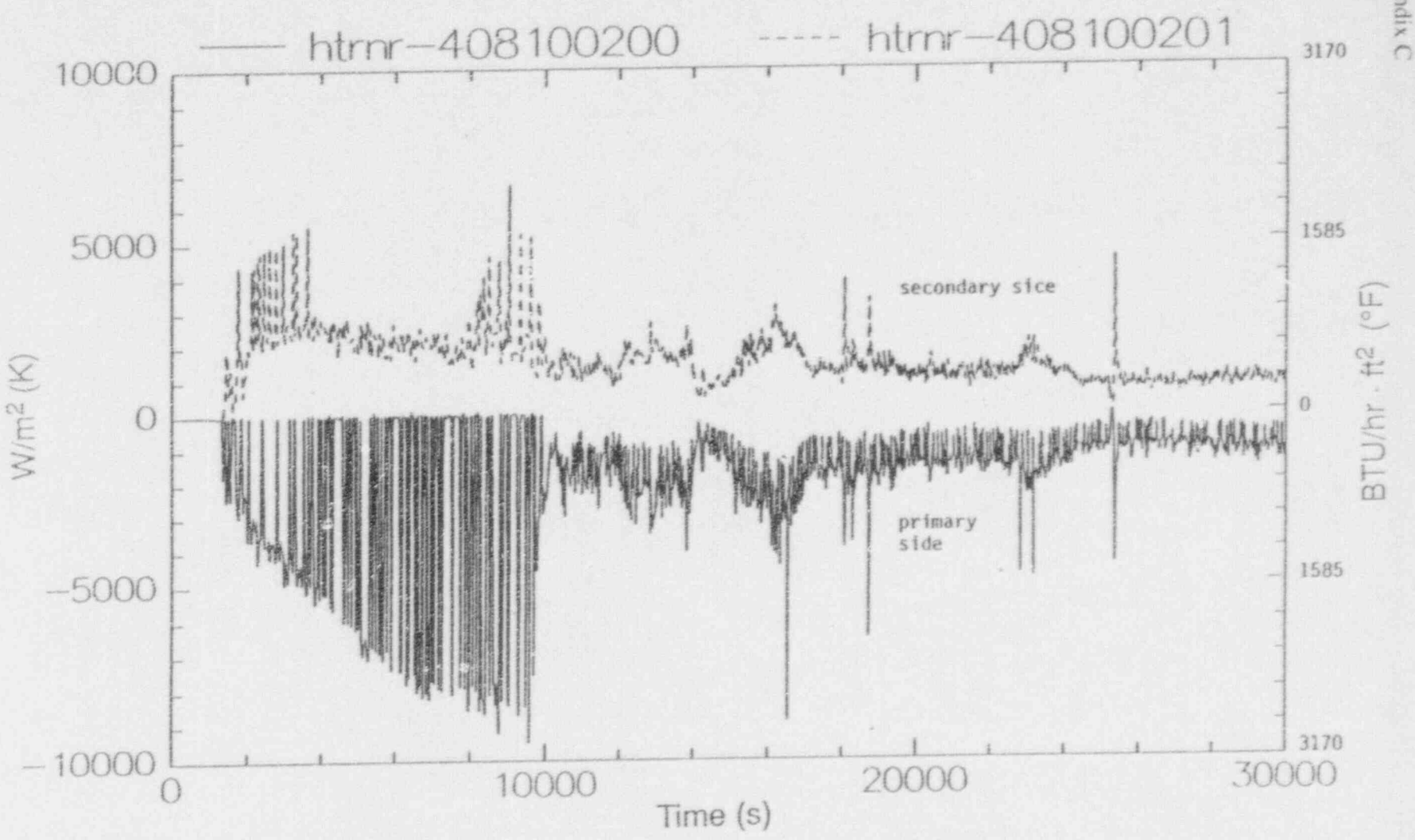

Figure C-47. Heat flux through the tubes in the second steam generator volume for Case 4.

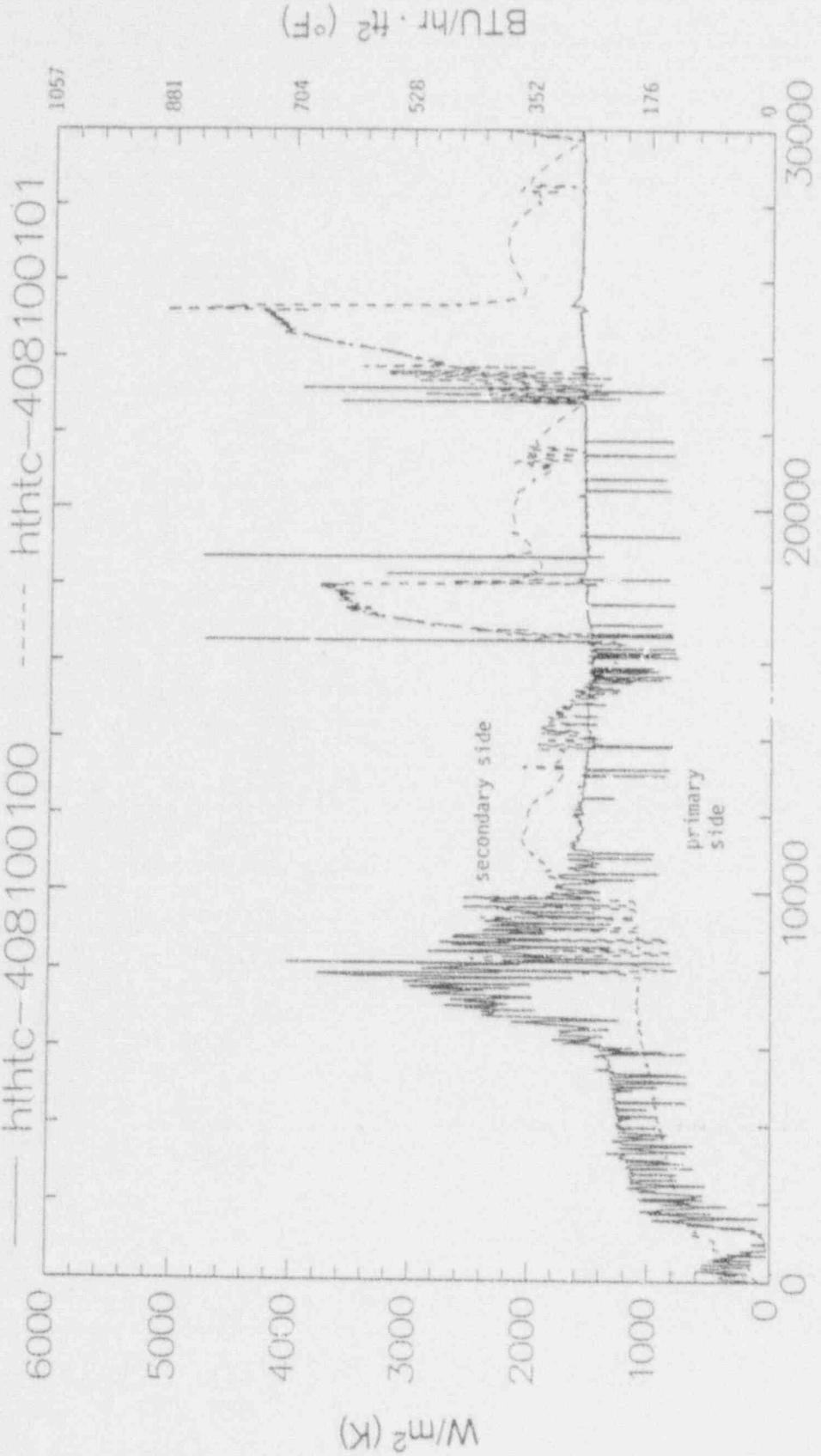

Figure C-48. Heat transfer coefficients in the first volume of the steam generator primary tubes for Case 4.

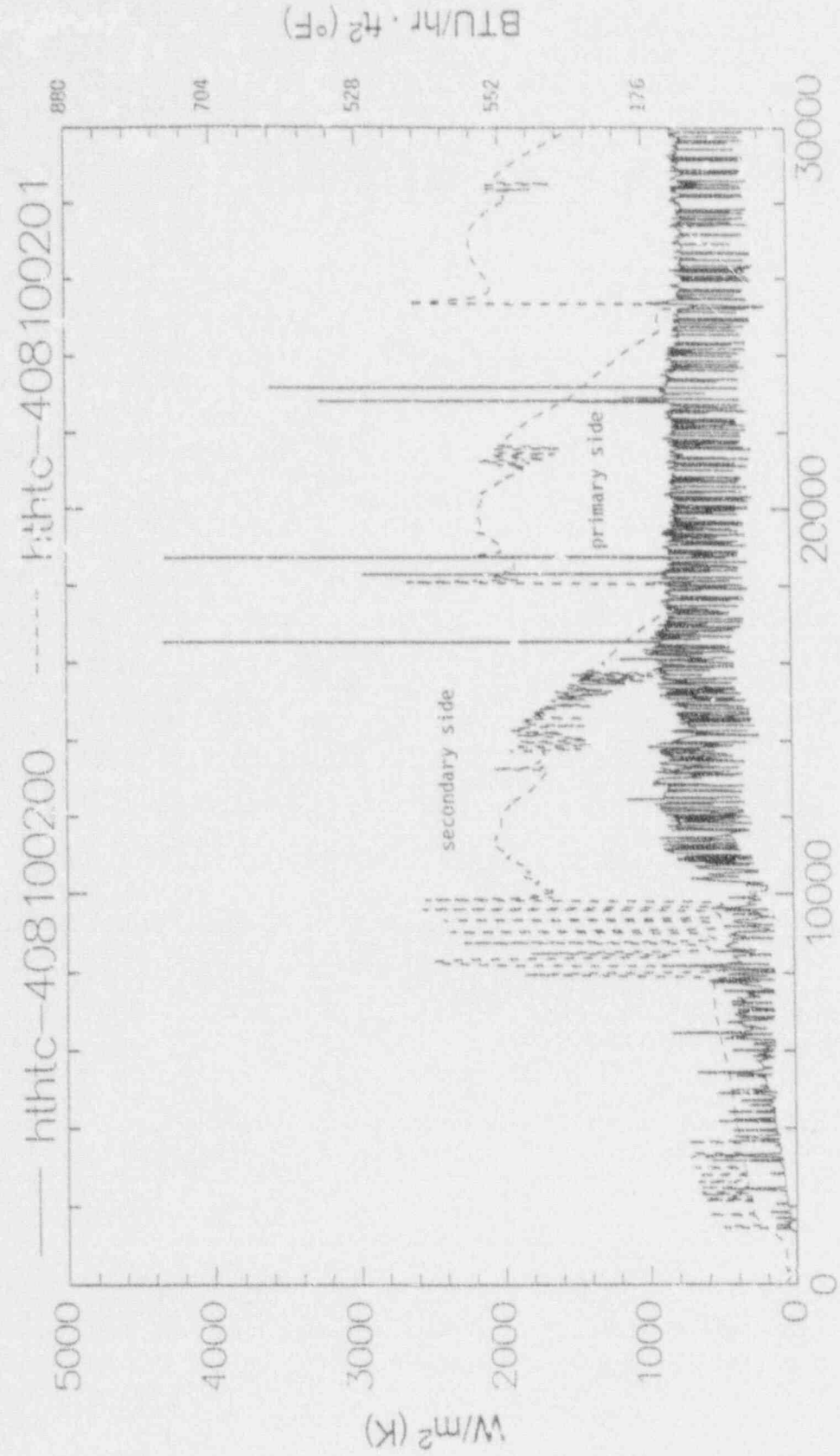

Figure C-49. Heat transfer coefficients in the second volume of the steam generator primary tubes for Case 4.

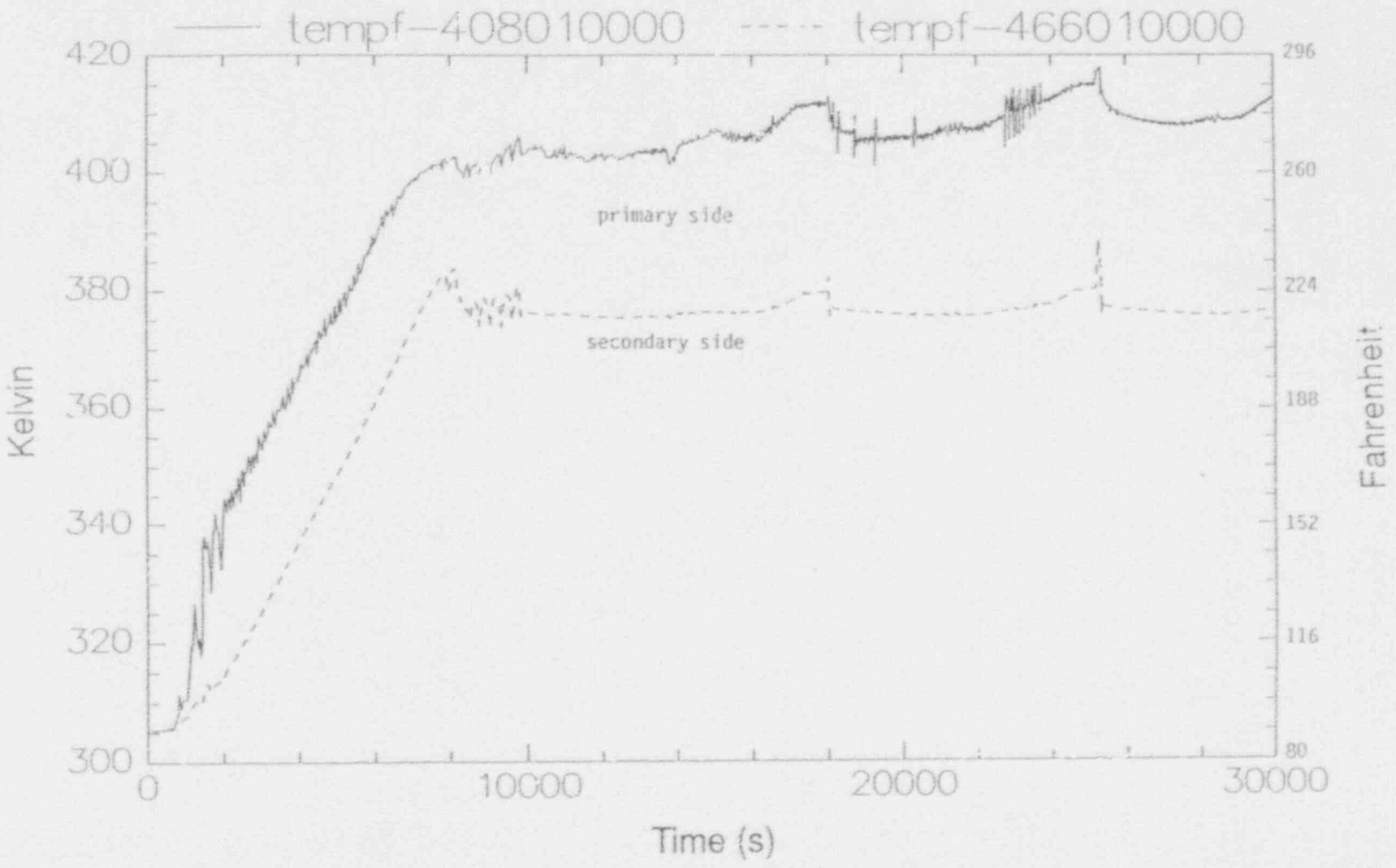

Figure C-50. Primary and secondary temperature in the first steam generator volume for Case 4.

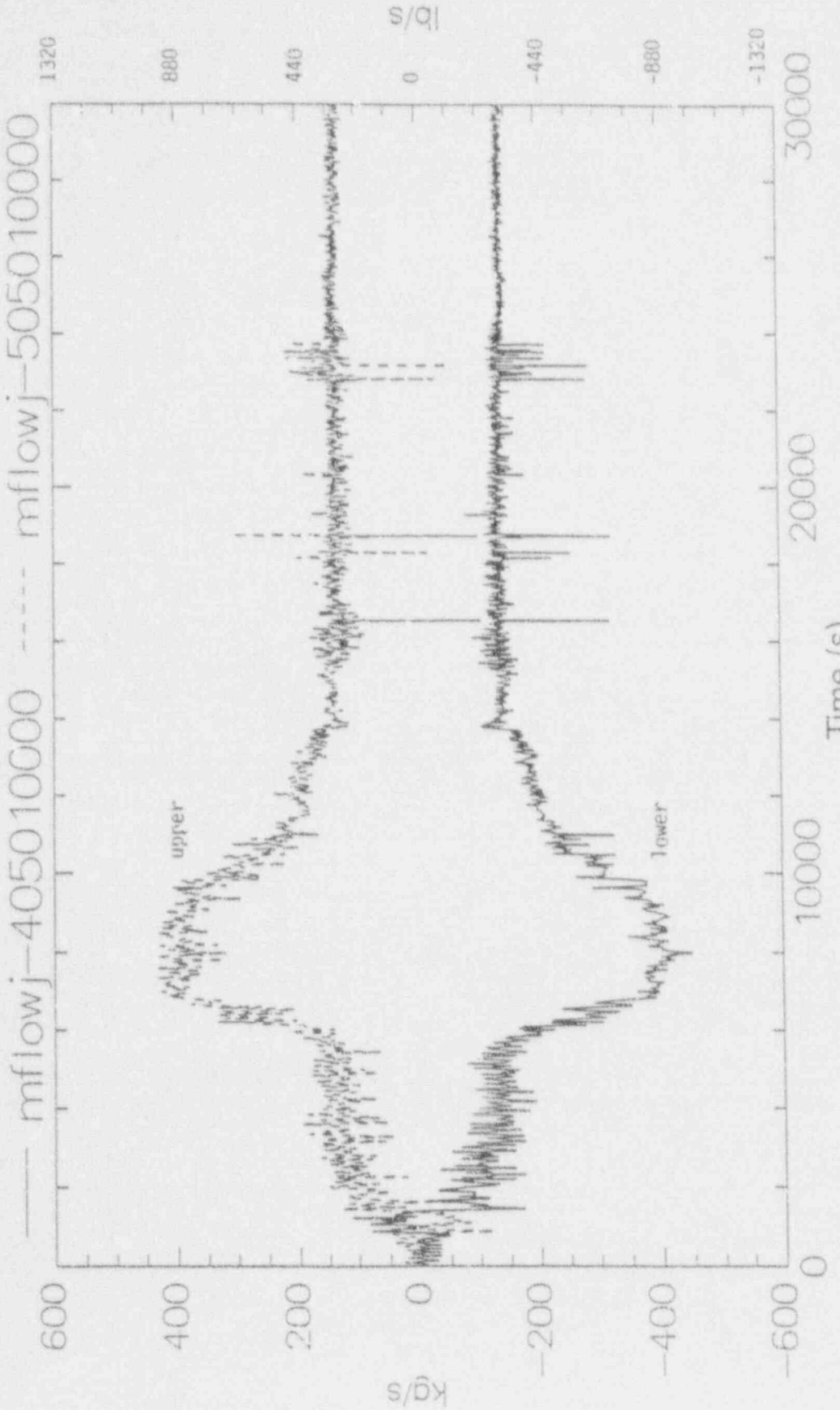

Figure C-51. Mass flow in the upper and lower parts of the hot leg for Case 4.

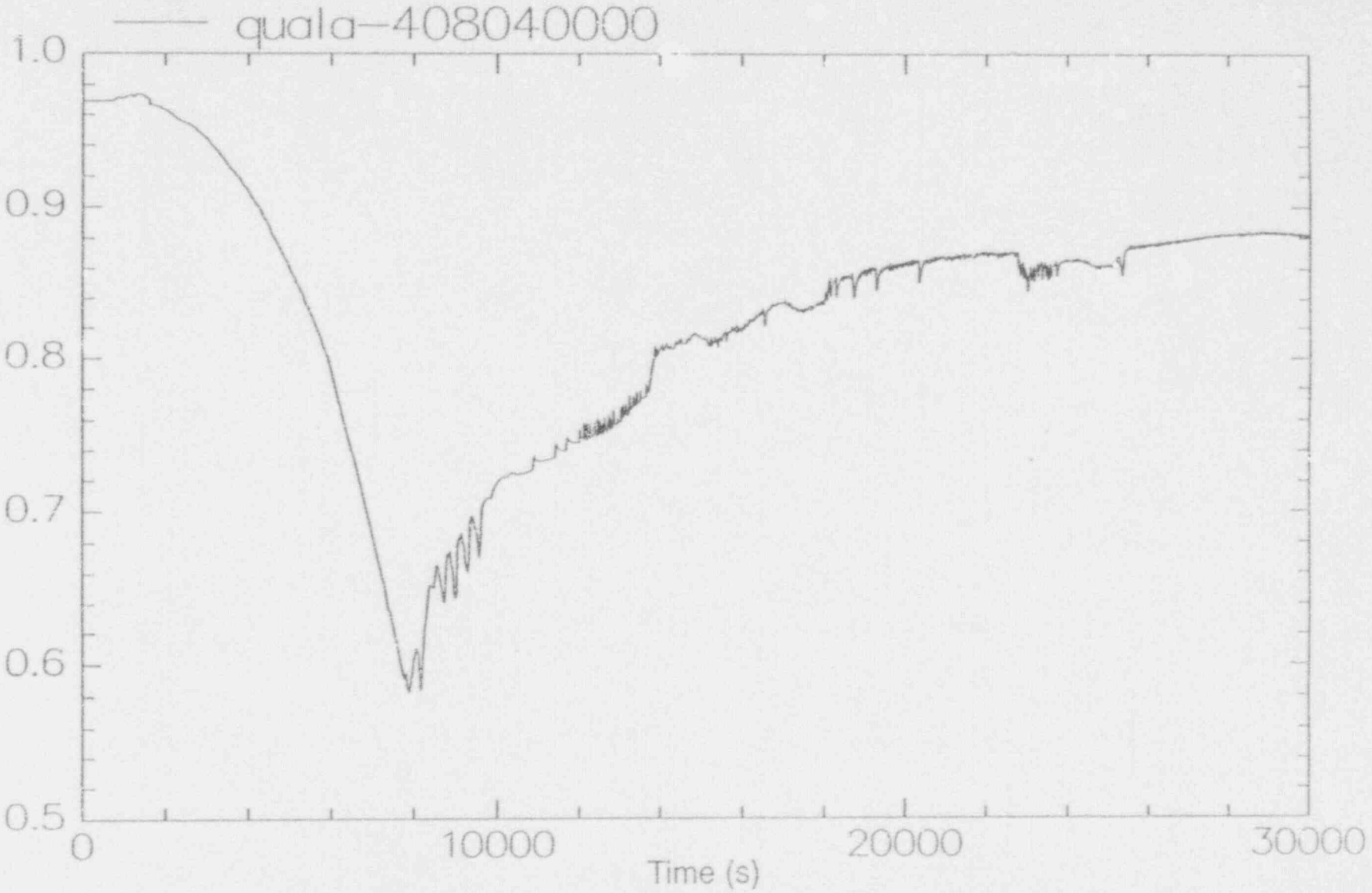

Figure C-52. Noncondensable mass fraction in the U-bend of the steam generator tubes for Case 4.

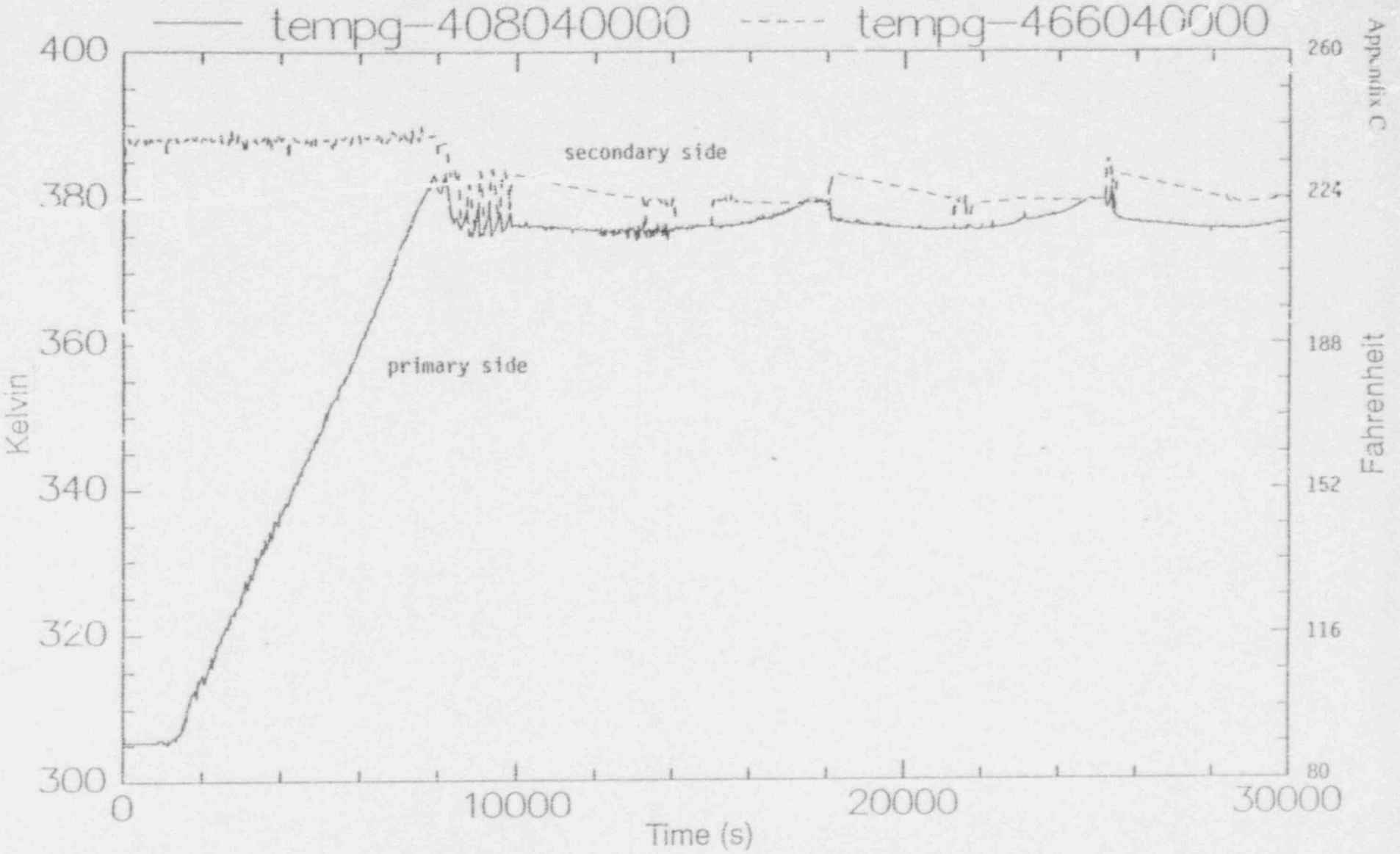

Figure C-53. Primary and secondary temperatures at the U-bend of the steam generator tubes for Case 4.

C-3. REFERENCES

1. K. E. Carlson et al., *RELAP5/MOD3 Code Manual*, NUREG/CR-5535, EGG-2596, Draft, (available from EG&G Idaho, Inc., P.O. Box 1625, Idaho Falls, ID 83415-2404), June 1990.

2. C. D. Fletcher et al., *RELAP5 Thermal Hydraulic Analyses of Pressurized Thermal Shock Sequences for the H. B. Robinson Unit 2 Pressurized Water Reactor*, NUREG/CR-3977, EGG-2341, April 1985.

Appendix D

Low-Pressure Reflux Boiling Condensation with Noncondensables in Pressurized Water Reactors

CONTENTS

Appendix D

Low-Pressure Reflux Boiling Condensation with Noncondensables in Pressurized Water Reactors

D-1. INTRODUCTION

The Vogtle Electric Generating Plant experienced a loss of the residual heat removal (RHR) system on March 20, 1990. The incident occurred with Unit 1 shutdown during a refueling outage. The water level in the reactor vessel had been lowered to the mid-loop level, and consequently a significant amount of air occupied the upper elevations of the primary system. The emergency diesel generator was manually restarted in the emergency mode 36 minutes after the loss of power. It was able to provide sustained power to the RHR system, eliminating the necessity for nonroutine actions to maintain adequate core cooling.

This appendix is concerned with the situation where restoration of power to the RHR system is not possible, and an alternative method of core cooling is necessary. The primary interest is the effectiveness of reflux/boiling condensation as an alternative cooling mechanism. The goal of this appendix is to synthesize the results of relevant experiments and analysis to improve the understanding of the plant thermodynamic behavior associated with reflux/boiling condensation cooling during reduced inventory operation with significant amounts of noncondensable gases present. This appendix gives a general, overall discussion of the reflux boiling process. Detailed calculations were performed and the results are reported in Appendices B and C.

On March 23, 1990 an Incident Investigation Team was sent to Vogtle by the U.S. Nuclear Regulatory Commission Executive Director for Operations. The results of the team's investigation are documented in Reference 1. Of particular interest to this discussion is Section 8.3 of that document, entitled "Reflux Cooling and Effect of Reactor Coolant System Water Level," which studies the feasibility of reflux cooling in the situation mentioned above. The reflux cooling option is desirable when boiling cannot be prevented by gravity-feed cooling, and when the reactor coolant system (RCS) is closed (ie., the steam generator and pressurizer manways and the reactor vessel head are sealed).

Reference 1 identified the need for additional analysis of the RCS following the loss of the RHR system. It was noted that the plant thermodynamic behavior associated with reflux cooling is not well understood during a plant shutdown situation. Little work has been done to provide guidance with regard to preventing core boiling, reasonably setting up for reflux cooling, and minimizing risk if electrical power is lost. The Incident Investigation Team envisioned the following problems with reflux condensation:

- If the hot leg water level is too high, the steam flow is impeded and reflux condensation may be disrupted
- If the steam generator tubes are full of liquid, drainage of the tubes must occur before steam can reach the tube surfaces and condense
- Air may prevent steam from entering the steam generator tubes.

The calculations performed by the Incident Investigation Team indicated that reflux cooling is effective regardless of the initial reactor system water level as long as the following requirements are satisfied:

- The initial vessel liquid level is above the top of the core

- Steam generators are operable
- Uncontrolled loss of reactor coolant does not occur.

It was also noted that stable modes of reflux cooling can be reached with operator adjustments to the RCS inventory. Thus, the need for accurate water level indication was identified.[1] This need was apparent after the Diablo Canyon incident in April of 1987.[2] Considerable uncertainty was associated with the Reactor Vessel Refueling Level Instrumentation System.

Experiments in integral test facilities such as SEMISCALE,[3,4,5,6] LOFT,[7] PKL,[8,9,10] FLECHT-SEASET,[11,12] EPRI/SRI,[13] LSTF,[14,15] and BETHSY[16] have demonstrated that reflux cooling is an effective means of decay heat removal in plants with U-tube steam generators (UTSGs). Local or separate effects experiments, such as those performed at the University of California at Santa Barbara,[17,18] the Massachusetts Institute of Technology (MIT)[19] the University of California at Berkley,[20] and one by Hein et al.[21] have discovered unstable U-tube flow characteristics during the reflux condensation mode of natural circulation. Several of the above references address potential adverse effects associated with flooding and steam generator liquid hold-up, and loop liquid seal formation that may occur during reflux cooling. The situation during the Vogtle incident was further complicated by the low system pressure and the presence of large amounts of air in the steam generator U-tubes. The experiments conducted by FLECHT-SEASET, PKL, EPRI/SRI, and the University of California at Santa Barbara considered the effects of noncondensables on reflux cooling at low pressure. Thus, these tests are considered more relevant to the Vogtle incident than the high pressure (≈1000 psi) experiments performed in SEMISCALE, LOFT, LSTF, and BETHSY, or the work by MIT and Hein, which did not examine the effects of significant amounts of noncondensable gases on boiling condensation.

Experiments in integral test facilities such as MIST,[22] OTIS,[23] and those at EPRI/SRI[24] and the University of Maryland at College Park (UMCP)[25] have demonstrated the effectiveness of boiling condensation as a heat removal mechanism in plants with once-through steam generators (OTSGs). MIST and EPRI/SRI experiments investigated the effects of noncondensable gases, but the MIST experiments were conducted at high pressure and with a cold leg break so that the primary system was not closed. OTIS and UMCP experiments did not consider the effects of noncondensables.

The results of these experiments were examined to determine the effects of noncondensable gases, flooding, loop seal formation and clearing, degraded secondary conditions, and low pressure. This appendix describes the phenomena associated with reflux condensation cooling in plants with a UTSG-type design, and addresses the phenomena associated with boiling condensation in plants with OTSGs.

D-2. REFLUX CONDENSATION PHENOMENA IN PLANTS WITH U-TUBE STEAM GENERATORS

In the reflux condensation mode of natural circulation, single-phase vapor generated in the core flows through the hot leg piping, is condensed in the steam generators, and flows back to the core as a liquid. Experiments have demonstrated that in the absence of noncondensables, an approximately equal condensation split exists between the upflow and downflow sides of the steam generator U-tubes.[3,5,26] In the upflow sides of the steam generator U-tubes, a countercurrent flow of vapor and condensate is established. Condensate drains back to the core through the hot leg while vapor continues to flow over the U-tube upper bend. In the downflow sides of the steam generator U-tubes, vapor and condensate flow co-currently into the cold leg suction piping. Figure D-1 illustrates this phenomena in a single U-tube. Since the primary heat transfer mechanism during reflux cooling is condensation, small primary-to-secondary temperature

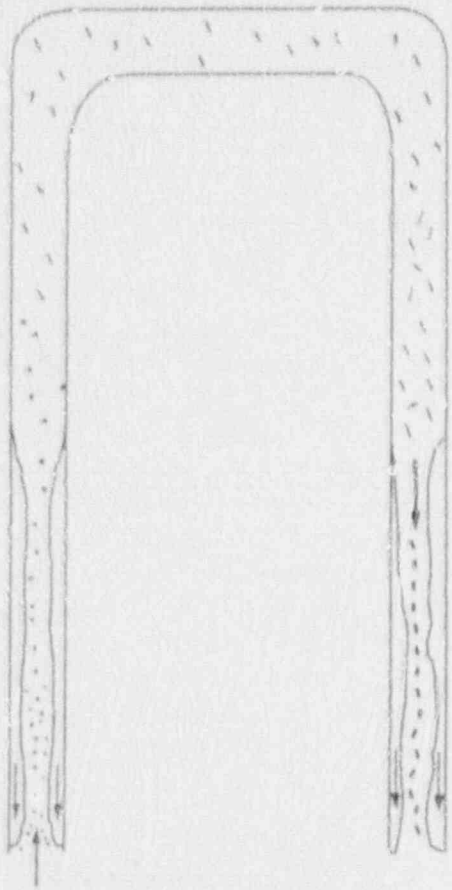

Figure D-1. Liquid distribution in a single U-tube during reflux condensation.

differences and mass flow rates are characteristic of this mode of natural circulation.[3,8,16,24]

Reference 2, which explains the loss of RHR at Diablo Canyon in April of 1987 during reduced inventory operation with noncondensables, describes the following three possible directions the steam-gas mixture can flow from the vessel.[2]

- The vessel upper head. As the pressure increases, the steam-gas mixture may be vented through the reactor vessel upper head vent or through the vessel bypass paths. However, the vent flow is much smaller than the steam generation rate so this path will not relieve the reactor coolant system pressure.

- The hot leg and into the pressurizer through the pressurizer surge line. A vent path exists in the pressurizer through the power operated relief valve.

- The hot leg and into the steam generator U-tubes. No vent path is available unless a steam generator manway is open.

Note that the steam-gas mixture will most likely follow the first two paths until the pressure increases sufficiently to expose a condensation surface in the steam generator U-tubes.

D-2.1 Flooding Effects (Nonuniform U-tube Flow)

During reflux condensation, flooding is possible in the counter-current flow regions in the upflow sides of the steam generator U-tubes, and the stratified counter-current flow regions in the hot legs. The tendency for flooding may be enhanced by a low system pressure and the presence of noncondensable gases. Low system pressure results in lower steam densities and hence, higher steam velocities. Noncondensable gases in the steam generator U-tubes cause a greater fraction of the condensation to occur in the upflow sides of the U-tubes. As a result, more condensate must drain from these tubes and the likelihood of liquid holdup is increased. Flooding has been observed in a number of reflux condensation experiments.[6,14,15,16,17,18,19]

To describe the flooding effects on the reflux flow behavior, the terminology of Nguyen et al. will be adopted.[17] They identified three distinct U-tube flow modes associated with reflux condensation. At low vapor velocities, the classical reflux condensation phenomena was observed. At the onset of flooding at the steam generator inlet, there is a transition from the classical reflux mode to what Nguyen et al. labeled the oscillatory mode.[17] This mode is characterized by the formation of liquid columns in the riser sections of the steam generator U-tubes. The transition to the oscillatory mode begins when portions of the liquid condensate are carried upward by the vapor flow. This phenomenon can be quantified with a Wallis-type flooding correlation. Liquid hold-up

was observed when the nondimensional superficial vapor velocity, j_g^*, was 0.50. This result is supported by high pressure large-scale test facility (LSTF) data in which liquid hold-up occurred for $j_g^* = 0.4$ and $j_g^* = 0.56$ corresponding to core powers of 5% and 7%, respectively.[14] Flooding also occurred in the FLECHT-SEASET facility for $j_g^* = 0.50$, which corresponds to core power levels of about 2.5% at a pressure of 140 psia. Thus, in the FLECHT-SEASET facility there were no stable reflux modes for decay heat levels greater than 2.5% core power.

The carry-over mode occurs when sufficiently high vapor velocities are able to carry the condensate over the upper U-bends of the U-tubes. In this situation, a co-current flow of liquid and vapor exists in both the upflow and downflow sides of the steam generator U-tubes, and a transition to two-phase natural circulation may occur. The transition to the carry-over mode was observed by Nguyen et al. to occur when $j_g^* = 0.9$,[17] while LSTF experiments observed this flow mode when $j_g^* = 0.8$ (10% core power).

Flow modes similar to those described above have also been observed by Calia and Griffith,[19] BETHSY,[16] Hein et al.,[21] Semiscale,[3] and in PKL.[8] The three modes of U-tube behavio described above are illustrated in Figure D-2.

Of particular concern with regard to nuclear reactor safety analysis is the oscillatory U-tube flow mode. A positive hydrostatic head in the steam generator U-tubes exerts a back pressure on the core liquid level and, while core cooling remains effective, core liquid level depression is possible.[18] This effect was first observed in Semiscale, where it was discovered that core coolant level depression during pump suction loop seal formation can be aggravated by the existence of a positive hydrostatic head in the steam generator U-tubes.[6]

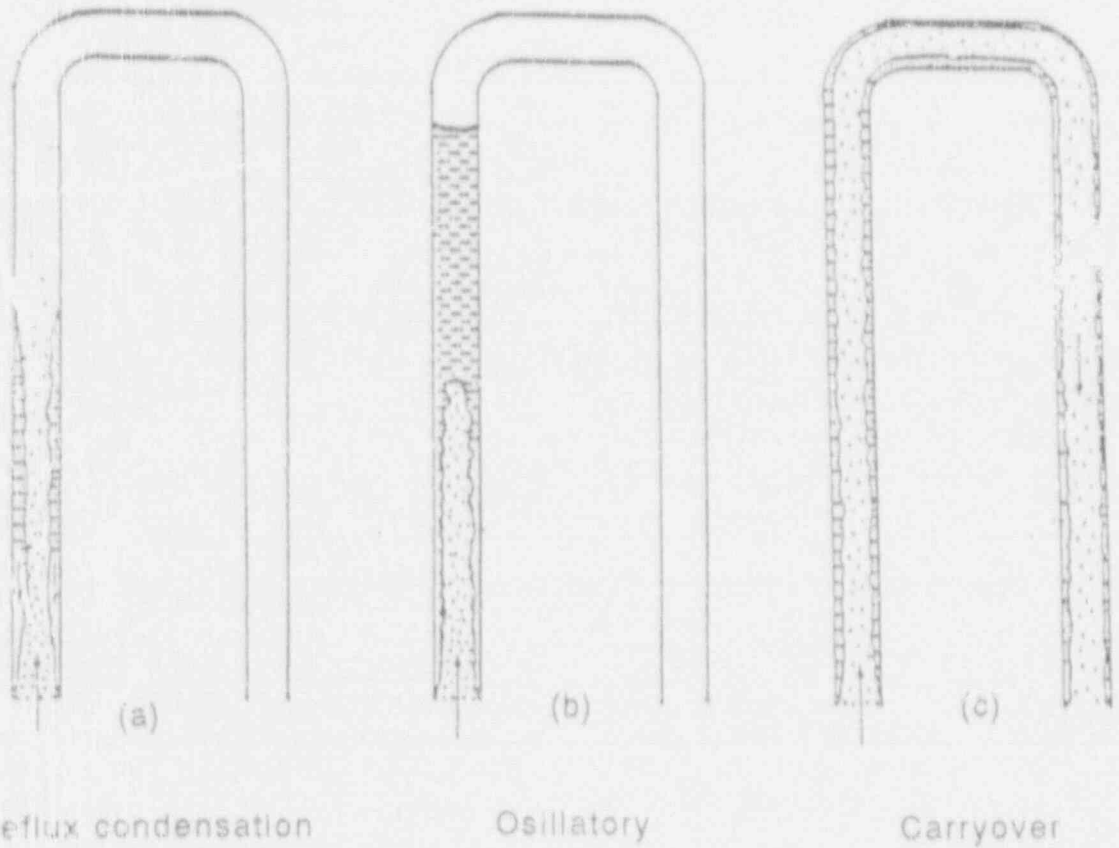

Figure D-2. Two-phase flow patterns in an inverted U-tube.[18]

The oscillatory mode was so named because of the observed periodic fill and dump behavior in the U-tubes. As the liquid column in a U-tube reached the top of the U-tube bend, spillover occurred. After spillover, a siphoning effect would pull the liquid column over the U-tube bend. Steam flow in this cleared tube would then increase significantly, allowing the remaining tubes to partially drain until the pressure drops in all tubes were equal. A liquid column would again form in the cleared tube and the pattern would repeat. The spillover event appeared to occur randomly in any one of the U-tubes. It is believed that the random nature of the fluctuations of the liquid columns is the cause of the randomness in the spillover event.[18] In the presence of noncondensable gases, spillover events may redistribute the noncondensables to other noncleared U-tubes or to other locations in the primary loop. The distribution of the noncondensables in the primary loop is very important in determining the thermal hydraulic behavior of the system. A redistribution of gases caused by U-tube spillover events should be considered when determining the system thermal hydraulic response.

It should be pointed out that calculations of steam velocities in the Vogtle steam generators as a function of decay heat, when compared with criteria for the onset of flooding, indicate that flooding would be unlikely to occur under conditions during reduced inventory operation. At decay heat levels as high as 30 MW, flooding would not occur as long as two or more steam generators are active. With only one steam generator available, flooding would not be expected at decay heats below 15 MW. Decay heat levels would be below this value two days after shutdown. The results of the flooding calculations are shown in Figure D-3.

Several additional comments should be made with regard to U-tube flow phenomena during reflux cooling. First, it is noted that the experimental results cited above are based on a limited number of U-tubes in the steam generators. In this situation, individual tube behavior has a greater effect on the system thermal hydraulic response than it would in an actual PWR steam generator with a much larger number of U-tubes (thousands of tubes).[5] In addition, the tube-to-tube interactions that may occur through the steam generator inlet and exit plena are not understood. Finally, the University of California at Santa Barbara research indicated that the common advanced thermal-hydraulic analysis systems codes, RELAP5 and TRAC-PF1, have difficulty predicting the onset of the oscillatory U-tube flow mode and the growth of the liquid column.[18]

D-2.2 Loop Seal Formation and Clearing Phenomena

During mid-loop operation, a liquid seal exists in the loop cold leg suction piping. During reflux cooling, the liquid seal impedes the flow of vapor through the loop piping. An experiment conducted in the Semiscale facility demonstrated that the effect of the loop seal is more complicated than a simple manometric balance between the reactor vessel and downflow leg of the loop seals.[6] The important parameters were identified as the core vapor generation rate, the core coolant bypass flow, the U-tube condensation rate, and flooding.

If the core vapor generation rate is sufficiently high, a differential pressure may develop between the reactor vessel (hot leg) and the downcomer (cold leg).[3] Consequently, the vessel coolant level may be depressed relative to the downcomer. In addition, this core liquid level depression may be intensified by liquid hold-up in the steam generator U-tubes resulting from flooding at the steam generator inlet.

There are often two sets of bypass paths in plants with UTSGs capable of removing steam from the upper vessel plenum to the downcomer. One set is the downcomer inlet annulus-to-upper head flow path, and the second set is leakages through the gaps at each hot leg penetration by the slip fit between the core barrel assembly and the reactor vessel.[27] The flow behavior through these core bypass paths during this type of transient is not well understood.

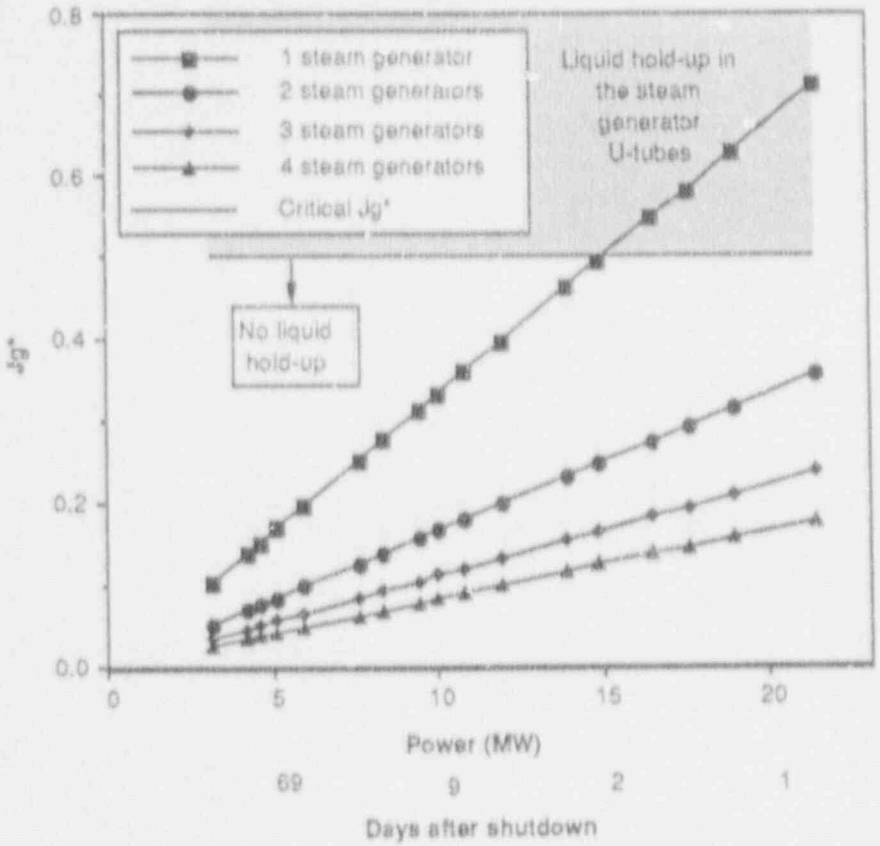

Figure D-3. J_g^* relative to decay heat levels and the number of active steam generators at atmospheric pressure.

The Semiscale experiment, mentioned above, demonstrated that core voiding was possible before the blowout of the pump suction liquid seals.[3,6] Figure D-4 demonstrates the hydrostatic heads in the primary system that lead to the core liquid level depression phenomena.[3]

Loop seal blowout during the high-pressure Semiscale experiments was observed to be a steady process. However, in experiments conducted in the low-pressure FLECHT-SEASET facility, the clearing of the loop seal was not steady. It was observed that steady-state reflux condensation was periodically interrupted by venting steam through the intact loop seal.[11] The core vapor generation rate was greater than the steam generator condensation rate and consequently, uncondensed vapor flowed into steam generator exit plenum and cold leg, displacing the liquid in those locations. The vapor depressed the liquid level in the downside of the cold leg suction piping until steam eventually vented through the loop seal. The differential pressure between the loop hot and cold leg nozzles was temporarily relieved, and the liquid seal re-formed. This process is illustrated in Figure D-5. The following effects resulted from venting steam through the loop seal.[11,12]

- Fluid from the downcomer was forced into the rod bundle by the vented steam. This liquid replaced the two-phase mixture in the lower elevations of the vessel and temporarily stopped vapor generation in the lower vessel elevations. The liquid from the downcomer also forced the two-phase froth level well above the hot leg nozzle elevation.

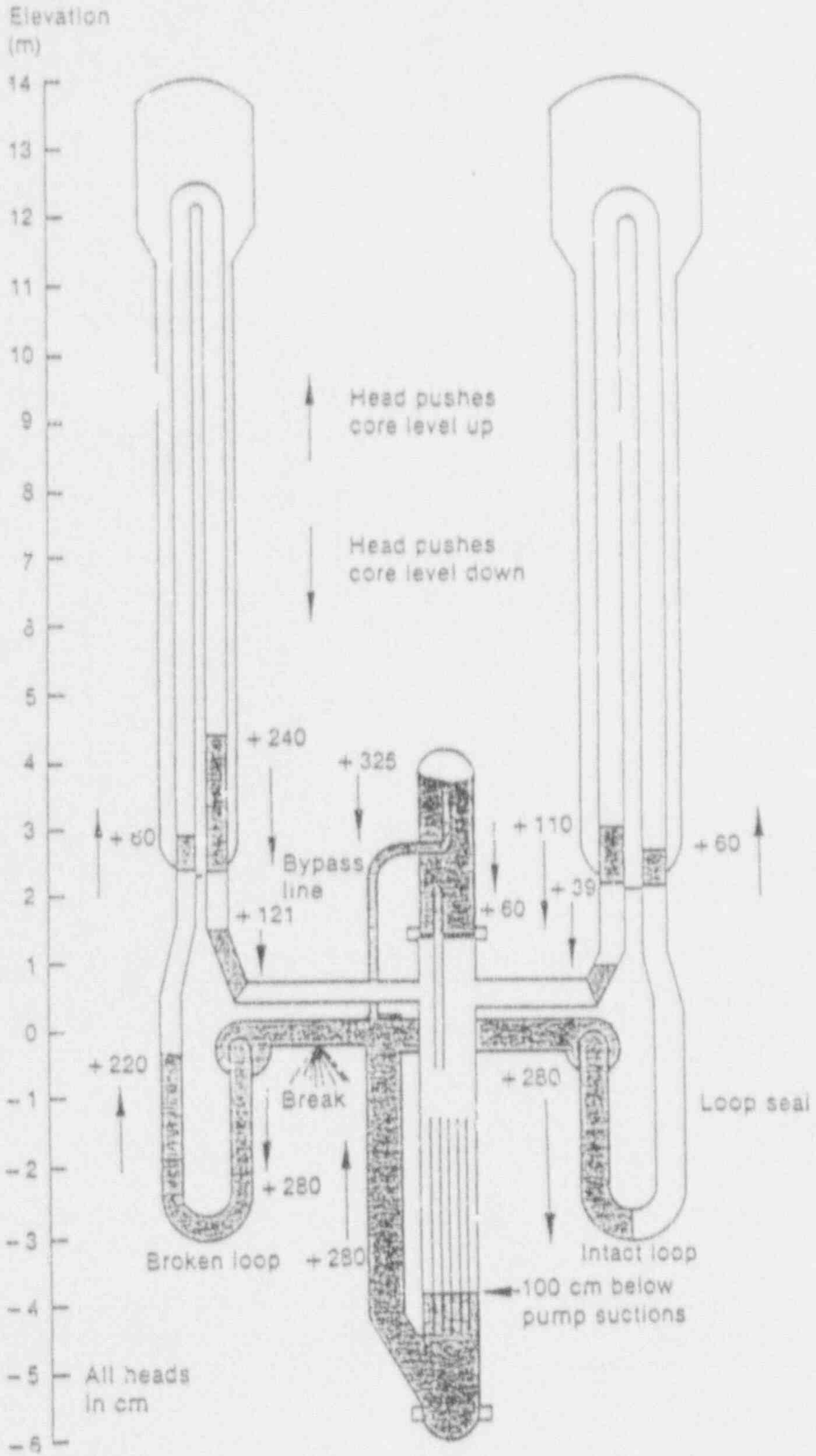

Figure D-4. Demonstrations of hydrostatic heads in the primary system that can lead to core level depression.[3]

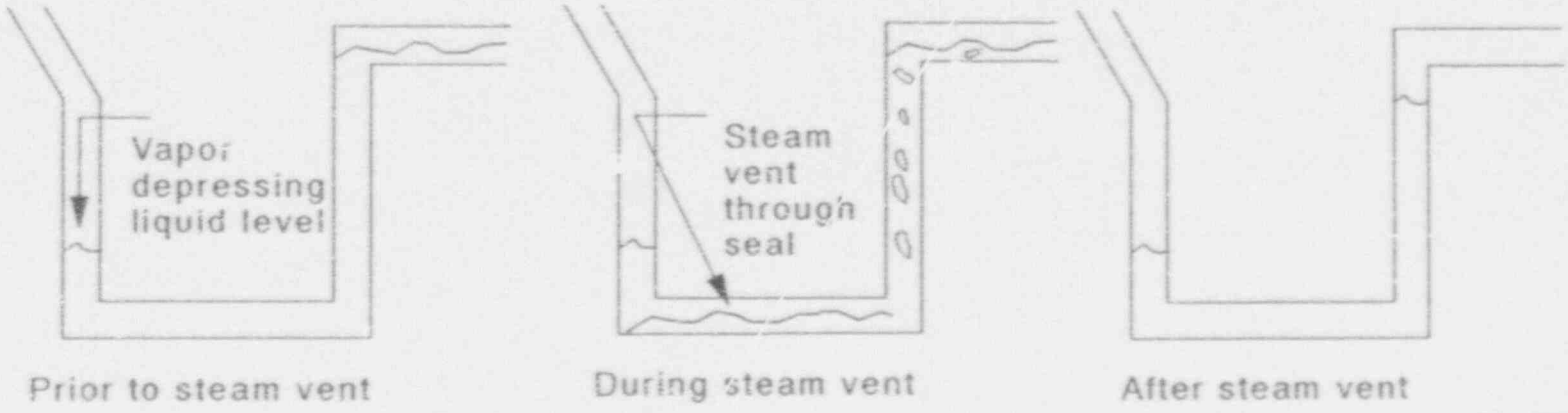

Figure D-5. Loop seal liquid distributions.[12]

- A two-phase mixture was forced into the steam generator inlet plenum.

- The flow in the steam generator U-tubes changed from countercurrent to co-current two-phase flow.

It is believed that the periodic venting of steam through the loop seal during reflux condensation is a low-pressure effect. This phenomena has also been observed in the low-pressure PKL facility.[12]

D-2.3 Effect of Noncondensable Gas on Reflux Cooling

Calia and Griffith[19] noted that at low pressure, a small mass fraction of noncondensable gas may become a significant volume fraction in the primary system. At low pressures, the influence of noncondensable gases on reflux cooling is more pronounced than at high pressures. The primary concern regarding noncondensable gases during reflux cooling is that they will accumulate in the steam generator U-tubes and disrupt the condensation of steam from the core. The following general effects of noncondensables on reflux condensation have been observed in Semiscale,[3,5] PKL,[8,9,10] FLECHT-SEASET,[12] and EPRI/SRI[13]:

- The condensation of vapor from the core is shifted to the upflow side of the steam generator U-tubes while noncondensable gas is deposited in the downflow sides of the steam generator U-tubes, the steam generator exit plenum, and above the loop seal liquid vapor interface.

- The steam generator is divided into active and passive zones thereby reducing the total condensing surface area. In the case of large amounts of noncondensable gases in the primary system, the condensing surface will be confined to a short distance above the tube sheet along the upflow sides of the steam generator U-tubes.

- If steam is unable to reach the steam generator U-tubes because of noncondensable gas blockages, the system pressure will increase until the noncondensable gas volume has been sufficiently compressed to allow condensation in the lower portions of the upflow sides of the steam generator U-tubes.

- An increase in the primary-to-secondary temperature difference is necessary to remove the core decay heat because of the reduced heat transfer area. An increase in the primary pressure also results.

Tests conducted by EPRI/SRI concluded that the amount of noncondensable gases that could be accommodated by the primary system is limited only by the design pressure of the system as long as secondary cooling is available.[13] In this low pressure (<75 psi) experiment, helium gas was injected into the primary system in increments that amounted to 60% of the total system volume. It was observed that reflux condensation is highly tolerant of significant amounts of noncondensable gases. When noncondensable gases prevented steam condensation, the system pressure would increase to compress the noncondensable gas volume, thereby exposing a condensing surface in the lower portions of the steam generator U-tubes. In this experiment, adequate core cooling was possible with reflux cooling even with significant amounts of noncondensable gases. However, this experiment was conducted at approximately 1% core power and problems associated with flooding did not occur.

Experiments in the low-pressure (approximately 140 psi) FLECHT-SEASET facility indicated that flooding is a potential problem during reflux cooling.[12] Low system pressures yield higher steam velocities and consequently, the flooding characteristics differ from those of high-pressure systems. Flooding problems are also complicated by the presence of noncondensable gases, which tend to shift the condensation to the upflow sides of the steam generator U-tubes. This results in more condensate trying to drain from the upflow sides of the U-tubes. Hence, the noncondensables increase the probability for liquid column formation in the steam generator U-tubes.

The combined effects of low pressure, noncondensable gases (helium), and flooding in experiments performed in the FLECHT-SEASET facility are discussed below.

Noncondensable gas would collect above the liquid-gas interface above the loop seal and extend upward into the steam generator exit plenum and the steam generator U-tubes. This noncondensable gas exerted a back pressure on the vessel liquid, forcing core liquid level depression. Periodic venting of the noncondensable gas through the loop seal temporarily relieved this pressure difference. However, the flooding tendency of the uphill sides of the steam generator U-tubes added to the pressure exerted on the vessel liquid level. The liquid level in the vessel was depressed to approximately two feet below the bottom of the loop seal elevation.[12] By comparing the tests with and without noncondensable gases, it was discovered that the frequency that steam vents through the loop seal was greater than the frequency of the noncondensable gas vents. Core uncovering did not occur in the test where noncondensable gases were not present.[12] The longer venting period in the noncondensable gas test may be due to the fact that helium is lighter than steam. Recall that air is heavier than steam, so similar behavior might not occur when air is the noncondensable gas present in the downflow side of the loop suction. Note also that the velocity of the vapor generated in the core exceeded the steam generator U-tube flooding limit in both these tests.

D-2.4 Secondary Side Effects

Experiments performed at the low-pressure PKL test facility investigated the effects of reduced secondary inventory on the effectiveness of reflux cooling.[10] The results indicated that the primary-to-secondary temperature difference increased because of the reduced heat exchanger area. A halving of the primary-to-secondary heat transfer area occurred when the secondary level was lowered to uncover half of the U-tubes, and this resulted in a doubling of the temperature difference when no noncondensable gases were present. When noncondensable gases were present, this temperature difference increased by a factor of four (from 2K to 8K).

Reference 1 stated that at a core power of 2.5 MW, 5 days would be required to boil-off the secondary liquid. However, it was also stated that if the Vogtle incident had occurred earlier in the refueling process, the core power could have been as high as 17.1 MW and the time to secondary boil-off would be significantly reduced.

The presence of significant amounts of noncondensable gases in the steam generator U-tubes reduces much of the heat transfer area in the higher elevations of the steam generator tubes. Therefore, one would expect that the effects of reduced secondary inventory would be significant only when the secondary liquid level drops to the lower elevations of the steam generator U-tubes where the majority of the heat transfer occurs.

D-2.5 Vent Operation

Many plants with UTSGs have reactor vessel upper head vent valves and pressurizer power operated relief valves. Vent operation may be used to control the primary pressure or to remove noncondensable gases. Plants equipped with these system vents have backup systems to ensure operation if a loss-of-power event occurs. However, if these backup systems fail, it is unclear whether the environment in containment would allow for manual operation of the vent valves. In addition, effectiveness of vent operation is not well understood.

D-2.6 Summary

Reflux condensation can be an effective means of heat removal in PWRs with UTSGs, even in the presence of significant amounts of noncondensable gases. Numerous experiments have demonstrated this fact.[3,7,8,16,26] Problems would arise if the decay heat level was high enough to cause flooding and/or to generate steam faster than it can be condensed in the steam generators. However, calculations indicate this is unlikely at decay heat levels typical during reduced inventory operation.

Under shutdown conditions, special equipment such as temporary thimble tube seals, nozzle dams, and liquid level instruments may be in place. These devices are vulnerable to failure at elevated pressures.[1,2] This equipment may impose

pressure limitations on the primary system. These limitations could subsequently remove the capability of the system to compress the noncondensable gas volumes to ensure a condensation surface in the steam generators.

The Diablo Canyon incident demonstrated that reflux cooling can occur during mid-loop operation upon the loss of the RHR system.[2] An order of magnitude estimate for the pressure increase necessary to initiate reflux was given in Reference 2 as 10 ± 5 psig. Note that this pressure is capable of causing Tygon tube rupture (failure at 2.5–5 psig), and in fact Tygon tube rupture did occur in the Diablo Canyon Incident.[2]

D-3. BOILING CONDENSATION PHENOMENA IN PLANTS WITH ONCE-THROUGH STEAM GENERATORS

In the case of plants with once-through steam generators (OTSGs), the natural circulation behavior with a partially filled RCS is quite different from the behavior encountered in plants with UTSGs. In the OTSG-type plant design, the hot legs consist of long vertical sections that lead to inverted U-bends ("candy cane" regions) and then drop into the top of the steam generators. The steam generators themselves consist of a very large number of vertical tubes connecting the candy cane regions and steam generator outlet plenum. Steam from the core flows through the hot leg to the steam generator, where it is condensed. The condensate then drains to the liquid level in the cold side of the primary loop. This mode of cooling is normally called boiling condensation.

Figure D-6 demonstrates the liquid distribution in the primary loop during boiling condensation. Boiler condensation operation requires the primary level to be lower than the secondary liquid pool. Consequently, this particular heat transfer process is commonly termed pool boiling condensation. A second type of boiling condensation, called emergency feedwater (EFW) boiling condensation, occurs when the primary liquid level is above the secondary pool within the steam generator, but a primary condensing surface exists below the EFW injection elevation. Figure D-7 presents the loop liquid distribution during this mode of natural circulation. Experiments have demonstrated that both types of boiling condensation are effective means of heat removal.[22,23,24]

D-3.1 Effect of Noncondensable Gas on Boiling Condensation

The primary question regarding boiling condensation in an OTSG with noncondensables present is the ability of the steam generated in the core to reach a condensing surface in the steam generators. Experimental data regarding this issue is very limited. High-pressure tests were performed at the Multiloop Integral System Test (MIST) facility to determine the effects of noncondensable gases, but these tests also included a cold leg break.[22] Consequently, MIST data may not be directly related to the situation discussed in this report. Additional low-pressure noncondensable gas experiments were conducted by EPRI/SRI in a facility modeled after Three Mile Island Unit-2.[24] The EPRI/SRI results are discussed below.

It was discovered in the EPRI/SRI experiment that the noncondensable gas in the steam generators dictated the elevation of the condensation region in OTSGs. High concentrations of noncondensable gas (nitrogen) accumulated above the primary steam generator liquid level because of the removal of steam from the gas mixture by condensation. Since the presence of noncondensables impedes condensation, the condensing region may be forced to a higher elevation in the steam generator. If this elevation is above the secondary pool level and EFW is not available, the heat removal ability of the steam generator may be lost. A loss of the heat sink results in increases in both primary pressure and temperature. Pressure increases compressed the noncondensable gas volume sufficiently to expose a condensing surface. These

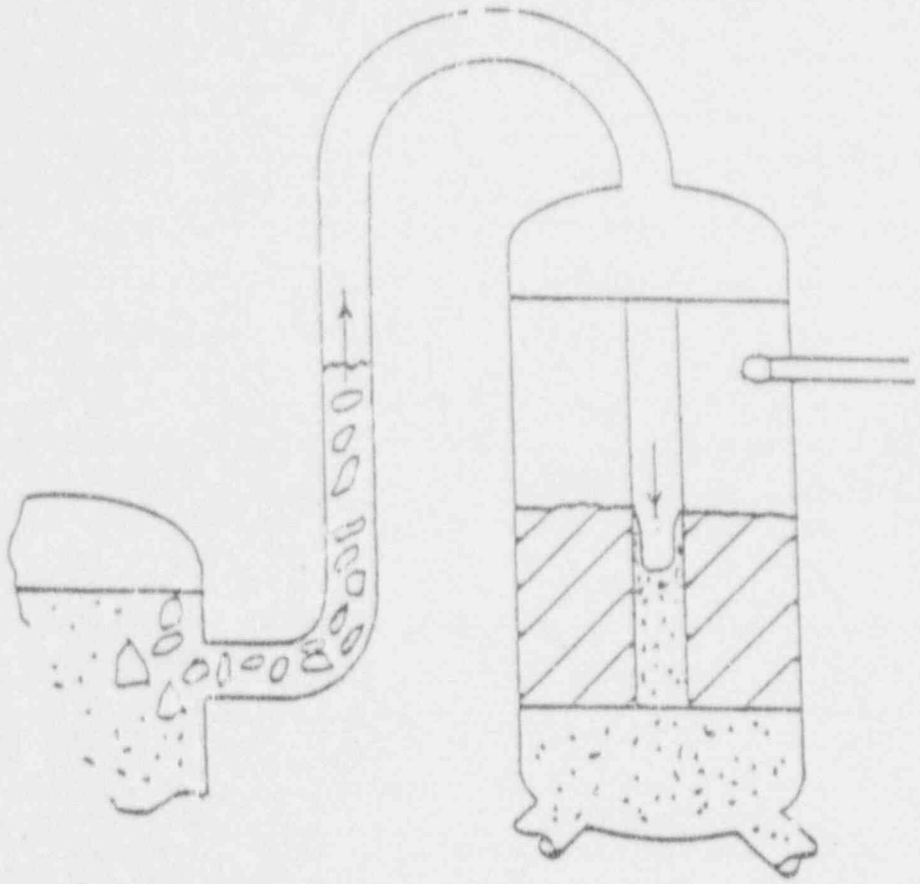

Figure D-6. OTSG liquid levels during pool boiling condensation.

observations led to the conclusion that the pressure limits of the facility determine the amount of noncondensable gas that may be accommodated by the system.[24] This pressure limit is very important, especially if it is determined by the vulnerability of equipment such as temporary liquid level instruments.

D-3.2 Secondary Side Effects

The availability of EFW is an important issue because the EFW availability guarantees the existence of a condensing surface high in the steam generators. If EFW is not operable because of loss of power, the secondary pool level must be high enough to provide a condensing surface in the steam generator. Otherwise, boiling condensation is not possible.

It appears that in the case of plants with OTSGs, the effect of noncondensable gas is to drive the condensing surface toward the top of the steam generator. Note that the opposite is true in the case of plants with UTSGs, where the condensing surface is driven toward the lower portions of the upflow sides of the steam generator U-tubes. Another adverse effect in the case of OTSGs is that stratification tends to place the hotter water at the top of the secondary, thus reducing the primary-to-secondary temperature difference in the region where condensation must occur. Therefore, the boil-off of the secondary liquid (without EFW) is a much greater concern in the case of an OTSG.

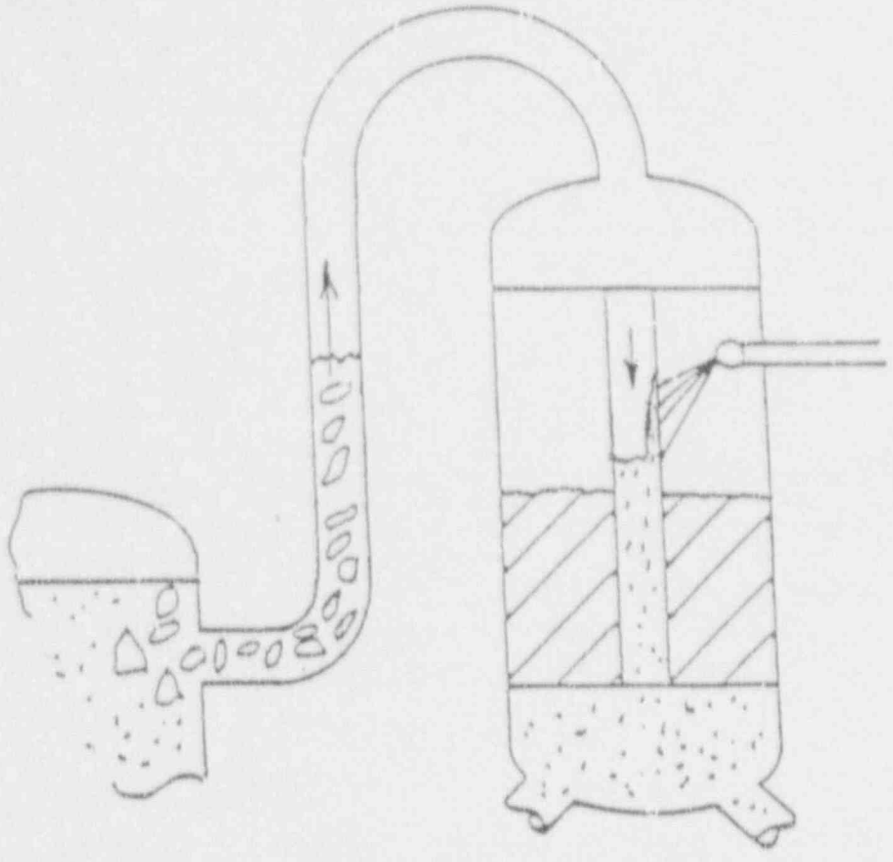

Figure D-7. OTSG liquid levels during auxiliary feedwater boiling condensation.

D-3.3 Vent Operation

In plants with OTSGs, reactor vessel vent valves may vent steam from the core into the downcomer region where condensation may occur. In addition, vents exist at the top of the hot leg U-bend region (hot leg upper head vent). These vents may be useful in removing noncondensable gas from the primary system.

The effectiveness of vent operation in plants with OTSGs, under conditions similar to the Vogtle incident, have been investigated. The results are reported in Appendix A.

D-3.4 Summary

The boiling condensation process in plants with OTSGs, under conditions similar to the Vogtle incident, is quite different than in plants with UTSGs. In plants with OTSGs, noncondensable gases must be compressed downward in the OTSG tubes, and the condensed liquid flows cocurrent (downward) to the steam flow. The availability of EFW and the effects of fluid thermal stratification in the secondary side are important issues with regard to the boiling condensation process. Availability of EFW ensures the existence of a condensing surface high in the steam generators, while thermal stratification in the secondary side effectively reduces the primary-to-secondary temperature difference where condensation must occur.

D-4. SUMMARY AND CONCLUSIONS

D-4.1 Plant Initial Conditions

This appendix discusses the important issues related to reflux (UTSGs) or boiling (OTSGs) condensation under the following conditions.

- Primary water level near mid loop
- Presence of large amounts of noncondensable gases in the upper elevations of the primary loop
- Complete loss of the RHR system
- A closed primary system, but with the possibility of reactor coolant system draining and vent operation
- Low primary system pressure (near atmospheric)
- Possible pressure limitations from the vulnerability of shutdown equipment such as temporary thimble tube seals or level instruments
- Wide range of decay heat levels.

Issues associated with plants with both UTSGs and OTSGs were considered. Since the behavior of these plants differs significantly in this situation, the important issues related to each type will be addressed separately.

D-4.2 Plants with UTSGs

Plants with UTSGs are capable of using the reflux condensation mode of natural circulation cooling under partial liquid inventory conditions. Experiments in many integral test facilities have investigated this mode of natural circulation cooling. Several of these include FLECHT-SEASET,[11,12] PKL,[8,9,10] Semiscale,[3,4,5,6] LSTF,[14,15] and an EPRI/SRI facility. Semiscale and LSTF are high-pressure facilities, while the others listed are low-pressure facilities. In addition, many local or separate effects experiments have also been performed. Several of these include University of California at Santa Barbara tests,[17,18] MIT tests,[19] and tests conducted by Hein et al.[21]

Flooding and steam generator liquid hold-up are issues of concern with regard to reflux cooling. Low system pressures result in low steam densities and high steam velocities that increase the possibility of flooding. However, calculations indicate that during reduced inventory operation, decay heat levels will probably be sufficiently low to prevent flooding. Uncertainties with regard to this issue include core vessel by-pass flow, spillover effects if the liquid columns reach the tops of the U-tubes, and loop seal behavior. Evidence of flooding and steam generator liquid hold-up can be found in the results of several experiments.[3,6,14,15,18]

The formation of loop seals in the cold leg suction piping impedes the flow of vapor during reflux cooling.[2,6,11,12] If the vapor generation rate is greater than the condensation rate, the liquid levels in the core and in the downflow side of the loop seal may be depressed. Liquid hold-up in the steam generator U-tubes will aggravate this effect and may result in a core liquid level depression to an elevation below the bottom of the loop seal elevation. Low-pressure experiments also observed the periodic venting of steam or noncondensable gases through the loop seal to relieve the loop differential pressure.[11,12] Uncertainties with regard to loop seal behavior include core bypass flow, steam generator liquid hold-up caused by flooding, and steam generation and condensation rates.

The presence of noncondensable gases in the steam generator U-tubes of the primary loop raises the question of whether the steam produced in the core can reach a condensing surface in the steam generators. Experiments have discovered that if a condensing surface does not exist, pressure increases will compress the noncondensable gas volume sufficiently to expose a condensing surface in the lower portions of the steam generator U-tubes.[3,5,8,9,10,12,13] The shift in the

condensation region to this location because of the presence of the noncondensable gases increases the possibility of liquid hold-up in the steam generator U-tubes. Other experimental observations include the accumulation of noncondensable gases above the gas-liquid interface of the loop seal. The venting period of noncondensables through the loop seal was found to be greater than the period observed for pure steam. Thus, the potential for core liquid level depression caused by the loop seal formation is greater when noncondensable gases are present. Uncertainties with regard to noncondensables include noncondensable gas-steam mixing, the potential for removing noncondensables through venting, and the redistribution or migration of noncondensables if a spillover events occur in the steam generator U-tubes.

Primary system pressure limitations from the presence of shutdown equipment, such as temporary thimble tube seals, nozzle dams, and liquid level instruments, could restrict the use of reflux cooling. If noncondensables prevent steam from reaching a condensing surface in the steam generators, reflux cooling is not possible unless primary pressure increases compress the noncondensable gas volume sufficiently to expose a condensing surface. Pressure and temperature increases will also occur because of the reduced heat transfer area in the steam generator U-tubes from the noncondensables present in the tubes.

D-4.3 Plants with Once-through Steam Generators

Plants with OTSGs are capable of using boiling condensation to remove core decay heat. Two types of boiling condensation are possible in the OTSG. Pool boiling condensation occurs when the primary level is below the secondary pool level within the steam generator. Auxiliary feedwater (AFW) boiling condensation normally occurs when pool boiling is not possible, but a condensing surface exists below the AFW sparger spray elevation. Experiments investigating boiling condensation include those performed at MIST,[22] EPRI/SRI,[24] OTIS,[23] and UMCP.[25] Low-pressure integral tests investigating the effects of noncondensables are limited to the work done by EPRI/SRI.[24]

In the presence of large amounts of noncondensable gases, the primary concern is the ability of steam to reach the steam generators. Observations at EPRI/SRI[24] indicated that the amount of noncondensable gases in a steam generator dictated the elevation of the condensation region. High concentrations of noncondensable gases accumulate above the primary liquid level in the steam generator because most of the steam has been condensed from the gas mixture. Condensation was impeded by these high concentrations of noncondensable gases and the condensation region was driven to a higher elevation in the steam generator. If the condensation region is driven above the top of the steam generator tube sheet or above the secondary liquid level, a pressure increase is necessary to compress the noncondensable gas volume and regain a heat sink. Uncertainties with regard to the effectiveness of boiling condensation with large amounts of noncondensables include the availability of AFW, limits on the primary pressure (level instruments, etc.), secondary liquid level, and operating vents to control pressure and/or to remove noncondensable gases.

D-5. REFERENCES

1. *NRC, Loss of Vital AC Power and the Residual Heat Removal System During Mid-Loop Operations at Vogtle Unit 1 on March 20, 1990*, NUREG-1410, June 1990.

2. J. L. Crews et. al., *Loss of Residual Heat Removal System, Diablo Canyon, Unit 2, April 10, 1987 (Augmented Inspection Team Report April 15–21, 29 and 1 May 87)*, NUREG-1269, June 1987.

3. G. Loomis, *Summary of the Semiscale Program (1965–1986)*, NUREG/CR-4945, EGG-2509, July 1987.

4. K. Soda and G. G. Loomis, "Effects of Noncondensable Gas on Natural Circulation in the Semiscale Mod-2A Facility," *Proceedings of the International Meeting Thermal Nuclear Reactor Safety, Chicago, Illinois, August 29–September 2, 1982*, NUREG/CR-0027, February 1983.

5. D. J. Shimeck and G. W. Johnsen, "Natural Circulation Cooling in a PWR Geometry Under Accident-Induced Conditions," *Nuclear Science and Engineering*, 5, 1984, p. 311.

6. M. T. Leonard, *Vessel Coolant Depletion During a Small Break LOCA*, EGG-SEMI-6010, September 1982.

7. C. L. Nalezny, *Summary of Nuclear Regulatory Commission's LOFT Program Research Findings*, NUREG/CR-3005, EGG-2231, April 1985.

8. R. M. Mandl, P. A. Weiss, "PKL Tests on Energy Transfer Mechanisms During Small-Break LOCAs," *Nuclear Safety, 23*, March–April 1982, p. 148.

9. H. Weisshauph and B. Brand, "PKL Small Break Tests and Energy Transport Mechanisms," *Proceedings of the ANS Specialists' Meeting on Small Break Loss-of-Coolant Accidents Analyses in LWRs, Monterey, California, August 25–27, 1981*, EPRI-WS-81-201, 1981.

10. D. Hein and F. Winkler "A Synopsis of PKL Small Break Tests," *Eighth Water Reactor Safety Research Information Meeting, Gaithersburg, Maryland, October 27–31, 1980*, NUREG/CP-0023, Vol. 2, 1980.

11. S.D. Rupprecht et al., "Results of the FLECHT-SEASET Natural Circulation Experiments," *American Nuclear Society Transactions, 45*, 1983, p. 460.

12. L. E. Hochreiter et al., *PWR FLECHT-SEASET Systems Effects Natural Circulation and Reflux Condensation*, NUREG/CR-3654, EPRI NP-3497, WCAP-10415, August 1984.

13. R. L. Kiang et al., *Decay Heat Removal Experiments in a UTSG Two-Loop Test Facility*, EPRI NO-2621, September 1982.

14. Y. Kukita et al., "Flooding at Steam Generator Inlet and Its Impacts on Simulated PWR Natural Circulation," *ASME Winter Meeting, Boston, Massachusetts, December 13–18, 1987*, FED-Vol. 61, HTD-Vol. 92.

15. Y. Kukita et al., "Nonuniform Steam Generator U-tube Flow Distribution during Natural Circulation Tests in ROSA-IV Large Scale Test Facility," *24th ASME/AIChE National Heat Transfer Conference, Pittsburgh, Pennsylvania, August 9–12, 1987*.

16. P. Bazin et al., "Natural Circulation Under Variable Primary Mass Inventories at BETHSY Facility," *Fourth International Meeting on Nuclear Reactor Thermal-Hydraulics, Karlsruhe, Federal Republic of Germany, October 10–13, 1989*, NURETH-4, p. 504.

17. Q. T. Nguyen and S. Banerjee, "Flow Regimes and Heat Removal Mechanisms in a Single Inverted U-Tube Steam Condenser," *American Nuclear Society Transactions, 43*, 1982, pp. 788–789.

18. Q. T. Nguyen, *Condensation in Inverted U-Tube Heat Exchangers*, Ph.D. dissertation, University of California at Santa Barbara, August 1988.

19. C. Calia, and P. Griffith, "Modes of Circulation in an Inverted U-Tube Array with Condensation," *Journal of Heat Transfer, 104*, November 1982, pp. 769–773.

20. C. L. Tien, *Reflux Condensation in a Closed Tube*, EPRI NP-3732, October 1984.

21. D. Hein et al., "The Distribution of Gas in a U-Tube Heat Exchanger and Its Influence on the Condensation Process," *Proceedings of the Seventh International Heat Transfer Conference, Munchen, Federal Republic of Germany, 1982*.

22. J. R. Gloudemans, *Multiloop Integral System Test (MIST): Final Report*, NUREG/CR-5395, EPRI/NP-6480, BAW-2066, Vol. 7, July 1989.

23. J. R. Gloudemans et. al., *Once-Through Integral System (OTIS): Final Report*, NUREG/CR-4567, EPRI NP-4572, BAW-1905, September 1986.

24. R. L. Kiang, *Two-Phase Natural Circulation Experiments in a Test Facility Modeled After Three Mile Island Unit-2*, EPRI-NP-2069, October 1981.

25. M. Massoud, *An Analytical and Experimental Investigation of Natural Circulation Transients in a Model Pressurized Water Reactor*, NUREG/CR-4788, Jan. 1987.

26. K. E. Carlson, *Improvements to the RELAP5/MOD3 Noncondensable Model*, EGG-EAST-8879, January 1990.

27. C. D. Fletcher and R. A. Callow, "Long-Term Recovery of Pressurized Water Reactors Following a Large Break Loss-Of-Coolant Accident," *Nuclear Engineering and Design, 110*, 1989, pp. 313–328.

Appendix E

Scoping Calculations

Appendix E

Scoping Calculations

E-1. STEAM GENERATOR U-TUBE FLOODING CALCULATIONS

This section discusses the Wallis-type flooding correlation calculations used to investigate the possibility of flooding in steam generator U-tubes.[1] In a number of experiments,[2,3,4,5,6] flooding has been shown to occur when the value of the nondimensional superficial vapor velocity, j_g^*, was greater than 0.5. Wallis defined j_g^* as

$$j_g^* = \frac{j_g \sqrt{\varrho_g}}{\sqrt{gD(\varrho_f - \varrho_g)}} \qquad \text{(E-1)}$$

where

j_g = superficial vapor velocity

ϱ_g = density of steam

g = acceleration due to gravity

D = tube diameter

ϱ_f = density of water.

A mass and energy balance in the primary loop is used to obtain the following expression for the superficial vapor velocity

$$j_g = \frac{Q}{\varrho_g h_{fg} A} \qquad \text{(E-2)}$$

where

Q = core decay heat

h_{fg} = latent heat of vaporization

A = cross-sectional area of the U-tubes in one steam generator times the number of active steam generators.

An active steam generator in this context means one that is capable of removing heat from the primary system. For simplicity, it is assumed that there is no flow through inactive loops, that is, through loops with inactive steam generators. This convention will be used throughout this appendix.

Calculations of j_g^* were performed by varying the decay heat and the number of active loops for pressures of both 1.0 atm and 2.0 atm. The results of these calculations are given in Figures E-1 and E-2. Relevant data used are given below [1979 American Nuclear Society (ANS) standard decay heat data]:

Rated plant power	=	3,411 MW
Number of U-tubes/steam generator	=	5,626
Steam generator U-tube piping inner diameter	=	0.688 inches
Number of primary loops	=	4.

Note that at atmospheric pressure, flooding is possible only when 15 MW of decay heat must be removed by one active steam generator. When the pressure is increased to 2.0 atm, this decay heat value is increased to approximately 20 MW. These calculations demonstrate that flooding in the steam generator U-tubes is not likely under reduced inventory conditions.

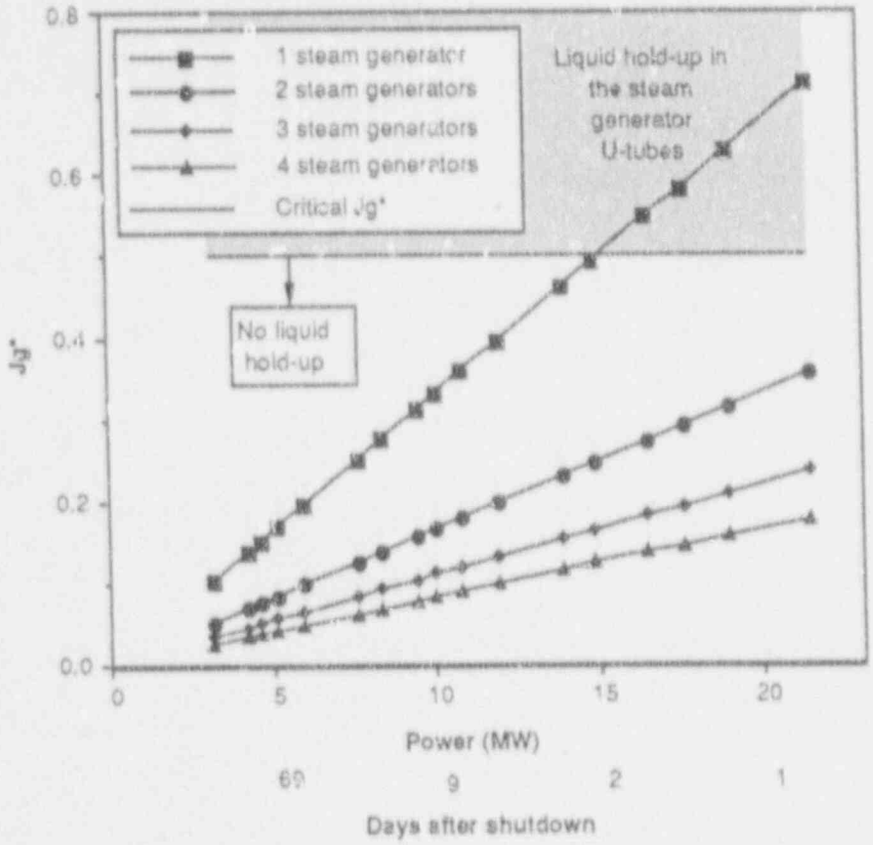

Figure E-1. Nondimensional superficial vapor velocity relative to decay heat and number of active steam generators at atmospheric pressure.

E-2. HORIZONTAL STRATIFICATION IN THE HOT LEGS

This section addresses the possibility of loss of horizontal stratification in the hot legs, which subsequently signals the loss of classical reflux condensation. These calculations are used to determine the range of decay heat where classical reflux is possible.

Three different hot leg liquid levels were considered in these calculations. These levels, measured from the bottom of the hot leg pipe (see Figure E-3), were (a) one quarter of the pipe diameter, (b) mid-pipe, and (c) three-quarters of the pipe diameter. The results of the calculations are shown in Figures E-4 through E-6, which demonstrate the behavior of the hot leg velocity as a function of the decay heat and the number of active loops. Figure E-4 shows that for h/D = 0.25 (where h = height and D = pipe diameter), the loss of horizontal stratification is not a concern. When the hot leg liquid level is at mid-pipe (h/D = 0.5), the loss of horizontal stratification is possible with one active loop for decay heat levels greater than 9 MW, and with two active loops for decay heat levels greater than 19 MW (Figure E-5). The results for h/D = 0.75 indicate that loss of horizontal stratification is possible for almost all cases considered, except when four loops are active and the decay heat is less than 5 MW (Figure E-6).

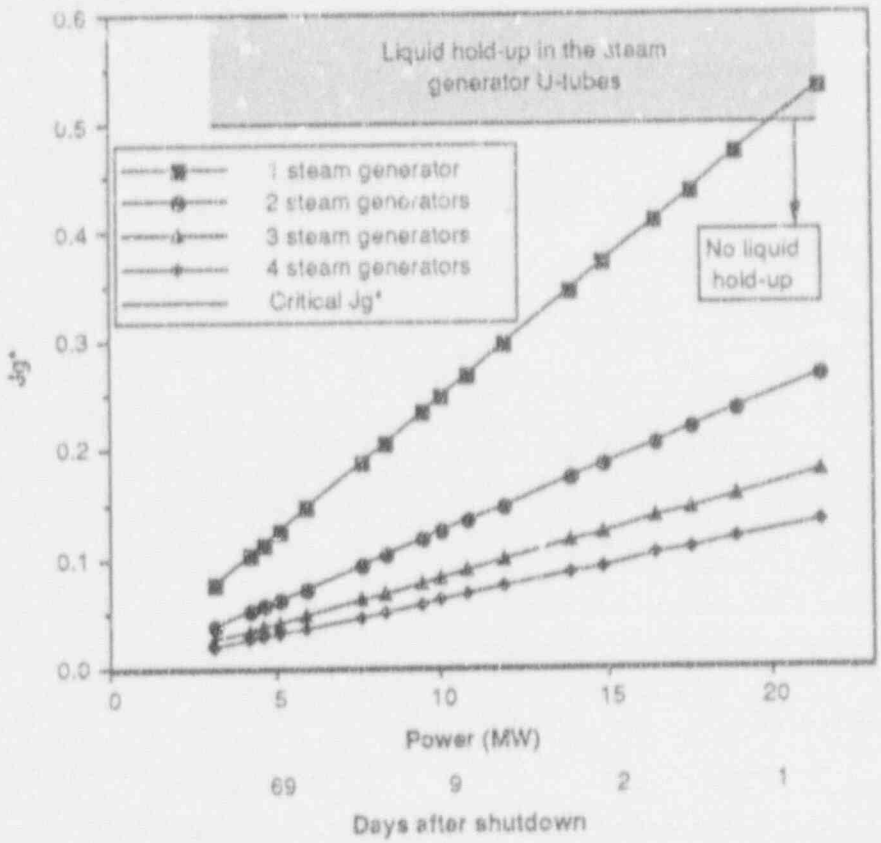

Figure E-2. Nondimensional superficial vapor velocity relative to decay heat and number of active steam generators at 2 atmospheres.

The loss of horizontal stratification is assumed to occur if the hot leg vapor velocity is greater than the critical velocity defined by Taitel-Dukler.[7] The critical velocity is defined as

$$V_{cr} = \frac{1}{2}(1 - \cos\theta)\sqrt{\frac{(\varrho_f - \varrho_g)g\alpha A}{\varrho_g D \sin\theta}} \quad \text{(E-3)}$$

where

θ = angle between a vertical line through the pipe center and the stratified liquid level at the pipe inner wall (see Figure E-3)

ϱ_f = density of water

ϱ_s = density of steam

g = acceleration due to gravity

α = hot leg void fraction

A = cross-sectional area of the hot leg piping

D = tube diameter.

The hot leg steam velocity is calculated from a mass and energy balance according to

$$V_g = \frac{Q}{\varrho_s h_{fg} A^*} \quad \text{(E-4)}$$

where

Q = core decay heat removed by each active steam generator

h_{fg} = latent heat of vaporization

A^* = cross-sectional steam flow area in the hot leg.

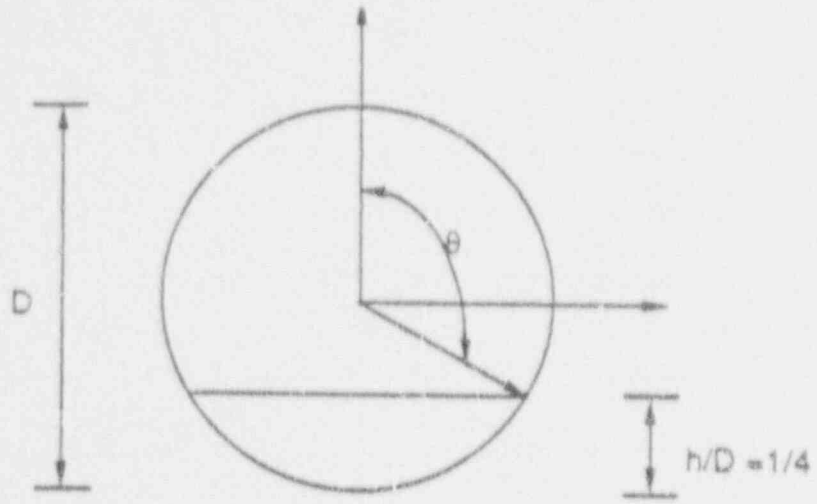

Figure E-3. The hot leg cross-sectional geometry.[1]

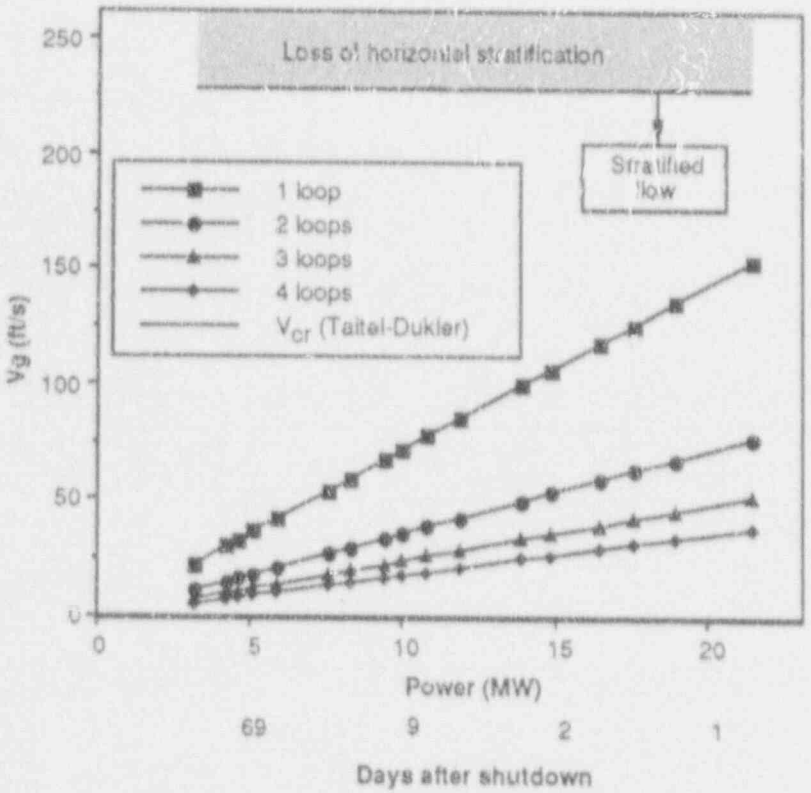

Figure E-4. Hot leg vapor velocity with a 0.25 liquid level in the hot leg pipe for various numbers of active loops.

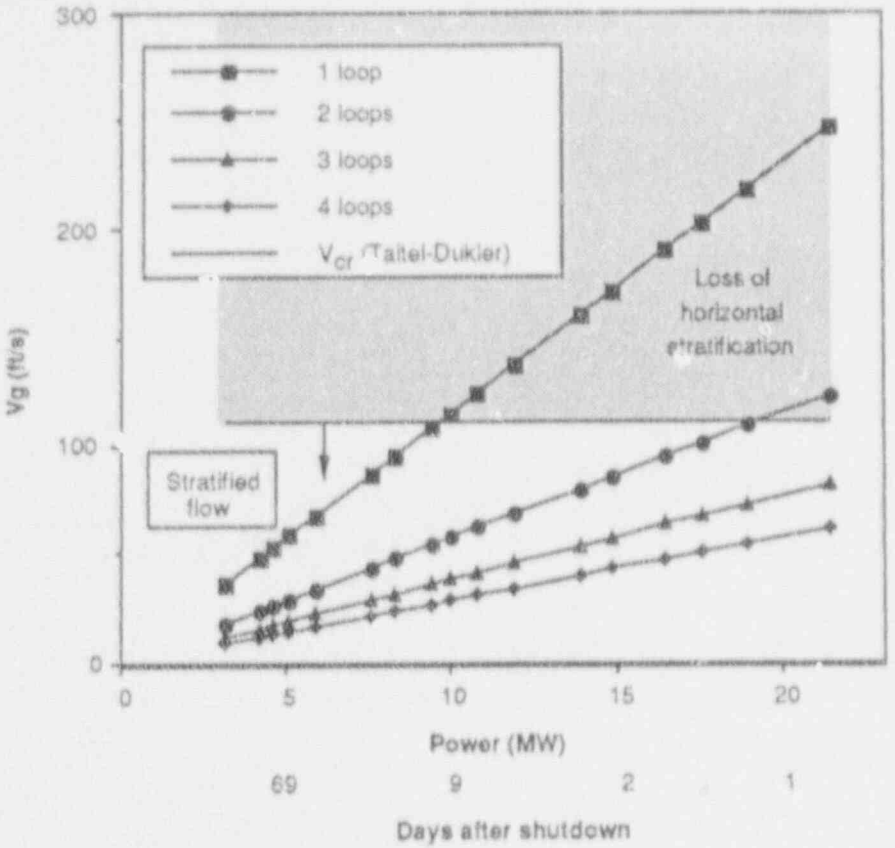

Figure E-5. Hot leg vapor velocity with a 0.5 liquid level in the hot leg pipe for various numbers of active loops.

The hot leg vapor velocity was calculated as a function of the decay heat, the hot leg liquid level, and the number of active loops. The results of the calculations are presented in Figures E-4 through E-6. Recall that it is assumed that there is no flow through an inactive loop. Relevant data used in these calculations are given below (1979 ANS standard decay heat data):

Rated plant power	=	3,411 MW
Hot leg piping inner diameter	=	29 inches
Number of primary loops	=	4.

E-3. FLOODING AT THE HOT LEG BEND

The calculations of hot leg flooding characteristics were based on the Kutateladze correlation.[8] Hot leg flooding can affect core level depression and reflux efficiency.

The Kutateladze correlation chosen is

$$\sqrt{K_g} + \sqrt{K_l} = \sqrt{3.2} \qquad \text{(E-5)}$$

Flooding occurs when there is no liquid downflow ($K_l = 0$) or when $K_g = 3.2$. K_g is defined by

$$K_g = j_g \left[\frac{(\varrho_f - \varrho_g)\sigma g}{\varrho_g^2} \right]^{-\frac{1}{4}} \qquad \text{(E-6)}$$

where

j_g = superficial vapor velocity

ϱ_f = density of water

ϱ_g = density of steam

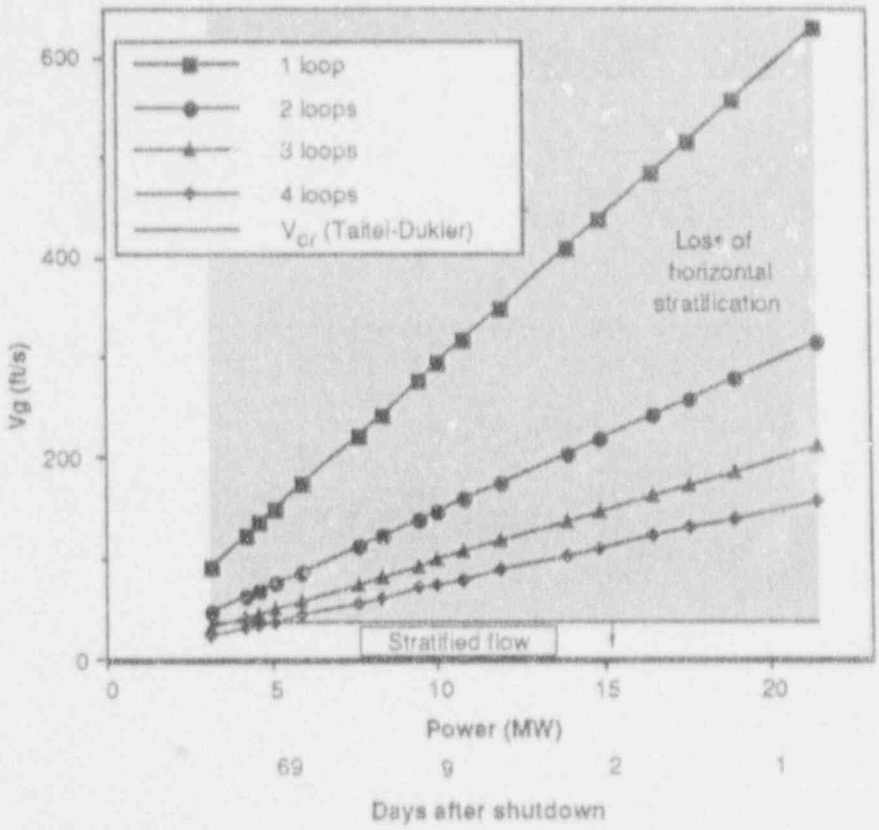

Figure E-6. Hot leg vapor velocity with a 0.75 liquid level in the hot leg pipe for various numbers of active loops.

σ = surface tension

g = acceleration due to gravity.

A mass and energy balance in the primary loop is used to obtain an expression for the superficial vapor velocity

$$j_g = \frac{Q}{\rho_g h_{fg} A} \qquad \text{(E-7)}$$

where

Q = core decay heat

h_{fg} = latent heat of vaporization

A = cross-sectional area of the hot legs.

Calculations of K_g at atmospheric pressure were performed by varying the decay heat and the number of active loops. The results are given in Figure E-7. Relevant data used in the calculations are (1979 ANS standard decay heat data)

Rated plant power = 3,411 MW

Hot leg piping inner diameter = 29 inches

Number of primary loops = 4.

The results show that at atmospheric pressure, flooding would occur only when one active steam generator is required to remove approximately 13 MW or more of decay heat.

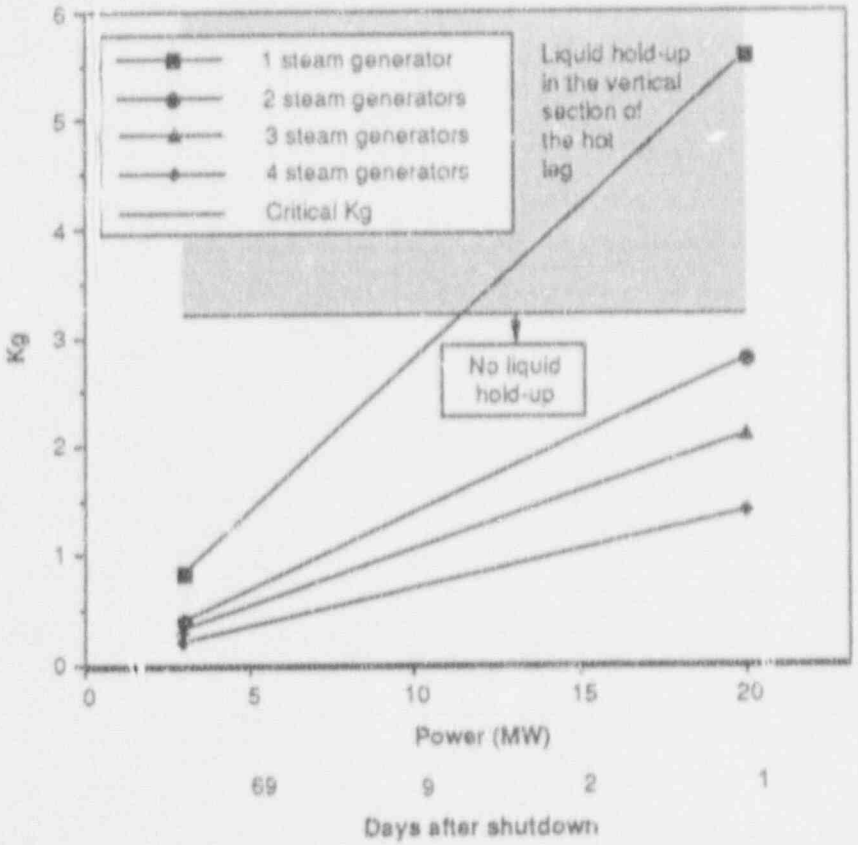

Figure E-7. K_g relative to decay heat at atmospheric pressure for various numbers of active loops.

E-4. FLOODING IN THE PRESSURIZER SURGE-LINE

The calculations of flooding characteristics in the pressurizer surge line are also based on the Kutateladze correlation.[8] Flooding in the vertical section of the pressurizer surge line can cause core level depression because of liquid hold-up in the pressurizer. Reference 9 shows that a column of water in the pressurizer can also cause erroneous reactor coolant system level indications when the temporary reactor vessel level indication system is used during reduced inventory operation. Equations (E-6), (E-7) are used to determine flooding characteristics in the pressurizer surge

Calculations of K_g were performed at atmospheric pressure. The fraction of the core generated steam entering the pressurizer surge line and the decay heat were varied to determine flooding tendencies. The results of these calculations are shown in Figure E-8. Relevant data used in the calculations are (1979 ANS standard decay heat data)

Rated plant power = 3,411 MW

Surge line piping inner diameter = 14 inches.

Figure E-8 demonstrates that if all the steam generated in the core enters the pressurizer surge line, flooding is possible at all decay heats considered. If one quarter of the steam produced in the core enters the pressurizer surge line, flooding is possible only if the decay heat is greater than 11 MW.

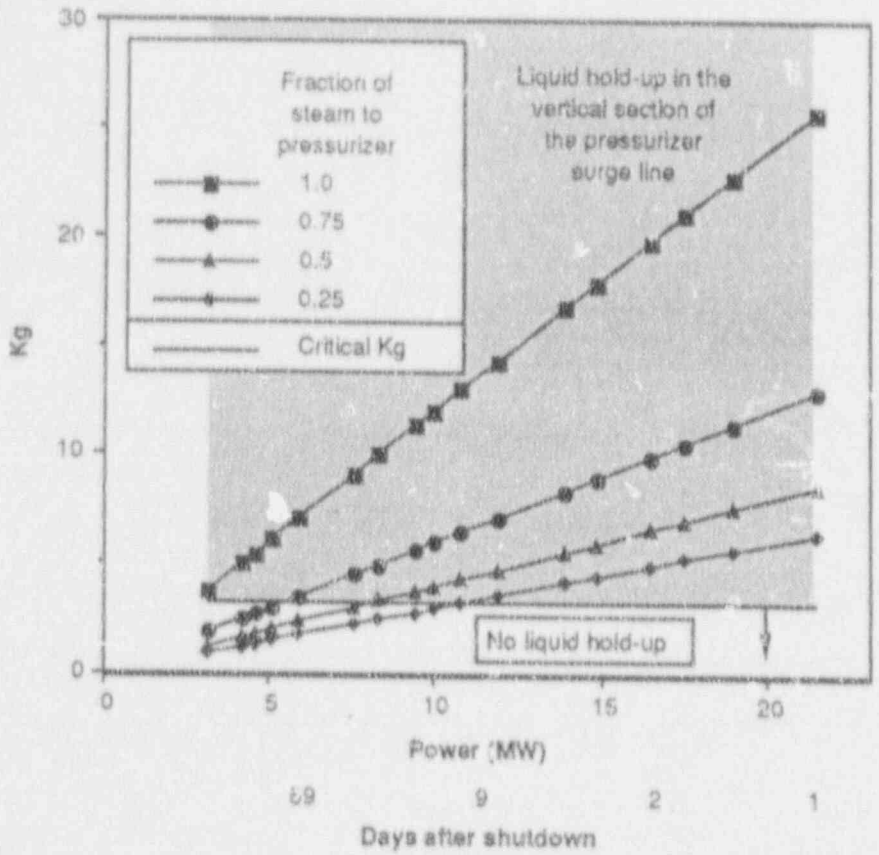

Figure E-8. K_g relative to decay heat and the fraction of steam entering the pressurizer surge line.

E-5. REFERENCES

1. G. B. Wallis, *One-Dimensional Two-Phase Flow*, New York: McGraw Hill, 1969, pp. 336–341.

2. G. Loomis, *Summary of the Semiscale Program (1965–1986)*, NUREG/CR-4945, EGG-2509, July 1987.

3. Y. Kukita et. al., "Flooding at Steam Generator Inlet and Its Impacts on Simulated PWR Natural Circulation," *ASME Winter Meeting, Boston, Massachusetts, December 13–18, 1987*, Fluids Engineering Division (FED)-Vol. 61, Heat Transfer Division (HTD)-Vol. 92.

4. Y. Kukita et. al., "Nonuniform Steam Generator U-tube Flow Distribution during Natural Circulation Tests in ROSA-IV Large Scale Test Facility," *24th ASME/AIChE National Heat Transfer Conference, Pittsburgh, Pennsylvania, August 9–12, 1987.*

5. P. Bazin et. al., "Natural Circulation Under Variable Primary Mass Inventories at BETHSY Facility," *Fourth International Meeting on Nuclear Reactor Thermal–Hydraulics, Karlsruhe, Federal Republic of Germany, October 10–13, 1989.*

6. Q. T. Nguyen and S. Banerjee, "Flow Regimes and Heat Removal Mechanisms in a Single Inverted U-Tube Steam Condenser," *American Nuclear Society Transactions, 43*, 1982, pp. 788–789.

7. Y. Taitel and A. Dukler, "A Model of Predicting Flow Regime Transitions in Horizontal and Near Horizontal Gas–Liquid Flow," *AICHE Journal*, 22, 1976.

8. R. A. Dimenna et. al., *RELAP5/MOD2 Models and Correlations*, NUREG/CR-5194, EGG–2531, August 1988.

9. *NRC, Loss of Vital AC Power and the Residual Heat Removal System During Mid-Loop Operations at Vogtle Unit 1 on March 20, 1990*, NUREG-1410, June 1990.

NRC FORM 335 (2-89) NRCM 1102, 3201, 3202

U.S. NUCLEAR REGULATORY COMMISSION

BIBLIOGRAPHIC DATA SHEET

(See instruction on the reverse)

1. REPORT NUMBER (Assigned by NRC, Add Vol., Supp., Rev., and Addendum Numbers, if any.)

NUREG/CR-5855
EGG-2671

2. TITLE AND SUBTITLE

Thermal-Hydraulic Processes During Reduced Inventory Operation with Loss of Residual Heat Removal

3. DATE REPORT PUBLISHED

MONTH	YEAR
April	1992

4. FIN OR GRANT NUMBER

L1893

5. AUTHOR(S)

S. A. Naff, G. W. Johnsen, D. E. Palmrose,
E. D. Hughes, C. M. Kullberg, W. C. Arcieri

6. TYPE OF REPORT

Technical

7. PERIOD COVERED (Inclusive Dates)

8. PERFORMING ORGANIZATION - NAME AND ADDRESS (If NRC, provide Division, Office or Region, U.S. Nuclear Regulatory Commission, and mailing address; if contractor, provide name and mailing address.)

Idaho National Engineering Laboratory
EG&G Idaho, Inc.
Idaho Falls, Idaho 83415

9. SPONSORING ORGANIZATION - NAME AND ADDRESS (If NRC, type "Same as above"; if contractor, provide NRC Division, Office or Region, U.S. Nuclear Regulatory Commission, and mailing address.)

Division of Systems Research
Office of Nuclear Regulatory Research
U.S. Nuclear Regulatory Commission
Washington, D.C. 20555

10. SUPPLEMENTARY NOTES

11. ABSTRACT (200 words or less)

Nuclear power plant conditions during outages differ markedly from those prevailing at normal full-power operation on which most past research has concentrated. This report identifies the topics needed to understand pressurized water reactor response to an extended loss-of-residual heat removal event during refueling and maintenance outages. By identifying the possible plant conditions and cooling methods that might be used, the controlling thermal-hydraulic processes and phenomena were identified. Gravity drain into the reactor coolant system, core water boil-off, and reflux condensation cooling were investigated in detail for example plants from each of the three U.S. pressurized water reactor vendors. The reactor coolant system pressure that would result from reflux cooling was calculated under various assumed conditions and compared to threshold pressures for various temporary closures that might be in use. The viability of various potential gravity feed-and-bleed approaches also was studied.

12. KEY WORDS/DESCRIPTORS (List words or phrases that will assist researchers in locating the report.)

loss of residual heat removal
reflux boiling
shutdown conditions
noncondensables

13. AVAILABILITY STATEMENT

Unlimited

14. SECURITY CLASSIFICATION

(This Page)
Unclassified

(This Report)
Unclassified

15. NUMBER OF PAGES

16. PRICE

UNITED STATES
NUCLEAR REGULATORY COMMISSION
WASHINGTON, D.C. 20555

OFFICIAL BUSINESS
PENALTY FOR PRIVATE USE, $300

SPECIAL FOURTH-CLASS RATE
POSTAGE AND FEES PAID
USNRC
PERMIT NO. G-67